Aalborg Universitet

Diffuse ceiling ventilation

Zhang, Chen

DIFFUSE CEILING VENTILATION

AIR DISTRIBUTION AND THERMAL COMFORT

BY
CHEN ZHANG

DISSERTATION SUBMITTED 2016

AALBORG UNIVERSITY
DENMARK

DIFFUSE CEILING VENTILATION

AIR DISTRIBUTION AND THERMAL COMFORT

by

Chen Zhang

AALBORG UNIVERSITY
DENMARK

Dissertation submitted 2016

.

CV

Personal Information

Name:	Chen Zhang
Date of Birth:	12.02.1987
Nationality:	Chinese
Phone:	+45-50272978
Email:	cz@civil.aau.dk; zclina@hotmail.com

Education

Jun 2013 – Sep 2016	Ph.D. student, Indoor Environment Engineering, Aalborg University, Denmark
Sep 2009 – Jul 2011	Master of Science, Applied Physics in Renewable Energy, University of Jyväskylä, Finland
Sep 2005 – Jul 2009	Bachelor of Engineering, Building Environment and Equipment Engineering, Tianjin University, China

Professional Experience

Jun 2013 – Sep 2016	Ph.D. student, Department of Civil Engineering, Aalborg University, Denmark
Jan 2015 – Jun 2015	Visiting Ph.D. student, School of Mechanical Engineering, Purdue University, USA
Aug 2011–May 2013	Research Assistant, Department of Civil Engineering, Aalborg University, Denmark
Jun 2008 – Sep 2008	Internship, Sunac China Holding Ltd., Tianjin, China

Fields of research interests

Ventilation

Computational fluid dynamics (CFD)

Energy efficient and sustainable buildings

ENGLISH SUMMARY

Diffuse ceiling ventilation is an innovative ventilation concept where the suspended ceiling serves as an air diffuser to supply fresh air into the room. Because of the large opening area, air is delivered to the room with very low velocity and unfixed direction, therefore named 'diffuse'. Compared with conventional ventilation systems (mixing or displacement ventilation), diffuse ceiling ventilation can significantly reduce or even eliminate draught risk in the occupied zone due to the low momentum supply. Moreover, this ventilation system uses a ceiling plenum to deliver air, which requires much lower pressure drop than the full-ducted systems. There is a growing interest in applying diffuse ceiling ventilation in offices and other commercial buildings because of the benefits from both thermal comfort and energy efficiency aspects. However, the present knowledge regarding the diffuse ceiling ventilation is very limited. It is essential to investigate the possibility and limitation of diffuse ceiling ventilation system and the parameters affecting the system performance.

By performing experimental studies in a room both with and without a diffuse ceiling, it was observed that diffuse ceiling ventilation effectively reduces local discomfort caused by draught, vertical temperature gradient and radiant temperature asymmetry. In addition, the comfort limit of diffuse ceiling ventilation was investigated by the design chart method. The results indicated that comfort requirements (such as draught and vertical temperature gradient) do not have strong limitations on the ventilation rate and the temperature difference between supply and return air. This characteristic allows the diffuse ceiling ventilation to have a higher cooling capacity than the conventional ventilation systems.

In addition to the stand-alone ventilation system, the potential to integrate diffuse ceiling ventilation with a radiant ceiling system (TABS) was also explored by full-scale experiments. In the integrated system, diffuse ceiling separates the TABS from the rest of the room, which consequently changes the energy efficiency of TABS. The measured results showed that diffuse ceiling ventilation plays a beneficial role on TABS' heating capacity. However, the cooling capacity was significantly reduced compared with the stand-alone TABS system.

Designing a diffuse ceiling ventilation system is challenging due to a large number of parameters encountered in practice. It is desirable to develop a numerical model to study the impacts of different parameters on the airflow pattern and thermal performance in the design stage. Two models were built and compared. One was a simplified geometrical model, and the other was a porous media model. Each model showed strengths and limitations. In order to provide an accurate prediction, two models were coupled. The simplified geometrical model was used to determine the radiative and convective heat transfers, and the results would provide necessary

boundary conditions for the porous media model for the detailed calculation on the flow behavior.

The validated model was further applied to conduct a series of parametrical studies. The numerical results proved that the airflow pattern is buoyancy controlled in the room with diffuse ceiling ventilation. The buoyancy flow was influenced by the location of heat sources and room geometry. From the aspect of thermal comfort, it is preferable to apply diffuse ceiling ventilation in rooms with low height and with even distributions of heat loads. On the other hand, the flow behavior in the room was not entirely independent of the supply air flow. The supply air flow was determined by the air distribution and thermal process within the plenum and the configuration of diffuse ceiling panel. The parametrical analysis indicated that the low plenum height and deep plenum deteriorated the uniformity of supply air flow and resulted in a higher velocity level in the occupied zone.

DANSK RESUME

Diffus loftsventilation er et innovativt ventilationskoncept, hvor det ophængte loft fungerer som luftdiffuser til forsyning af frisk luft i rummet. På grund af det store loftsareal forsynes rummet med luften i meget lav hastighed og uden fast retning, deraf navnet 'diffus'. Sammenlignet med konventionelle ventilationssystemer (blanding eller fortrængningsventilation) kan diffus loftsventilation betydeligt reducere eller helt eliminere risiko for træk i den beboede zone på grund af den lave fremdriftsforsyning. Desuden bruger dette ventilationssystem et loftsplenum til at levere luften, hvilket kræver et meget lavere trykfald end systemer med komplet udførelsesgang og muliggør også brug af naturlig ventilation. Der er en stigende interesse i brugen af diffus loftsventilation i kontorer og andre kommercielle bygninger på grund af fordelene fra både termisk komfort and energieffektive aspekter. Men den nuværende viden omkring diffus loftsventilation er meget begrænset. Det er essentielt at undersøge muligheden for og begrænsningen ved diffus loftsventilation og de faktorer der påvirker systemets præstation.

Ved at udføre eksperimentelle studier i rummet med og uden et diffust loft observeres det, at diffus loftsventilation effektivt reducerer det lokale ubehag forårsaget af træk, vertikal temperatur gradient og radiant asymmetri. Ydermere bliver komfortgrænsen for diffus loftsventilation undersøgt ved beregningsdiagram-metoden. Resultaterne indikerer, at komfortkravene (så som træk og vertikal temperatur gradient) ikke har større begrænsninger på ventilationsraten og temperaturforskellen mellem forsynings- og retur-luft. Disse karakteristika muliggør en højere køleevne for den diffuse loftsventilation end ved de konventionelle ventilationssystemer.

Foruden det selvstændige ventilationssystem udforskes også potentialet for at integrere diffus loftsventilation med et termisk aktiveret bygningssystem (TABS) ved hjælp af eksperimenter i fuld skala. I det integrerede system deles diffus loftsventilation TABS fra resten af rummet, hvilket betyder ændringer i energieffektiviteten af TABS. De målte resultater viste, at den diffuse loftsventilation havde en afgørende rolle i varmekapaciteten for TABS.

Det er udfordrende at designe et diffus loftsventilationssystem på grund af et større antal parametre der indgår i praksis. Det vil være ønskeligt at udvikle en numerisk model til at studere parametrenes indflydelse på luftstrømsmønstret og den termiske præstation. To forenklede modeller blev udviklet og sammenlignet; den ene er en forenklet geometrisk model og den anden en porøs medie-model. Hver model udviste styrker og svagheder. For at kunne give en nøjagtig forudsigelse blev de to modeller sammenkoblet, hvor den forenklede model blev brugt til at afgøre den radiative og konvektive varmeudveksling, og resultaterne ville give de nødvendige forhold for den porøse medie-model til en detaljeret beregning af luftstrømsadfærden.

Den validerede numeriske model blev yderligere brugt til at udføre en serie af parametriske studier. De numeriske resultater viste, at opdriftsstrømmen spiller en væsentlig rolle i luftstrømsmønstret i rummet med diffus loftsventilation. Opdriftsstrømmen bliver påvirket af varmekilders placering og rumgeometri. Ud fra et termisk komfort-perspektiv foretrækkes det at tilføje diffus loftsventilation i et rum med lavt loft med en jævn distribution af varmebelastning. På den anden side er strømmens adfærd i rummet ikke fuldstændig afhængig af forsyningsluftstrømmen. Den lave plenum højde and lange plenum længde forringer ensartetheden af forsyningsluftstrømmen og øger hastighedsniveauet i den beboede zone.

ACKNOWLEDGEMENTS

Chen Zhang

June 2016, Aalborg

TABLE OF CONTENTS

TABLE OF FIGURES

NOMENCLATURE

A	area [m^2]
Ar	Archimedes number
a_0/A	area ratio
C_2	inertial resistance coefficient
C_d	discharge coefficient
C_o	contaminant concentration in the supply opening [ppm]
C_{oc}	contaminant concentration in the occupied zone [ppm]
$C_{p,w}$	specific heat of water [J/kg.k]
C_R	contaminant concentration in the return opening [ppm]
DR	draught rate %
E_f	total fluid energy [m^2/s^2]
h_{ins}	heat transfer coefficient of the insulation layer [W/m^2.K]
h_{TABS}	heat transfer coefficient of TABS [W/m^2.K]
g	gravitational acceleration [m/s^2]
K_{sp}	a constant which depends on parameters outside the wall jet
k_{eff}	effective thermal conductivity of the medium [W/m.K]
k_f	fluid thermal conductivity [W/m.K]
k_s	solid medium thermal conductivity [W/m.K]
L	length of the room [m]
$\dot{m}$	mass flow rate [kg/s]
M_w	water flow rate [kg/s]
ΔP	pressure drop [Pa]
Q	heat load [W]
q_0	air flow rate [m^3/s]
S_E	energy source term [W/m^3]
S_M	momentum source term [N/m^3]
ΔT_0	temperature difference between supply and return air [K]
Tu	local turbulence intensity %
T_{op}	operative temperature [^{o}C]
$t_{a,l}$	local air temperature [^{o}C]
$t_{a,up}$	upper zone air temperature [^{o}C]
$t_{s,up}$	TABS upper surface temperature [^{o}C]

$t_{w,su}$	supply water temperature [°C]
$t_{w,re}$	return water temperature [°C]
u_o	supply air velocity [m/s]
u_{max}	maximum air velocity in the occupied zone [m/s]
$v_{a,l}$	local mean air velocity [m/s]
x_s	penetration length [m]
α	permeability [m^2]
β	expansion coefficient [1/C]
ε	ventilation effectiveness
ϵ^a	air exchange efficiency
τ_n	nominal time constant, which is the theoretically shortest exchange time for all air in the room
$\langle \overline{\tau} \rangle$	mean age of all air present in the room
ρ	air density [kg/m^3]
μ	dynamic viscosity [kg/m.s]

CHAPTER 1. INTRODUCTION

1.1. BACKGROUND

In the European Union, buildings are responsible for approximate 40% of the total energy consumption, which making buildings the largest 'energy-using sector'. To limit the expanding energy demand of buildings, EU launched the Energy Performance of Buildings Directive (Directive 2010/31/EU) [1], which emphasised the need to improve the energy efficiency and towards the goal of cutting overall energy consumption and greenhouse gas emissions by 20% by 2020 compared with 1990 level. In order to comply this directive, Denmark introduced new energy performance requirements BR10 in 2010 [2]. In addition to a general tightening by 25% of the energy performance frameworks compared with BR08 (2008), the new building regulations introduced a classification system for low energy buildings, i.e. low energy class 2015 and low energy class 2020 buildings, corresponding to a reduction of 50% and 75% of the minimum requirement respectively. Therefore, energy conservation becomes the most critical issue for building designer and developer.

However, minimizing the energy use in buildings must not be achieved at the expense of a comfortable and healthy indoor environment. An increasing number of studies support that there is a strong relation between indoor environment and the occupants' satisfaction and productivity. The investigation showed that the performance of office work improves when the air quality is increased [3]. Study with an extended scope revealed that the impact exists in not only the office, but also effects on the performance of schoolwork by children [4]. Therefore, from the perspective of occupants, the primary concern is to have a healthy and comfortable indoor environment that satisfies most of the occupants.

Sometimes, there are conflicts between the strategies to minimize the energy use and to create an acceptable indoor environment. For example, ventilation with cool outdoor air is usually employed to remove internal heat load in the office buildings. However, draught is a major complaint by using conventional ventilation systems, such as mixing and displacement ventilation. To avoid draught risk in the occupied zone, the supply air needs to be preheated before delivering to the room in winter or part of transitional seasons, which considerably reduces the cooling capacity of ventilation. As a result, the ventilation rate may increase many times larger than necessary to provide adequate cooling. The large ventilation rate leads to significant increases in both energy consumption and investment cost.

The conflict is expected to be reduced or even eliminated by an novel ventilation system, which is called diffuse ceiling ventilation. This ventilation concept is characterized by air being supplied through a large area occupying entire or a considerable part of the ceiling. Thus, the air is delivered to the room with very low velocity and unfixed flow direction, therefore the name 'diffuse' [5]. This ventilation system has been evidenced that it can reach a high cooling capacity by supplying cold outdoor air directly but without compensating indoor comfort [5][6][7][8]. In addition, the open space between suspended ceiling and ceiling slabs is employed as a plenum to distribute air instead of ductwork systems. The pressure loss of this ventilation system is much lower than the conventional ventilation systems, making it even possible to be driven by natural ventilation [5][7][9]. On the other hand, diffuse ceiling ventilation presents a high potential to combine with the night cooling strategy, because the ceiling slabs typically are exposed to the supply air pathways, which increases the efficiency of the thermal storage and improves the pre-cooling effect [10]. This ventilation concept presents many potential opportunities on energy saving and at the same time creating a comfortable indoor environment.

1.2. AIR DISTRIBUTION
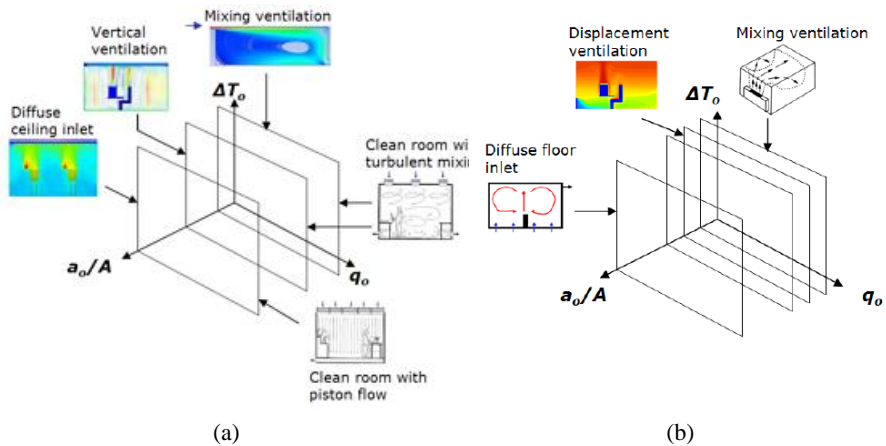
Figure 1-1: Three-dimensional chart of different air distribution systems for cooling (a) High location of supply opening (b) Low location of supply opening [11]

The pattern of air distribution in the room plays a decisive role in the ventilation performance. The primary variables determined the air distribution include: operative mode (heating or cooling), Archimedes number (or flow rate q_0 and the temperature difference between supply and return air ΔT_0), the area ratio between the supply opening a_0 and the surface it located A, and the location of the supply opening [11]. Based on these variables, Nielsen [11] introduced a 'family tree' to connect all types

of air distribution systems, as described by three-dimensional charts in Figure 1-1. The air distributions for non-industrial application are discussed below.

Mixing ventilation: The principle of mixing ventilation is to dilute the polluted and warm room air with clean and cool supply air. The air is delivered into the room with high initial velocity and generates a flow jet in front of the opening. The high turbulence jet and the entrainment of surrounding air promote a good mixing and create a uniform temperature and pollution distribution in the occupied zone, where the ventilation effectiveness is close to 1. The mixing air distribution is controlled by the momentum flow generated by the supply opening. In order to create a high momentum flow, the opening needs to have a small area, where the area ratio a_0/A is typically less than 10^{-3}. The supply opening must be located outside of the occupied zone. Nielsen analyzed a wall jet model of mixing ventilation [12][13]. It was found that the maximum velocity in the occupied zone is located close to the floor due to the reverse flow. The amount of heat load removed by mixing ventilation is proportional to the cube of the maximum velocity in the occupied zone, as expressed by Eq (1). Therefore, in order to deal with high heat load, the mixing ventilation system must provide a high velocity, which commonly results in a high risk of draught in the occupied zone [14].

$$Q = 3.5 \cdot 10^3 K_{sp}^{1.5} \left(\frac{L}{x_s}\right)^{1.5} \frac{u_{rm}^3}{L} \qquad \text{Equation 1}$$

Displacement ventilation: The basic idea of displacement ventilation is to replace instead of mixing the fresh air with the polluted room air. The cool and fresh air is supplied close to the floor and then rises into the occupied zone by the natural buoyancy flow generated by the heat sources. Therefore, the airflow pattern in the room with displacement ventilation is controlled by buoyancy flow. The supply opening area is larger than that of mixing ventilation, where the area ratio a_0/A is typical 6×10^{-3} [11]. Displacement ventilation can provide better air quality than mixing ventilation due to the stratification effect. However, the low location of the supply opening results in the highest velocity and lowest temperature occur near the floor. To avoid draught and cold feet, the supply air is introduced into the room with at a low velocity (< 0.25 m/s) and moderate temperature (2-4 °C below room temperature), which restricts the cooling capacity of the ventilation system [15]. Thus, displacement ventilation is preferable to use in the situations where the air quality is the major problem instead of surplus heat [16]. On the other hand, the vertical temperature gradient is another concern in the room with displacement ventilation, where the temperature gradient should be limited to 3 K/m to avoid discomfort. High location of exhaust opening is required in this system. Displacement ventilation can only apply for cooling purpose because short circuit will occur for the heating case.

Diffuse floor inlet is a type of displacement ventilation where the area ratio equals to 1.0. Air is also introduced at floor level, but at a higher flow rate and greater temperature difference are allowed. Care must be taken to avoid draught near the opening.

Vertical ventilation: Vertical ventilation is a distribution system where the air is supplied through a large ceiling mounted diffuser. The opening area ratio is around 3×10^{-2} [11]. The air distribution in the room with vertical ventilation is mainly controlled by the buoyancy flow. However, it also depends on the location of the supply opening. The flow in the room will present a high mixing level when the supply openings are located above the heat sources. On the contrary, a displacement effect will occur when supply openings are located near the side wall. Due to the buoyancy force play a dominant role in this ventilation concept, the draught is dependent on the strength and location of heat sources. Vertical ventilation is suitable for the cooling purpose, while stratification effect will take place in the heating case.

Diffuse ceiling ventilation could be regarded as a version of vertical ventilation, where the air is supplied through the ceiling panels. The supply area covers most of the ceiling or even the whole ceiling, where the area ratio a_0/A is close to 1.0. The detailed analysis regarding the diffuse ceiling ventilation will be addressed in this study.

1.3. THERMAL COMFORT CRITERIA

Before evaluating the thermal comfort in a ventilated room, it is necessary to specify the area that the indoor environment requirements should be fulfilled. Based on EN 13779 [17], an occupied zone is defined that all the measurements regarding the comfort criteria should be within this zone, where the dimension of the occupied zone is demonstrated in Figure 1-2. The regions outside the occupied zone are not guaranteed to satisfy the criteria.

Thermal discomfort can be related to the thermal balance of the whole body, but also can be caused by unwanted cooling or heating of one particular part of the body, called local discomfort. The thermal comfort evaluation presented in this study focuses on the steady-state conditions, where the long-term evaluation is not taken into consideration. Thermal comfort criteria are based on Category B, which is suitable for the spaces like single and landscape offices, classrooms and conference rooms.
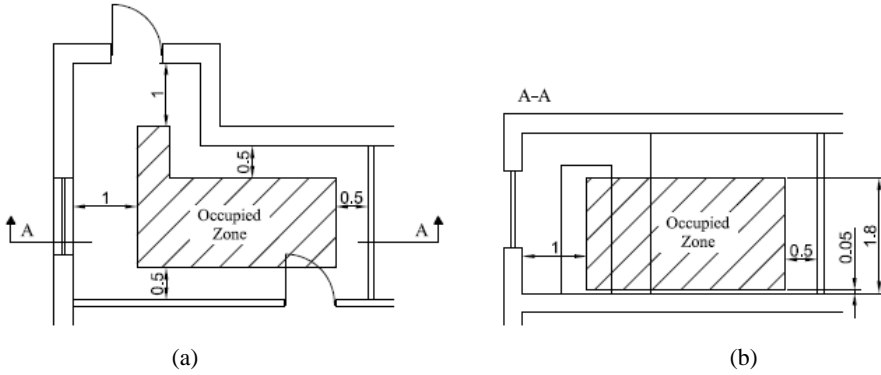
Figure 1-2: Description of the occupied zone, unit (m) (a) Plan view (b) Vertical section
[17][18]

A predicted mean vote (PMV) model proposed by Fanger is commonly used to evaluate the thermal sensation of the whole body [19]. This model is based on the heat balance theory and predicts the thermal sensation as a function of people's activity and clothing, as well as environmental factors: air temperature, mean radiant temperature, air velocity and humidity. The advantage of this model is flexible to apply in the indoor environment with different HVAC systems and a wide range of activity levels and clothing habits[19][20]. The PMV limit in this study is between -0.5 to +0.5, corresponding to predicted percentage dissatisfied (PPD) less than 10 %.

Draught is the most common reason for local discomfort in ventilated or air conditioned buildings, and is caused by air movement [21][22]. The occupants often counteract the draught by stopping the ventilation systems or plug up the diffusers, resulting in a poor indoor environment at the end. The risk of draught is evaluated by the draught rate (DR), which expresses the percentage of people dissatisfied due to draught. DR is not only determined by the local air velocity, but also influenced by air temperature and turbulence intensity, as presented in Eq. (2). This model applies to people with sedentary activity and with a neutral thermal sensation for the whole body. In addition, the model is designed to predict the draught rate at the neck level, and an overestimation is expected when predicts the draught at arms or feet level [23].

$$DR = (34 - t_{a,l})(\bar{v}_{a,l} - 0.05)^{0.62}(0.37 \cdot \bar{v}_{a,l} \cdot Tu + 3.14) \quad \text{Equation 2}$$

Besides the draught rate, maximum mean air velocity is also regarded as a design criterion in the ventilated buildings. ISO 7730 [23] and CR 1752 [22] provide the maximum mean air velocities allowed in summer and winter conditions, while, ASHRAE 55-2013[24] gives a limit on the mean air velocity based on the operative temperature of 22.5 °C. Different standards are based on different assumptions on the

air temperature and turbulence intensity, therefore, the tolerances on the air velocity present slightly discrepancy (Table 1-1).

Table 1-1: Criteria related to draught [23][22][24]

Draught rate	Maximum mean air velocity ISO 7730		Maximum mean air velocity CR1752		Maximum mean air velocity ASHRAE 55-2013
	Summer	Winter	Summer	Winter	Summer/Winter
< 20 %	0.19 m/s	0.16 m/s	0.22 m/s	0.18 m/s	0.2 m/s

In addition to draught, local discomfort can also be caused by vertical temperature difference and radiant temperature asymmetry. Temperature differences between the diffuse ceiling and the rest of the room surfaces are expected in the room with diffuse ceiling ventilation. The radiant temperature asymmetry is estimated as the difference between the plane radiant temperatures in two opposite directions. Compare to the cool ceiling, people are more sensitive to the warm one, as indicated in Table 1-2.

Table 1-2: Local thermal discomfort limits [23]

Vertical temperature difference between head and ankles	Radiant temperature asymmetry	
	Warm ceiling	Cool ceiling
< 3 ºC	< 5 ºC	< 14 ºC

1.4. OBJECTIVE OF THE THESIS

Despite growing interest in diffuse ceiling ventilation, the knowledge and experiences regarding this innovative ventilation concept are very limited. Further investigation on a number of issues is needed to fully understand the possibility and limitation of diffuse ceiling ventilation system.

The objectives of this study are to:

- Provide a critical review on the diffuse ceiling ventilation based on the most current research results from both laboratory and field experiments as well as numerical simulations. Discover the characteristic of diffuse ceiling ventilation.

- Evaluate the thermal comfort in a room with diffuse ceiling ventilation and investigate the influence of the opening area of diffuse ceiling panels on the system cooling capacity. A design chart method will be implemented to explore the limits of the system in term of ventilation rate and supply air temperature.
- Explore the potential to integrate diffuse ceiling ventilation with a radiant ceiling system (TABS). Special attention will be drawn to whether the integrated system can provide an energy-efficient and comfortable indoor environment under different climate conditions.
- Develop a numerical model which can describe the flow behavior of diffuse ceiling ventilation. In addition to simulating the flow in the conditioned space, this model should also be able to predict the air distribution and thermal process within the plenum.
- Identify the critical parameters with influence on the performance of diffuse ceiling ventilation. Propose the optimal system solution based on a series of parametrical analysis.

The investigation will be conducted by both full-scale experiments and numerical modeling by CFD. This study focuses on the steady-state analysis, where the transient flow situation and dynamic effect of thermal mass will not be taken into consideration.

1.5. THESIS OUTLINE

Chapter 1 presents the background and objective of this study, where the air distribution principle and thermal comfort criteria are addressed.

Chapter 2 provides a literature review of the currently available studies and applications of diffuse ceiling ventilation in the non-industrial buildings, where the airflow pattern, type of diffuse ceiling supply, ventilation performance and the characteristics are discussed.

Chapter 3 describes two full-scale experimental studies, one aims to discover the comfort limit of the diffuse ceiling ventilation system, and the other one explores the possibility and limitation to cooperate with a radiant ceiling system (TABS).

Chapter 4 proposes and compares two numerical models regarding the diffuse ceiling ventilation. The validated model is applied to conduct a series of parametrical studies on the selected design parameters.

Chapter 5 provides the general conclusions drawn from this study.

Chapter 6 summarizes the limitations of the current study and recommends the future research directions.

Appendix A-E contains publications during the Ph.D. study, included journal and conference articles.

CHAPTER 2. LITERATURE REVIEW OF DIFFUSE CEILING VENTILATION

2.1. ROOM AIRFLOW PATTERN

The airflow in the room with diffuse ceiling ventilation can be either momentum controlled or buoyancy controlled, which depend on the Archimedes number. Based on similarity principles, air distribution in a room with the fully developed flow can be described by Archimedes number ($Ar \sim \Delta T/q_0^2$), which represents the ratio between buoyancy force and the momentum forces [11]. Figure 2-1 shows a design graph (q_0-T_0) for a diffuse ceiling ventilation system with a whole ceiling supply ($a_0/A = 1$).
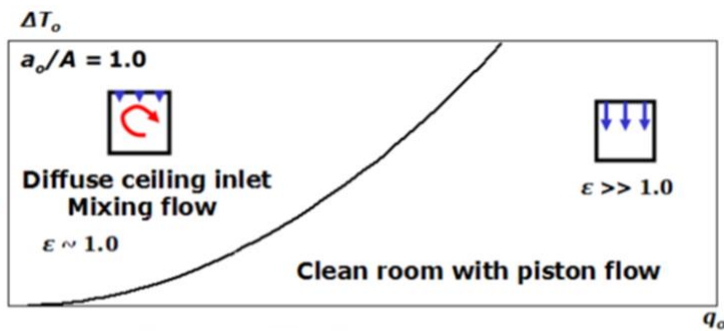
Figure 2-1 The airflow pattern in the room with diffuse ceiling ventilation and examples of its application: office and clean room[11]

The lower right side of the graph defines the momentum driven flow. In this case, the large ventilation rate is required (50-100 h^{-1}) and the piston-flow takes place. The momentum driven flow is specially utilized in clean rooms where high ventilation effectiveness is expected. In addition, exhaust opening is required to place in the lower zone.

When the ventilation rate ranges from 1 to 5 h^{-1}, the airflow pattern is controlled by buoyancy flow, and the ventilation effectiveness is close to 1, which could be regarded as a mixing flow. *" This air distribution concept is suitable for buildings requiring high cooling demand and high thermal comfort level, like offices or classrooms [25]".* In the thesis, attentions have been paid on buoyancy controlled pattern because of the wide application potential.

2.2. DIFFUSE CEILING SUPPLY

The configurations of diffuse ceiling, for example shape, material and perforation level, as well as the ceiling suspensions, have significant influences on the performance of the air supply. Generally, we can divide diffuse ceiling supply into three categories depending on the air path, as listed in Table 2-1 [25].
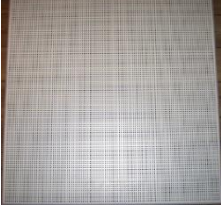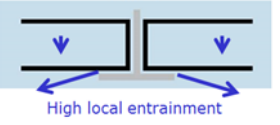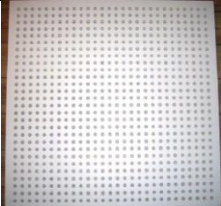
In the first category, diffuse ceiling is built by ceiling panels impenetrable to air [25]. The air is delivered only through the connection slots between the panels, called crack flow. Micro-jets will be formed by this category of supply, and generate high local entrainments. Consequently, the shape and location of connections potentially influence the ventilation performance. The micro-jets may have high air velocity and penetrate to 0.25 m down into the room. Therefore, it is recommended to keep a minimum distance of 0.25 m from the occupied zone to the suspended ceiling, in order to avoid draught at the head level [26].

The second category is composed of air permeable ceiling panels [25]. The air is discharged through both perforations on the ceiling panels and connection slots. Similar to the first category, high locate entrainments occur below the slots. The proportions of crack flow and panel flow strongly depend on the connection profiles and the perforation level. The first two categories of diffuse ceiling supply have significant application potential because the acoustic ceiling panels can be directly applied as air diffusers, which reduce the investment cost of the ventilation system.

The third category is called 'Fully diffuse ceiling' [25]. This kind of diffuse ceiling supply is built by porous material. Because it is not composed of ceiling panels, no slot exists. The whole ceiling area is used to distribute air, thus, the air velocity through diffuse ceiling diffuser is very low and without any micro-jet, therefore with low local entrainment. The pressure drop of this category of supply could vary considerably depending on the porous material, thickness, porosity, as well as coating and painting layer, which will be discussed in Section 2.4.1.

Table 2-1: Three categories of diffuse ceiling supply based on air path and examples [25]

Category	Example	Description	Ref.
High local entrainment		• Impermeable mineral wool acoustic tiles • 50 mm thickness	[26]
		• Impermeable aluminium lamellas • 15 mm mineral wool acoustic plates above lamella	[27]
High local entrainment		• Aluminium acoustic tiles • 0.6 mm thickness Circle perforation: $\emptyset$ =2.5 mm, pitch 5.6 mm • Perforation level 16.2%	[28]
		• Gypsum acoustic tiles • 12.5 mm thickness Hexagon perforation: $\emptyset$ =11 mm, pitch 20 mm • Perforation level 17%	[28]
		• Large perforations: $\emptyset$ = 25 mm, pitch 300 mm • Perforation level 0.5%	[8]
		• Small perforations: 12×12 mm^2, pitch 25 mm • Perforation level 18%	[8]
Low local entrainment		• Perforated structure • Three layers: base layer 25 mm diffusive layer 3 mm paint layer	[18] [29]

2.3. THERMAL COMFORT AND INDOOR AIR QUALITY

Thermal comfort and indoor air quality are the two crucial factors to evaluate a ventilation system. The thermal comfort parameters include vertical air temperature difference, draught rate and radiant asymmetry. Indoor air quality is evaluated by ventilation effectiveness and air exchange efficiency [25].

2.3.1. VERTICAL AIR TEMPERATURE DIFFERENCE

Table 2-2 presents the vertical temperature differences (0.1-1.1 m above the floor) obtained from several studies. The temperature difference in the cooling cases ranges from 0.1-1.0 ºC, depending on the different boundary conditions in the experiments, such as heat loads, flow rates, supply air temperature and diffuse ceiling configurations. These results show that diffuse ceiling ventilation provides a good mixing between supply air and room air, and the occupants experience no discomfort caused by the vertical temperature difference. However, in the heating case, which demonstrates an unoccupied situation, a high temperature difference up to 2.5 ºC was observed. This is due to the low-momentum supply flow can not generate sufficient mixing in the room without the presence of heat sources. Nielsen [26] recommended using convector or floor heating to support heating the room with diffuse ceiling ventilation.

Table 2-2: Vertical air temperature difference between head and ankles (0.1-1.1 m)

Reference	Condition	Temperature difference [ºC]
[26]	Cooling	0.2-1.0
	Heating	0.5-2.5
[27]	Cooling	0.3
[28]	Cooling	0.5
[18]	Cooling	0.1-0.7

Note: Detail information regarding test conditions can be found in Paper 1[25]

2.3.2. DRAUGHT RATE

Diffuse ceiling ventilation has been proved to have lower draught risk compared with the other conventional ventilation system. Nielsen et al. [6], Fan et al. [27] and Hviid et al. [5] demonstrated that this ventilation system is able to maintain a draught free environment even with a low supply air temperature.

Figure 2-2 demonstrates the relation between air flow rate and DR, as well as the effect of other design parameters, such as room height and heat load distribution. It

was observed that DR in the occupied zone does not strongly depend on the air flow rate. While the air flow rate increases from 0.05 m³/s to 0.3 m³/s, the DR only increases less than 5%. This result explains well that the air distribution in the room is not dominated by the supply air flow. However, it is influenced by other parameters. By comparing the DR in the rooms with three heights (2.5 m, 4.1 m and 4.4 m), it can be concluded that the increase of room height results in an increase of the DR in the occupied zone. The DR is below 15% within 2.5 m room, while it is above the limit of 20% when the room is 4.4 m height.
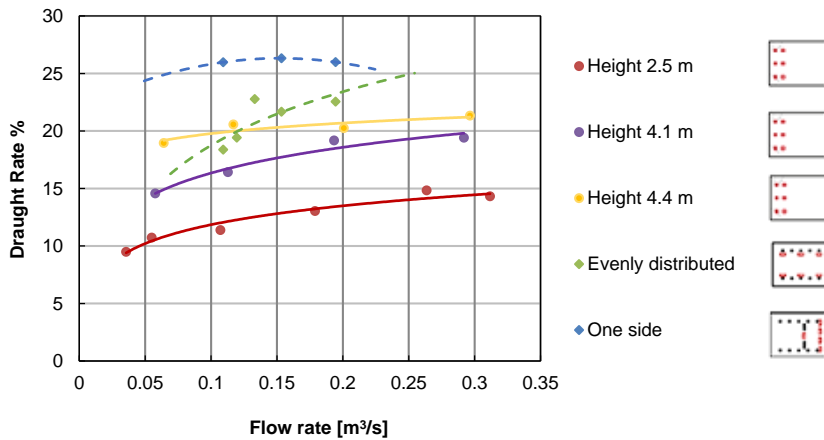
Figure 2-2: Draught rate vs. flow rate with different design parameters[18][30]

Table 2-3: Design parameters and test conditions

References	Design parameters	Heat load
[30]	Room height	454-497 W or 16-18 W/m²
[18]	Heat load location	2000 W or 72W/m²

The effect of heat load distribution can be observed in Figure 2-2. The buoyancy flow generated by heat sources determines the airflow pattern in the room and consequently determines the draught rate. Even distribution of heat sources provides a more comfortable environment than that located on one side. Finally, by comparing these two studies, it is clear that [18] gives a high draught environment than [30]. This can be attributed to the high heat load in [18], which is approximate four-time of that in [30], see Table 2-3. The intense buoyancy flow above the heat sources creates a strong air movement in the room and increases the draught risk.

2.3.3. RADIANT TEMPERATURE ASYMMETRY

(a) Al ceiling   (b) Gyp ceiling
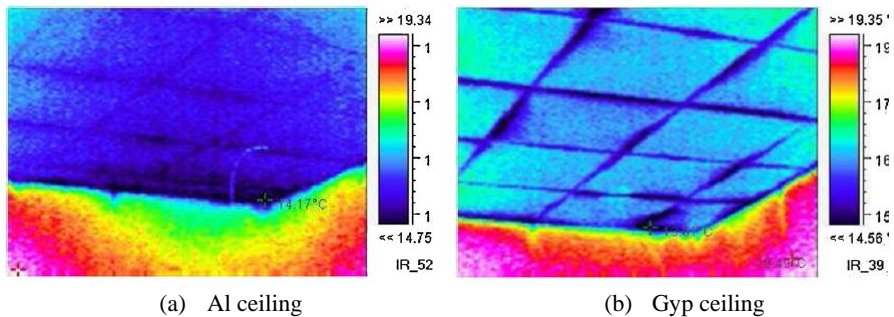
Figure 2-3: Thermovision of Al ceiling and Gyp ceiling [5]

People may experience discomfort due to the temperature differences between room surfaces, named radiant temperature asymmetry. The temperature differences between diffuse ceiling and other enclosure surfaces are determined by supply air temperature and the materials of ceiling panels. The ceiling panels with high thermal conductivity may increase the temperature asymmetry. For example, Figure 2-3 shows the thermal image of the aluminum (Al) ceiling and gypsum (Gyp) ceiling[5]. When the supply air temperature was -3 ºC, Al ceiling had a surface temperature of 14 ºC, while that of Gyp ceiling was about 16 ºC. Although the low ceiling temperature will not generate discomfort due to radiant asymmetry, there is a condensation risk if the surface temperature is below dew point temperature. Radiant asymmetry is also influenced by the heat load condition. By conducting the tests under different heat load conditions, the radiant asymmetry ranged from 1.5 to 8.4 K was observed by Chodor et al. [18], where the lowest temperature asymmetry occurred when lighting was the only heat source in the room.

2.3.4. INDOOR AIR QUALITY

The indoor air quality can be evaluated by ventilation effectiveness and air exchange efficiency [25]. Ventilation effectiveness represents the ability of a ventilation system to remove air-bone contaminants from the occupied zone, expressed by Eq. (3) [12]:

$$\varepsilon = \frac{C_R - C_o}{C_{oc} - C_o} \qquad \text{Equation 3}$$

"The ventilation effectiveness is determined by the air distribution and the location of the pollution sources in the room. A complete mixing of air and pollutants will result in the ventilation effectiveness equals to one. The ventilation effectiveness can be measured by tracer gas method. Fan et al. [27] mentioned that the ventilation effectiveness in the breathing zone is around 0.9 to 1 by diffuse ceiling ventilation.

These results correspond well with the other studies [26][18][31], which mean the room equipped with diffuse ceiling can generate good mixing in the occupied zone by the convective flow. Furthermore, the results indicated that ventilation flow rate has a limited influence on ventilation effectiveness in case of non-isothermal load [25]."

Another index is air exchange efficiency, which indicates the ability of a ventilation system to exchange the air in the room. It can be expressed by Eq. (4) [5]:

$$\epsilon^a = \frac{\tau_n}{\overline{\tau_r}} \times 100\% \qquad \text{Equation 4}$$

The actual air change time $\overline{\tau_r}$ can be derived from the room mean age of air $\langle \overline{\tau} \rangle$ by [5]:

$$\overline{\tau_r} = 2\langle \overline{\tau} \rangle \qquad \text{Equation 5}$$

"The air exchange efficiency is dependent on the air distribution system in the room, the geometry of the room and location of heat source, but it is not dependent on the location of the contaminant sources. Hviid et al. [5] investigated the air exchange efficiency, and the results support the good mixing finding as mentioned above. On the other hand, no evidence indicated there is any stagnant zone or short-circuiting ventilation in the room [25]."

2.4. CHARACTERISTICS OF DIFFUSE CEILING VENTILATION

2.4.1. PRESSURE DROP AND ITS EFFECT

The air transport power is determined by the pressure drop of the system. It is desirable to decrease the pressure drop of ventilation systems, which is possible to avoid noise problem and at the same time save the power consumption of the fan. Most of the studies pointed out that diffuse ceiling ventilation has the advantage of low pressure drop [5][27].

The low-pressure drop of diffuse ceiling ventilation is caused by two reasons. First of all, suspended ceiling panel is employed as air diffusers, which requires significantly lower pressure drop than the conventional diffusers. Figure 2-4 illustrates the pressure drop across the diffuse ceiling as a function of air flow rate. " *A significant variance on pressure drop can be observed for different types of diffuse ceiling. Diffuse ceiling supply cargorey 1 (mineral wool ceiling, Al lamella ceiling) and category 2 (Al-16 and Gyp-17 ceiling) present very low-pressure drops of less than 5 Pa when flow rate ranges from 1-10 l/s.m². However, the pressure drops across 'fully diffuse ceiling' (FDC) show a big variation 5-70 Pa when the airflow rate is 20 l/s.m². The large range of the pressure resistance of 'fully diffuse ceiling' is attributed to different*

thicknesses and different types of diffusive layer, as well as the coating and paint layers. Most of 'fully diffuse ceiling' samples show higher pressure drop than the other types of diffuse ceiling supply. [25]"

On the other hand, connection profile plays an important role in the pressure drop. As illustrated in Figure 2-4, the single mineral wool panel presents a large resistant to airflow, which is almost air impermeable. The pressure drop reaches 74 Pa when the air flow rate is 8.5 l/s.m². However, the pressure drop of the mineral wool ceiling system is decreased to 5 Pa at the same flow rate. The large difference between the single panel and the whole ceiling is because almost of the air flow discharges through the connection slots but not the ceiling panels [25].
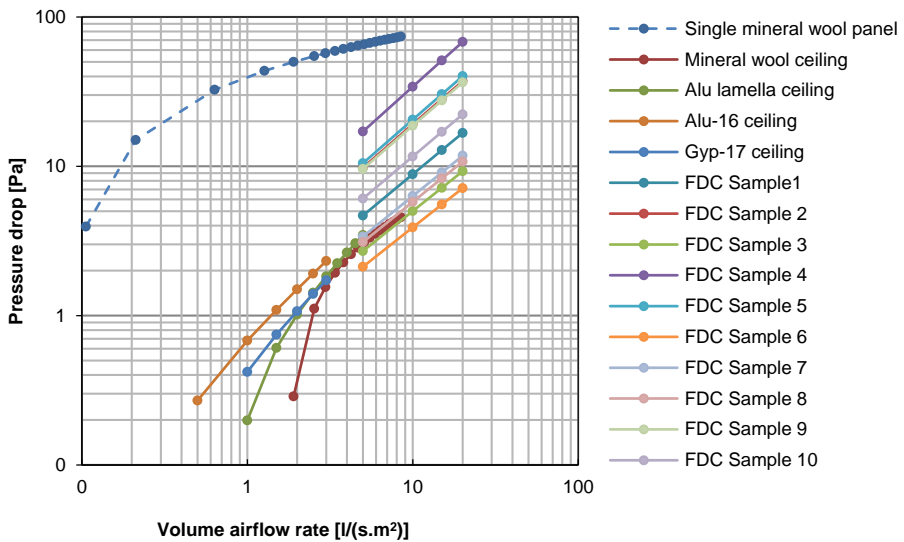
Figure 2-4: Pressure drop for different diffuse ceiling types [5][9][18][27][32]

Table 2-4: The diffuse ceiling types used in pressure drop measurements

References	Diffuse ceiling supply
[27]	Al lamellas
[5]	Al-16 (open area 16%)
	Gyp-17 (open area 17%)
[18][32]	'Fully diffuse ceiling' by porous material
[9]	Mineral wool panels and ceiling

Secondly, plenum is a primary air distribution route for diffuse ceiling ventilation. The use of plenum eliminates the need of ductwork, and the large size of the plenum creates a little restriction to the air flow. Consequently, the amount of pressure required to deliver air by diffuse ceiling ventilation is much lower than that required by the conventional ventilation system. Therefore, the influence factors of diffuse ceiling pressure drop include: diffuse ceiling panels, air tightness of connections, suspension systems and plenum configuration.

The pressure loss through the air distribution system is a dominant parameter of energy consumption of fans. *"P Jacobs et al. [7] described two field studies of the classroom with diffuse ceiling ventilation systems. By comparing with traditional and modern ventilation systems for schools in Netherlands* [33]*, they found out the specific fan power (SPF) and energy cost of diffuse ceiling ventilation systems was considerably lower than other ventilation systems [25]".* The low-pressure drop even makes the system possible to be driven by natural ventilation. For example, in the typical Danish climate, the annual mean wind speed is about 4.4 m/s, providing a pressure difference above 3.5 Pa in building with natural ventilation [34]. This pressure difference is sufficient to drive the airflow into the conditioned space with diffuse ceiling supply.

However, the low pressure drop of the diffuse ceiling panels may result in a problem of reverse flow. The reverse flow may raise hygiene problem, and the humid and warm airflow forced back into the plenum may cause condensation on the surfaces of suspended ceiling panel and concrete slab. The situation will even deteriorate when the thermal plume from heat sources is strong. Reverse flow can be examined by tracer gas method, where trace gas is dosed in the conditioned space and the concentration of tracer gas in the plenum is measured after reaching the steady–state. The plenum concentrations need to compare with background level to evaluate whether the reverse flow exists or not [28][35].

2.4.2. THE EFFECT OF PLENUM AND SUSPENDED CEILING

Distributing air by an overhead plenum is an important feature that distinguishes diffuse ceiling ventilation from the fully-duct ventilation systems. The plenum needs to keep a positive static pressure to the conditioned space in order to drive the plenum air through diffuse ceiling supply.

The thermal process within the plenum is more complicated than that in the ducted system. As the air traveling through the plenum, it directly contacts with the concrete slabs and suspended ceiling, which leads to heat transfer to or from the air depending on the air–surface temperature difference and ventilation rate [25]. It is desirable to

design a plenum which can provide an even air distribution through the diffuse ceiling supply from both quantity and quality (temperature) aspects. The air distribution in the plenum is determined by plenty of design parameters, including plenum inlet, plenum dimension and shape, obstructions within the plenum, etc. [36][37]. Currently, the researches regarding the ceiling plenum are very limited, and no comprehensive design guideline is available. Therefore, one of the objectives of this study is to investigate the effect of these design parameters and propose an optimized plenum design solution.

Diffuse ceiling ventilation presents a high potential to combine with night cooling strategy. The ceiling slabs are exposed to the supply air pathway, which may increase the efficiency on removing the heat stored in the thermal mass and improve the pre-cooling effect. The night-cooling potential of diffuse ceiling ventilation was investigated by Hviid [10] by comparing it with conventional mixing ventilation. Simulation results demonstrated that diffuse ceiling ventilation enables additional cooling potential by activating the thermal mass of the ceiling slabs. However, this study was conducted by numerical modeling and it neglected the heat transfer from the room side to the plenum. The effect of diffuse ceiling ventilation on the energy efficiency of thermal mass requires further investigation by experimental study.

2.4.3. RADIANT COOLING POTENTIAL AND CONDENSATION RISK

Different from centralized air terminals, diffuse ceiling supply shows a radiant cooling potential because of the large supply area and low surface temperature [28][18][25]. Therefore, a portion of sensible heat load is removed by radiative heat transfer between cold diffuse ceiling surface and the rest of the room. The radiant cooling potential strongly depends on the properties of diffuse ceiling panel. Ceiling panel with a higher thermal conductivity is easy to reach a lower surface temperature and therefore a higher radiant cooling potential, as discussed in Section 2.3.3.

"Since the diffuse ceiling has the radiant cooling potential, condensation becomes a problem facing by this system. In a humid climate, the suspended ceiling surface can form condensation easily if humidity is not properly controlled [25]." Condensation will impact the visual perception and the function of the diffuse ceiling as air diffusers.The ceiling surface grows wet dirty and microorganism so that disease breeds heavily, and drop water from the ceilings forming the "Office Rain" [38].

In the humid climate, approximately 50% - 80% of the moisture load in the office buildings is from the outdoor air [39]. On the other hand, the extra latent load generated by the occupants has the risk to create a condensation problem [40]. The condensation will deteriorate by the reverse flow, where the humid and warm room

air is pushed back to the plenum and condenses on the the diffuse ceiling surface, causing early failure [25].

"The supply air temperature needs to be carefully controlled to ensure the diffuse ceiling surface temperature is above the dew-point temperature of the ambient air. Usually, the surface temperature should not be lower than 15 ºC to make sure that the indoor air temperature is maintained within the comfortable range. Moreover, it is necessary to control the pressure of the plenum properly and carefully design of the plenum and suspended ceiling to avoid the reverse flow [25]". Finally, the risk of condensation is possible to be reduced if the suspended ceiling is made of moisture absorbent materials, for example, wood-cement board. The absorbent materials can serve as a humidity buffer and give a substantial stability to the indoor relative humidity if transient moisture situation occurs.

2.5. CONCLUSION

Several conclusions could be drawn in this chapter:

- The air movement in the room with diffuse ceiling ventilation can be either driven by buoyancy flow or momentum flow, which depends on *Ar* number. The buoyancy controlled pattern presents a large potential to apply in the commercial buildings (offices or classrooms) because of the ability to handle high heat loads and high ventilation demand without generating discomfort.
- The diffuse ceiling supply can be seperated into three categories based on the air pathway: air supply through connection slots, through perforated ceiling, and through both connection slots and perforated ceiling. Micro-jets and high local entrainment may take place below connection slots, because of the relatively high air velocity. A minimum distance of 0.25 m should be kept between the diffuse ceiling to the occupied zone, to avoid draught risk at the head level. The supply area of diffuse ceiling inlet is more flexible than conventional air diffuser, which could take up the entire ceiling area or a part of the ceiling.
- Because of the low momentum supply from the diffuse ceiling, the mixing level in the room is determined by the buoyancy flow created by the heat sources. With the help of the buoyancy flow, low temperature gradients can be reached, and the ventilation effectiveness is as good as mixing ventilation.
- Diffuse ceiling ventilation can provide a low draught environment compared with the conventional ventilation systems. The draught rate in the occupied zone is not strongly determined by the ventilation rate, but depends on the

heat load conditions, like the geometry, intensity and location. The room height also has significantly impact on the draught rate.

- The diffuse ceiling can obtain a lower surface temperature than the surrounding surfaces, depending on the supply air temperature and the material of ceiling panel. The radiant temperature asymmetry will not result in discomfort but will provide a radiant cooling potential. However, the ceiling surface temperature should be kept above dew point temperature to avoid condensation risk.

- The low pressure drop of diffuse ceiling ventilation attributes to two reasons. First, the suspended ceiling as diffuser requires much lower pressure drop than the conventional air diffusers. Second, the use of plenum to distribute air eliminates the need for ductwork and creates a little resistance to the airflow. The low pressure drop of diffuse ceiling ventilation system reduces the energy use of fan and even makes the system able to be driven by natural ventilation.

- The air distribution in the plenum enables the air to directly contact and therefore to have heat exchange with the thermal mass of ceiling slab and diffuse ceiling panel. The plenum configurations have an impact on the air distribution in the plenum and further impact the air distribution in the conditioned space. Further study should be conducted to find out the critical design parameters and optimize the system solution.

For further information, please refer to <u>Paper 1</u>: "Diffuse ceiling ventilation: a review."

CHAPTER 2: LITERATURE REVIEW OF DIFFUSE CEILING VENTILATION

CHAPTER 3. EXPERIMENTAL STUDY OF DIFFUSE CEILING VENTILATION

The studies of ventilation systems mainly use two approaches: experimental and numerical studies. Experimental studies are typically carried out in climate chambers with certain boundary conditions. There are also some monitoring studies that measure the system performance under real operating conditions. The present thesis includes two sets of full-scale experiments in a climate chamber. The first set of experiment focus on the performance of diffuse ceiling ventilation combined with a radiant ceiling system, which aims to evaluate the impact of diffuse ceiling ventilation on the energy performance of radiant ceiling and indoor thermal comfort. The second set of experiment investigates the stand-alone diffuse ceiling ventilation system, which focus on the comfort limit of the ventilation system and the impact of the opening area of diffuse ceiling supply on the system cooling capacity. The second set of experiments was performed by Martin H. Kristensen and Jakob S. Jensen, and the author conducted the interpretation and analysis of the results.

3.1. DIFFUSE CEILING VENTILATION WITH A RADIANT CEILING SYSTEM

3.1.1. INTRODUCTION OF THE INTEGRATED SYSTEM

One of the limitations of natural ventilation is that it strongly depends on the outdoor climate. An additional heating and/or cooling system is required when natural resources are insufficient to maintain an acceptable indoor environment, for example, in winter or extremely summer. Based on the heat transfer mechanism, the heating and/or cooling systems can be classified into two categories: air based (or convective) and radiant systems [41]. Different from the all air-based systems, which transfer heat mainly by convection, radiant systems can transfer heat partly by radiation with the rest of the room surfaces and partly by convection with the indoor air. Therefore, it could provide a more comfort environment and is able to make use of low-grade energy [42][43][44].

Thermally activated building system (TABS) is an innovative heating and/or cooling system, with the hydronic pipes embedded in the concrete building construction [45]. By taking advantage of high thermal inertia of concrete slabs, TABS can shave the peak load and transfer some of the heating or cooling load beyond the time of

occupancy. At the same time, the big surface allows significant heat exchange even with a slight temperature difference between the concrete slabs and the space. This feature enables the energy system to run efficiently and even makes it possible to use some low grade energy resources, for example, groundwater, heat pump and solar collectors[44][46] [47].

A schematic diagram of the integrated system is shown in Figure 3-1. In this system, the outdoor air is supplied into a ceiling plenum, which is the space between ceiling slabs and suspended ceiling. As the air distributing in the plenum, it is gradually warmed up or cooled down by the TABS. The conditioned air is then delivered into the room through the perforations and/or slots in the suspended ceiling panels. The harmony of these two techniques is the key issue of the integrated system. Normally, the TABS is required to operate with a large surface expose to the space. However, in this system, the diffuse ceiling covers the TABS and consequently affects the heat transfer between the TABS and the rest of the room [48].
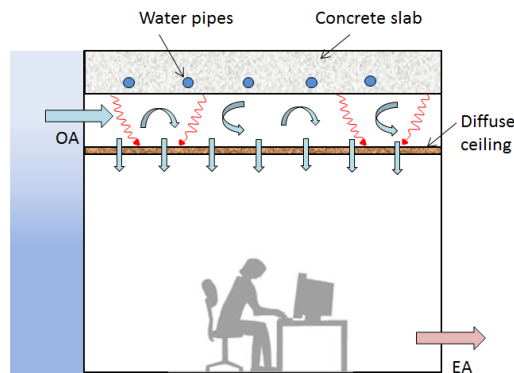
Figure 3-1: Schematic diagram of the system combining diffuse ceiling ventilation and TABS

The following sections describe the experimental study of the integrated system, based on Paper 2 [48]. The effect of diffuse ceiling ventilation on the TABS' heating and cooling capacity is investigated, at the same time, the thermal process within the plenum and its impact on the indoor comfort are also evaluated.

3.1.2. EXPERIMENTAL DESCRIPTION

3.1.2.1 Test facility

The experiments were conducted in an environmental chamber located in the laboratory of Aalborg University, Denmark (Figure 3-2 a). The environmental chamber consisted of two parts: a climate chamber simulating the outdoor environment and a test chamber simulating a two-floor office building, as illustrated

in Figure 3-2 (b). The test chamber included three subzones: the lower zone simulated a typical office with an inner dimension of 4.8 m × 3.3 m × 2.72 m; the upper zone represented the upper floor office and was used to study the TABS' thermal performance; a surrounding zone enclosed the lower and upper zone and eliminated the heat transfer from the outside [48] .

(a)
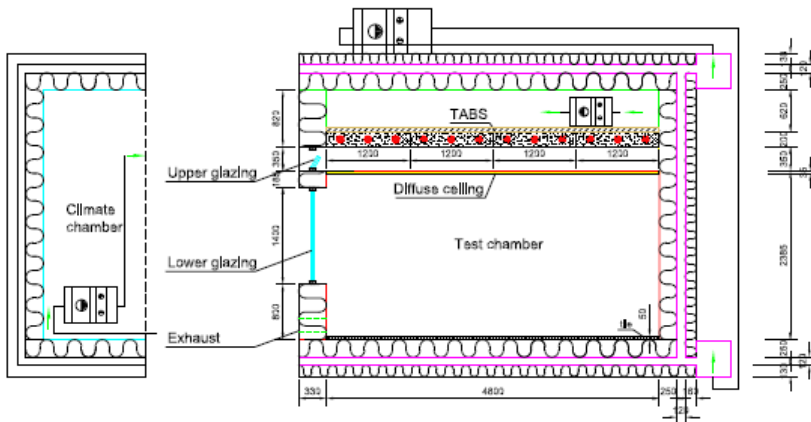
(b)

Figure 3-2: Environmental chamber (a) Photo (b) Vertical section [48]

The two chambers were separated by a façade with two glazing areas [48]. The lower glazing area, with three panels and overall dimensions of 2.4 m × 1.4 m, was shut down during the measurements; while the upper glazing area, with three panels and overall dimensions of 2.4 m × 0.35 m, was opened to function as plenum inlets. The plenum inlet kept a geometrical opening area of 0.0207 m² (0.01 m × 0.69 m × 3 panels) during the measurements. The exhaust was placed at the lower corner of the façade with 160 mm diameter. A fan connected to the exhaust opening and recirculated the exhaust air into the climate chamber. The recirculated air was re-

supplied into the plenum after treating by the AHU. The effective heat transfer coefficient of the facade was tested to be 0.61 W/m^2.K based on ISO 8990 [49].

The lower zone and upper zone were separated by the TABS. The TABS consisted of four hollow-core concrete slabs and each slab had a dimension of 3.56 m× 1.197 m × 0.2 m. The water carrying pipes were with a diameter of 20 cm and embedded 4 mm above the lower surface to ensure a quick thermal response. There was a layer of 50 mm insulation above the concrete slab to reduce the heat transfer to the upper floor. The water circuit of the TABS was connected with a chiller and an electric-heater, and operated with a controlled temperature and flow rate (Figure 3-9) [48].

3.1.2.2 Diffuse ceiling and its properties

The tested diffuse ceiling was made by wood-cement panels. These panels were air permeable and typically used for the acoustic purpose, as shown in Figure 3-3 (a) [50]. Each ceiling panel had a dimension of 35 mm × 600 mm ×1200 mm. The physical properties of wood-cement panel are present in Table 3-1.

Table 3-1: Properties of wood-cement panel

Density	Conductivity	Specific heat capacity	Porosity
kg/m^3	W/m.K	J/kg.K	%
359	0.085	932.31	65%

The ceiling panels were positioned 0.35 m below the ceiling slabs and separated the test chamber into a ceiling plenum and a conditioned space. The panels were installed by C-profile suspension system with a non-overlapping layout, as shown in Figure 3-3 (b) (c) [50]. Therefore, the air discharged through both ceiling panels and slot opening was expected.

(a)

(c)

(b)
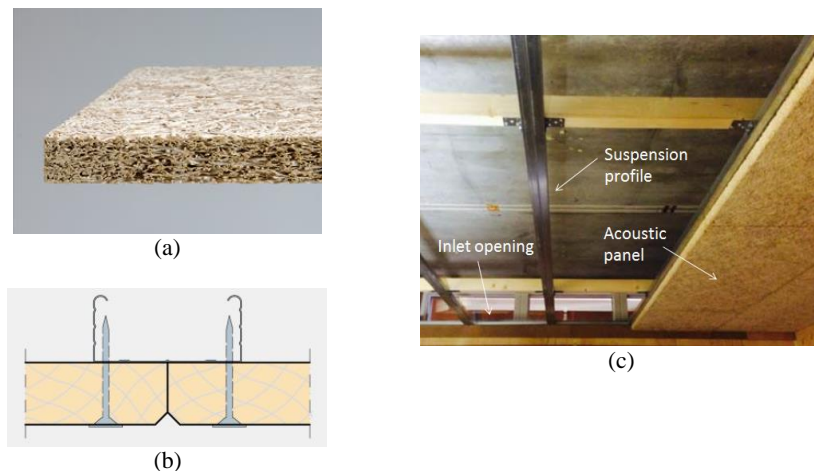
Figure 3-3: Description of the tested diffuse ceiling system (a) Wood-cement panel (b) Suspension system (c) Diffuse ceiling set-up [50]

3.1.2.3 Measurements

The measurements were performed under 12 cases with various boundary conditions (climate, heat loads, TABS operating mode), detailed information regarding test conditions can be seen in Table 3-2 [48]. The cases without diffuse ceiling were employed as references. It needs to be noticed that the TABS water supply temperature was lower than the dew-point temperature in some summer cases and resulted in condensation problem. Operating at such low temperature aimed to identify the application limits, but did not represent the practical situation [48].

The internal heat load conditions refer to Paper 2 [48]. " The test room was set up to represent a two-person office, as presented in Figure 3-4 (a). The layout included two desks with two computers (55W and 45 W), two monitors (16 W and 21.5 W) and two task lamps (54 W and 59 W). Two persons were simulated by thermal manikins (100 W each). To simulate the heat gain by solar radiation, an electric carpet (464 W) was placed on the floor close to the window (Figure 3-4 (b)). The total heat load in the test room without solar radiation was 450.5 W (28.4 W/m^2), while it with solar radiation was 914.5 W (57.73 W/m^2)."

Table 3-2: Test conditions [48]

Case	Air change rate	Supply air temperature	Heat load	TABS water supply temperature	TABS water flow rate	Diffuse ceiling
	h^{-1}	^{o}C	W	^{o}C	m^3/h	
1	2	-7.1	450.5	36.38	134.5	-
2	2	9.21	450.5	-	-	-
3	2	23.82	450.5	17.29	140	-
4	4	-6.87	914.5	38.91	208	-
5	4	8.92	914.5	-	-	-
6	4	23.89	914.5	10.95	273	-
7	2	-6.87	450.5	30.89	136	Y
8	2	9.46	450.5	-	-	Y
9	2	24.1	450.5	8.1	221	Y
10	4	-7.23	914.5	35.63	138	Y
11	4	9.41	914.5	-	-	Y
12	4	24.07	914.5	4.27	294	Y

(a) (b)

Figure 3-4: Heat sources in the test room (a) Two workplaces (b) Electric carpet [48]

Measurement sensors and locations are described below, refer to Paper 2 [48]:

- Temperature: In total, there were 115 K-type thermocouples used to monitor temperatures, with an accuracy of ± 0.15 K. The temperatures were logged by Helios data logger connected to an ice point reference.
  - Air temperature: The vertical temperature profiles in the test room were measured by three movable columns. In each column, there were seven thermocouples mounted in different heights and the heights were

distinguished between the cases with and without the diffuse ceiling, see Figure 3-5. To measure the temperature distribution in the horizontal direction, each column changed four positions during the measurements. In total twelve columns have been measured in the test room, as indicated in Figure 3-6. In the cases with the diffuse ceiling, nine thermocouples were evenly distributed in the plenum to measure the plenum air temperature, see Figure 3-7. Beside the air temperatures in the test room and plenum, the air temperatures in the other zones (climate chamber, upper zone and surrounding zone, laboratory) were also measured.

o Operative temperature: Based on the literature [51][52], a grey sensor of 3-5 cm diameter is the best option to measure the operative temperature. In this study, the operative temperature was measured by thermocouples positioned in the grey spheres with a diameter of 4 cm. The sensors were placed at the heights of 0.1 m, 0.7 m and 1.1 m and measured in four positions (A-2, B-2, C-2, and D-2). The average value was used as the operative temperature in the test room.

o Surface temperature: The surface temperatures were measured by thin thermocouples mounted with thermally conductive paste. Beside internal wall surface, the surface temperature of concrete slabs and diffuse ceiling panels were also measured (Figure 3-8, Figure 3-9).

o Water temperature: TABS water temperatures were measured at 5 points along the water pipes. For each slab, the water supply and return temperatures were measured in order to calculate their cooling or heating capacity (Figure 3-9).

- Velocity: Air velocities were measured by hot sphere anemometers with the accuracy of ±0.01 m/s +5% of reading. In total 19 anemometers were used to measured air velocity in the occupied zone and plenum, see Figure 3-5 and Figure 3-7. Velocities were logged by Dantec multichannel flow analyzer type 54N10.

- Flow rate: The air flow of the ventilation system was measured by an orifice plate connected to the exhaust fan. The pressure drop across the orifice plate was measured by a micromanometer. The accuracy of the air flow rate was ± 5%.
  The water flow rate through the TABS system was recorded by Brunata energy meter type HGQ1 with an accuracy of $\pm (2 + 0.02q_p/q)$. Both the flow rate and supply and return water temperatures were logged by specific LabView interface.

- Pressure difference: The pressure drop of the diffuse ceiling was measured by FCO510 micromanometer (accuracy ± 0.25%) by placing sensors in both the plenum and lower zone, see Figure 3-7.

- Humidity: The indoor humidity was measured by HIH-4602 humidity sensor located in the middle of test room, with an accuracy ± 7.5%.

In order to reach high accuracy, all the sensors were calibrated before performing the real measurements. All the measurements were conducted under steady-state. The indoor conditions took 2-4 days to reach stable depending on whether the diffuse ceiling panels was installed or not. Data were recorded every 10 s, for at least 6 hours after stabilization.
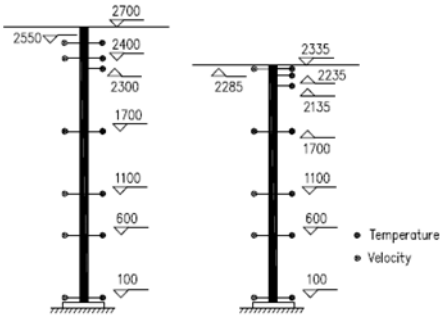
Figure 3-5: Temperature and velocity sensors in the columns [48]
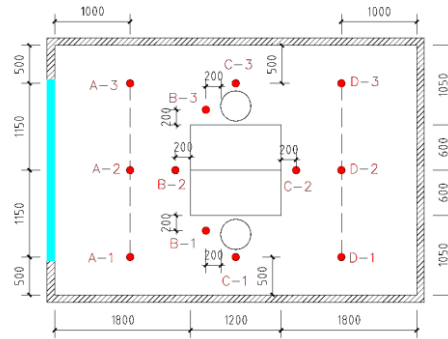
Figure 3-6: Plan view of the test room and location of the columns [48]
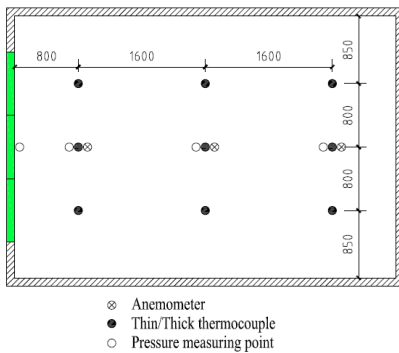
Figure 3-7: Measurement sensor locations in the plenum [48]
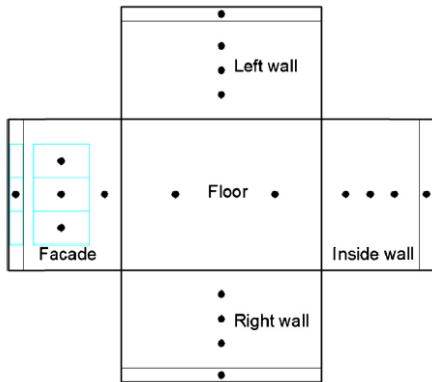
Figure 3-8: Surface temperature of internal wall [53]
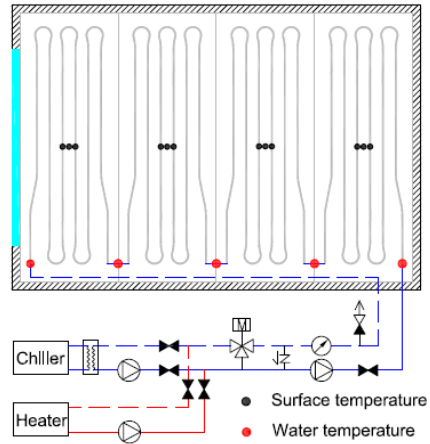
Figure 3-9: TABS water circuit and temperature sensor locations [53]

3.1.3. COMPARISON OF THERMAL COMFORT

The vertical temperature profiles are presented in Figure 3-10, where the air temperature at each height was the mean value at twelve locations [48]. In the cases without diffuse ceiling, large temperature gradients were observed in the winter conditions, for example, Case 1 and Case 4. The large temperature gradients were because of the insufficient mixing between room air and supply air. The cool supply air quickly dropped to the floor by attaching the façade, while the warm room air stagnated near the ceiling. The temperature stratification restricted the heat exchange between the heated ceiling and the space, which is a common reason that the heated ceiling is less efficient than cooled one [54]. On the contrary, diffuse ceiling ventilation eliminated the temperature gradients. The cool supply air was distributed in the plenum and preheated by the heated ceiling. Therefore, the conditioned air was delivered to the room with a moderate temperature and very low velocity. Moreover, the convective flow generated by the heat sources improved the mixing level, making the airflow pattern in the room was comparable to mixing ventilation [48].

Although diffuse ceiling ventilation presented a remarkable advantage on reducing the temperature gradients, a risk of overheating was observed in summer or even transition seasons. The room with diffuse ceiling were approximately 2-3 ºC warmer than those without diffuse ceiling. As a matter of fact, diffuse ceiling acted as a layer of insulation between the TABS and the room and restrained the heat exchange between the two zones [48]. Detailed analysis on the energy performance will be described in the following section.

(a)   (b)
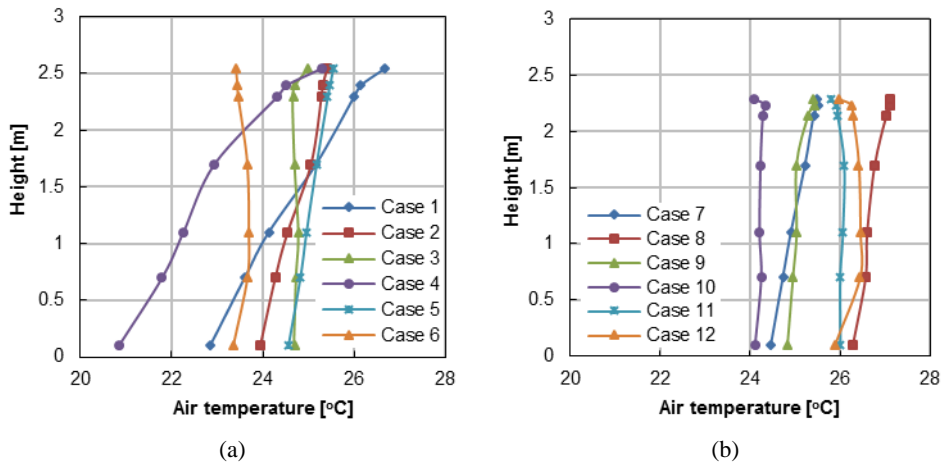
Figure 3-10: Vertical air temperature gradients (a) Cases without diffuse ceiling (b) Cases with diffuse ceiling [48]

Draught is one of the major concerns in the room with ventilation systems. The draught rate was evaluated at 0.1 m height at four critical locations (locations refer to Figure 3-6), as illustrated in Figure 3-11. First of all, diffuse ceiling ventilation significantly reduced draught in the occupied zone, especially in winter. The maximum draught rates decreased from 24% to 9% with the help of the diffuse ceiling. The ventilation system itself did not generate draught because of the low impulse flow through diffuse ceiling supply. In addition, the preheating effect of plenum further reduced the draught risk in the occupied zone [48].
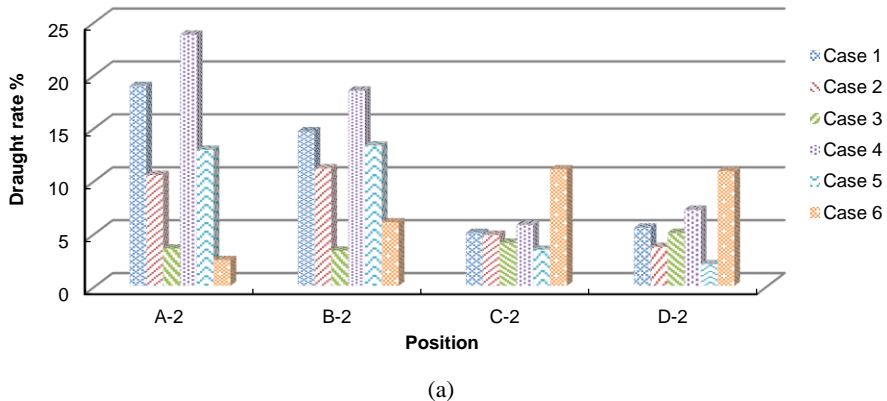
(a)
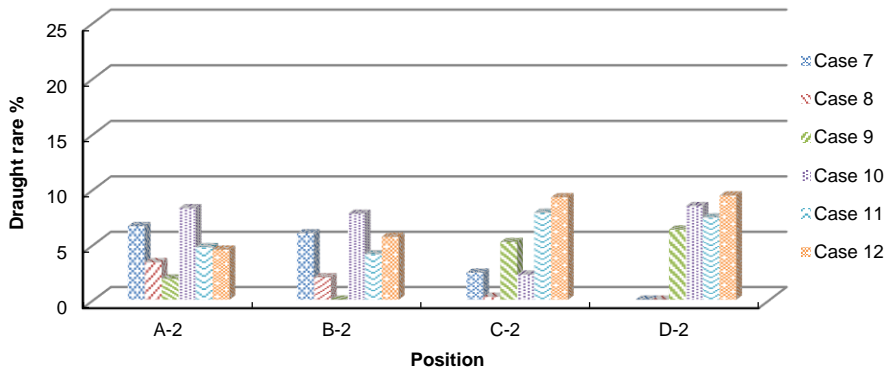
(b)

Figure 3-11: Draught rate at ankle level (a) Cases without diffuse ceiling (b) Cases with diffuse ceiling [48]

By comparing the draught at four critical locations, it can be observed that the highest draught rate moved A-2 to D-2 while increasing the supply air temperature. The tendency was significant in the cases without diffuse ceiling but also showed in the cases with diffuse ceiling. This can be explained by that the jet flow in the plenum is strongly depended on the supply air temperature, where the warm air can travel deeper while the cold air will drop immediately. This results further proved that diffuse ceiling did not provide a uniform air distribution through the entire ceiling area, which was determined by the supply air temperature and TABS operating modes [48].

People may feel discomfort due to the temperature difference between the room surfaces. It is essential to evaluate the asymmetry when TABS operates as a heated or cooled ceiling. For the cases without the diffuse ceiling, occupants directly exposed to the TABS surface. Discomfort is observed when TABS was activated as a heated ceiling. The asymmetries reached 4.5 °C and 5.9 °C in Case 1 and Case 4, which was close or even above the limit of 5 °C by ISO 7730 [23]. However, the discomfort was eliminated by using the diffuse ceiling. Instead of exposure to the conditioned space directly, the TABS was covered by ceiling panels and the radiation effect was weakened considerably. No discomfort was observed when TABS operated as a cooled ceiling, regardless with or without the diffuse ceiling, which is because people are less sensitive to the cooled ceiling than the warm one [48].
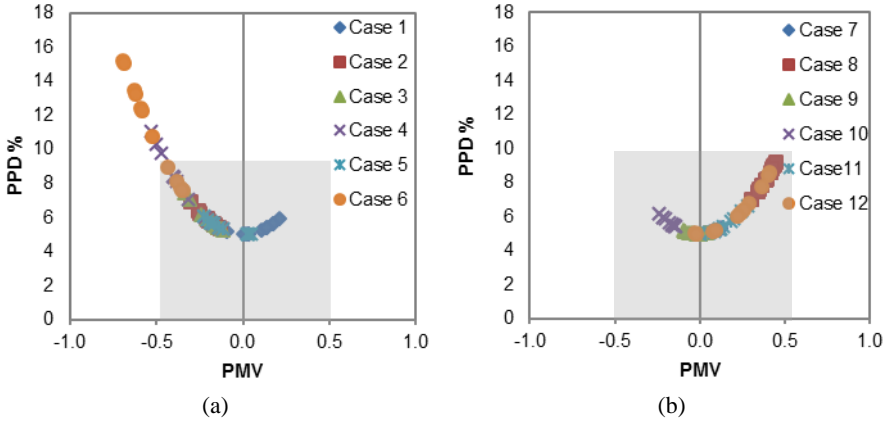
Figure 3-12: PMV and PPD (a) Cases without diffuse ceiling (b) Cases with diffuse ceiling
[48]

The PMV and PPD values of a seated person were calculated in twelve positions, as shown in Figure 3-12 [48]. The PMV varied between −0.69 to 0.21 in the cases without the diffuse ceiling, exceeding the limit of ±0.5 for Category B [23]. Occupants felt slightly cool in Case 4 and Case 6, and the percentages of dissatisfied (PPD) reached 11% and 15%, respectively. In the cases with the diffuse ceiling, the PMV was within the range of −0.24 to 0.45. A neutral indoor environment was created and less than 10% of people felt dissatisfied. Detailed discussions regarding thermal comfort refer to Paper 2 [48].

3.1.4. COMPARISON OF ENERGY PERFORMANCE

As mentioned above, the existence of diffuse ceiling changes the heat transfer mechanism between the TABS and the rest of the room, which consequently influences the energy performance of TABS. The energy efficiency of TABS under steady-state was evaluated by the heat transfer coefficient (h-value), based on the operative temperature in the test room and the average surface temperature of the TABS, as expressed by Equation 6 and 7 [48]:

$$Q_{TABS,down} = Q_{TABS} - Q_{TABS,up}$$

$$= C_{p,w} \cdot M_w \cdot (t_{w,su} - t_{w,re}) - h_{ins} \cdot A \cdot (t_{s,up} - t_{a,up}) \quad \text{Equation 6}$$

$$h_{TABS} = \frac{Q_{TABS,down}}{A \cdot (T_{op} - T_{s,avg})} \quad \text{Equation 7}$$

Using the equations above, the h-value of TABS under both the conditions with and without diffuse ceiling were calculated and compared, as shown in Figure 3-13 [48].

Without diffuse ceiling, the h-values of TABS was close to the design values (6 W/m^2·K for ceiling heating and 11 W/m^2·K for ceiling cooling) [55][56]. However, the h-values changed significantly after coupling with diffuse ceiling, approximately 13 W/m^2·K for heating and 2.5 W/m^2·K for cooling. Diffuse ceiling presented very opposite effects on the energy efficiency of TABS under heating and cooling modes. The heat exchange was promoted under heating mode. The enhancement was due to that the distribution of cool supply air in the plenum provided a larger air-surface temperature difference and relatively higher air velocity near the TABS surface. Therefore, the increase of convective heat transfer offset the loss of radiative heat transfer. Oppositely, the air-surface temperature difference was decreased under cooling mode. Both convective and radiative heat exchange were weakened after installing diffuse ceiling [48]. More information regarding energy performance of TABS refers to Paper 2 [48].
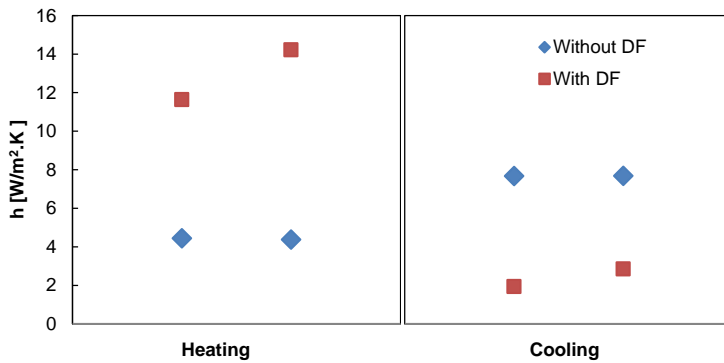
Figure 3-13: Heat transfer coefficients of TABS under heating and cooling modes [48]

3.1.5. THE EFFECT OF PLENUM AND DIFFUSE CEILING

Using a plenum to distribute air is one of the key features of diffuse ceiling ventilation. There are complex thermal processes within the plenum, where the heat exchanges between TABS, diffuse ceiling panels and plenum air. The thermal processes have significant effects on the effectiveness of TABS as a cooling and/or heating system and the effectiveness of diffuse ceiling ventilation as an air distribution system [48].

The air temperature distributions at the mid-height of plenum are presented in Figure 3-14. *"In winter, the cool supply air was gradually warmed up by the TABS surface and ceiling panels as it travelled deeper in the plenum. In contrast, the warm supply air was slowly cooled down in summer, when TABS operated in the cooling mode. In transient season, although the TABS was not activated, the supply air was still warmed up by the heat conducted from the room side through the diffuse ceiling panel*

[48]. *"From the design consideration, it is desirable to limit the amount of temperature variation in order to provide a uniform air distribution through diffuse ceiling supply. The parameters influenced the plenum air distribution will be analyzed by the numerical model and presented in Section 4.2.*

Figure 3-14 indicates that there were remarkable temperature differences between diffuse ceiling lower and upper surfaces even up to 10 ºC. *"The temperatures of the lower surface were close to the room air, and the peak temperature located in the middle of the room as the surface was warmed up by the thermal plume from heat sources. On the contrary, the upper surface temperature was close to the plenum air temperature* [48]*"*. However, different from the study with Al ceiling panels performed by Hviid et al. [28], no clear radiate cooling potential was observed in this study. The different results regarding radiant cooling potential are due to the properties of diffuse ceiling panel, where the wood-cement panel used in this study has a low conductivity of 0.085 W/m.K, while the conductivity of Al is up to 205 W/m.K.

(a)

(b)

(c)
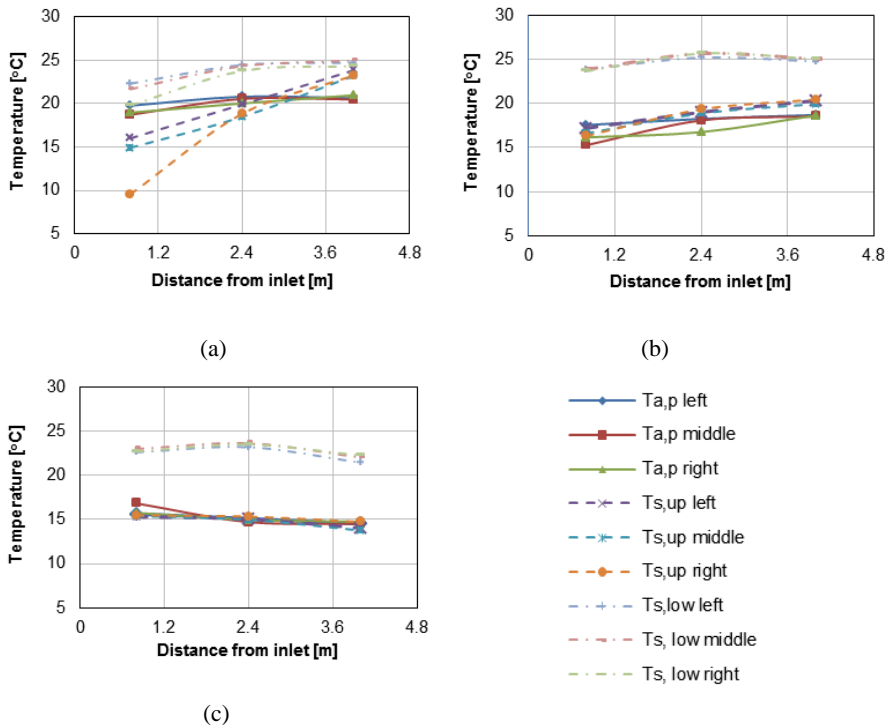
Figure 3-14: Plenum air and diffuse ceiling surface temperature distributions (a) Case 7 (b) Case 8 (c) Case 9 [48]

3.2. DIFFUSE CEILING VENTILATION WITH DIFFERENT OPENING AREA

The second set of experiments aims to investigate a stand-alone diffuse ceiling ventilation system [50]. Compared with momentum-driven ventilation systems, the opening area of diffuse ceiling supply is more variable. The supply can either take up the entire ceiling or part of the ceiling. Nevertheless, the impact of opening area on the system performances has not been analyzed in detail. A design chart method was implemented to make a direct comparison of three diffuse ceiling configurations and also intend to explore the comfort limit of each configuration, regarding ventilation rate and supply air temperature. The air path of diffuse ceiling supply and the factors influencing the air path are also discussed here.

3.2.1. EXPERIMENTAL DESCRIPTION

The experiments were conducted in the same test facility as in the first set of experiments. This study focused on the stand-alone diffuse ceiling ventilation, so the TABS was not activated during the entire measurements. The upper glazing served as the plenum inlet was fully opened with a geometrical opening area of 0.0675 m^2. The exhaust was located 80 mm below the ceiling on the back wall, see Figure 3-15.

(a)   (b)

Figure 3-15: The test room with a classroom layout (a) Front side (b) Back side [50]

(a)   (b)

(c)
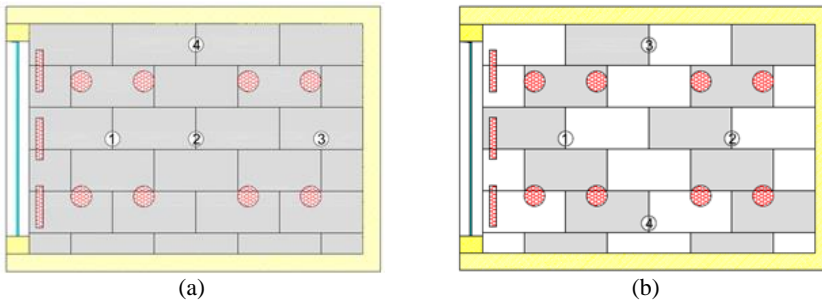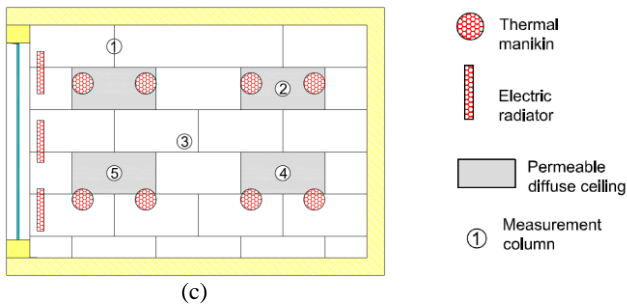
Figure 3-16: Diffuse ceiling layouts and placement of measured columns (grey panels are air permeable, and white ones are covered by vapor barrier) (a) 100% DF (b) 50% DF (c) 18% DF [50]

Table 3-3: Test conditions [50]

Case	DF	$\Delta T = T_{ex} - T_{in}$	ACR
	%	°C	h^{-1}
1 - 6		10	12 - 17
7 - 15		15	4 - 12
16 - 22	100	20	4 - 12
23 - 33		25	4 - 12
34 - 36		30	7 - 8
37 - 39		10	11 - 12
40 - 42		15	9 - 10
43 - 47	18	20	8 - 11
48 - 51		25	9 - 11
52 -55		30	8 - 11
56 - 61		30	6 -11
62 - 63		25	6 - 7
64 - 65	50	20	9 - 11
66 - 67		15	10 - 11
68 - 70		10	9 - 14

Note: ΔT is the temperature difference between exhaust and supply air

The test room was set up to represent a classroom layout, as shown in Figure 3-15. *"Eight thermal manikins with heat load of 80 W each were used to simulate eight pupils with the sedentary activity of 1.2 Met. There were also three electric radiators placed just below the windows to maintain a desired indoor temperature under*

different operating conditions. The heat load of radiators varied in different cases and was recorded by a power meter [50].*"*

The parameter focused in this study was the diffuse ceiling opening area. Measurements were conducted under three area ratios: 100%, 50%, and 18%, as illustrated in Figure 3-16. The opening area was reduced by covering the suspended ceiling panels with vapor barrier from the room side. *"Under each diffuse ceiling configuration, several tests were conducted with different combinations of air flow rate and supply air temperature. Supply air temperatures varied from -5 ºC to 15 ºC to represent the system operating in different climates. To find out the comfort limit of the system, the air flow rate covers a wide range and reaches a very high value in the tests* [50].*"* Table 3-3 described the detailed test conditions.

In the second set of measurements, the temperature profile and draught rate were measured by columns placed in the critical area within the occupied zone, see Figure 3-16. The positions of columns were determined by smoke test. The pressure difference between the plenum and the room was measured to analyze the air path of the diffuse ceiling supply [50]. Detailed descriptions regarding measurement sensors and locations refer to Section 3.1.2.3.

3.2.2. DESIGN CHART

In order to maintain a comfortable environment, it is desirable to explore the limit of a ventilation system in the design phase. Nielsen [57][58] developed a design chart that enables a direct comparison between different ventilation systems and to select the optimal solution for a given condition. The design chart is presented as a q_0 - ΔT_0 chart, which identifies an area that satisfies both indoor air quality and thermal comfort requirements.

The limits presented in the design chart refer to the possible ventilation rate and the temperature difference between supply and return. The limits of diffuse ceiling ventilation can be obtained by experiments and similarity principle [58]. In the room with the fully developed flow, the non-dimensional velocity can be given as function of Archimedes number. This phenomenon is called the similarity principle and expressed by Eq. (8-9) [58].

$u_{max}/u_0 = func(Ar)$ Equation 8

$Ar = \frac{\beta \cdot g \cdot l \cdot \Delta T_0}{u_0^2}$ Equation 9

Figure 3-17 shows the design chart of diffuse ceiling ventilation with three opening areas. The dashed line indicates that the minimum airflow rate of 7 l/s per person is required to fulfill for the indoor air quality purpose [22]. The q_0 - ΔT_0 curve represents the maximum cooling capacity of the system without generating discomfort. The draught risk is limited by the maximum velocity in the occupied zone of 0.2 m/s. As mentioned in Section 3.1.3, diffuse ceiling ventilation produces very low temperature gradient. Therefore, the comfort limit of temperature gradient less than 2.5 K/m is not considered here [50].
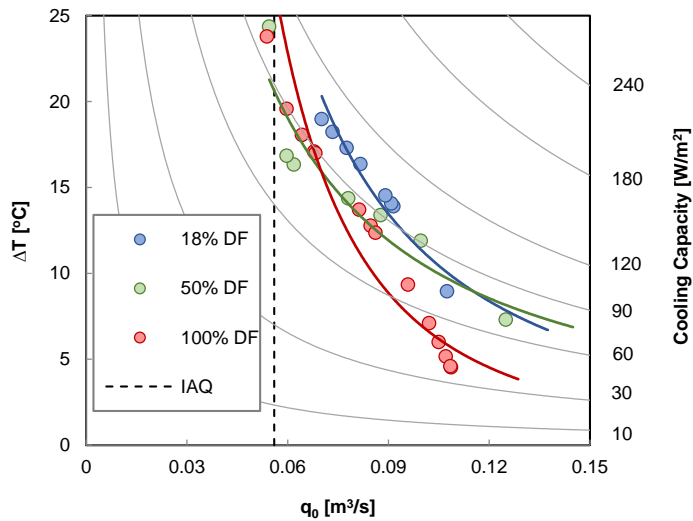
Figure 3-17: Design chart for diffuse ceiling ventilation with different opening area, u_{max}=0.2 m/s [50]

The design chart indicates that the diffuse ceiling with 18% opening area could remove the highest heat load without thermal discomfort. The high cooling capacity of 18% DF case might be attributed to that heat sources were placed just below the permeable ceiling panels. Therefore, the cool supply air could directly deal with the thermal plume generated by the heat sources. In addition, 18% DF could produce relatively higher momentum flow than the other two openings, which to some extent had impact on the airflow pattern in the room [50]. However, the cooling capacity of the system reduced while increasing the airflow rate. These results indicate the draught rate was not completely independent of the ventilation rate or the supply air temperature, where the airflow in the room was not entirely buoyancy controlled and to some extent still influenced by the supply flow.

Figure 3-18 presents the design chart for different air distribution systems. In order to make it more comparable, the maximum velocity in the occupied zone was limited to

0.15 m/s for air distribution systems. Compared with the other systems, the comfort requirements such as draught risk and vertical temperature gradient did not have strong limitation on the ventilation rate and temperature difference between the supply and return air in the diffuse ceiling ventilation. The system could provide a draught free environment even with a high flow rate above 10 h^{-1}, because of the low velocity flow from the large ceiling surface. The tolerance of the high air temperature difference was because the cold supply air did not enter the occupied zone directly and a mixing has been reached with the room air by the buoyancy flow. Therefore, the diffuse ceiling ventilation had a higher cooling capacity than the other ventilation systems. The difference between the diffuse ceiling in this study and reference one measured by Nielsen. et al. [9][31] can be attributed to the room geometry, layout, heat sources, which had a notable impact on the system capacity. On the other hand, it was also because of the different diffuse ceiling types. The ceiling panels used in the reference case were mineral wool panels, which had remarkable higher pressure resistance to the flow than the wood-cement panels. The high pressure drop restricted the downward supply flow and decreased the draught in the occupied zone, especial when the cold air was supplied directly.
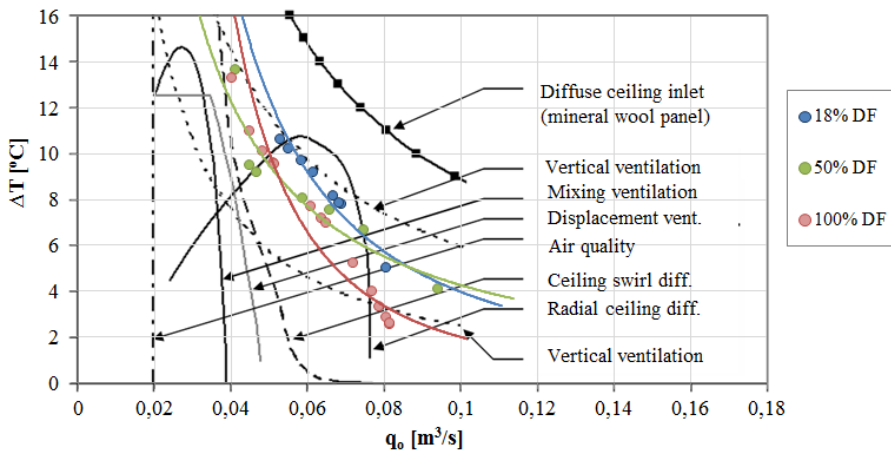
Figure 3-18: Design chart for different air distribution systems, u$_{max}$=0.15 m/s [31]

3.2.3. AIR PATH OF DIFFUSE CEILING VENTILATION

By comparing the pressure drop of a single ceiling panel with that of the mounted ceiling, we can estimate the air path of diffuse ceiling supply. As illustrated in Figure 3-19, air was supplied into the room through both perforated ceiling panels (panel flow) and slots between the panels (crack flow), where the proportion of these two types of flow was related to the diffuse ceiling opening area and ventilation rate. The panel flow was the primary pathway in the 100% DF case. However, while decreasing

the opening area, crack flow became more and more significant. On the other hand, air was mainly delivered through the ceiling panels at low flow rate. The proportion of crack flow increased while increasing the air flow rate. The crack flow was in part caused by the suspension profile, where the non-overlapping layout leaded to the air jet between panels. Meanwhile, the leakage through the vapour barrier was unavoidable [50].
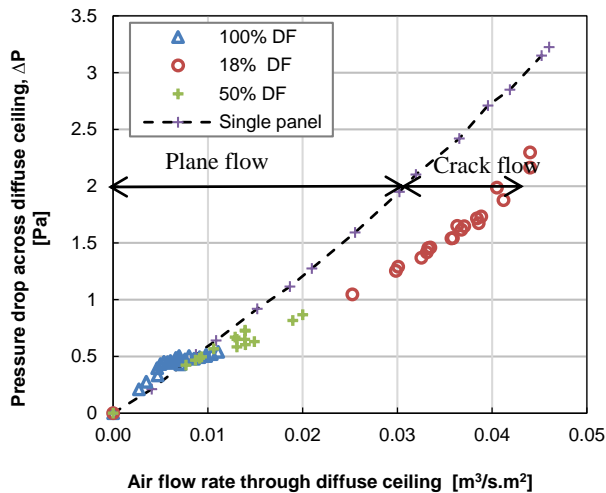
Figure 3-19: Pressure drop for the different diffuse ceiling configurations [50]

3.3. CONCLUSION

Two sets of experiments were conducted in a full-scale test facility with different focuses. The first set investigated the potential of diffuse ceiling ventilation combining with a radiant heating or cooling system, and the second set highlighted the impact of diffuse ceiling opening area on the indoor comfort and cooling capacity of a stand-alone ventilation system.

The results from the first set of experiments revealed that diffuse ceiling ventilation significantly improves indoor thermal comfort. It effectively eliminated local discomfort caused by draught, vertical temperature gradient and radiant temperature asymmetry, especially in winter. From the perspective of energy efficiency, the diffuse ceiling ventilation had opposite effect on the heating and cooling capacity of TABS. After installing the diffuse ceiling, the heat transfer coefficient of TABS increased from 5 W/m^2 to 13 W/m^2 in the heating mode, but the value reduced from 8 W/m^2 to 2.5 W/m^2 in the cooling mode. The integrated system presented a promising potential as a heating system than stand-alone heated ceiling. However, the reduction in the cooling capacity limited the application of the integrated system in the space

with high heat load. Finally, the variations of the plenum air temperature and the diffuse ceiling surface temperature indicated that the air was not perfectly mixed in the plenum and was not evenly distributed through the diffuse ceiling. Instead, they were as function of the distance from the plenum inlet. Although the non-uniform distribution did not result in discomfort in the current study, it is essential to find out the impact factors and explore the optimal design solution in the further study.

For the stand-alone ventilation system, diffuse ceiling with 18% opening area was able to remove the highest heat load without generating draught risk. Nevertheless, it is too early to draw the conclusion that smaller opening area will lead to a higher cooling capacity. The relative location of heat sources and the diffuse ceiling opening plays an important role. It is essential to explore the interaction between the heat source location and the diffuse ceiling opening location in the further study. Secondly, when the opening area reduces to a certain level, the airflow pattern will turn from the buoyancy controlled to the momentum controlled, and draught will become a primary concern in that situation. It is necessary to investigate the limit of the opening area ratio of diffuse ceiling supply. Comparing diffuse ceiling ventilation with the other air distribution systems through the design chart, it can be observed that the comfort requirements did not present a strong limitation on the ventilation rate, or the temperature difference between the supply and return air. Therefore, the diffuse ceiling ventilation can handle higher heat loads than the other systems. Finally, the pathway of diffuse ceiling supply can be estimated by comparing the pressure drop of single and mounted panels. Panel flow was the primary pathway at low ventilation rate and with the large opening area. On the contrary, the crack flow became important with an increase of flow rate and a decrease of opening area.

For further information, please refer to Paper 2: "Experimental study of diffuse ceiling ventilation coupled with a thermally activated building construction in an office room."

& Paper 4: "Parametrical analysis on the diffuse ceiling ventilation by experimental and numerical studies."

CHAPTER 4. NUMERICAL STUDY OF DIFFUSE CEILING VENTILATION

Compared with experimental studies, numerical studies are reputed for their low cost and time efficiency, since the boundary conditions can be easily adjusted to investigate different scenarios. The present investigation aims to use computational fluid dynamics (CFD) to solve the airflow and temperature distributions in the plenum and the occupied zone, where the commercial CFD program Fluent is used [59]. It is important to have a suitable model to specify the airflow through the diffuse ceiling supply. However, the ceiling panel employed in this study has a porous property due to the particular structure of the wood-cement material (Figure 3-3). It is difficult to model the air distribution through the panels directly using CFD. Therefore, two simplified models aimed to describe the main characteristic of the diffuse ceiling ventilation are presented and compared: one is a simplified geometrical model, and the other is a porous media model. The strengths and limitations of each model are described in this chapter.

According to experimental study [48][50], the airflow pattern and thermal process within the plenum have remarkable impacts on the effectiveness of diffuse ceiling ventilation. There are many plenum configurations encountered in practice, such as plenum height, plenum depth, the location and shape of plenum inlet, etc. It is essential to explore the impact of these design parameters on the system performance. On the other hand, the buoyancy flow from the heat sources dominants the airflow pattern in the room with diffuse ceiling ventilation. The location of heat sources is an essential parameter to consider. Furthermore, the experimental study by Vilsbøll [29] revealed that there is a relation between the room height and the draught rate in the occupied zone. Therefore, another objective of the numerical study is to use the validated model to perform a series of sensitivity analysis on the design parameters.

4.1. DEVELOPMENT OF NUMERICAL MODEL

4.1.1. SIMPLIFIED GEOMETRICAL MODEL

A simplified geometrical model is a common approach to simulate air diffusers, which is to replace the complex diffuser by one or more simple rectangular slots [60][61][62]. This method is proved to be able to give accurate predictions in regions remote from the initial jet development [60].

The effective opening area of the diffuse ceiling supply was difficult to measure directly. Because it is not only related to the porosity of the panels, but also depends on the shapes of the small holes (pores) in the media and their level of connectedness [63]. Alternatively, the effective opening area of air diffuser was estimated based on the results from pressure drop measurement (detail refer to Figure 2, Paper 3 [64]), and expressed by equation below:

$$C_d A = \frac{\dot{m}}{\sqrt{2\rho\Delta P}} \qquad \text{Equation 10}$$

As a result, three slot openings with an effective area of 0.032 m² (3.2 m × 0.01 m) each were built to model the air pathway of diffuse ceiling supply [64], as illustrated in Figure 4-1 (a).

(a)   (b)
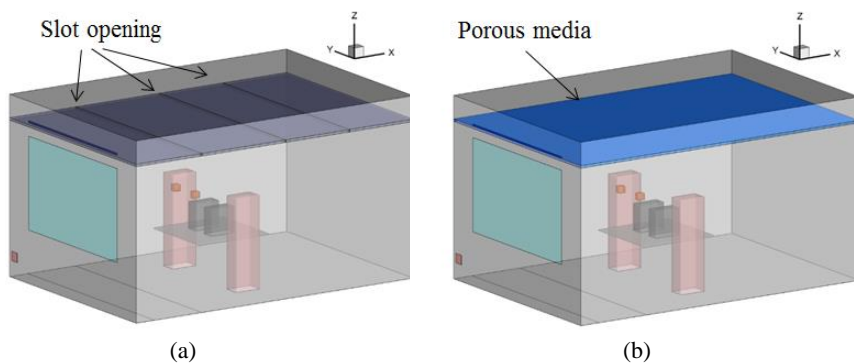
Figure 4-1: Numerical models of the office room with diffuse ceiling ventilation (a) Simplified geometry model (b) Porous media model

Based on the previous studies [18][65], the diffuse ceiling may have a large temperature difference from the rest of the room surfaces depending on the supply air temperature and the conductivity of ceiling panel. It is essential to consider the radiative heat exchange in the room with diffuse ceiling ventilation. On the other hand, the thermal processes within the plenum includes both convective heat transfer between the plenum air and the thermal mass and radiative heat exchange between ceiling slab and diffuse ceiling panel, especially when the TABS is activated [64]. A surface-to-surface radiation model was applied, in which the radiative heat transfer between surfaces were calculated by use of the Stefan-Boltzmann law and the view factors.

In the simplified geometrical model, the wall boundaries were defined by the U-value and the measured air temperatures in the climate chamber and surrounding zone. The ceiling slabs were defined by a uniform surface temperature, where the thermal decay

alone the water-pipes was ignored. The total heat released by the heat sources were specified as surface heat fluxes [64][66].

4.1.2. POROUS MEDIA MODEL

In the second model, the diffuse ceiling panel was defined by a porous media model [50][64][67], where the flow experiences a resistance when it passes through, as seen in Figure 4-1 (b). The porous media model includes an additional momentum source in the governing equation, based on Darcy-Forchheimer Law [68]. When the flow goes with very low velocity, the viscous resistance is dominant. For high-velocity flow, the inertial effect becomes significant. The momentum source term is expressed by:

$$S_M = - \left(\frac{\mu}{\alpha} v + C_2 \frac{1}{2} \rho |v| v \right) \qquad \text{Equation 11}$$

The viscous resistance coefficient $1/\alpha$ and inertial resistance coefficient C_2 were determined by the properties of the diffuse ceiling panel, like porosity and equivalent perforation diameter. The resistance coefficients were also calculated by the pressure drop results, where $1/\alpha$ is 1.14×108 m^{-2} and C_2 is 33055 m^{-1} [64].

The energy equation for the porous media model was modified on the conduction flux only, where an effective thermal conductivity k_{eff} was introduced to consider the effect of both the fluid and solid conductivities [67].

$$\nabla \cdot \left(\bar{v} (\rho_f E_f + P) \right) = \nabla \cdot \left[k_{eff} \nabla T + (\bar{\tau} \cdot \bar{v}) \right] + S_E \qquad \text{Equation 12}$$

$$k_{eff} = \gamma k_f + (1 - \gamma) k_s \qquad \text{Equation 13}$$

Unfortunately, the porous media model treats the diffuse ceiling panel as flow zone and thus could not calculate the radiative heat exchange directly. To overcome this limitation, the wall surface temperatures derived from the simplified geometrical model were used as boundary inputs in the porous media model for the detailed simulation on the air velocity and air temperature distribution. Instead of directly specifying the diffuse ceiling's surface temperature, the radiative heat flux to the diffuse ceiling panels was applied as an energy source S_E [67].

The internal heat sources exchange heat with the space through both convection and radiation. *"The radiative exchange has been already considered when calculates the wall surface temperatures. A feasible approach is to estimate the radiative heat flow and to specify the convective heat flow boundary condition for the heat sources [69]. The convective fraction for different heat sources were specified in ASHRAE*

Handbook [70], for occupants with moderately active office work was about 50%, while the values of computers and desk lamps were 90% and 50%, respectively [67]."

4.1.3. TURBULENCE MODEL AND NUMERICAL METHOD

The airflow through the diffuse ceiling can be regarded as laminar flow due to the low air velocity. On the other hand, the airflow in the room is turbulent because of strong convective flow generated by the various heat sources and room enclosures. The Re-normalized group (RNG) *k-ε* model is suitable for this situation, which considers the low-Reynolds-number effects compared with standard k-ε model [68]. This turbulence model was recommended by Chen [71] to simulate the turbulent flow in the indoor environment, and the accuracy for the porous media zone was proved by Yang et al. [72]. In addition, the buoyancy effect was taken into account by the Boussinesq hypothesis, where treated density as a constant value in all solved equations, except for the buoyancy term in the momentum equation [68].

The geometrical model was a simplified version of the test chamber. To simplify the geometrical model and create high-quality meshes, room geometry and the other objects were built as rectangular. Structured meshes were generated in the entire domains, and the finest meshes were built in the critical areas, for instance, diffuse ceiling, inlet, outlet, walls, and internal heat sources. Grid independence check was conducted for the numerical models, and the detail description can refer to Paper 5 [67]. The SIMPLE numerical algorithm was employed. The convergence were reached when the absolute residuals are lower than 10^{-3} except that for energy less than 10^{-6}.

All the simulations were conducted under steady-state conditions, where the transient flow and the dynamic effect of thermal mass (diffuse ceiling panels and ceiling slabs) were not considered in the current study.

4.1.4. MODEL VALIDATION

To evaluate the ability to predict the airflow pattern and thermal performance of diffuse ceiling ventilation, the numerical models need to be validated by the experimental data. Case 7, 8 and 9 were chosen as examples to validate the models under different operating conditions (coupled or uncoupled with TABS), and detailed boundary conditions can be seen in Table 3-2. To keep the brief of the thesis, only the velocity and air distribution of Case 8 are illustrated here. More information regarding the other two cases can refer to Paper 5 [67].

(a)   (b)

Velocity Magnitude: 0.00 0.03 0.07 0.10 0.13 0.17 0.20 0.23 0.26 0.30
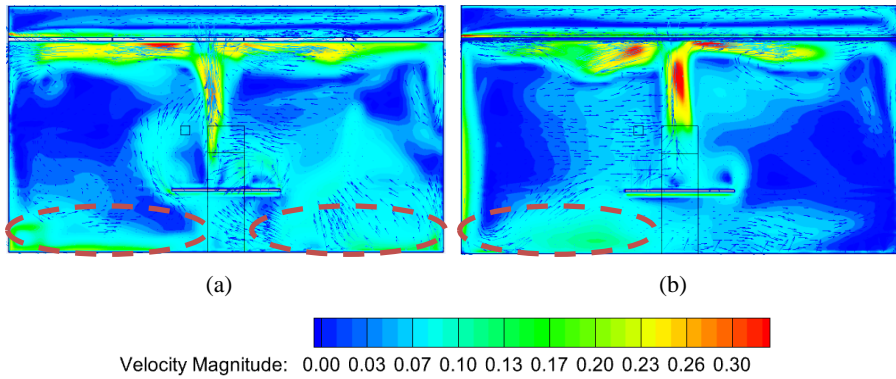
Figure 4-2: Velocity distribution across the central plane of the room, Case 8 (a) Simplified geometrical method (b) Porous media method [64]

T_{in}= -6.87 ºC

(a)

T_{in}= 9.46 ºC

(b)

T_{in}= 24.1ºC

(c)

Velocity Magnitude

0.0030
0.0027
0.0023
0.0020
0.0017
0.0013
0.0010
0.0007
0.0003
0.0000
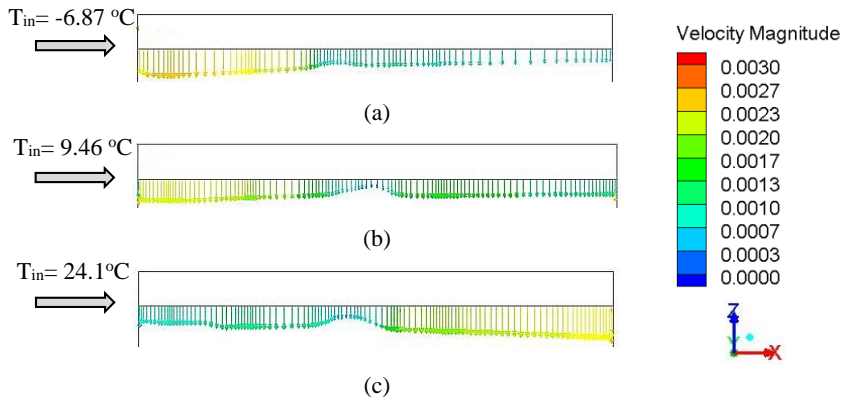
Figure 4-3: Velocity vector of airflow through the diffuse ceiling by porous media model (a) Case 7 (b) Case 8 (c) Case 9

The airflow patterns predicted by the two numerical models are shown in Figure 4-2. The uprising thermal plumes from the heat sources and the downward flow attached the wall worked together and generated air recirculation in the room [64]. The recirculated airflow entered into the occupied zone along the floor and caused the high velocity at the ankle level. The simulated results proved that the buoyancy force is the dominant driving force in the room with diffuse ceiling ventilation. However, the simplified geometrical model mis-predicted that two symmetrical vortexes occur in both sides of the room, while, the porous media model gave a correct prediction on one strong vortex in the front side of the room. The deviation was due to the different air passage of diffuse ceiling supply defined by these two models. The simplified geometrical model restricted the air flow to be supplied through the slots, where the location and shape of slots strongly influenced the air distribution. Porous media model showed a clear advantage in representing the airflow characteristic of the

diffuse ceiling supply. As present in Figure 4-3, the air was distributed through the entire ceiling area, and the air delivery was a function of distance from the plenum inlet depending on the inlet air temperature. The high density of cold air leaded to a significant proportion of air drop in a short distance to the inlet, and vice versa. In addition, the uprising thermal plume reached the ceiling and blocks the downward supply flow, causing the low air delivery just above heat sources (in the mid-length of the room). If the thermal plume is very strong, there is a risk of reverse flow through the diffuse ceiling into the plenum, referred to Paper 4 [50]. It need to notice that the velocity presented in Figure 4-3 was the superficial velocity regardless the impact of porosity.
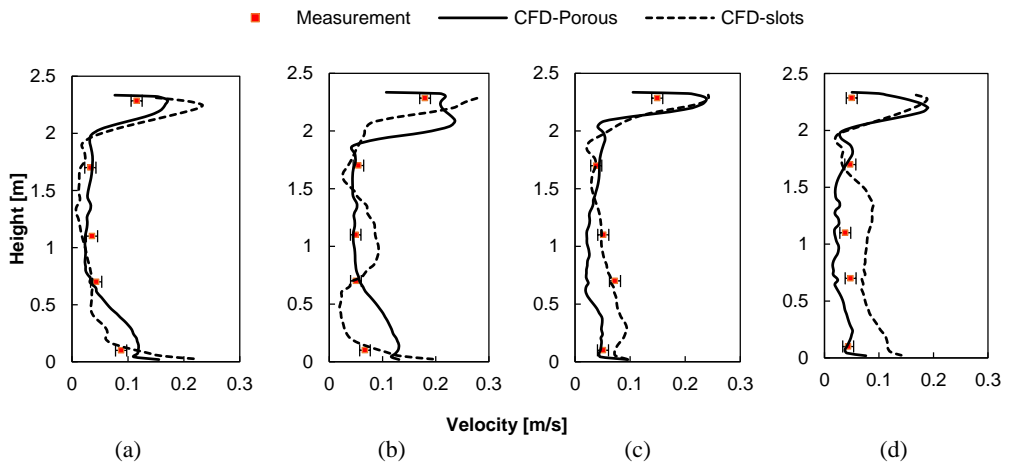
Figure 4-4: Comparison of the vertical velocity profiles at four locations (a) A-2 (b) B-2(c) C-2 (d) D-2 [64]

The simulated velocities were compared with the measured ones at four locations (Figure 3-6) in the room. Figure 4-4 indicates that porous media model had a superior performance to the simplified geometrical model on predicting the velocity distribution, especially the velocity at floor level [64]. Both models indicated that peak velocities occur 5-10 cm below the diffuse ceiling. However, the measured data were not sufficient enough to validate this finding, detailed measurement of air velocity blew the diffuse ceiling is required in the future study.

Both models yielded similar results on the temperature distribution, as illustrated in Figure 4-5. There was a clear temperature difference between the plenum and the room. This is due to the positive pressure in the plenum prevents the mix of the plenum air and the room air, and the diffuse ceiling panel served as a layer of insulation ensures temperature difference between the two zones [64]. Although the plenum air temperature varied along the depth of plenum, the impact on the room temperature

distribution was not significant. The air temperature was predicted to be uniformly distributed in the occupied zone (except the region below the diffuse ceiling), because of the convective flow improves the mixing. "*However, a slight displacement tendency occurred in the room, where the warmest air layer was found just below the diffuse ceiling. The displacement effect of diffuse ceiling ventilation was mentioned by Petersen et al. [73], they pointed out that a displacement tendency takes place at low heat loads and development towards fully mixing with an increase of heat loads [67].*"
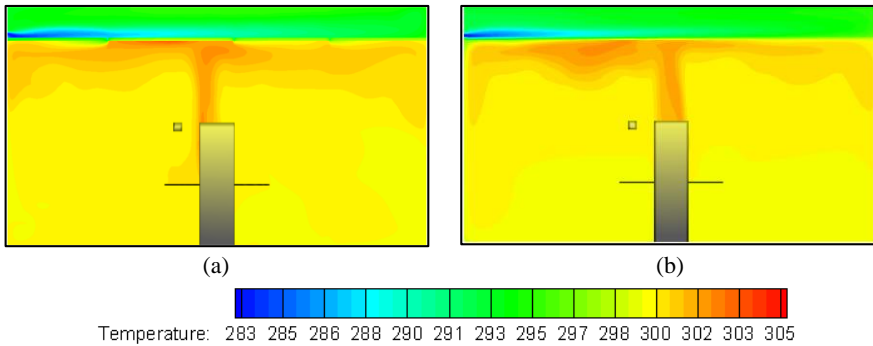
Figure 4-5: Temperature distribution across the central plane of the room, Case 8 (a) Simplified geometrical method (b) Porous media method [64]
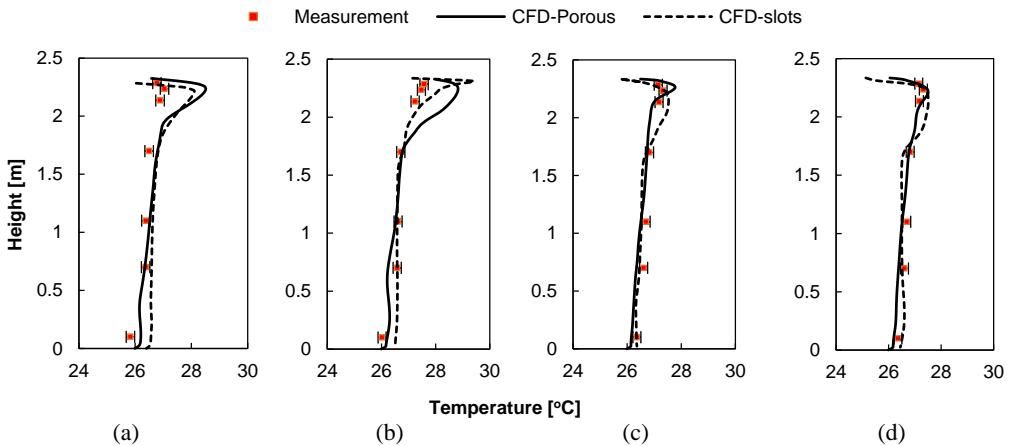
Figure 4-6: Comparison of the vertical temperature profiles at four locations (a) A-2 (b) B-2 (c) C-2 (d) D-2 [64]

The calculated air temperatures agreed quite well with the measured data in the occupied zone, see Figure 4-6. The largest deviation occurred below the diffuse ceiling in both models. The CFD models seemed to overestimate the effect of the thermal plume generated by the heat sources, which leaded to a higher air temperature in this region. The calculated temperature distributions in the plenum were also

validated by the experimental results, as presented in Figure 4-7. Both models gave acceptable predictions on the temperature variation along the length of the plenum. Although the deviation was above 1 ℃ in some locations, if consider the complex thermal processes and the large temperature range within the plenum, the prediction can be considered acceptable [64].
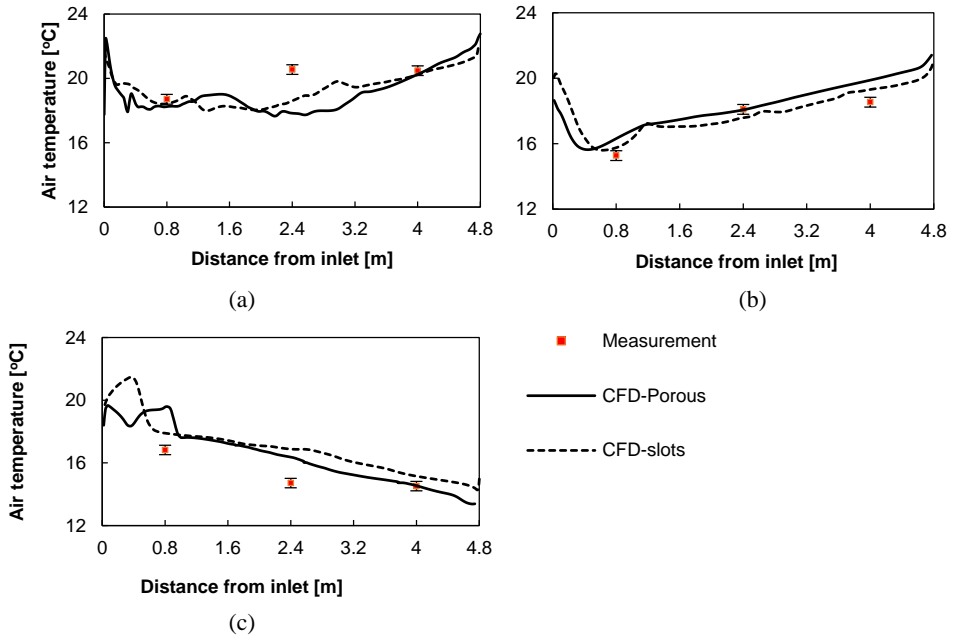
Figure 4-7: Comparison of the plenum air distribution (a) Case 7 (b) Case 8 (c) Case 9 [64]

In conclusion, both numerical models showed their strength and limitation. The simplified geometrical model could directly calculate the radiative heat exchange in both the plenum and in the conditioned zone, while, porous media model required a separate radiation model to provide the necessary boundary condition for the simulation. However, porous media model showed promising results on capturing the flow characteristic of diffuse ceiling supply and provided an accurate prediction on the velocity distribution in the occupied zone. Therefore, coupling of these two models will overcome their own limitation and provide a more accurate prediction of diffuse ceiling ventilation, where the simplified geometrical model is used to determine the convective and radiative heat exchange and results serve as boundary conditions of the porous media model for the detail calculation of flow behavior. The coupled model will be applied in the further study to conduct a series of paramedical analysis.

4.2. PARAMETRICAL STUDY

From the standpoint of the flow element, the design parameters can be divided into two main categories: parameters related to the supply air flow and parameters related to the buoyancy flow.

The supply air flow is mainly determined by the air distribution and thermal process within the plenum and the configuration of diffuse ceiling panels. It is desired to have the supply air uniformly delivered to the entire space with required quantity and conditions. On the other hand, when diffuse ceiling ventilation works together with TABS, it is essential to reduce the negative impact of the diffuse ceiling on the energy performance of TABS. The design parameters considered in this study include the material of diffuse ceiling panel, plenum height, plenum depth and plenum inlet configuration [67].

The buoyancy flow is the air current rising above the heat sources or descending from cold envelopes, like windows or walls. It occurs in the conditioned space and does not have a significant impact on the airflow in the plenum. The buoyancy flow is determined by the type and location of heat sources, as well as the room geometry [50].

Different boundary conditions were specified in the parametrical studies for the various design parameters. The heat load distribution and room geometry were analyzed with the stand-alone diffuse ceiling ventilation system. The diffuse ceiling was modelling with 100% opening area, and ventilation was operated with an air change rate of 4 h^{-1} and supply air temperature of 15.5 °C. The heat load composed of eight pupils and electric radiators are not activated (40 W/m^2).

For the parameters related to the plenum and diffuse ceiling configurations, the integrated system was investigated. The system was operated under three weather conditions: winter, transient season, and summer, referred to the boundary conditions of case 7, 8, 9 in Table 3-2. The room was with office layout, and the heat load is 450.5 W (30 W/m^2).

4.2.1. DISTRIBUTION OF HEAT LOAD

According to the literature review [18][30][74][75], the location of heat sources plays a significant role in the buoyancy driven flow pattern. Four different heat load distributions were analyzed in the study, as shown in Figure 4-8, including heat sources evenly distributed, located in the center, located in the front side of the room and located in the back side of the room [50].
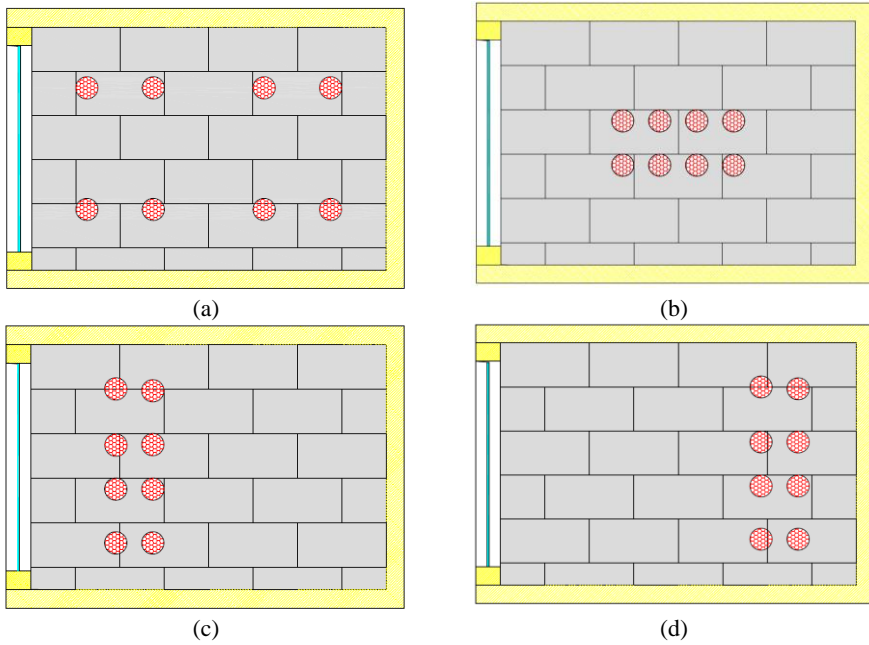
Figure 4-8: Different heat load distributions (a) Evenly distributed (b) Centered (c) Front side (d) Back side [50]

Velocity Magnitude: 0.00 0.03 0.05 0.08 0.11 0.14 0.16 0.19 0.22 0.25 0.27 0.30
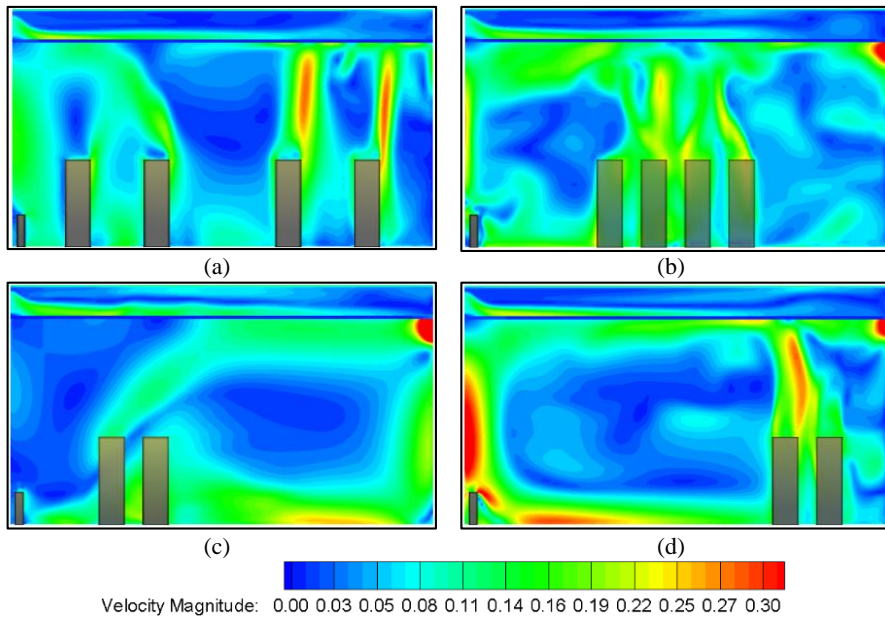
Figure 4-9: Velocity distribution in the vertical plane across the occupants with different heat load layouts (a) Evenly distributed (b) Centered (c) Front side (d) Back side [50]

The velocity distributions are presented in Figure 4-9. The flow pattern changed significantly by varying the location of heat sources [50]. The heat sources located in one side of the room generated a strong air recirculation with the flow direction opposite to the heat source location. When the heat sources located in the center, two recirculation appeared: a strong one in the front side and a weak one in the back side. However, no clear air recirculation occurred when the heat sources were evenly distributed. This result reaches a good agreement with Nielsen et al. [30]. By performing smoke tests, they observed that the air movement was unstable in the room with an even distribution of heat sources. The flow direction was either unclear or not consistent.

The impact of heat load distribution on the local discomfort was further evaluated by the draught rate at the ankle level [50]. As expected, evenly distributed heat sources gave the lowest draught rate. When the heat sources were centralized, the intensity of thermal plume increased. The strong recirculation was formed and resulted in the high-velocity flow entering the occupied zone along the floor. The maximum draught rate was presented with the back side located heat sources, reaching the limit of 20%. However, the draught rate with the front located heat sources was less than 15%. The result revealed that diffuse ceiling supply does not provide a uniform air distribution. Due to the gravity, a high proportion of air was delivered near the inlet. The downward supply flow met the uprising buoyancy flow and aggravated the recirculation.

4.2.2. ROOM HEIGHT

Room geometry is another important parameter in the design of a ventilation system. For example, displacement ventilation is preferable to apply in a high space due to the stratification principle, where the room height should be above 3 m. On the contrary, the standard mixing ventilation is a better solution for space with room height less than 2.3 m, where surplus heat is the primary concern instead of air quality [16]. The impact of room height on the performance of diffuse ceiling ventilation was analyzed by numerical studies. Three room heights were discussed here: 2.335 m (as in the test facility), 3.0 m and 4.0 m.
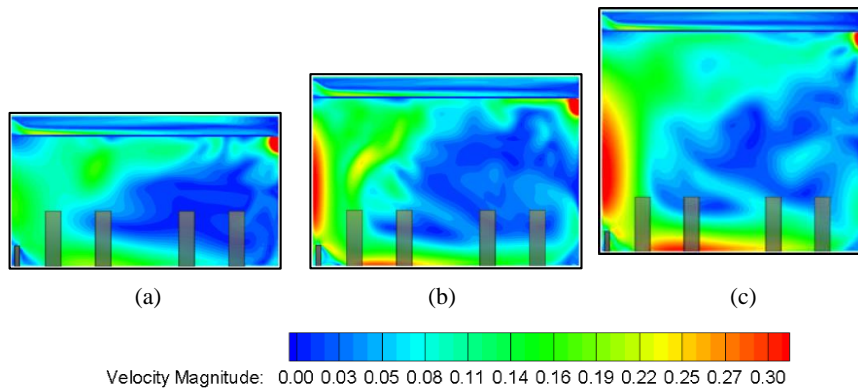
Figure 4-10: Velocity distribution across the central panel with different room heights (a) 2.335 m (b) 3.0 m (c) 4.0 m [50]

As illustrated in Figure 4-10, the airflow patterns under different room heights presented a similar trend. However, the intensity of the recirculation increased dramatically with the rise of the room height. This can be explained by the fact that the engine of the recirculation is the convective flow generated by the heat sources. The amount of air involved in the convective flow increases with room height because of the entrainment of ambient air[16]. When the convective flow free rising height is larger than the ceiling height, it becomes downward flow and interacts with the downward supply flow accelerating the recirculation. As a result, the draught risk in the occupied zone is proportional to the room height, where the draught rate in the 4.0 m case (20%) was approximately doubled that in the case with 2.335 m height (12%) [50].

4.2.3. THE CONDUCTIVITY OF DIFFUSE CEILING PANEL

Two types of diffuse ceiling panels were compared regarding their impact on the energy performance of the TABS. *"One was wood-cement panel, and the other was Al panel. Wood-cement panel was 35 mm thick and with a thermal conductivity of 0.085 W/m.K (U-value 2.43 W/m2.K), while, Al panel had a thickness of 5 mm and thermal conductivity of 202.4W/m.K (U-value 40480 W/m2. K). To limit the number of variables, it assumed both panels have the same porosity and the same pressure resistance. Moreover, to avoid the influence of the materials' emissivity on the radiative heat exchange, it was assumed that the Al panel is painted into black and has the same emissivity as the wood-cement panel [67]."*

Table 4-1: The impact of different design parameters on the energy performance of TABS [67]

Design Parameter		Operating condition	Room air temp [ºC]	TABS Q_{tot} [W]	TABS Q_{rad} [W]	TABS Q_{conv} [W]
Diffuse ceiling material	Wood-cement	Winter	25.11	517	312	205
	Al		23.62	450	259	191
	Wood-cement	Transient season	26.72	-	-	-
	Al		25.94	-	-	-
	Wood-cement	Summer	24.46	-461	-172	-289
	Al		22.17	-557	-236	-321
Plenum height	35 cm	Winter	25.11	517	312	205
	20 cm		26.04	540	273	267
	10 cm		27.94	604	204	400
	5 cm		28.76	636	175	461
Plenum depth	4.8 m	Winter	25.11	517	312	205
	9.6 m		25.05	965	576	389
Plenum inlet	Original	Winter	25.11	517	312	205
	Corner		25.32	541	294	246

Note: Winter, transient season and summer represent the case 7, 8, 9 in Table 3-2, respectively. '+' presents heating capacity and '-' presents cooling capacity.

In term of energy performance, the increase in the diffuse ceiling conductivity played a beneficial role in the cooling capacity of the TABS. An enhancement of 22% was achieved by using Al panels, as shown in Table 4-1. However, the opposite effect was observed in the heating case, where the heating capacity reduced by 13%. In the transient season, although the TABS was not activated, the diffuse ceiling had an indirect impact on the heat transfer from the upper floor. The Al panel limited the heat conducted from the upper floor and kept a lower room temperature than the wood-cement panels [67].

Based on the previous experimental study [48][53], the cooling capacity of TABS significantly reduced after utilizing the diffuse ceiling, which limited the application of the integrated system in the room with high cooling demand. The negative effect can be weakened by using diffuse ceiling panel with high thermal conductivity, for instance, Al panel. It is recommended to use ceiling panel with a high conductivity if cooling is the primary demand during the year. The conductivity of the diffuse ceiling panel did not influence the airflow pattern. Thus, no discussion regarding the thermal comfort is presented here [67].

4.2.4. PLENUM HEIGHT

The effect of plenum height was evaluated by varying the height from 35 cm to 5 cm under winter condition. Winter is more critical situation, because the cool supply air deteriorates the uniformity of the air distribution through the diffuse ceiling and enhances the draught risk in the occupied zone.

The decrease in the plenum height showed a positive impact on the energy performance of TABS. The low plenum enabled the force convection on the TABS surface. Consequently, the convective heat exchange had a remarkable increase. Although the radiative heat transfer reduced, the total heating capacity of TABS increased from 516 W to 636 W as the plenum height reduced from 35 cm to 5 cm, see Table 4-1 [67].
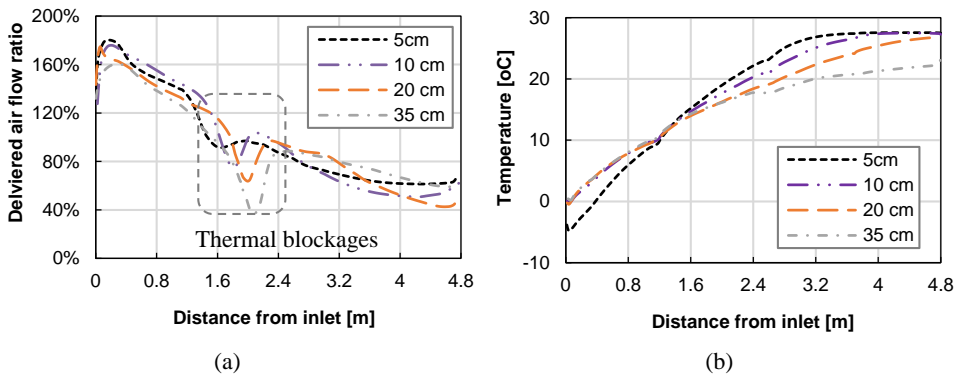
Figure 4-11: Air distribution through the diffuse ceiling with different plenum heights (a) Delivered air flow ratio (b) Temperature distribution [67]

The effect of plenum height on the supply air flow through diffuse ceiling can be analyzed by two factors: delivered air flow ratio and supply air temperature distribution. As indicate in Figure 4-11, both the amount and temperature of supply air varied significantly as the distance from the inlet [67]. Bauman mentioned that the distribution variance should be limited to ±10% in the plenum for the underfloor air distribution [37]. However, the delivered air flow ratios were above 100% in all plenum heights. The large distribution variations can be attributed to three reasons. First, the pressure drop of the diffuse ceiling panel was much lower than that of conventional air diffusers, where the pressure drop was lower than 0.2 Pa when the air change rate was 2 h^{-1}. Secondly, the inlet air was with extremely low temperature (-7 °C). The high density of cold air caused that a large amount of air dropped in a short distance from the inlet. Finally, the continued heat transfer from the TABS enhanced the thermal variation of plenum air. Nevertheless, the reduction in the

plenum height deteriorated the situation. The low height plenum limited the mixing between the inlet air and the plenum air and aggravated the temperature variation [67].

Although the buoyancy flow plays a dominant role, the airflow pattern in the room is still influenced by the supply flow from the diffuse ceiling, which can be concluded from Figure 4-12. When the plenum height decreased, the cold downward flow from diffuse ceiling accelerated the air recirculation and leaded to high-velocity reverse flow penetrated from the front side to the entire room, as illustrated in Figure 4-12. The maximum air velocity at the ankle level exceeded 0.29 m/s and the area above 0.2 m/s reached 50% of the entire space, when the plenum was 5 cm height [67]. It is surprising to see that the draught rate in the occupied zone presented a different manner than the velocity, as shown in Figure 4-13. This is because the low plenum height enabled a high heating capacity of TABS and resulted in a higher indoor air temperature (Table 4-1). It needs to be noticed that the low draught risk under low plenum only applies to the integrated system. For the stand-alone diffuse ceiling ventilation system, the local draught will be a major concern when uses a low plenum. *"Finally, although the temperature variation in the plenum reached 30 ºC, the air temperature in the occupied zone was very uniform, as shown in Figure 4-14. An efficient mixing between supply air flow and convective flow from heat sources was expected [67]. "*

(a)   (b)

(c)   (d)

Velocity Magnitude: 0.00 0.03 0.05 0.08 0.11 0.14 0.16 0.19 0.22 0.25 0.27 0.30
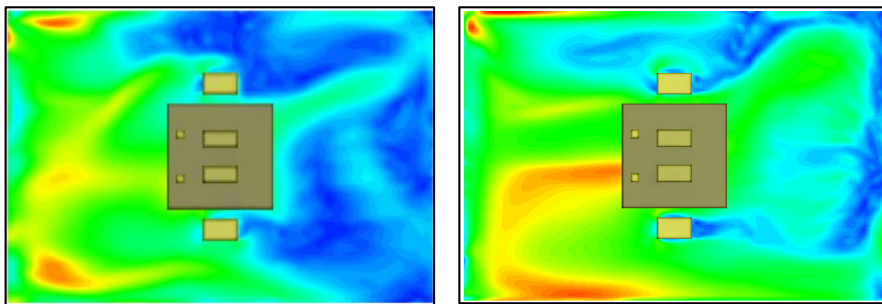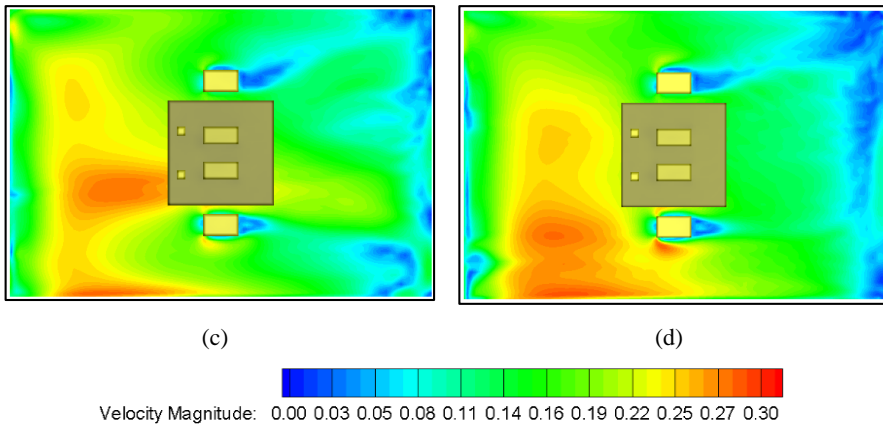
Figure 4-12: Velocity distribution at ankle level with different plenum heights (a) 35 cm, (b) 20 cm, (c) 10 cm, and (d) 5 cm [67]
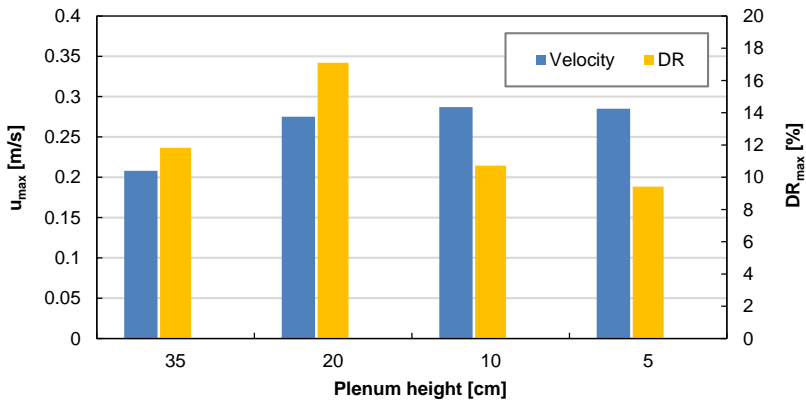
Figure 4-13: Maximum velocity and draught rate with different plenum heights

(a)   (b)

(c)   (d)

Temperature: 283 284 285 286 288 289 290 291 292 293 295 296 297 298 299 300 302
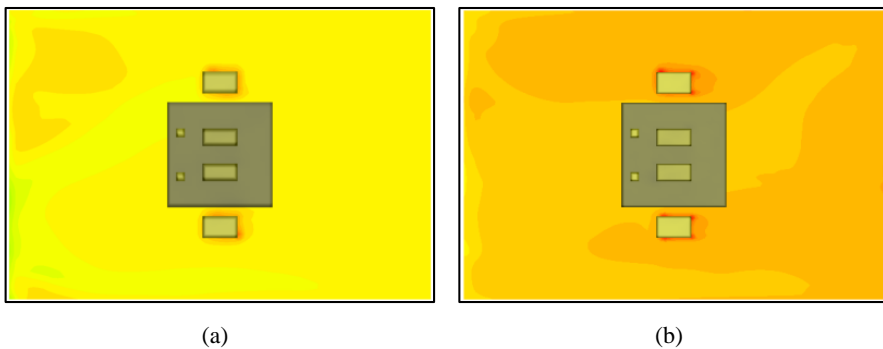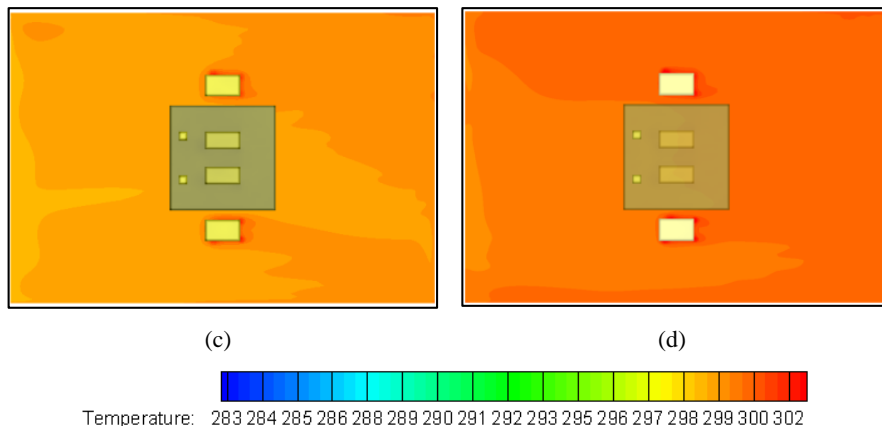
Figure 4-14: Temperature distribution at ankle level with different plenum heights (a) 35 cm, (b) 20 cm, (c) 10 cm, and (d) 5 cm

4.2.5. PLENUM DEPTH

Another consideration is whether the diffuse ceiling ventilation can be applied in deep rooms, for instance, landscape offices. This question was explored by doubling the plenum depth.

As demonstrated in Table 4-1, doubling the plenum depth did not lead to a double of the heat released from the TABS. Both air velocity and air-surface temperature differences decreased as the air traveling further in the plenum. Consequently, both convective and radiative heat fluxes were slightly decreased by increasing plenum depth [67].

As expected, the deep plenum is another contributor to the uneven supply air distribution. The variation in the air delivery rate exceeded 140%. *"The uneven supply flow influenced the flow behavior in the occupied zone, where the velocity magnitude and region with high velocity were dramatically higher than those in 4.8 m room. The maximum air velocity at the ankle level reached 0.33 m/s and the maximum draught rate reached 22%, exceeding the limit of 20% in Category B ISO 7730 [23]. The occupants located near the facade experienced significantly higher draught than the ones located in the back side of the room. From both energy efficiency and thermal comfort point of view, diffuse ceiling ventilation performed better in the room with 4.8 m length than that with 9.6 m [67]."* However, the impact of plenum depth is expected to be reduced by using diffuse ceiling panel with higher pressure drop, where the higher resistance can provide a more uniform distribution through diffuse ceiling

supply. The relation between the maximum plenum depth and the pressure drop of diffuse ceiling panel is recommended to investigate in the future study.

(a)

(b)

Velocity Magnitude: 0.00 0.03 0.05 0.08 0.11 0.14 0.16 0.19 0.22 0.25 0.27 0.30
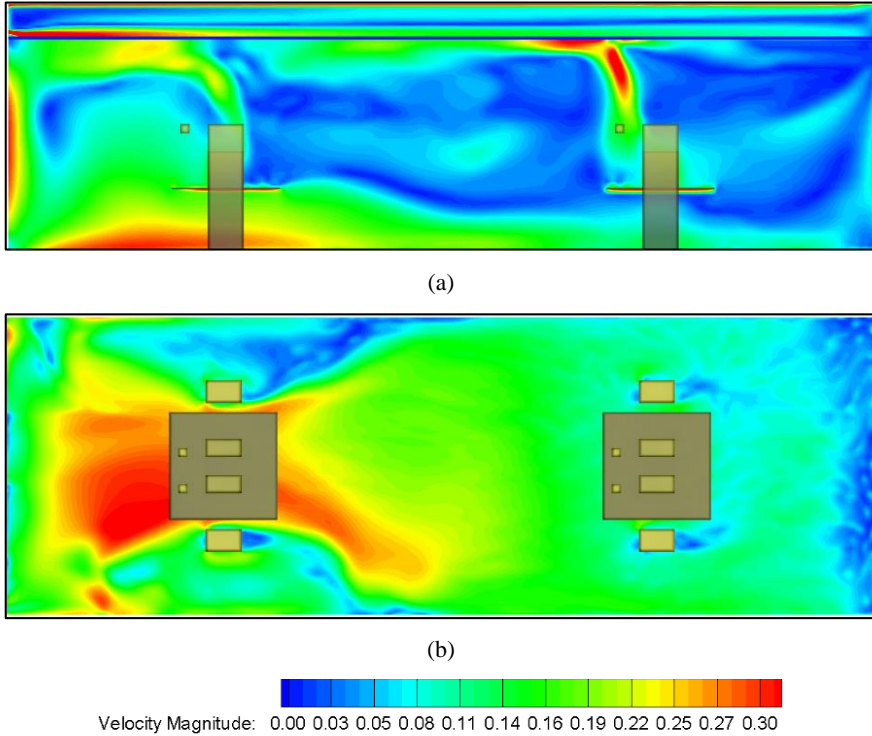
Figure 4-15: Velocity distribution at ankle level with 9.6 m length (a) The central panel x-z (b) The ankle level x-y [67]

4.2.6. PLENUM INLET

"Two plenum inlet configurations were studied, as illustrated in Figure 4-16. The original plenum inlet setup served as a reference, the other configuration was a square opening located at one corner of the plenum, which simulates a duct opening. Both inlets had the same effective opening area, and the plenum height was 35 cm. In order to build structured mesh, both inlets were simplified as squared shape [67]."
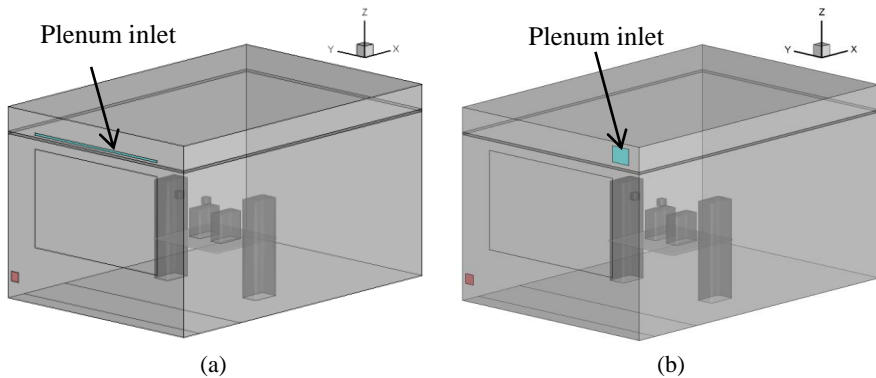
Figure 4-16: Plenum inlet configurations: (a) slot opening and (b) duct opening [67]

The location of plenum inlet had an impact on the energy performance of TABS. An enhancement of TABS' heating capacity was observed by using the duct opening. The air was distributed near the TABS surface, which leaded to forced convection between the air and TABS surface.

By comparing the velocity distribution at the ankle level with two inlet configurations, we conclude that the plenum inlet does not only determine the airflow pattern in the plenum but also influences the air flow in the occupied zone. The concentrated shape of duct opening caused a large amount of air delivered to the room through the corner, and then the air penetrated into the entire space along the floor. The slot opening enabled a more even distribution along the width of the room. In the case with duct opening, although high velocity was observed near the corner, it did not have a significant impact on the velocity in the occupied zone. The draught risk was at the same level in both cases [67].

<div align="center">(a)   (b)</div>

Velocity Magnitude: 0.0000 0.0005 0.0010 0.0015 0.0020 0.0025 0.0030
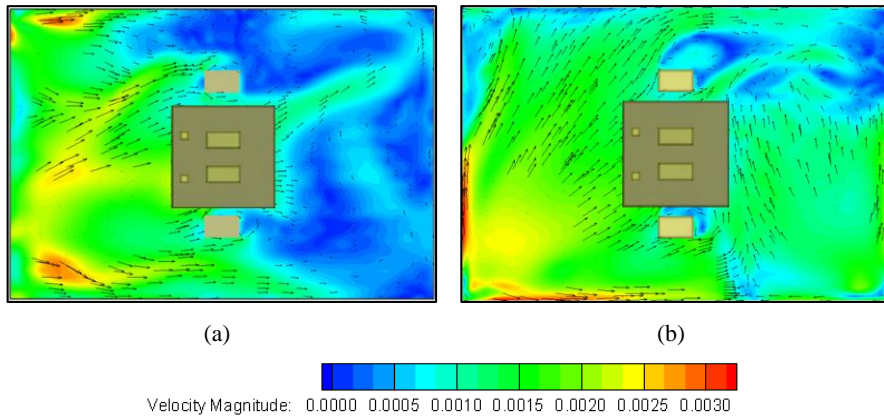
Figure 4-17: Velocity distribution at ankle level with different plenum inlet (a) slot opening and (b) duct opening [67]

4.3. CONCLUSION

When designing the diffuse ceiling ventilation system, a large number of design parameters are encountered in practice, accompanied by the complex flow and thermal behaviors. It is desirable to develop a validated numerical model that could provide a reliable prediction of the diffuse ceiling ventilation in the design stage. The major challenge we faced is how to specify the diffuse ceiling supply, as the wood-cement panel has a porous structure. Two simplified models were built and compared: one was a simplified geometrical model, and the other was porous media model. Porous media model presented a superior performance on capturing the flow characteristic through the ceiling panel and provided a more accurate prediction on the airflow pattern in the occupied zone. However, the limitation of the porous media model was that it not able to calculate the radiative heat exchange directly. Therefore, the simplified geometrical model was used to calculate the energy performance and the results were served as boundary conditions for the porous media one. The validated model was further applied to conduct a series of parametric studies. The following conclusions can be drawn:

- The simulated results proved that buoyancy flow from the heat sources plays a dominant role on the airflow pattern in the room with diffuse ceiling ventilation. The buoyancy flow was strongly influenced by the location of heat sources and the room geometry. From the standpoint of draught rate, it is recommended to evenly distribute heat sources rather than concentrated location. In addition, large room height aggravated the air recirculation and resulted in a high draught risk at the ankle level. Thus, the diffuse ceiling ventilation is preferable to apply in cases with low room height.

- The plenum and diffuse ceiling configurations determined the airflow pattern and thermal process in the plenum, and further affected the supply flow through the diffuse ceiling, especially when the system cooperated with the TABS. The diffuse ceiling panel with higher thermal conductivity could reduce its impact on the energy performance of the TABS, and enabled the integrated system to operate more efficiently in summer. On the other hand, the low plenum height and deep plenum deteriorated the uniformity of supply air distribution and resulted in the high air velocity in the occupied zone. The effect of plenum configurations on the supply flow is expected to be reduced by utilizing diffuse ceiling panel with higher pressure drop. The relations between the pressure drop of diffuse ceiling panel and the optimal plenum height as well as plenum depth are recommended to investigate in the future study.

For further information, please refer to Paper 3: "Airflow Pattern and performance analysis of diffuse ceiling ventilation in an office room using CFD Study."

& Paper 4: "Parametrical analysis on the diffuse ceiling ventilation by experimental and numerical studies."

& Paper 5: "Numerical study of an integrated system with diffuse ceiling ventilation and thermally activated building constructions."

CHAPTER 5. CONCLUSION OF THE THESIS

The objective of the present study was to characterize the air distribution and thermal comfort in the rooms with diffuse ceiling ventilation. In addition to investigating the stand-alone diffuse ceiling ventilation, the possibility and limitation to integrate it with a radiant ceiling system (TABS) were also discussed. The investigations were based on both full-scale experiments and numerical modeling by CFD. The present study focused on the steady-state analysis, where the dynamic effect of thermal mass (ceiling slab and diffuse ceiling panel) was not taken into account. However, it is recommended to consider this in future studies. This chapter describes the general conclusions drawn from this study.

The thermal comfort levels in the room with and without diffuse ceiling ventilation were compared by an experimental study. The results indicated that diffuse ceiling ventilation could effectively eliminate the local discomfort caused by draught, vertical temperature gradient, and radiant asymmetry, especially in winter. By means of the design chart method, one can observe that the thermal comfort requirements such as draught rate and vertical temperature gradient do not have strong limitations on the ventilation rate and temperature difference between the supply and return air temperature. This characteristic allows the diffuse ceiling ventilation to have a higher cooling capacity than the conventional ventilation systems (Figure 3-18), which is preferable for the spaces with high heat loads and high ventilation demands, such as classrooms and offices.

In the integrated system, the TABS was encapsulated by the diffuse ceiling panel and the energy efficiency of TABS was changed accordingly. The diffuse ceiling ventilation played a beneficial role in the heating performance of the TABS, because it enlarged the air-surface temperature difference and enabled a forced convection between TABS and the supply air. Consequently, the increase of convective heat transfer offset the loss of radiative heat transfer. On the contrary, the effect on the cooling performance presented a different manner. The air-surface temperature difference was decreased when the TABS was operated as a cooling surface. Therefore, both the convective and radiative heat transfers were weakened by the existence of the diffuse ceiling. The reduction in the cooling capacity required TABS to operate with a lower surface temperature to maintain a desirable indoor environment at a certain heat load conditions. To reduce the negative impact on the cooling performance, it is recommended to use diffuse ceiling panel with high thermal conductivity, for example, Al panel. The cooling capacity of TABS enhanced 21% compared with that using the wood-cement panel.

Both experimental and numerical analyses proved that the flow pattern in the room with diffuse ceiling ventilation is mainly controlled by buoyancy flow produced by the heat sources. The uprising thermal plumes met the downward flow from diffuse ceiling supply and generated air recirculation in the room level. As a result, the ventilation performance was comparable to mixing ventilation. Two parameters affecting the buoyancy flow were investigated, one was the location of the heat sources, and the other was the height of the room. The simulated results demonstrated that even distribution of heat source provides a lower draught environment than the concentrated placement. In addition, high ceiling level aggravated the air recirculation in the room and resulted in significant draught at the ankle level. Consequently, it is preferable to utilize diffuse ceiling ventilation in the rooms with low ceiling height and with even distribution of heat sources.

Using suspended ceiling as air diffusers presented an advantage of low pressure loss. The pressure drop of the wood-cement ceiling was measured to be less than 2.5 Pa even when the air change rate reached 17 h^{-1}. Furthermore, the ceiling plenum was applied to distribute air instead of conventional ductwork, which created less resistance to the airflow. The low pressure loss of diffuse ceiling ventilation allowed a remarkable energy saving on the fan power and even made the system able to driven by natural ventilation. However, the low pressure drop of the ceiling panel was a potential contributor to the uneven air distribution through the diffuse ceiling supply. The distribution variance was observed to be more than 100% when the system was operated in the winter conditions (Figure 4-11). The situation further deteriorated with reduced plenum height or increased plenum depth. The non-uniform supply led to higher air velocity occurred in the occupied zone, but did not have a significant impact on the temperature distribution in the room. Therefore, there is a tradeoff between the energy saving of the fan and the uniform air supply when selecting the diffuse ceiling panel. On the other hand, when the diffuse ceiling ventilation is coupled with the TABS, the decrease of the plenum height increased the convection and promoted the heating/cooling capacity of the TABS.

CHAPTER 6. FUTURE WORK

Despite the promising results from the present study, further investigation on a number of issues is still needed to fully understand the potentials and limitations of diffuse ceiling ventilation.

- Air quality is another leading factor to evaluate the performance of a ventilation system. In the existing test facility, the air was recirculated between the test chamber and the climate chamber, which prohibited air quality measurement using tracer gas. Although the measured temperature distribution indicated a good mixing level in the occupied zone, the effectiveness of temperature distribution and effectiveness of concentration distribution can only give same results when the contaminant source at the same time is the significant heat source in the room[12]. It is essential to investigate whether the ventilation system is able to remove the contaminant in an efficient way and whether there are any short-circuiting or stagnant air zones, with different contaminant sources.

- The experiments on diffuse ceiling with different opening areas found out that the system with 18% area ratio can handle the highest heat load without discomfort (Figure 3-17). However, it is too cursory to conclude that reducing diffuse ceiling opening area can increase the system cooling capacity, because the location of the heat sources to the location of the diffuse ceiling opening may play a crucial role. For instance, by analyzing the vertical ventilation with the textile terminal, it found out that a large of mixing occurred when the textile terminal was located directly above the heat sources, but a displacement flow took place when the terminal was located close to the side wall [76]. It is essential to investigate the interaction between the heat sources location and the diffuse ceiling opening location in future study. On the other hand, when the opening area reduces to a certain level, the flow pattern will turn from the buoyancy controlled to the momentum controlled and the draught will become a major concern in that situation. It will be important to find the minimum opening area which can maintain the buoyancy controlled pattern.

- The present study mainly focused on the cooling situations, where the ventilation was used to cool down spaces. Although winter conditions were considered when the system worked together with the TABS, the supply air temperature through the diffuse ceiling was still lower than the room air temperature due to

the presence of the internal heat loads. The heating condition represents the unoccupied period with the heat loss through the envelope (cold window and external wall). The ventilation needs to supply warm air to maintain an acceptable indoor environment until people come to work. Nielsen et al. [26] mentioned that high vertical temperature gradient was observed in the heating case due to the absence of heat sources. The possibility to use diffuse ceiling ventilation for heating will be investigated in future study, whether sufficient mixing can be reached by only the convective flow from the cold envelope surface.

- Night-time ventilation becomes a promising technique for passive cooling, especially for the commercial buildings in the moderate or cold climate[77]. Diffuse ceiling ventilation presents a high potential to combine with the night cooling strategy, due to the ceiling slabs are typically exposed to the supply air pathways, which increases the efficiency of the thermal storage and improves the pre-cooling effect. The diffuse ceiling ventilation can circulate the cool air throughout the space, remove the stored heat and pre-cool the building constructions for the next day. The energy saving potential by implementing the night–time ventilation strategy requires further analysis by both experimental and numerical approaches. On the other hand, the diffuse ceiling panel also presents thermal storage potential depending on the thermal capacity of the materials. In the current study, Al panel showed a superior performance on the cooling efficiency than the wood-cement panel, if only considering their thermal conductivity. However, the difference maybe reduces or show a different manner if thermal capacity of ceiling panel is taken into account.

REFERENCES

[1]   EU, "Directive 2010/31/EU. European parliament and of the council of 19 May 2010 on the energy performance of buildings," *Off. J. Eur. Union*, pp. 13–35, 2010.

[2]   The Danish Ministry of Economic and Business Affairs, *Building Regulations 2010*. 2010.

[3]   P. Wargocki, P. D. Wyon, and P. O. Fanger, "Productivity is affected by the air quality in offices," in *Healthy Buildings 2000*, 2000, vol. 1, pp. 635–640.

[4]   P. Wargocki and D. P. Wyon, "The Effects of Outdoor Air Supply Rate and Supply Air Filter Condition in Classrooms on the Performance of Schoolwork by Children (RP-1257)," *HVAC&R Res.*, vol. 13, no. 2, pp. 165–191, 2007.

[5]   C. A. Hviid and S. Svendsen, "Experimental study of perforated suspended ceilings as diffuse ventilation air inlets," *Energy Build.*, vol. 56, pp. 160–168, Jan. 2013.

[6]   P. V Nielsen and E. Jakubowska, "The Performance of Diffuse Ceiling Inlet and other Room Air Distribution Systems," in *Cold Climate HVAC*, 2009, p. 7.

[7]   P. Jacobs and B. Knoll, "Diffuse ceiling ventilation for fresh classrooms," in *4 th Intern. Symposium on Building and Ductwork Air tightness*, 2009, pp. 1–7.

[8]   P. Jacobs, E. C. M. Van Oeffelen, and B. Knoll, "Diffuse ceiling ventilation, a new concept for healthy and productive classrooms," in *Indoor Air*, 2008, pp. 17–22.

[9]   E. M. Jakubowska, "Air distribution in rooms with the diffuse ceiling inlet," Department of Civil Engineerging, Aalborg University, 2007.

[10]   C. A. Hviid, "Integrated ventilation and night cooling in classrooms with diffuse ceiling ventilation," in *11th Ökosan*, 2011.

[11]   P. V Nielsen, "The 'Family Tree' of Air Distribution Systems," in *Roomvent*, 2011, p. 12.

[12]   P. V. Nielsen, *Lecture Notes on Mixing Ventilation*. Department of Civil Engineering, Aalborg University, 1995.

[13]   P. V. Nielsen, "Mathematical Models for Room Air Distribution Nielsen," in *System Simulation in Buildings*, vol. 1, pp. 455–470.

[14]   T. Arghand, T. Karimipanah, H. B. Awbi, M. Cehlin, U. Larsson, and E. Linden, "An experimental investigation of the flow and comfort parameters forunder-floor, confluent jets and mixing ventilation systems in an open-plan office," *Build. Environ.*, vol. 92, pp. 48–60, 2015.

[15]   CIBSE, *AM13 Mixed mode ventilation*. CIBSE, 2000.

[16]   H. Skistad, E. Mundt, P. V. Nielsen, K. Hagström, and J. Railio, *Displacement ventilation in non-industrial premises*. REHVAC: Federation of European Heating, Ventilation and Air - conditioning Associations, 2007.

[17]   D. Standards, "DS/EN 13779 Ventilation for non-residential buildings – Performance requirements for ventilation and room-conditioning systems," 2007.

[18]   A. D. Chodor and P. P. Taradajko, "Experimental and Numerical Analysis of Diffuse Ceiling Ventilation," Department of Civil Engineering, Aalborg University, 2013.

[19]   P. O. Fanger, *Thermal comfort: Analysis and applications in environmental engineering*. Danish Technical Press, 1970.

[20]   P. Ole Fanger and J. Toftum, "Extension of the PMV model to non-air-conditioned buildings in warm climates," *Energy Build.*, vol. 34, no. 6, pp. 533–536, 2002.

[21]   P. O. Fanger, A. K. Melikov, H. Hanzawa, and J. Ring, "Air Turbulence and Sensation of Draught," *Energy Build.*, vol. 12, pp. 21–39, 1988.

[22]   CEN Report, "CR 1752, Ventilation for buildings - Design criteria for the indoor environment," 1998.

[23]   International Standard, "ISO 7730:2005 Ergonomics of the thermal environment -- Analytical determination and interpretation of thermal comfort using calculation of the PMV and PPD indices and local thermal comfort criteria." 2005.

[24]   ASHRAE, *ASHRAE 55-2013: Thermal Environmental Conditions for Human Occupancy*. 2013.

[25]   C. Zhang, P. Heiselberg, and P. V Nielsen, "Diffuse Ceiling Ventilation : A

REFERENCES

Review," *Int. J. Vent.*, vol. 13, no. 1, pp. 49–63, 2014.

[26]   P. V Nielsen, R. L. Jensen, and L. Rong, "Diffuse Ceiling Inlet Systems and the Room Air Distribution," in *Clima 2010: 10th REHVA World Congress*, 2010.

[27]   J. Fan, C. A. Hviid, and H. Yang, "Performance analysis of a new design of office diffuse ceiling ventilation system," *Energy Build.*, vol. 59, pp. 73–81, Apr. 2013.

[28]   C. A. Hviid and S. Svendsen, "Experimental study of perforated suspended ceilings as diffuse ventilation air inlets," *Energy Build.*, vol. 56, pp. 160–168, Jan. 2013.

[29]   R. W. Vilsbøll, "Diffuse ceiling ventilation - Experimental and numerical analysis based on variation of room geometry and heat load distribution," Department of Civil Engineering, Aalborg University, 2014.

[30]   P. V. Nielsen, R. W. Vilsbøll, L. Liu, and R. L. Jensen, "Diffuse ceiling ventilation and the influence of room height and heat load distribution," in *Healthy buildings Europe 2015*, 2015, pp. 2–9.

[31]   P. V Nielsen and E. Jakubowska, "The Performance of Diffuse Ceiling Inlet and other Room Air Distribution Systems," in *COLD CLIMATE HVAC*, 2009.

[32]   R. L. Jensen and L. M. Jensen, "Airflow Test of Acoustic Board Samples Airflow Test of Acoustic Board Samples," 2012.

[33]   J. Railio and P. Mäkinen, "SPECIFIC FAN POWER – a tool for better performance of air handling systems," in *Clima 2007 Well Being Indoors*, 2007.

[34]   P. Heiselberg, "Modelling of Natural and Hybrid Ventilation," Lecture Notes, Department of Civil Engineering, Aalborg University, 2006.

[35]   R. Václavík, "Analyses and Test of Diffuse Ventilation System in Test Building," Technical University of Denmark, 2013.

[36]   H. Jin, F. Bauman, and T. Webster, "Testing and modeling of underfloor air supply plenums," *ASHRAE Trans.*, vol. 112, no. 2, pp. 581–591, 2006.

[37]   F. S. Bauman, *Underfloor Air Distribution (UFAD) Design Guide*. USA: American Society of Heating, Refrigerating and Air-Conditioning Engineers, Inc., 2013.

[38]   S. Li, M. Yuan, H. Wang, and T. Xu, "Study on Condensation Control of Radiant Cooling Ceiling," *2011 Second Int. Conf. Digit. Manuf. Autom.*, pp. 1149–1153, Aug. 2011.

[39]   Price HVAC, "Displacement Ventilation Design Guide," 2013.

[40]   S. A. Mumma, "Condensation Issues With Radiant Cooling Panels," *ASHRAE IAQ Appl.*, pp. 1–3, 2001.

[41]   J. Le Dréau, "Energy flow and thermal comfort in buildings Comparison of radiant and air-based heating & cooling systems," PhD Thesis, Department of Civil Engineering, Aalborg University, 2013.

[42]   L. Su, N. Li, X. Zhang, Y. Sun, and J. Qian, "Heat transfer and cooling characteristics of concrete ceiling radiant cooling panel," *Appl. Therm. Eng.*, vol. 84, pp. 170–179, 2015.

[43]   J. Niu and J. v d Kooi, "Indoor climate in rooms with cooled ceiling systems," *Build. Environ.*, vol. 29, no. 3, pp. 283–290, 1994.

[44]   T. Active and B. Systems, "Using Building Mass To Heat and Cool," *ASHRAE J.*, pp. 44–52, 2012.

[45]   F. I. Z. Karlsruhe, "Thermo-active building systems," *FIZ Kalsruhe*, 2007.

[46]   B. Lehmann, V. Dorer, and M. Koschenz, "Application range of thermally activated building systems tabs," *Energy Build.*, vol. 39, no. 5, pp. 593–598, May 2007.

[47]   B. Lehmann, V. Dorer, M. Gwerder, F. Renggli, and J. Tödtli, "Thermally activated building systems (TABS): Energy efficiency as a function of control strategy, hydronic circuit topology and (cold) generation system," *Appl. Energy*, vol. 88, no. 1, pp. 180–191, Jan. 2011.

[48]   C. Zhang, P. K. Heiselberg, M. Pomianowski, T. Yu, and R. L. Jensen, "Experimental study of diffuse ceiling ventilation coupled with a thermally activated building construction in an office room," *Energy Build.*, vol. 105, pp. 60–70, 2015.

[49]   British Standards, "BS EN ISO 8990-1996:Thermal insulation. Determination of steady-state thermal transmission properties. Calibrated and guarded hot box." 1996.

[50]   C. Zhang, M. H. Kristensen, J. S. Jensen, P. K. Heiselberg, R. L. Jensen, and

REFERENCES

M. Pomianowski, "Parametrical analysis on the diffuse ceiling ventilation by experimental and numerical studies," *Energy Build.*, vol. 111, pp. 87–97, 2016.

[51]   A. Simone, J. Babiak, M. Bullo, G. Landkilde, and B. W. Olesen, "Operative temperature control of radiant surface heating and cooling systems," in *Clima 2007 Well Being Indoors*, 2007.

[52]   T. L. Madsen, B. W. Olesen, and N. K. Christensen, "Comparison between operative and equivalent temperature under typical indoor conditions," *ASHRAE Trans.*, 1984.

[53]   T. Yu, P. Heiselberg, B. Lei, M. Pomianowski, C. Zhang, and R. Jensen, "Experimental investigation of cooling performance of a novel HVAC system combining natural ventilation with diffuse ceiling inlet and TABS," *Energy Build.*, vol. 105, pp. 165–177, 2015.

[54]   H. B. Awbi and a. Hatton, "Mixed convection from heated room surfaces," *Energy Build.*, vol. 32, pp. 153–166, 2000.

[55]   British Standards, "BS-EN-15377-2-2008: Heating systems in buildings. Design of embedded water based surface heating and cooling systems. Design, dimensioning and installation." 2008.

[56]   B. W. Olesen and G. Zöllner, "New European standards for design , dimensioning and testing embedded radiant heating and cooling systems .," *Clima 2007 WellBeing Indoor*. Helsinki, Finland, 2007.

[57]   P. V Nielsen, T. S. Larsen, and C. Topp, "Design methods for air distribution systems and comparison between mixing ventilation and displacement ventilation," in *Proceedings of the 7th International Conference on Healthy Buildings*, 2003.

[58]   P. V Nielsen, "Analysis and Design of Room Air Distribution Systems," *HVAC&R Res.*, vol. 13, no. 6, pp. 987–997, 2007.

[59]   ANSANSYS Inc., "Ansys Fluent release 16.0.," 2015. [Online]. Available: http://www.ansys.com/.

[60]   A. D. Lemaire, Q. Chen, M. Ewert, J. Heikkinen, C. Inard, A. Moser, P. V. Nielsen, and G. Whittle, *IEA Annex 20: Air flow patterns within buildings*. 1993.

[61]   Q. Chen and A. Moser, "Simulation of a multiple-nozzle diffuser," in *12th*

AIVC Conference on Air Movement and Ventilation Control within Buildings, 1991, pp. 1–13.

[62] C. Topp, R. L. Jensen, D. N. Pedersen, and P. V. Nielsen, "Validation of Boundary Conditions for CFD Simulations on Ventilated Rooms," in *4th International Conference on Indoor Air Quality, Ventilation & Energy Conservation in Buildings, IAQVEC 2001*, 2001, pp. 295–302.

[63] Wikipedia, "Permeability," 2016. [Online]. Available: https://en.wikipedia.org/wiki/Permeability_(earth_sciences).

[64] C. Zhang, Q. Chen, P. K. Heiselberg, and M. Z. Pomianowski, "Airflow Pattern and Performance Analysis of Diffuse Ceiling Ventilation in an Office Room using CFD Study," in *Building Simulation Conference*, 2015.

[65] C. A. Hviid and S. Terkildsen, "Experimental study of diffuse ceiling ventilation in classroom," in *33rd AIVC conference, 2nd TightVent conference*, 2012.

[66] C. Zhang, P. Heiselberg, Q. Chen, M. Pomianowski, and T. Yu, "Numerical study of an integrated system with diffuse ceiling ventilation and thermally activated building constructions," 2016.

[67] C. Zhang, P. Heiselberg, Q. Chen, and M. Pomianowski, "Numerical analysis of diffuse ceiling ventilation and its integration with a radiant ceiling system," *Submitt. to Build. Simul.*, 2016.

[68] I. ANSYS, *ANSYS FLUENT User's Guide*. 2009.

[69] J. Srebric and Q. Chen, "An example of verification , validation , and reporting of indoor environment CFD analyses (RP-1133)," *ASHRAE Trans.*, vol. 108, no. 2, pp. 185–194, 2002.

[70] ASHRAE, *2009 ASHRAE Fundamentals Handbook (SI)*. 2009.

[71] Q. Chen, "Comparison of Different K-E Models for Indoor Air Flow Computations," *Numer. Heat Transf. Part B Fundam. An Int. J. Comput. Methodol.*, vol. 28, no. 3, pp. 353–369, 1995.

[72] Y.-T. Yang and C.-H. Chen, "Numerical simulation of turbulent fluid flow and heat transfer characteristics of heated blocks in the channel with an oscillating cylinder," *Int. J. Heat Mass Transf.*, vol. 51, no. 7–8, pp. 1603–1612, 2008.

REFERENCES

[73]   S. Petersen, N. U. Christensen, C. Heinsen, and A. S. Hansen, "Investigation of the displacement effect of a diffuse ceiling ventilation system," *Energy Build.*, vol. 85, pp. 265–274, 2014.

[74]   R. Harish and K. Venkatasubbaiah, "Numerical simulation of turbulent plume spread in ceiling vented enclosure," *Eur. J. Mech. B/Fluids*, vol. 42, pp. 142–158, 2013.

[75]   K. Venkatasubbaiah and Y. Jaluria, "Numerical Simulation of Enclosure Fires with Horizontal Vents," *Numer. Heat Transf. Part A Appl.*, vol. 62, no. November, pp. 179–196, 2012.

[76]   H. B. Awbi, *Ventilation Systems- Design and Performance*. Taylor & Francis, 2008.

[77]   N. Artmann, H. Manz, and P. Heiselberg, "Climatic potential for passive cooling of buildings by night-time ventilation in Europe," *Appl. Energy*, vol. 84, no. 2, pp. 187–201, Feb. 2007.

PUBLICATIONS FOR THE THESIS

Thesis Title: Diffuse Ceiling Ventilation – Air Distribution and Thermal Comfort

Name of Ph.D. Student: Chen Zhang

Name of Supervisors: Professor Per Heiselberg and Associate Professor Michal Pomianowski

List of Publications:

1. C. Zhang, P. Heiselberg, and P. V Nielsen, "Diffuse Ceiling Ventilation : A Review," International Journal of Ventilation, vol. 13, no. 1, pp. 49–64, 2014.

2. C. Zhang, P. K. Heiselberg, M. Pomianowski, T. Yu, and R. L. Jensen, "Experimental study of diffuse ceiling ventilation coupled with a thermally activated building construction in an office room," Energy and Buildings, vol. 105, pp. 60–70, 2015.

3. C. Zhang, Q. Chen, P. K. Heiselberg, and M. Z. Pomianowski, "Airflow Pattern and performance analysis of diffuse ceiling ventilation in an office room using CFD Study," Proceedings of Building Simulation Conference IBPSA 2015, p925-932, 2015.

4. C. Zhang, M. H. Kristensen, J. S. Jensen, P. K. Heiselberg, R. L. Jensen, and M. Pomianowski, "Parametrical analysis on the diffuse ceiling ventilation by experimental and numerical studies," Energy and Buildings, vol. 111, pp. 87–97, 2016.

5. Paper 5: C. Zhang, P. Heiselberg, Q. Chen, M. Pomianowski, and T. Yu, "Numerical analysis of diffuse ceiling ventilation and its integration with a radiant ceiling system," Submitted to Building Simulation, 2016.

This thesis has been submitted for assessment in partial fulfilment of the PhD degree. The thesis is based on the submitted or published scientific papers which are listed above. Parts of the papers are used directly or indirectly in the extended summary of the thesis. As part of the assessment, co-author statements have been made available to the assessment committee and are also available at the Faculty. The thesis is not in its present form acceptable for open publication but only in limited and closed circulation as copyright may not be ensured.

Appendix A. Diffuse Ceiling Ventilation : A Review

Paper 1

Diffuse Ceiling Ventilation - A Review

Chen Zhang, Per Heiselberg and Peter V. Nielsen

Department of Civil Engineering, Aalborg University, Sohngaardsholmsvej 57,
DK-9000 Aalborg, Denmark

Abstract

As a novel air distribution system, diffuse ceiling ventilation combines the suspended acoustic ceiling with ventilation supply. Due to the low-impulse supply from the large ceiling area, the system does not generate draught when supplying cold air. However, heat sources play an important role on thermal comfort in the occupant zone. Another characteristic of this system is its lower pressure drop compared with conventional ventilation systems, which reduces the noise problem and, at the same time, the energy consumption of the fan can be reduced. This review is based on a number of experimental and numerical studies on diffuse ceiling ventilation. Performance in terms of thermal comfort, air quality, pressure drop as well as radiant cooling potential are examined. Finally, a discussion on the proper design of the suspended ceiling and plenum to achieve a uniform air distribution and surface temperature as well as optimizing the radiant cooling potential by combining with thermal mass is conducted and gives a direction for further investigation.

Key words: diffuse ceiling, thermal comfort, indoor air quality, design chart.

1. Introduction

The main purpose of ventilation systems in buildings is to supply fresh air to the occupants and remove heat, gases and particulates from the building. In addition to these basic requirements, ventilation systems must be energy efficient and provide a high level of thermal comfort. The most widely used non-residential ventilation systems are based on mixing ventilation and displacement ventilation, as shown in Figure 1 (a), (b). In mixing ventilation, the air is supplied to the room at high initial velocity and turbulence. This promotes good mixing with uniform temperature and pollution distribution in the occupied zone. In contrast, the principle of displacement ventilation is to replace but not to mix the room air with fresh air, where the fresh and cold air is supplied close to the floor. Therefore, the highest velocity and the lowest temperature occur near the floor and a vertical temperature gradient exists in the room (Nielsen, 2001). Jacobs et al. (2009) note that, in the case of high ventilation demand and cold supplied air, draught always occurs for these two ventilation systems due to flow concentration at the air inlets.
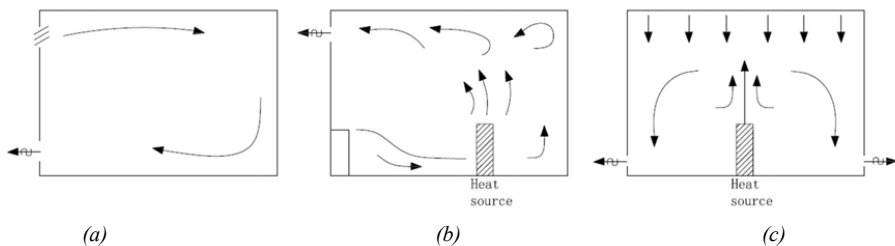

Figure 1. Three different types of air distribution systems:
(a) mixing ventilation, (b) displacement ventilation, (c) diffuse ceiling ventilation.

A novel solution is diffuse ceiling ventilation, Figure 1(c), where the space above a suspended ceiling is used as a plenum and fresh air is supplied to the occupied zone through perforations in the suspended acoustic ceiling. Because of the low-impulse supply from the ceiling area, the system does not generate draught from cold supply air. A common application is in livestock buildings. In Denmark, approximately 90% of livestock buildings are ventilated by diffuse ceiling inlets. This is because it provides fresh air to the animals at a high level of thermal comfort and at low energy and investment cost (Jacobsen, 2008). This ventilation concept is also used in special applications such as clean rooms where high ventilation effectiveness is required (see Nielsen, 2001; Brohus et al., 2004; Chow et al., 2004). However in this case the air change rate is high (50 to 100 h^{-1}) giving a high supply momentum flow and unidirectional flow in the room. Currently the application of the diffuse ceiling concept in spaces occupied by human beings is quite limited.

Studies of diffuse ceiling ventilation systems mainly use two approaches i.e. experimental and numerical. Experimental studies are normally carried out in climate chambers where certain boundary conditions are set up (Fan et al., 2013; Hviid et al., 2013; Nielsen et al., 2010; Jacobs et al., 2008; Chodor and Taradajko, 2013; Yang, 2011). There are also some monitoring studies that have measured performance under real operational conditions (Jacobs et al., 2008, 2009; Hviid et al., 2012). Different designs of diffuse ceiling ventilation systems, in terms of shape, material, porosity of the ceiling tiles as well as the airflow distribution are documented in these studies. Measurement results have been used to evaluate the thermal comfort, air quality and energy efficiency of the systems. Compared with numerical modelling, the results obtained by experimental studies are considered to be more reliable. However, numerical research is characterized by its low cost and time efficiency. Also boundary conditions can be easily changed to study different scenarios. Numerical simulations include investigation of fluid flow by CFD (Fan et al., 2013; Nielsen et al., 2010; Chodor and Taradajko, 2013; Yang, 2011) and heat transfer and energy performance by dynamic building simulation tools (Hviid, 2011). In addition to these two approaches, a design chart method based on the "flow element" theory has been created, which is based on analysis of measurement results or predicted results of validated CFD models (Fan et al., 2013; Nielsen et al., 2009). The design chart approach can serve as a guideline for the design and dimensioning of diffuse ceiling ventilation systems.

This paper aims to provide a critical review of diffuse ceiling ventilation systems based on the most current research results from laboratory field experiments and simulation studies. First of all, the air distribution patterns and various types of diffuse ceiling inlet are summarized to provide a good knowledge about this air distribution system. Secondly, the performance of diffuse ceiling ventilation is analysed in terms of thermal comfort, air quality, energy efficiency (minimising pressure drop) as well as its radiant cooling potential. Finally, a discussion is conducted regarding the design chart method and its application as well as the effect of the plenum and suspended ceiling on system performance and condensation issues.

2. Characteristics of Diffuse Ceiling Ventilation

2.1 General Description

A diffuse ceiling ventilation system uses the open space between the ceiling slab and suspended ceiling as a plenum to deliver conditioned air. As there is a pressure difference between the plenum and the occupied zone, the air penetrates through the entire ceiling into the occupied zone. This concept is characterized by the large ceiling area used as the supply opening. Thus, air flows into the occupied zone at low velocity and with no fixed jet direction, hence the name "diffuse". This system has the potential to reduce draught risk in the occupied zone, even when supplying cold air. Instead, it is the convective flows generated by the heat sources such as people, equipment or windows that generates a risk of draught in the occupied zone (Nielsen et al., 2009).

2.2 Air Distribution Pattern

The air distribution patterns in rooms with diffuse ceiling inlets may be controlled either by buoyancy flows from heat sources or by momentum flow depending on the air change rate (see Nielsen, 2001 and Figure 2). In the case of an air distribution pattern controlled by momentum flow a high air change rate is needed (e.g. 50 - 100 h^{-1}), which creates piston-flow. This air distribution concept is especially applied in clean room where very high
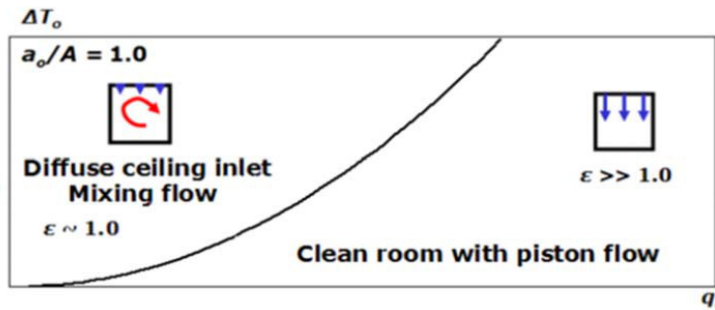
Figure 2. Diffuse ceiling ventilation presented on a q-ΔT graph (Nielsen, 2001).

ventilation effectiveness is expected. Nielsen (2001) also mentioned that low return openings are required in this case.

For air change rates in the range1 to 15 h^{-1}, the air distribution pattern in the room is controlled by buoyancy flows, and this could be defined as mixing ventilation because the ventilation effectiveness is close to one when a heat load is present. For this situation Hviid et al. (2012) state that the ventilation effectiveness of diffuse ceiling ventilation is comparable to conventional mixing ventilation, which is generated by the convective plumes of the heat load. The main advantage of this air distribution system is that it can handle high heat load without significant draught, because the air flow is determined by the heat sources and not by momentum flow from the supply openings. This characteristic makes the concept especially suitable for buildings requiring high cooling demand and high thermal comfort levels such as in offices or classrooms. In this paper, special attention is given to the buoyancy control of the air distribution pattern, due to its wide application potential.

2.3 Types of Diffuse Ceiling Inlet

The design of diffuse ceiling inlets such as the shape and material of ceiling tiles, perforation patterns and ceiling suspensions, etc. has a significant influence on the performance of ventilation systems. As illustrated in Table 1, diffuse ceiling inlets can be generally divided into three types based on their air path. In the first type, the diffuse ceiling is made of ceiling tiles which are impermeable to air. In this case air is supplied through connection slots between tiles (crack flow) thus forming micro-jets

that will generate high local entrainment. Consequently, the ceiling installation determines the connections, the slot locations and micro-jet characteristics that will potentially affect ventilation performance. This type of diffuse ceiling inlet was analyzed by Nielsen et al. (2010) in a full-scale experiment in a one person office. Smoke experiments showed that high velocity with high entrainment took place in micro-jets below the ceiling penetrating to a depth of 0.25 m into the room. Therefore, a distance of at least 0.25 m from the occupied zone to the ceiling surface is needed. Linear micro-jets were also observed at both ends of aluminium lamellae by Fan et al. (2013).

The second type of inlet consists of perforated ceiling tiles which are permeable to air. Thus, the air is supplied through ceiling perforations as well as connection slots. The air flow pattern of this inlet approach is strongly dependent on the connection profiles and the perforation profiles. Hviid et al. (2013) carried out an experimental study on two types of perforated suspended ceiling (aluminium and gypsum), as illustrated in Table 1. The aluminium tiles were fixed by pushing taps into the suspension profile, while the gypsum tiles were connected by a reverse T-profile. By comparing the volume flow at the same pressure drop for a single tile and for the mounted suspended ceiling, the crack flow for the aluminium and gypsum ceiling was estimated to constitute 17% and 64% of the total flow, respectively. The different crack flow rates were attributed to the different connection profiles i.e. the more airtight the connection, the lower the crack flow. The influence of perforated area ratio was investigated by Jacobs et al. (2008) in a pilot study of a classroom by comparing two

Table 1. Three types of diffuse ceiling inlet based on air path and their examples.

Type	Example inlet	Description	Reference
High local entrainment		• Impermeable mineral wool acoustic tiles • 50 mm thickness	Niesen et al. (2010)
		• Impermeable aluminium lamellae • 15 mm mineral wool acoustic plates above lamella	Fan et al. (2013)
High local entrainment		• Aluminium acoustic tiles • 0.6 mm thickness Circle perforation: $\Phi = 2.5$ mm, pitch 5.6 mm • Degree of perforation 16.2%	Hviid and Svendsen (2013)
		• Gypsum acoustic tiles • 12.5 mm thickness Hexagon perforation: $\Phi = 11$ mm, pitch 20 mm • Degree of perforation 17%	Hviid and Svendsen (2013)
		• Large perforations: $\Phi = 25$ mm, pitch 5300 mm • Degree of perforation 0.5%	Jacobs et al. (2008)
		• Small perforations: 12 x 12 mm, pitch 25 mm • Degree of perforation 18%	Jacobs et al. (2008)
Low local entrainment		• Perforated structure • Three layer Base layer 25mm Diffusive layer, 3 mm paint layer	Chodor and Taradajko (2013)

perforated ceilings with ventilation grilles. One ceiling tile had large perforations, where the perforation diameter was 25 mm and the perforated area ratio was 0.5%. The other has small perforations, where the perforation was 12 x 12 mm^2 and the perforated area ratio was 18%. The measurement results indicated that the diffuse ceiling with the large perforated area ratio contributed to lower draught risk in the occupied zone. However, both showed better thermal comfort than ventilation grilles.

The third type of inlet is the 'fully diffuse ceiling'. This type of inlet is made of perforated material instead of consisting of ceiling tiles Therefore no connection slots exist. The advantage of this type of diffuse ceiling is an aesthetic aspect without any visible diffusers. The air penetrates through the entire ceiling area. Thus the air velocity is very small and no micro-jet is present and hence there is low local entrainment. This type of diffuse ceiling was was investigated by Chodor and Taradajko (2013) as a possible application for Oslo National Museum. As illustrated in Table 1, the diffuse ceiling is made of large particles with diameter

varying between 1 to 2 mm. The particles are connected with each other to form a 25 mm layer. The results showed that a higher pressure drop was generated by this type of ceiling construction, with a value of between 20 and 107 Pa for an airflow rate between 5 to 20 l/s.m^2. Jensen et al. (2012) conducted airflow tests on 10 'Fully diffuse ceiling' samples and the results indicated that the pressure drop could vary considerably depending on the thickness and type of diffusive layer, coating and paint layer. A detailed introduction of pressure drop is discussed in the following section.

As well as single type designs, some diffuse ceiling ventilation systems are designed by combining several inlet types. Hviid et al. (2012) presented an experimental study in a real classroom, where two types of ceiling tiles were used: active and passive. The active tiles of cement bonded wood-wool were permeable while the passive tiles incorporated impermeable mineral wood glued to the back. The active panels were non-uniformly placed and covered 13% of whole ceiling area while the remaining area incorporated the passive panels. The experimental results indicated that the mineral wool

Table 2. Tested conditions of different studies.

References	Case	Flow rate (l/s.m^2)	Heat load (W)	Supply temp. (°C)
Fan et al. (2013)	1	3.4	670	16.7
	2	4.96	1137	17.2
Hviid & Svendsen (2013)	1	1.85	1080	-3.2
	2	2.45	1080	3.2
	3	4.86	1080	11.2
Nielsen et al. (2010)	Cooling 1	5.4	1 mankin, 1 PC, 1 lamp	N/A
	Heating 1	2.38	0	N/A
	Heating 2	4.08	0	N/A
Nielsen and Jakubowska (2009)		1.9-7.3	480	ΔT_0=12-3.5
Jacobs et al. (2008)	Floor heating 1	3.12	750	N/A
	Radiator 1	3.12	750	N/A
	Floor heating 2	6.24	750	N/A
	Radiator 2	6.24	750	N/A
Chodor and Taradajko (2013)		5.0-20.0	1000-2000	4.8-15.7
Hviid (2011)	1	2.23		10
	2	2.23	24 pupils+ 1 radiator	17
	3	4.46	(1100 W) + light (324 W)	10
	4	4.46		17

layer improved the acoustic properties and permitted control of the supply air distribution in the room. From infrared pictures, it was clearly observed that the active panels had a lower surface temperature than the passive panels.

3. Performance Evaluation

Performance studies on diffuse ceiling ventilation systems can be generally grouped in the following four aspects:

- Thermal comfort: air temperature gradient, draught and radiant asymmetry;
- Indoor air quality: ventilation effectiveness and air exchange efficiency;
- Pressure drop and its effect on energy consumption;
- Radiant cooling potential.

These aspects are discussed below and are based on a number of experimental and simulation results. The tested conditions of different studies are presented in Table 2.

3.1 Thermal Comfort

The air distribution system needs to be designed for high thermal comfort. Therefore, it is important that the occupied zone has the optimum climate with respect to air temperature, draught level, and asymmetric radiant temperature. ISO 7730 (2005) specifies the design criteria for different types of spaces, where category B for types of rooms such as single and landscaped offices, classrooms and conference rooms are addressed in this paper.

3.1.1 Air Temperature Gradient

Temperature stratification that results in the air temperature at head level being higher than at ankle level may cause thermal discomfort. In order to avoid discomfort, ISO 7730 (2005) gives the limitation of temperature difference between ankle level and head level (0.1 – 1.1 m above floor) as less than 3 K for Category B.

Diffuse ceiling ventilation can provide good mixing of room air, as has been addressed by a number of studies, and consequently a low risk of discomfort caused by vertical temperature gradient has been reported. Fan et al. (2013) analyzed the temperature gradient of a climate chamber using both experimental measurements and CFD simulations. The results showed that there was 1 K temperature difference from floor to ceiling for two scenarios corresponding to an equivalent temperature gradient of 0.3 K/m. A similar finding was reported by Hviid et al. (2013) who showed that the vertical temperature gradient between head and ankle height was approximately 0.5 K.

Nielsen et al. (2010) measured the vertical temperature gradients in an office for both cooling and heating cases. Their study proved that there is a small vertical temperature gradient in the cooling case, where the temperature difference between head and ankle level was less than 1 K. In the heating case, which looked at a night situation without any heat load in the room, a high vertical temperature gradient was observed and the temperature difference between head and ankle level reached 2.5 K. However, this was still within the limitations of Category B. It should be noted that the absence of heat loads in the occupied zone minimizes the mixing flow in the room. Thus, in the heating case, using diffuse ceiling ventilation, it is always recommended to use a convector or a floor heating system for heating.

3.1.2 Draught

Draught is defined as an unwanted local cooling of the body caused by air movement (Fanger et al. 1988). This is one of the most common causes of complaint in ventilated or air conditioned buildings. The draught rate (DR) is determined by local air temperature, local mean air velocity and local turbulence intensity.

The DR by diffuse ceiling ventilation was explored by Fan et al. (2013) at three heights: 0.1 m, 1.1 m (for a seated person) and 1.7 m (for a standing person) and for two airflow rate scenarios (Table 2). The highest DR was found to be 7% for the high airflow rate scenario of 4.96 l/s.m^2. This was well within the maximum limit set by environment category B of 20%. This finding was in good agreement with the investigations carried out by Nielsen et al. (2009) and Hviid et al. (2013), which conclude that the use of a diffuse ceiling as the air terminal device can provide a draught free indoor environment, even under high airflow rate. Furthermore, the highest risk of draught was found at ankle level, which corresponds well with the finding that maximum velocity in the occupied zone is located close to the floor.
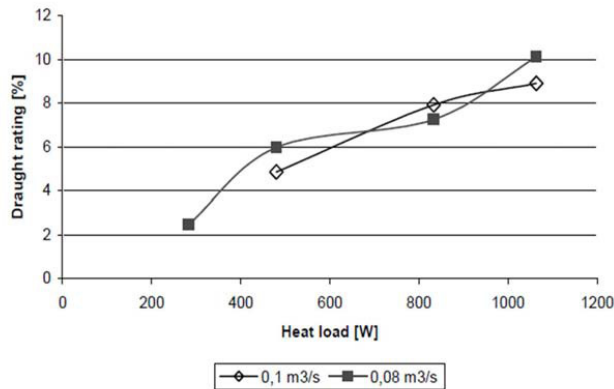
Figure 3. Draught rating for different heat loads (Jakubowska, 2007).

A parametric analysis was carried out to investigate the influences of ventilation flow rate on DR for a room equipped with diffuse ceiling ventilation (Fan et al., 2013). The results indicated that there was no clear dependence of DR on ventilation flow rates within the range 1.48 to 11.62 l/s.m². This finding was confirmed by Nielsen et al. (2009), who showed that the DR is, to some extent, independent of the supply flow, because the momentum of supply flow is very low. On the other hand, the influence of total heat load (including human and equipment heat load) on the DR was investigated by Jakubowska (2007). This showed that the DR at ankle level for four heat load conditions (283 W, 480 W, 833 W and 1063 W) depended on heat load and draught. As illustrated in Figure 3, the DR increased from 2% to 10% when the heat load increased from 283 W to 1063 W, but the difference due to flow rates was insignificant. Thus, it can be deduced that the diffuse ceiling ventilation does not generate draught by itself; instead, it is the heat sources that cause the draught in the occupied zone. Moreover, the importance of heat sources was investigated by Hviid (2010) who used CFD simulations to indicate that thermal plumes force the supply air to regions with no heat sources, leading to cold downdraught and a risk of draught in those regions. The same phenomenon was also found by Chodor and Taradajko (2013).

3.1.3 Radiant Temperature Asymmetry

Differences in room enclosure temperatures can lead to thermal discomfort due to radiant asymmetry, even when the mean radiant temperature is within

acceptable limits (Fanger et al,. 1985). However, occupants are less sensitive to radiant asymmetry caused by cool ceilings than warm ceilings or cool walls (windows). The radiant temperature asymmetry for cool ceiling should be less than 14 K to satisfy indoor environment category B (ISO 7730, 2005).

The temperature difference between the suspended ceiling and other surrounding surfaces increases with the reducton of supplied air temperature, as reported by Hviid et al. (2013). They measured the surface temperature of aluminium and gypsum ceilings for three test conditions (Table 2), and the results show that the maximum temperature asymmetry of the cold ceiling was approximately 6 K when the supply temperature was -3.2 °C.

Chodor and Taradajko (2013) confirmed that radiant asymmetry caused by a cool ceiling did not generate a notable amount of percentage dissatisfied occupants. They measured the temperature asymmetry ranging from 1.5 K to 8.4 K depending on different heat load and flow rate conditions, which are clearly within the limit value of 14 K. They also pointed out that the lowest temperature asymmetry, 1.5 K, occurred when the only heat source was from lighting (heat load of 1000 W) in the room.

3.2 Indoor Air Quality

The parameters used to evaluate indoor air quality include ventilation effectiveness and air exchange efficiency. Ventilation effectiveness describes how

efficiently the ventilation system removes the indoor contaminants from the occupied zone and how certain areas are influenced by contaminant sources in the room, which is calculated using Equation (1).

$$\varepsilon = \frac{C_R - C_o}{C_{oc} - C_o} \tag{1}$$

Where C_R, C_o and C_{oc} are the contaminant concentration in the return opening, contaminant concentration in the supply opening and contaminant concentration in the occupied zone. The ventilation effectiveness depends on the air distribution system and the location of the pollution sources in the room. If there is complete mixing of air and pollutants, the ventilation effectiveness is one.

The ventilation effectiveness was analyzed by means of tracer gas measurements. Fan et al. (2013) reported that the ventilation effectiveness by diffuse ceiling ventilation is between 0.9 and 1 in the breathing zone and in the middle of the room for the two air change rate scenarios given in Table 2. These results correspond well with the studies of (Nielsen et al., 2010: Chodor and Taradajko, 2013; Nielsen et al., 2009). This means that rooms equipped with diffuse ceiling ventilation can generate good mixing in the occupied zone by convective flow. In addition, the results indicated that ventilation flow rate has a limited influence on ventilation effectiveness in the case of non-isothermal load.

Another indoor air quality index is air exchange efficiency, ε^a, which shows how fast the air is exchanged in a ventilated room. This is a measure of the average time it takes to replace the air in the room $\overline{\tau_r}$ compared to the theoretically shortest possible air change time τ_n, and is expressed by Equation (2):

$$\epsilon^a = \frac{\tau_n}{\overline{\tau_r}} \times 100\% \tag{2}$$

The actual air change time $\overline{\tau_r}$ can be derived from the room mean age of air $\overline{\tau}$ by:

$$\overline{\tau_r} = 2\overline{\tau} \tag{3}$$

The air exchange efficiency is dependent on the air distribution system in the room, geometry of the room and location of heat source, but it is not dependent on the location of the contaminant sources. Hviid et al. (2013) investigated the air exchange efficiency and the results support the good mixing finding as mentioned above. Also there was no evidence of any stagnant zone or short-circuiting ventilation in the room.

3.3 Pressure Drop and its Effect on Energy Consumption

Normally, it is preferable to reduce pressure drop across the diffuser to avoid noise problems and reduce fan power consumption. As documented by several studies (Jacobs et al., 2009; Fan et al., 2013; Hviid et al., 2013; Yang, 2011; Jakubowska, 2007), one advantage of the diffuse ceiling as an air terminal device is the low pressure drop.

Figure 4 illustrates the pressure drop across different diffuse ceiling constructions (see Table 3), as a function of airflow rate. It can be observed that there is a large variance on pressure drop for different types of diffuse ceiling inlet. Diffuse ceiling inlet type 1 (mineral wool ceiling, aluminium lamella ceiling) and type 2 (Alu-16 and Gyp-17 ceiling) show very low pressure drops of less than 5 Pa for airflow rates ranging from 1 l/s.m^2 to 10 l/s.m^2. However, the pressure drops across different 'fully diffuse ceiling' (FDC) samples show a large span

Table 3. The diffuse ceiling types used in pressure drop measurements.

References	Diffuse ceiling type
Fan et al. (2013)	Aluminium lamellae
Hviid and Svendsen (2013)	Aluminium tiles (open area 16%)
	Gypsum tile (open area 17%)
Jensen et al. (2012)	Ten 'Fully diffuse ceiling'(FDC) samples
Jakubowska (2007)	Mineral wool panels and profiles
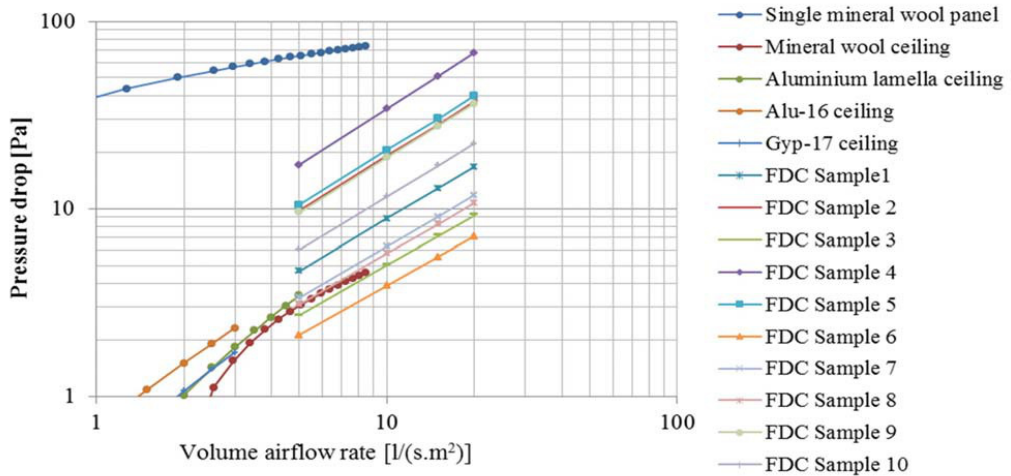
Figure 4. Pressure drop for different diffuse ceiling types.

ranging from 5 Pa to 70 Pa when the airflow rate is 20 l/s.m². The large span of possible variation on the 'fully diffuse ceiling' is attributed to different thicknesses and types of diffusive layer, as well as the coating and paint layers. Generally, most of 'fully diffuse ceiling' samples showed higher pressure drop then the other types of diffuse ceiling inlet.

In addition, the connection profile has been found to have a significant impact on the pressure drop of diffuse ceiling systems. A proper connection profile can reduce the pressure drop and control the air distribution over the ceiling. As reported by Jakubowska (2007), the pressure drop from a single mineral wool panel was very high due to the high resistance of the material. In this example a pressure drop of 74 Pa was reached for an airflow rate of 8.5 l/s.m² (see Figure 4). However, the pressure drop reduced to 5 Pa when measured over the whole diffuse ceiling system. This was due to almost all the airflow penetrating through the connection slots instead of ceiling panels. A similar study was made by Hviid et al. (2013) who found that 64% of the airflow was through the connection slots for the gypsum ceiling and 17% for the aluminium ceiling. Thus, it can be concluded that major factors influencing pressure drop are the diffuse ceiling inlet type, porosity and air tightness of connections as well as the suspension system.

The pressure drop across the ventilation system is a dominant parameter of fan energy consumption. Jacobs et al. (2009) described two field studies of classrooms with diffuse ceiling ventilation systems: Sliedrecht primary school and Tilburg primary school. The air was distributed by 25 mm perforations of pitch 300 mm drilled in the existing ceiling tiles, and was discharged through the façade in the first case and to an atrium in the second case. By comparing with traditional and modern ventilation systems for schools in the Netherlands (Railio et al., 2007), they found that the specific fan power (SPF) and energy cost of diffuse ceiling systems were considerably lower than other ventilation systems, as shown in Table 4. In addition, they pointed out that the investment cost for implementing diffuse ceiling ventilation in an existing classroom is very low because air ducts were not needed and the existing suspended ceiling could be used.

3.4 Radiant Cooling Potential

A radiant cooling system refers to a temperature-controlled surface that cools indoor temperatures by removing sensible heat (ASHRAE, 2000) and which relies on the process of radiant heat flow from heated objects and occupants to the cooled surface. Different from other air distribution devices, diffuse ceiling inlets have radiant cooling potential due to

Table 4. Comparison of specific fan power (SPF) and electricity consumption of different ventilation systems. Occupancy 1040 h/a, flow rate 200 dm3/s, electricity costs 0.2 euro/kWh (Jacobs and Knoll, 2009).

Systems	SPF [kW/m^3/s]	Electricity costs [€/a]
Traditional system	5 - 10	290
Modern system	2 – 2.5	90
Primary shool Sliedrecht	0.04	2
Primary shool Tilburg	0.5	20

their large supply area and low surface temperature. Consequently, instead of removing the entire heat load by cold air, a part of the sensible heat load can be removed by the cold suspended ceiling panel.

Hviid et al. (2013) measured the suspended ceiling surface temperature in three scenarios with air flow rates from 1.85 to 4.86 l/s.m^2 and supply air temperature from -3.2 °C to 11.2 °C. The results showed that the ceiling surface temperature was in the range of 14.3 to 17.7 °C. The low surface temperature increases radiant heat transfer between the ceiling and other warm surfaces in the room. Additionally, the radiant heat transfer not only occurs between the suspended ceiling and room surfaces, but also occurs between the ceiling slab, plenum surface and supply air. In this study, the preheating effect of the plenum was significant for low temperature supply, where the supply air temperature increased by 12.9 °C in the plenum (from -3.2 °C to 9.7 °C). This phenomenon indicates that the occupied zone is at low draught risk regardless of the supply air temperature because the radiant cooling part increases relatively over the convective part. Hviid (2011) also investigated the radiant cooling potential by comparing the simulated thermal indoor environment for two ventilation strategies (diffuse ceiling ventilation and mixing ventilation). The results showed that the diffuse ceiling ventilation results in a 1 K lower operative temperature than mixing ventilation.

The radiant effect was also analysed by Chodor and Taradajko (2013) by calculating the radiant heat transfer to the diffuse ceiling. In their study, the heat transfer to the diffuse ceiling by radiation was approximately 510 W when the heat load in the room was 2000 W, which means that 25% of the heat load is eliminated by radiation.

4. Discussion

4.1 Design Chart

When designing a ventilation system, one important task is to find the limits of flow rate to the room and the temperature difference between supply and return air that provides both sufficient cooling capacity while maintaining an acceptable comfort level. In order to make decisions more clearly, a design chart was developed and used to compare different systems and to find the optimal solution to satisfy requirements (Nielsen, 2007). The resultant chart is expressed as a q_0 - ΔT_0 chart. The limits for the design chart consist of maximum air velocity in the occupied zone, maximum vertical temperature gradient, and minimum flow rate to obtain air quality. In addition, sometimes, other restrictions are applied including maximum cooling capacity, minimum supply temperature (when outdoor air is used for cooling), and the maximum flow rate associated with acceptable noise level.

A design chart for a diffuse ceiling inlet was developed by Fan et al., (2013) based on their particular experimental setup. From Figure 5, the vertical line on the left represents the minimum flow rate to satisfy indoor air quality, while the vertical line on the right is the limit of the system capacity which corresponds to an air change rate of 6 h^{-1} for a traditional design office building. The horizontal line represents the maximum temperature difference in order to avoid condensation in the duct systems. Condensation in the duct system or suspended ceiling is an important problem in densely occupied room, such as classrooms. The curved line represents the flow rate and temperature difference within the design range for a constant heat load limit of 30 W/m^2. These four lines enclose an area
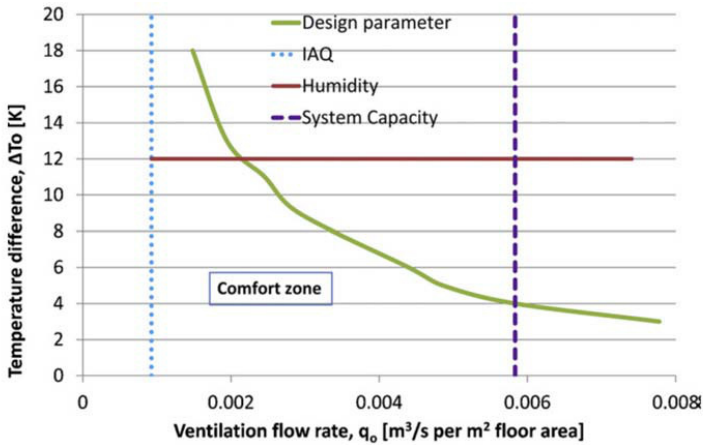
Figure 5. Design chart for the diffuse ceiling ventilation system(Fan et al. 2013).
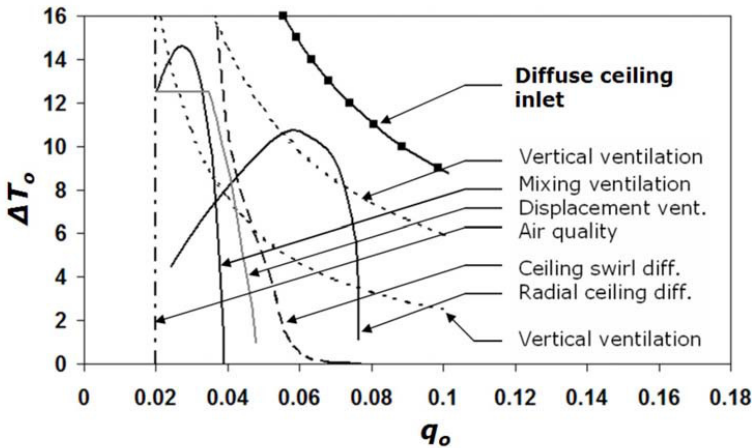
Figure 6. Design chart for a diffuse ceiling inlet and five other air distribution systems.
(Nielsen and Jakubowska 2009).

representing the comfort zone for diffuse ceiling ventilation.

It is possible to make a direct comparison between different air distribution systems by means of a design chart. As shown in Figure 6, the performance of a diffuse ceiling inlet and five other air distribution systems are compared (Nielsen et al., 2009). The design chart was drawn based on the experimental results obtained by testing different air distribution systems for the same room and same heat load. This shows that the diffuse ceiling inlet is

able to handle the highest load compared to all the other systems. In addition, the draught limit of the diffuse ceiling inlet is close to a line representing a constant load of approximately 1100 W (72 W/m²). This is because the draught is generated by the thermal plume, which is independent of the flow rate and temperature difference.

4.2 The Effect of Plenum and Suspended Ceiling

The use of a ceiling plenum to deliver conditioned air directly into the occupied zone is one of the key features that distinguishes diffuse ceiling ventilation from conventional ducted air distribution systems. The plenum is the space between the ceiling slab and the suspended ceiling, which can operate as pressurized or at zero pressure. A pressurized plenum has a small positive static pressure applied which is created by a central fan in the air-handling unit or by wind and buoyancy effect generated by temperature differences. In the case of a zero-pressure plenum, the air is exhausted from the conditioned space using an extractor fan which creates a negative pressure in the space. Thus, the pressure difference between plenum and conditioned space will drive the air through a diffuse ceiling. The pressurized plenum has advantages of simplicity and low installation costs. However, there is evidence from some completed projects that uncontrolled air leakage from a pressurized plenum can impair system performance (Valadez, 2013). However, since the pressure in a diffuse ceiling ventilation system is relatively low, proponents of the pressurized plenum approach claim that leakage is minimal, and much of the leakage will be into the same zone as the conditioned space.

Since the pressure difference between the plenum and conditioned space is low and convective currents are strong, two directional flows may occur and cause a warm air buffer to form in the plenum. This reverse flow may raise hygiene problems if particulate matter deposits in the plenum (Hviid et al., 2013). Reverse flow across the perforated ceiling was investigated by Hviid et al. (2013) using tracer gas. Results showed that only insignificant reverse flows were observed at a pressure drop of approximately 1 - 2 Pa. In this study, the sampling points in the plenum had almost identical concentration levels, even at the lowest inlet speed of 1.3 m/s, while the concentration in the plenum was slightly higher than the background level in the supply. This indicated that reverse flow was very low. Jakubowska (2007) also performed tracer-gas experiments, but did not observe reverse flows. In

these measurements the under pressure differences were approximately 1.5 - 4.5 Pa.

By distributing the supplied air via the plenum, continuous direct contact between the cold air and thermal mass of the ceiling slab occurs. This enables heat transfer to take place depending on the temperature difference and airflow rate. Various studies (Høseggen et al., 2009; Kolokotroni et al., 1998) have shown that thermal mass together with ventilation may reduce indoor maximum temperature and cooling demand. In addition, free night cooling with thermal mass can provide a heat sink during the following day (Artmann et al., 2008). However, in the case of diffuse ceiling ventilation, the thermal mass of the ceiling slab is encapsulated by the suspended ceiling. Høseggen et al. (2009) pointed out that the suspended ceiling decreases night free cooling significantly and also increases the number of hours with excessive temperature considerably. Some studies have demonstrated that it is only necessary to partly cover the suspended ceiling to improve thermal cooling while still maintaining acceptable acoustic conditions. Jensen et al. (2012) and Weitzmann (2008) show that even a large covering percentage still gives significant cooling from the ceiling. However, this solution, when integrated with a diffuse ceiling ventilation system, still needs further investigation. In addition, the heat exchange between supply air and thermal mass of the concrete slab and suspended ceiling may influence supply air temperature variations as a function of distance travelled through the plenum (Bauman, 2013).

In the design of the plenum, the primary objectives are to ensure:

· Generation of uniform air distribution through the entire ceiling area;

· Generation of uniform temperature distribution at the surface of the diffuse ceiling;

· Creation of a low momentum air supply in the occupant zone;

· Increase of heat transfer by activating the thermal mass.

The performance of plenum and diffuse ceiling systems are influenced by a number of design parameters such as: plenum height, the location and configuration of the inlet to the plenum, obstructions within the plenum and the covering percentage of the suspended ceiling, etc. For example, it was documented that the plenum depth is often

inadequate in the direction of airflow, which results in localized areas of high velocity flow (U of I Facilities Standards, 2011). However research regarding the plenum design of diffuse ceiling ventilation systems is quite limited and no design guide is available at present. Thus, further investigation should be conducted on the proper design of these parameters.

4.3 Condensation Problems

Since the diffuse ceiling has radiant cooling potential, condensation is also a problem faced by this technology. In humid climates a suspended ceiling surface can form condensation easily if humidity is not properly controlled in the room. The condensation of moisture will affect visual perception and function. Also, the surface of the ceiling can become wet and contaminated with dirt and micro-organisms. Condensation can drop from such ceilings forming "office rain" (Li et al., 2011). Condensation risk can be aggravated by reverse-flow in diffuse ceiling ventilation systems. Thus condensation will occur when high humidity and high temperature airflow from the conditioned space is forced back to condense on the back of suspended ceiling panels causing early failure.

In a humid climate, the largest source of moisture is the ventilation air from outside, which accounts for about 50 to 80% of the building moisture load in typical commercial buildings (Price HVAC, 2013). Therefore, it is essential that ventilation air is dehumidfied before being delivered to the plenum. On the other hand, the supply air temperature needs to be controlled to ensure that the suspended ceiling surface temperature is above the dew-point of the ambient air. In particular, the temperature of the cool ceiling surface should not be reduced below the limit of 15 °C (Stetiu, 1997) to ensure that the indoor air temperature is maintain within the range specified by EN 15251 (2007). In addition, proper control of the pressure of the plenum and correct design of the plenum and suspended ceiling may avoid reverse flow and associated condensation problems.

5. Conclusion

Based on the literature review, this study reaches several conclusions:

- The flow pattern of diffuse ceiling ventilation can be either buoyancy controlled or momentum

controlled, depending on the ventilation rate. However, the buoyancy controlled pattern has great potential for non-industrial applications because it is possible to handle high heat loads without generating draught.

- Based on the air path, diffuse ceiling inlets can be divided into three types: air supply through connection slots, air supply through both connection slots and perforated ceiling tiles, and air supply through a perforated ceiling. Micro-jets and high local entrainment may occur below connection slots, due to the relatively high air velocity. Therefore, a certain vertical distance should be kept between the occupied zone and the diffuse ceiling surface for the first two types of inlet.

- In rooms with diffuse ceiling ventilation, small vertical temperature gradients ranging from 0.3 to 1 K/m have been observed in the case of cooling, while values up to 2 K/m have been observed in the heating case. These values satisfy the requirement of ISO 7730 Category B. In addition, heat loads in the occupied zone can increase air mixing which is beneficial to thermal comfort. In the case of space heating, convector heating should be used.

- The diffuse ceiling as an air terminal device can provide a low draught risk to the indoor environment. The highest risk of draught is found at ankle level. Draught is independent of flow rate, but it is influenced by heat sources. It has been found that thermal plumes force the supply air to regions with no heat sources, leading to cold downdraught and risk of draught in those regions. Discomfort caused by radiant asymmetry of a cool ceiling can be negligible.

- The ventilation effectiveness of diffuse ceiling ventilation is comparable to perfect mixing ventilation. There is no stagnant zone or short-circuiting ventilation in a room with diffuse ceiling ventilation.

- Pressure drop is dependent on the design of the diffuse ceiling inlet. Parameters include shape, material, porosity of the ceiling and connection profile, etc. Generally, diffuse ceiling ventilation has a significantly lower pressure drop than conventional ventilation systems.

- Critical issues for future research include plenum design for uniform air distribution and

surface temperature, and suspended ceiling design to optimize the radiant cooling potential of thermal mass.

References

Artmann N, Manz H and Heiselberg P: () 2008 "Parameter study on performance of building cooling by night-time ventilation", *Renewable Energy*, **33**, (12), pp.2589-2598.

ASHRAE: (2000) "HVAC Systems and Equipment-Chapter 6: Panel Heating and Cooling Design".

Bauman FS: (2013) "Underfloor Air Distribution (UFAD) Design Guide", American Society of Heating, Refrigerating and Air-Conditioning Engineers Inc., USA.

Brohus H and Balling KD: (2004) "Local Exhaust Efficiency in an Operating Room Ventilated by Horizontal Unidirectional Airflow", In *Proceedings of Roomvent 2004, 9th international conference on Air Distribution in Rooms*. Coimbra, Portugal.

Chodor AD and Taradajko PP: (2013) Personal commonucation, Department of Civil Engineering, Aalborg University.

Chow TT and Yang XY: (2004) "Ventilation performance in operating theatres against airborne infection: review of research activities and practical guidance", *The Journal of Hospital Infection*, **56**, (2), pp85-92.

European Standard. EN 15251: (2007) "Indoor environmental input parameters for design and indoor air quality, thermal environment, lighting and acoustics".

Fan J, Hviid CA and Yang H: (2013) "Performance analysis of a new design of office diffuse ceiling ventilation system", *Energy and Buildings*, **59**, pp73-81.

Fanger PO et al.: (1988) "Air Turbulence and Sensation of Draught". *Energy and Buildings*, **12**, pp21-39.

Fanger PO et al.: (1985) "Comfort Limits for Asymmetric Thermal Radiation". *Energy & Buildings*, **8**, pp225-236.

Hviid CA: (2010) "Building integrated passive ventilation systems". PHD thesis, Department of Civil Engineering, Technical University of Denmark.

Hviid CA: (2011) "Integrated ventilation and night cooling in classrooms with diffuse ceiling ventilation!. In *11th Ökosan*. Graz.

Hviid CA and Svendsen S: (2013,) "Experimental study of perforated suspended ceilings as diffuse ventilation air inlets". *Energy and Buildings*, **56**, pp160-168.

Hviid CA and Terkildsen S: (2012) "Experimental study of diffuse ceiling ventilation in classroom". In *33rd AIVC conference, 2nd TightVent conference*. Copenhagen, Denmark.

Høseggen R, Mathisen HM and Hanssen SO: (2009). "The effect of suspended ceilings on energy performance and thermal comfort". *Energy and Buildings*, 41, (2), pp234-245.

International Standard. ISO 7730:2005 (2005) "Ergonomics of the thermal environment - Analytical determination and interpretation of thermal comfort using calculation of the PMV and PPD indices and local thermal comfort criteria".

Jacobs P and Knoll B: (2009) "Diffuse ceiling ventilation for fresh classrooms". In *4th International Symposium on Building and Ductwork Air tightness*. Berlin, Germany.

Jacobs P, Van Oeffelen ECM and Knoll B: (2008) "Diffuse ceiling ventilation, a new concept for healthy and productive classrooms". In *Indoor Air*. Copenhagen, Denmark,, pp17-22.

Jacobsen L: (2008) "Air Motion and Thermal Environment in Pig Housing Facilities with Diffuse Inlet". PHD thesis, Department of Civil Engineering, Aalborg University.

Jakubowska, E.M. *Air distribution in rooms with the diffuse ceiling inlet*. PHD thesis, Department of Civil Engineerging, Aalborg University,2007.

Jensen RL and Jensen LM: (2012) "Airflow test of acoustic board samples". DCE Contract Reports, Department of Civil Engineering, Aalborg University.

Jensen, Rasmus Lund et al. (2012) Master ' s Thesis Ideas 2012. Department of Civil Engineering, Aalborg University.

Kolokotroni M, Webb BC and Hayes SD: (1998) "Summer cooling with night ventilation for office buildings in moderate climates". *Energy and Buildings*, **27**, (3), pp231-237.

Li S et al: (2011) "Study on Condensation Control of Radiant Cooling Ceiling". *In 2nd International Conference on Digital Manufacturing & Automation*, pp1149-1153.

Nielsen PV: (2007). "Analysis and Design of Room Air Distribution Systems". *HVAC&R RESEARCH*, 13, (6), pp987-997.

Nielsen PV: (2011). "The "Family Tree" of Air Distribution Systems". In *Roomvent 2011*. Trondheim, Norway.

Nielsen PV and Jakubowska E: (2009). "The Performance of Diffuse Ceiling Inlet a nd other Room Air Distribution Systems". In *COLD CLIMATE HVAC 2009*. Sisimiut, Greenland.

Nielsen PV, Jensen, Rasmus L and Rong L: (2010) "Diffuse Ceiling Inlet Systems and the Room Air Distribution". In *Clima 2010: 10th REHVA World Congress*. Antalya.

Price HVAC: (2013) "Displacement Ventilation Design Guide". Available from: http://www.price-hvac.com/literature/pdfs/br409_displacementdesign guide.pdf

Railio J and Mäkinen P: (2007) "SPECIFIC FAN POWER – a tool for better performance of air handling systems". In *Clima 2007 Well Being Indoors*. Helsinki, Finland.

Stetiu C: (1997) "Radiant Cooling in US Office Buildings: Towards Eliminating the Perception of Climate-Imposed Barriers". Energy and Resources Group, University of California at Berkeley.

U of I Facilities Standards: (2011) "Ventilation Systems (Previously Air Distribution Systems)". Available from: http://cfapps.fs.illinois.edu/2010Standards/II. %20General%20Guidelines/Building %20Systems/Ventilation%20Systems.pdf

Valadez E: (2013) "Underfloor air technology." *Journal - Oklahoma Dental Association*, 104, (1), pp34-5. Available at: http://www.ncbi.nlm.nih.gov/pubmed/23713382.

Weitzmann P: (2008). "The cooling capacity of the Thermo Active Building System combined with acoustic ceiling". In *8th Symposium on Building Physics in Nordic Countries*. Copenhagen, Denmark.

Yang H: (2011). "Experimental and Numerical Analysis of Diffuse Ceiling Ventilation". Master thesis, Department of Civil Engineering, Technology University of Denmark.

Appendix B. Experimental study of diffuse ceiling ventilation coupled with a thermally activated building construction in an office room

Paper 2

Author's Right

Re: Add the article into Ph.D. thesis [ref 160704-007781] [160704-007781]

Dear Zhang,

Thank you for chatting with us.

Please be informed that as an author, you have the right to use your article for your thesis or dissertation as long as it is for non-commercial purposes.

I wish to advise that you do not need to obtain permission in some instances if you are the author of the article you wish to use. You also have certain rights in using your article.

For further details on this, please visit the link below:

https://www.elsevier.com/about/company-information/policies/copyright#permissions

Kind regards,

Marc Toneza

Researcher Support
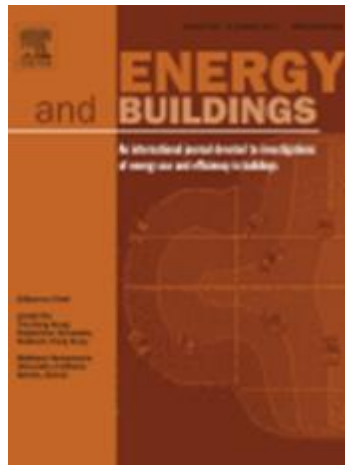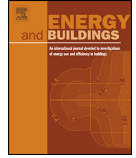
Experimental study of diffuse ceiling ventilation coupled with a thermally activated building construction in an office room

Chen Zhang [a,*], Per Kvols Heiselberg [a], Michal Pomianowski [a], Tao Yu [b], Rasmus Lund Jensen [a]

[a] Department of Civil Engineering, Aalborg University, Sofiendalsvej 11, 9200 Aalborg, Denmark
[b] School of Mechanical Engineering, Southwest Jiaotong University, Chengdu 610031, Sichuan, China

ARTICLE INFO

ABSTRACT

This paper presents and analyses the performance of an integrated system with diffuse ceiling ventilation and a thermally activated building construction. A full-scale experiment is carried out in a hot box with an office setup. The performance of the integrated system is evaluated under different boundary conditions, considering different weather conditions, internal heat loads, TABS activation modes and with/without diffuse ceiling. The measurement results indicate that the diffuse ceiling plays a beneficial role improving thermal comfort in the occupied zone. However, the diffuse ceiling has the opposite effect on energy performance when TABS is activated in heating or cooling mode. Finally, the air temperature distribution in the plenum and the surface temperature distribution of the diffuse ceiling point out that the air does not perfectly mix in the plenum, the air is not evenly distributed throughout the entire ceiling area and the radiation cooling potential of diffuse ceiling is not sufficient. Thus, a further study should be conducted on optimizing diffuse ceiling and plenum design.

© 2015 Elsevier B.V. All rights reserved.

1. Introduction

The demand for comfort cooling is dramatically increasing in all European countries. As predicted by EECCAC [1], a four-fold growth of energy consumption for cooling will occur between 1990 and 2020 in EU 15. The reasons for the expansion of cooling demand are manifold. First of all, the constructional and physical boundary conditions of buildings have been changing. For example, the buildings are designed to be more airtight, with better thermal insulation and intensive use of glazed façades. These changes considerably reduce the energy demand on heating, but also lead to an increase on cooling demand. Secondly, the tightened requirements on indoor comfort and the increase of internal loads (IT equipment) contribute to a rise on cooling demand. Finally, the climate change with an increase of outdoor temperature in the summer period exacerbates the situation.

Passive cooling by ventilation is regarded as a promising strategy, which has been proved to have a significant free cooling potential in the moderate or cold climates of Central, Eastern and Northern Europe [2]. For the conventional ventilation solutions, it

is necessary to preheat the outdoor air during winter to avoid the draught risk in the occupied zone. This rises the energy use and investment cost. An alternative ventilation concept is known as diffuse ceiling ventilation (DIFCV), where the fresh air is supplied through perforations in suspended ceiling panels [3]. Due to the large opening area, air flow is delivered into the room with very low velocity and with no fixed jet direction, so the name 'diffuse'. This ventilation system has been demonstrated that it has superior performance on handling high heat load by directly supplying low temperature air and without significant draught risk [4,5]. On the other hand, a plenum above suspended ceiling is used to deliver air instead of conventional duct system, thus the pressure drop of the system is largely reduced, making it possible to implement with natural ventilation [5–7]. This ventilation concept is wildly used in the livestock buildings because of its low investment cost and high thermal comfort [8,9]. Recent years, more and more applications and studies have been reported regarding utilization of DIFCV in the indoor space for human being, especially for offices and classrooms with high heat load and high ventilation demands [6,5,10,11].

Natural ventilation as a passive cooling strategy strongly depends on the climatic conditions. When natural ventilation is insufficient to cool down the building or heating is required, thermally activated building system (TABS) could serve as a supplementary system to deal with the excessive cooling or heating

---

* Corresponding author. Tel.: +45 9940 7232.
  E-mail address: cz@civil.aau.dk (C. Zhang).

Nomenclature

A	area [m^2]
ACH	air change rate [1/h]
DR	draught risk [%]
PD	percentage of dissatisfied [%]
PMV	preceded mean vote
C_p	specific heat [J/kg K]
M	flow rate [kg/s]
t	temperature [°C]
Q	heat flow [W]
h	heat transfer coefficient [W/m^2 K]

Subscripts

a	air
avg	average
DIFCV	diffuse ceiling ventilation
down	lower zone
envelop	other envelop
ex	return
façade	façade
in	inlet
op	operative
re	return
s	surface
source	heat source
su	supply
surround	surrounding zone
TABS	thermally activated building construction
up	upper zone
vent	ventilation
w	water

demands. TABS is a type of radiant cooling and heating system, where the water carrying pipes are embedded in the building elements [12]. Because of the high inertia of thermal mass, the peak load will be reduced and some of cooling load will be transferred beyond the time of occupancy. In addition, due to the large heat transfer surface, it is possible to heat or cool effectively, even with very slight temperature differences between the concrete slab and the room. This will result in a high efficiency of energy system and increasing application of renewable energy resource such as ground water, heat pump and solar collectors [13–15]. Therefore, the integrated system has the potential to provide cooling, heating and ventilation for an office building all year around with high thermal comfort and low energy consumption.

The combination of radiation cooling/heating and ventilation systems has been extensively studied. The most common application is cooled ceiling with displacement ventilation. This integrated system has been proved to be more energy efficient than conventional air conditioning systems, since it could work together with night cooling and heat storage facilities [16,17]. However, in order to avoid the risk of draught in the occupied zone, the cooling load should be restricted to below 100 W/m^2, the height from floor to ceiling should be higher than 2.5 m and the cooling outputs of ceilings should also be regulated appropriately [16]. In addition, the downward convective flow produced by cooling panels mix with the upward displacement flow, which gives a more mixed condition than pure displacement [17,18]. The combination of floor cooling with displacement ventilation is also considered possible, although the draught risk at the ankle level and vertical temperature gradient need to be controlled carefully [19]. Since the advantage of displacement flow in respect to the air quality is receded when cooled ceiling is used to remove high cooling load, another solution

of cooled ceiling coupled with mixing ventilation were studied. The results indicated that a mixing ventilation system could provide uniform pollutant distribution if the entire ceiling be covered by cooled areas. However, a draught risk was observed if high cooling load was presented, in the same manner as displacement ventilation [20].

The new system solution combining DIFCV and TABS has been proposed recently by Tao Yu et al. [21]. They specified five operation models based on different climatic and occupied conditions. A case study of a typical office using this solution was compared with those with other traditional HVAC system by energy simulation. The results indicated that the new system has a large energy saving potential once it is properly designed and controlled and the ventilation period is extended by using diffuse ceiling supply. This study mainly conducted by theoretical analysis, therefore, the performance of the system should be further evaluated and validated by experimental study. A key issue is the harmony of the combination between these two techniques. Most of studies regarding TABS have pointed out it is necessary to have large surface areas with exposed concrete. However, in this coupled system, the TABS is encapsulated by a suspended ceiling. A reduction on the radiation heat exchange between the TABS and the room surfaces will be expected. On the other hand, distributing the supplied air by a plenum allows direct contact between the air and the thermal mass of the concrete slabs. As a result, the convection heat exchange between TABS and air will vary, depending on the temperature difference and air flow rate. A research of integrated ventilation and night cooling with DIFCV in a classroom was performed by Hviid [22], and the results indicated that the extra free cooling potential made available by activating the thermal mass of the concrete slab in the plenum. Therefore, the impact of suspended ceiling on the thermal performance of TABS should be investigated in the experimental study. Second, in the simulation, the air was predicted to be perfectly mixed in the plenum and evenly distributed through entire ceiling area. Actually, the air condition in the plenum is influenced by the heat exchange between supply air and thermal mass and the mixing level is determined by configuration of plenum and inlet. It is critical to exam the air flow pattern in the plenum and through diffuse ceiling.

The objective of this study is to analyze the performance of the system combining DIFCV and TABS by means of an experimental study. Special attention has been paid on whether the integrated system could achieve an energy-efficient and comfortable indoor environment. A typical office layout is simulated in a hot box equipped with TABS ceiling and diffuse ceiling panels. The performance of integrated system is evaluated under different boundary conditions, including weather, internal heat load, TABS activation mode. The cases without diffuse ceiling are used as reference to estimate the effect of diffuse ceiling on the air distribution and heat exchange.

2. Experimental investigations

2.1. The hot box

The study was made as full-scale experiments in a hot box located in a laboratory. According to EN ISO 8990 [23], two types of hot box apparatus are introduced: guarded hot box (GHB) and calibrated hot box (CHB). In this study, the constructed hot box was designed based on the GHB concept. Fig. 1 shows the vertical section view of the hot box. The hot box is separated into a cold chamber representing the outdoor climate and a hot chamber representing a two-floor office building. The hot chamber is divided into three different zones. The lower zone represents a two-person office where the thermal comfort and energy performance are mainly

Fig. 1. Vertical section view of hot box.

investigated. And upper zone represents a second floor office which is used to investigate the thermal behavior of TABS. It needs to notice that the concrete slabs are separated from the upper zone by means of a 50 mm insulation layer, which aims to simulate the construction in a real building. There is always a layer of floor board or floor covering TABS, reducing the heat exchange between TABS and upper zone and preventing sound transmission. Lower and upper zones are enclosed by another zone, which is named as surrounding zone. The set temperature in the surrounding zone was kept to identical to upper and lower zones to eliminate heat gain or heat loss from the laboratory. Air is re-circulated through the air handling unit (AHU) to provide cooling and heating to each individual zone depending on the predefined temperature profile.

The façade between the cold chamber and the hot chamber is made by a sandwich element (wood panel 15 mm – rock wool 300 mm – wood panel 15 mm). There are 6 windows mounted in the façade. The lower three have a dimension of 2.4 m length and 1.4 m height, and are closed during the whole experiments. The upper three serve as supply openings with a dimension of 2.4 m length and 0.35 m height. The opening size can be changed by adjusting opening angle of upper windows and a geometrical open area of 0.0207 m^2 (1 cm × 69 cm × 3 window) is used in this study. The exhaust opening is located on the left corner of the façade, with a diameter of 160 mm. The exhaust air is recirculated to the cold chamber driven by an exhaust fan, and it is treated by the air handling unit to maintain the same temperature as the cold chamber. The heat transfer coefficient of the facade is measured to be 0.61 W/m^2 K based on ISO 8990 [23].

The diffuse ceiling is installed in the lower zone at 2.335 m height. It is composed of perforated ceiling tiles with 600 mm width, 1200 mm length and 35 mm thickness occupying the entire ceiling area. The ceiling tiles are made of wood and cement and are known as cement-bonded wood wool panels, which have good sound-absorbing properties and are penetrable to air. The ceiling tiles are fixed by suspension brackets, as shown in Fig. 2.

The thermally activated ceiling is composed by four pieces of concrete slabs with a dimension of 3560 mm × 1197 mm × 200 mm each. The water-carrying pipes with a diameter of 20 mm are connected in series between four slabs. The pipes are located 4 mm above the slab lower surface to ensure most of the heat can be

Fig. 2. Diffuse ceiling set-up.

transferred to the test room. The water is circulated at a defined supply temperature and flow rate in the TABS system.

The lower zone, also called test room, is set up to represent an office layout, as shown in Fig. 3. Two workplaces are arranged, which consist of two desks with two computers (55 W and 45 W), two monitors (16 W and 21.5 W) and two task lamps (54 W and 59 W). Two persons are simulated by thermal manikins (100 W for each). In order to simulate the heat gain by solar radiation, an electric carpet is positioned on the floor closed to the façade, with a heat load of 464 W. Thus, the total heat load in the room without solar radiation is 450.5 W (28.4 W/m^2), and with solar radiation is 914.5 W (57.73 W/m^2).

2.2. Measurements and location of sensors

The experiments are carried out for 12 cases with different boundary conditions. The basic idea of the measurement is to provide an acceptable indoor environment (24–26 °C) by using TABS and ventilation with/without diffuse ceiling supply in different climatic conditions (varying on outdoor temperature and solar radiation). The TABS water supply temperature and flow rate are determined so that a certain amount of energy can be transferred

Table 1
Boundary conditions for different.

Case	Air change rate (h^{-1})	Supply air temperature (°C)	Heat load (W)	TABS water supply temperature (°C)	TABS water flow rate (m^3/h)	Diffuse ceiling
1	2	−7.1	450.5	36.38	134.5	–
2	2	9.21	450.5	–	–	–
3	2	23.82	450.5	17.29	140	–
4	4	−6.87	914.5	38.91	208	–
5	4	8.92	914.5	–	–	–
6	4	23.89	914.5	10.95	273	–
7	2	−6.87	450.5	30.89	136	Y
8	2	9.46	450.5	–	–	Y
9	2	24.1	450.5	8.1	221	Y
10	4	−7.23	914.5	35.63	138	Y
11	4	9.41	914.5	–	–	Y
12	4	24.07	914.5	4.27	294	Y

Fig. 3. Lay-out of the test room.
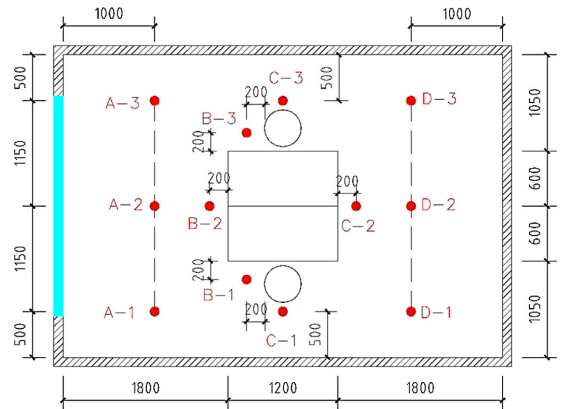
Fig. 4. Plan view of the test room indicating the layout of the room and showing temperature and velocity measurement locations.

into the test room in the steady state conditions. For example, TABS provides the same amount of heating as heat sources in winter and removes the entire heat load in summer. This results that TABS supply water temperature is much lower than the dew point temperature in some cases and raises the condensation risk. However, in order to identify the applied limits even cases leading to condensation risk are still investigated in this study. The boundary conditions are described in detail in Table 1.

In the temperature measurements, besides PT100 located in each zone (except the test room) to control the indoor air temperature there are 115 K type thermocouples in total to monitor the temperature, with an uncertainty of ±0.15 K. The vertical temperature profiles in the test room are measured by three moveable columns, and there are 7 thermocouples mounted in different heights in each column (the heights are distinguished between the cases with/without diffuse ceiling), see Fig. 5. The three moveable columns can also be used to measure horizontal air temperature distribution. Each column changes 4 positions, so in total 12 columns have been measured in the occupied zone, as indicated in Fig. 4. The operative temperature is measured by thermocouple positioned in a gray sphere with a diameter of 4 cm at the height of 1.1 m. Internal surface temperatures (wall, façade, floor) are measured at 3–5 points distributed in each surface. The surface temperature of TABS and inlet and outlet water temperatures in each slab are measured as well. In the cases with diffuse ceiling, 9 thermocouples are evenly distributed in the plenum to measure plenum air temperature, and 18 thermocouples are symmetrically installed on both sides of the diffuse ceiling surface. All the thermocouples are scanned every 10 s, and temperatures are logged by the Helios Fluke data logger.

Air velocity is measured by hot sphere anemometers with uncertainty of ±0.01 m/s +5% of reading. In total 19 anemometers are

used to measured air velocity in the occupied zone and plenum, see Figs. 5 and 6. Velocities are logged by Dantec multichannel flow analyzer type 54N10.

The cooling capacity of TABS is calculated by water flow rate and inlet and outlet water temperature. The water flow rate is recorded by Brunata energy meter type HGQ1 with a uncertainty of $\pm(2+0.02q_p/q)$. Both the flow rate and supply and return water temperatures are logged by specific LabView interface.

Finally, the indoor humidity is measured by HIH-4602 humidity sensor (accuracy ±7.5%). And the pressure drop of diffuse ceiling is measured by FCO510 micromanometer (accuracy ±0.25%) by locating pressure sensors in the plenum and lower zone.

3. Analytic criteria

3.1. Thermal comfort criteria

According to ISO 7730:2005[24], when assessing thermal comfort in the occupied zone, both whole-body thermal comfort and local thermal comfort should be taken into account. Thermal comfort of the whole-body can be evaluated by the PMV and PPD indexes, and local thermal comfort can be assessed by draught risk, vertical temperature difference and radiant asymmetry.

The PMV is an index that predicts the mean value of the votes of a large group of persons on the 7-point thermal sensation scale (from Hot to Cold), and PPD gives a quantitative prediction of thermally dissatisfied. These two indexes are calculated based on the heat balance of the human body, depending on the thermal environmental variables (air temperature, relative humidity, mean radiant
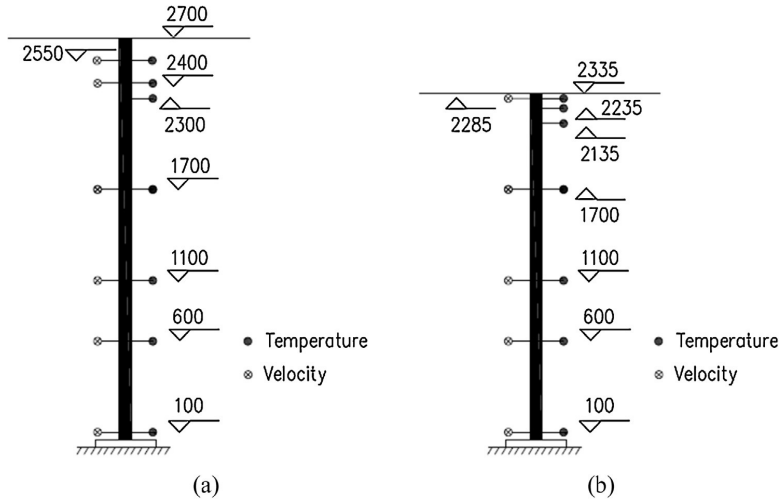
Fig. 5. Temperature and velocity sensors in the moveable columns. (a) Without diffuse ceiling. (b) With diffuse ceiling.
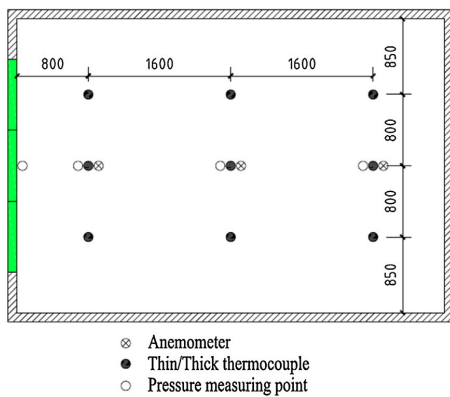

Fig. 6. Measurement points in the plenum.

temperature and relative air velocity), as well as activity level and insulation of clothing. A metabolic rate of 1.2 and a clothing value of 0.7 for winter and 0.5 for the other seasons are assumed in this study. And the discomfort due to draught is evaluated by the percentage of people predicted to be bothered by draught, so called as draught rate (DR). A constant turbulence intensity of 40% is used in DR calculation.

3.2. Energy performance

3.2.1. Energy balance and heat transfer coefficient of TABS

TABS serves as ceiling for the lower zone and floor for the upper zone, thus, the heat released by TABS will transfer to both zones. The energy balance of TABS in the steady state conditions is expressed as Eq. (1):

$$Q_{TABS} = Q_{TABS,up} + Q_{TABS,down} \tag{1}$$

The first term expresses the energy provided by water flow, and the two later terms express the heat flow through the upper and lower surface. The energy flow in the pipe can be determined by

supply and return water temperature multiplied by the water flow rate. Since the pipe is located far away from the upper surface and there is a layer of insulation on the top, thus the temperature is almost evenly distributed on the upper surface. The heat delivered to the upper zone can be calculated by the temperature difference between the upper zone and the upper surface. Therefore, the energy delivered to the lower zone by TABS is expressed by the equation below:

$$
\begin{aligned}
Q_{TABS,down} &= Q_{TABS} - Q_{TABS,up} \\
&= C_{p,w} \cdot M_w \cdot (t_{w,su} - t_{w,re}) - h_{ins} \cdot A \cdot (t_{s,up} - t_{a,up})
\end{aligned}
\tag{2}
$$

The heat transfer coefficients between radiant surfaces and the room is an important and fundamental parameter to evaluate the energy performance of radiant heating/cooling system. The total heat transfer coefficient between TABS and the room, based on the operative temperature at a height of 1.1 m height and average TABS surface temperature is calculated as:

$$h = \frac{Q_{TABS,down}}{A \cdot (t_{op} - T_{s,avg})} \tag{3}$$

3.2.2. Energy balance of the test room

The test room energy balance for a steady state can be expressed by Eq. (4).

$$Q_{vent} + Q_{TABS,down} + Q_{facade} + Q_{envelop} + Q_{source} = \Delta Q \qquad (4)$$

The heat gain/loss by ventilation is defined as:

$$Q_{vent} = C_{p,a} \cdot \rho_a \cdot M_a \cdot (t_{a,ex} - t_{a,in}) \qquad (5)$$

Due to the temperature difference between the cold chamber and the test room, there is a heat gain/loss through the façade. The façade is made by inhomogeneous components (sandwich element with 6 windows), so the thermal transmittance of façade cannot be easily calculated by using material thermal conductivities. Therefore, a thermal testing of the façade was conducted with the hot box method before the real measurement [23]. The heat transfer coefficient of the façade is measured to be 0.61 W/m^2 K. On the other hand, although the surrounding zone tries to keep the same temperature as the test room, there is still a slight temperature difference between these two zones. The heat gain/loss through other envelop is estimated as a function of the measured surface temperature of each wall and floor. It needs to be noted that $Q_{envelop}$ also includes the heat transfer from upper zone when TABS is not activated.

$$Q_{facade} = h_{facade} \cdot A_{facade} \cdot (t_{s,facade} - t_{a,out}) \qquad (6)$$

$$Q_{envelop} = h_{envelop} \cdot A_{envelop} \cdot (t_{s,envelop} - t_{a,surround}) \qquad (7)$$

ΔQ indicates the error on the energy balance, which is associated with some uncertainties due to the measurement and the simplifications used in the equation formulation.

4. Result of experimental investigations

4.1. Thermal comfort

4.1.1. Temperature distribution

Vertical air temperature difference is critical on evaluating local thermal comfort. Occupants will feel discomfort when high temperature difference exists between head and ankles. The vertical temperature profiles are analyzed and presented in Fig. 7, where the air temperature at each height is the average values of 12 positions. Due to TABS activation modes and the impact of diffuse ceiling, different trends can be observed from the temperature profiles. First of all, high temperature gradients are noticed in the cases without diffuse ceiling under TABS operating as heating mode, as indicated by Case 1 (1.56 °C/m) and 4 (1.82 °C/m). Due to the gravity, cold outdoor air generates a downward flow and drops to the floor just after it supplied into the room. At the same time, the warm air stagnates at the ceiling level without significant mixing with supply air, which causes temperature stratification in the room. The thermal stratification also limits the heat exchange between heated ceiling and the room, for this reason heated ceiling is normally less efficient than the cooled ceiling, as pointed out by Awbi et al. [25]. On the other hand, DIFCV contributes to reducing vertical temperature gradient under the similar boundary condition, as shown by Fig. 7 (Case 7 and 10). Instead of direct supplying cold outdoor air into the room, the outdoor air firstly distributes in the plenum and is preheated by the heated ceiling surface. As a result, the fresh air is sent into the room with higher temperature and lower velocity. In addition, the convection flow generated by the heat source improves the mixing degree in the room, which makes the air flow pattern comparable to mixing ventilation. This result corresponds well with the finding by Fan [26] and Nielsen [10]. When TABS runs by cooling mode in summer or without activating in transition season, no discomfort is observed in both cases with and without diffuse ceiling.

Although DIFCV exhibits a superior performance on eliminating the vertical temperature gradient, an overheating phenomenon is found in summer or even transition season after installing diffuse ceiling, where the average air temperatures are 23 °C higher than those without diffuse ceiling under the similar boundary conditions. This is because diffuse ceiling works as a layer of insulation between TABS and the room, impeding the heat exchange between them. Therefore, the cooling capacity of ventilation or radiant cooling is reduced. The detail evaluation on energy performance will be presented in Section 4.2.

In order to investigate air flow patterns in the room, the horizontal air temperature distributions are analyzed by locating temperature columns along the length of the room. Case 1 and Case 7 are selected as examples to present the room without and with diffuse ceiling under winter condition. As shown in Fig. 8, a remarkable horizontal air temperature difference is observed at the floor level if the air is directly supplied into the room. The air temperature rises while increasing the distance to the façade. This indicates that cold fresh air drop toward the floor in a short distance to the inlet, causing the low floor air temperature on the side closed to the façade. While the air flow penetrates to the deeper part of the room, the air is warmed up by the heat sources located in the middle of the room. This can explain the temperature gap between positions A/B and C/D.

The temperature distribution shows a different trend by using diffuse ceiling. The horizontal temperature difference is very small in the occupied zone. This means the occupants will experience the same thermal environment, no matter their locations. The largest horizontal air temperature difference (1.01 °C) occurs 5 cm below diffuse ceiling. This reveals the fact that air is not uniformly distributed throughout the entire ceiling area. However, the thermal plume generated by heat sources helps the mixing process in the occupied zone.

4.1.2. Draught

Draught is defined as an unwanted local cooling of the human body caused by air movement, which is strongly related to local air velocity. Draught rates are analyzed at 4 positions along the length of the room and at 3 heights 0.1 m, 1.1 m and 1.7 m corresponding to ankle, head of sitting person and head of standing person, respectively. Based on the measurement results, the highest draught risk is observed at the ankle level in all cases. Therefore, only the draught rate at ankle level is discussed and shown in Fig. 9. First of all, a general conclusion could be drawn that occupants experience low draught risk in the room with diffuse ceiling, especially in the winter. A maximum draught rate of 24% is found in the cases without diffuse ceiling, which exceeds the limit of 20% in Category B [24]. For all cases with diffuse ceiling, the draught rate even satisfy the Category A of 10% [24]. The results also exhibit that the supply air temperature and TABS activation mode has less effect on the draught risk by using diffuse ceiling than the other cases. As a matter of fact, due to the low-momentum flow generated by DIFCV, the system does not generate significant draught by itself, the draught is generated by the heat sources, such as the occupants and equipment [4,7].

Second, from the view of horizontal distribution, the highest draught risk moves from the place closed to the façade to the deeper part of the room since the supply air temperature rises. This phenomenon is significant in the cases without diffuse ceiling but also appears in the cases with diffuse ceiling. This is easy to understand that supply air temperature has a large impact on the air jet pattern, where the warm air can travel further along the ceiling while the cold air will drop in a short distance. This phenomenon proves again that air is not evenly distributed throughout diffuse ceiling, where the same trend is also found by horizontal temperature
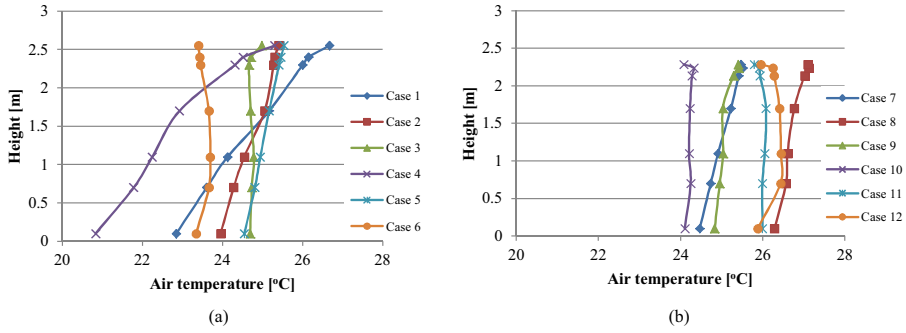
Fig. 7. Vertical air temperature gradient. (a) Cases without diffuse ceiling. (b) Cases with diffuse ceiling.
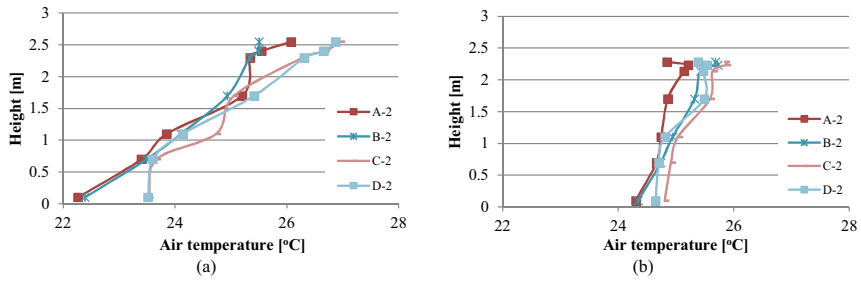

Fig. 8. Air temperature distribution measured at different horizontal positions. (a) Case 1. (b) Case 7.
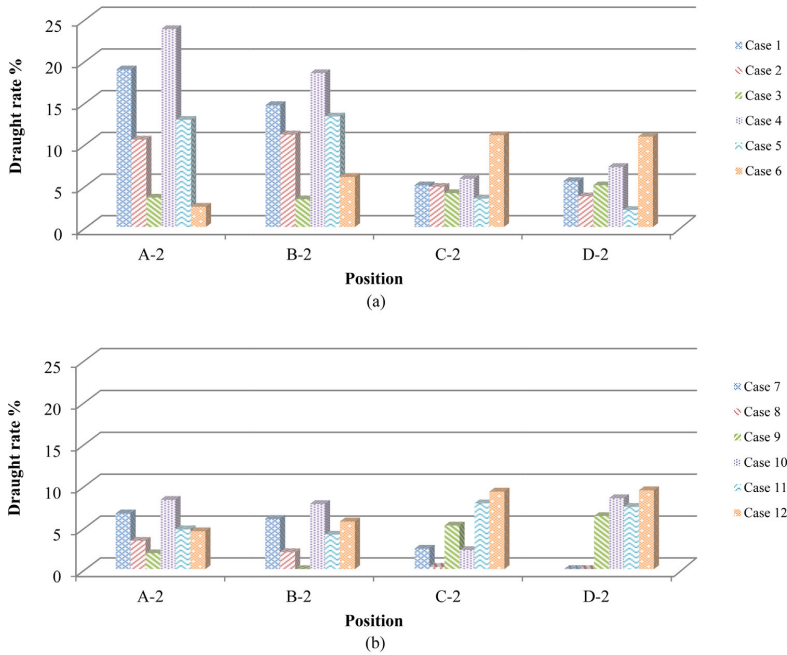

Fig. 9. Draught rate at ankle level measured at different horizontal positions. (a) Cases without diffuse ceiling. (b) Cases with diffuse ceiling.
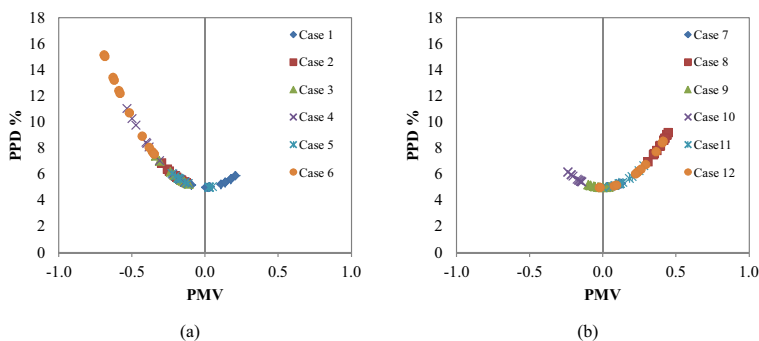
Fig. 10. PMV and PPD. (a) Cases without diffuse ceiling. (b) Cases with diffuse ceiling.

distribution (Fig. 7). Nevertheless, the impact is too low to cause thermal discomfort in the cases with diffuse ceiling.

4.1.3. Radiant asymmetry

Differences in room enclosure temperatures can lead to thermal discomfort due to radiant asymmetry, even when the mean radiant temperature is within acceptable limits [27]. The radiant temperature asymmetry is estimated as the difference between the plane radiant temperatures in two opposite directions. As described by Fanger [27], it refers to a small plane element 0.6 m above the floor (the height of the center of a seated person) and horizontal to characterize radiant asymmetry caused by a warm or cool ceiling. Table 2 illustrates the asymmetric radiation from a cool or warm ceiling and percentage dissatisfied due to cool or warm ceiling. For the cases without diffuse ceiling, the ceiling surface temperature represents by lower surface temperature of TABS, while that is replaced by the lower surface temperature of diffuse ceiling when the diffuse ceiling is mounted. The PD values reveal that high dissatisfaction occurs when directly exposing a warm TABS surface to the room, where the PD of Case 1 and Case 4 exceed the limitation of 5% in Category B [24]. However, the radiant asymmetry due to warm ceiling is reduced after installing diffuse ceiling. Because instead of directly exposing warm TABS surface to the room, the TABS is encapsulated by diffuse ceiling and the radiation effect is reduced simultaneously.

On the contrary, no discomfort due to radiant asymmetry is found when TABS is activated as a cooling system, no matter with or without diffuse ceiling. This is due to the fact that occupants are more sensitive to warm ceiling instead of cool one. As stated in ISO 7730, occupants will feel discomfort when the radiant asymmetry is larger than 5 °C by warm ceiling, and larger than 14 °C by cooling ceiling.

4.1.4. PMV, PPD

The whole-body thermal comfort of occupants in the test room is evaluated by PMV and PPD, as shown in Fig. 10. The PMV and PPD values of a seated person is determined by an mean values of air temperature, mean radiant temperature and air velocity at 0.1 m, 0.6 m and 1.1 m heights and calculated in 12 locations (detailed location see Fig. 5). The PMV is range from −0.69 to 0.21 in the cases without diffuse ceiling, which exceeds the limit of ±0.5 for thermal environment Category B [24]. Occupants will feel slightly cool in Case 4 and Case 6, and the percentage of dissatisfied (PPD) reach 11% and 15%, respectively. In the cases with diffuse ceiling, the PMV is within the range of −0.24–0.45. Although occupants will experience a slightly warm in Case 8, 11 and 12, they are still in the acceptable level and less than 10% of people will feel discomfort.
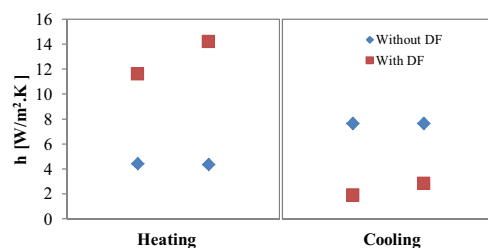

Fig. 11. Heat transfer coefficients of TABS under heating and cooling modes.

4.2. Energy performance

The energy balance of TABS and the proportion of cooling/heating transfer to the test room are presented in Table 3. The results of heat flow into the test room is used to calculated the total heat transfer coefficients of TABS in both heating and cooling conditions, as presented in Fig. 11. First of all, a conclusion could be drawn that diffuse ceiling has significant influence on the thermal performance of TABS. The total heat transfer coefficients in the cases without diffuse ceiling are closed to the typical design values, 6 W/m² K for ceiling heating and 11 W/m² K for ceiling cooling [28,29]. However, the values in the cases with diffuse ceiling are in a different manner, which is around 13 W/m² K for heating and 2.5 W/m² K for cooling. As an obstacle between the test room and TABS, diffuse ceiling changes the air flow pattern near the TABS surface as well as the view factors between the TABS and the other room surfaces. Consequently, the convection and radiation heat transfers between the TABS and the test room change as well. On the other hand, since diffuse ceiling separated the whole space into two thermal zones: plenum and test room, the TABS directly interacts with the thermal conditions in the plenum instead of that in the test room. Secondly, diffuse ceiling has very opposite effect on the heat transfer coefficient under heating and cooling models. It is clear that diffuse ceiling promote the heat transfer under heating conditions. This is because the cold outdoor air distributes in the plenum before supplying into the room, which gives a larger air–surface temperature difference and relative high air velocity near TABS surface. Thus, the increase of convective heat transfer offsets the loss of radiation heat transfer. On the contrary, the air-surface temperature is decrease in the cooling mode, therefore, both convection heat exchange and radiation heat exchange are weaken by the existence of diffuse ceiling. As a result, the heat transfer coefficient of TABS is only one third of that without diffuse ceiling in the cooling mode. As a matter of fact, heat transfer

Table 2
Radiant temperature asymmetry. (a) Cases without diffuse ceiling. (b) Cases with diffuse ceiling.

(a)

Case	1	2	3	4	5	6
$T_{TABS, low}$ [°C]	32.1	24.9	20.6	33.8	25.5	15.8
Δt_{pr} [°C]	4.5	0.3	1.5	5.9	0.5	3.1
PD %	5.86	0.01	0.01	8.49	0.01	0.02

(b)

Case	7	8	9	10	11	12
$T_{TABS, low}$ [°C]	27.3	20.1	10.8	28.6	15.0	8.2
$T_{diff, low}$ [°C]	23.4	24.8	22.7	21.5	22.5	23.0
Δt_{pr} [°C]	0.6	0.7	0.9	1.6	2.8	1.8
PD %	0.01	0.01	0.01	0.01	0.02	0.01

Table 3
Energy balance of TABS.

(a) Without diffuse ceiling

Energy terms	Case 1	Case 2	Case 3	Case 4	Case 5	Case 6
Q_{TABS} [W]	651.52	–	−521.95	897.9264	–	−1034.93
$Q_{TABS, up}$ [W]	95.07	–	−49.06	125.1764	–	−113.786
$Q_{TAB, down}$ [W]	556.45	–	−472.89	772.75	–	−921.14
Proportion of TABS to test room	85.41%	–	90.60%	86.06%	–	89.01%

(b) With diffuse ceiling

Energy terms	Case 7	Case 8	Case 9	Case 10	Case 11	Case 12
Q_{TABS} [W]	567.45	–	−598.34	1067.91	–	−1020.52
$Q_{TABS, up}$ [W]	42.23	–	−168.01	56.47	–	−209.41
$Q_{TAB, down}$ [W]	525.23	–	−430.32	1011.44	–	−811.11
Proportion of TABS to test room	92.56%	–	71.92%	94.71%	–	79.48%

coefficient represents the relationship between heat flow intensity and the temperature difference between room and the TABS surface. This means if want to keep the same room air temperature and remove the same heat load, TABS need to be operated with a lower surface temperature after installing diffuse ceiling. This explains why the water supply temperature reaches 4 °C in case 12, much lower than the recommended water supply temperature of 18–20 °C. Operating at an excessively low temperature will raise a condensation risk and limit the application of renewable cooling source. Finally, air flow rate has relatively larger impact on the TABS thermal performance after installing diffuse ceiling. In fact, if directly supply outdoor air into the room, the air cannot spread through the entire ceiling area before it dropping into the occupied zone. Diffuse ceiling provide a pressure difference between plenum and room which force air distributes in the plenum. Therefore, the air movement is stronger closed to the TABS and the influence of air flow rate is stronger than without diffuse ceiling.

Energy balance of the test room in three weather conditions are presented in Table 4. Cases 1, 4, 7, 10 represent winter, where TABS will be activated as heating system to compensate the heat loss generated by ventilation and transferred through the facade. Cases 2, 5, 8, 11 represent transition season, where the heat load will mainly be removed by ventilation and TABS is not activated. While Cases 3, 6, 9, 12 simulate summer season where the outdoor environment has the same temperature as the indoor environment, TABS will be used to absorb the entire heat load. In most cases, the energy in the test room reaches good balance that the unbalance rate is below 10%. The only exception is Case 7, that energy unbalance rate reaches to 12.21%. On the other hand, the reason of high indoor temperature in Case 8 and Case 11 is that instead of removing the entire heat load by ventilation, a part of the cooling is used to cool down the thermal mass of concrete slabs and further transfer to the upper zone, as indicated by the energy term of $Q_{envelop}$. The

ventilation cooling capacity is reduced and not sufficient to keep an acceptable indoor temperature in the test room.

4.3. The effect of plenum and diffuse ceiling

The use of a ceiling plenum to deliver air into the occupied zone is one of the key features that distinguish DIFCV from the conventional ducted air distribution system. Thermal processes within the plenum have an important impact on the effectiveness of TABS as a cooling or heating system and diffuse ceiling as an air distribution system. The thermal processes include: heat transfer between TABS and plenum air, heat transfer between diffuse ceiling panel and plenum air as well as heat transfer between TABS and diffuse ceiling panel. Fig. 12 illustrates the plenum air temperature distribution and the surface temperature distribution of diffuse ceiling. Because the temperature in the plenum have similar trends in both air change rate conditions, only the cases with air change rate of $2 \, h^{-1}$ are discussed here.

Even though the supply air temperature ranges from −6.87 to 24.1 °C, the air temperature in the plenum remain relatively stable (average air temperature from 15.2 to 20.1 °C). This result declares a pre-heating or pre-cooling effect of plenum. With the help of diffuse ceiling, the draught risk in the room can be significantly reduced regardless of the supply air temperature.

As stated by Bauman [30], the heat exchange between supply air and TABS and diffuse ceiling panel influences air temperature variation as a function of distance traveled through the plenum. It is clear that in Case 7 the supply air is gradually heated up by heated ceiling and diffuse ceiling panel when it travels further in the plenum. On the contrary, the supply air is gradually cooled down in Case 9, when TABS is activated as cooled ceiling. While, in Case 8, although the TABS is not activated, the air temperature is still heated up by warm diffuse ceiling surface. From the horizontal air

Table 4
Energy balance of the test room.

(a) Without diffuse ceiling

Energy terms	Case 1	Case 2	Case 3	Case 4	Case 5	Case 6
Q_{source} [W]	450.5	450.5	450.5	914.5	914.5	914.5
$Q_{ventilation}$ [W]	−852.66	−397.02	−13.4	−1569.55	−810.76	−19.97
$Q_{TAB, down}$ [W]	556.45	–	−472.89	772.75	–	−921.14
Q_{facade} [W]	−139.62	−67.35	−2.28	−133.59	−76.37	0.57
$Q_{envelop}$ [W]	−14.7	−14.59	−0.72	−6.01	−30.15	13.31
ΔQ [W]	−0.03	−28.46	−38.79	−21.9	−2.78	−12.73
Unbalance rate	−0.01%	−6.32%	−8.61%	−2.39%	−0.30%	−1.39%

(b) With diffuse ceiling

Energy terms	Case 7	Case 8	Case 9	Case 10	Case 11	Case 12
Q_{source} [W]	450.50	450.50	450.50	914.50	914.50	914.50
$Q_{ventilation}$ [W]	−892.73	−498.95	−28.44	−1835.28	−998.83	−152.99
$Q_{TAB, down}$ [W]	525.23	–	−430.32	1011.44	–	−811.11
Q_{facade} [W]	−135.91	−72.75	−1.83	−138.58	−75.38	−13.53
$Q_{envelop}$ [W]	−2.11	80.14	5.51	9.07	98.43	−5.02
ΔQ [W]	−55.02	−41.06	−4.59	−38.86	−61.28	−68.16
Unbalance rate	−12.21%	−9.11%	−1.02%	−4.25%	−6.70%	−7.45%
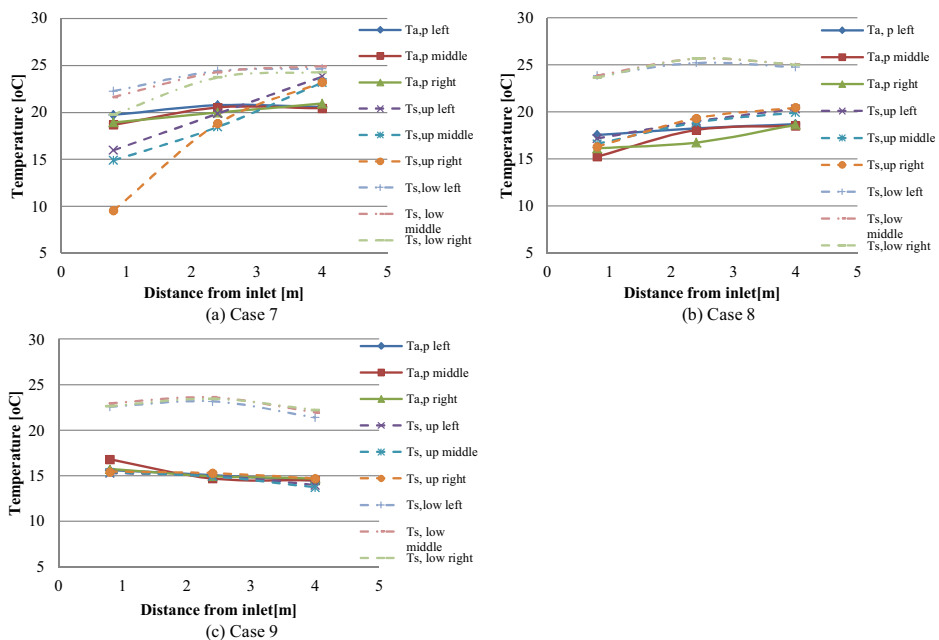
Fig. 12. Plenum air temperature distribution and surface temperature distribution of diffuse ceiling. (a) Case 7. (b) Case 8. (c) Case 9.

temperature distribution in the plenum, it is possible to see that the air is not totally mixed in the plenum, and a temperature difference up to 2 °C is noticed.

A noticeable temperature difference between diffuse ceiling lower and upper surface can be observed in these cases, as the temperature difference up to 10 °C. The lower surface has closed temperature to the room air and a peak surface temperature can be found corresponding to the middle of the room as the surface is heated by thermal plume generated by heat sources. While, the upper surface has the similar temperature as the plenum air. Therefore, unlike the study performed on the perforated aluminum ceiling tile by Hviid et al. [5], no clear radiation cooling potential of diffuse ceiling is found in this study. This is due to the low

conductivity of cement-wood ceiling tile used in this study, with λ-value of 0.085 W/m K, while the conductivity of aluminum is up to 205 W/m K.

5. Conclusion

This study investigates the performance of an integrated system combining diffuse ceiling ventilation with thermally activated building construction. Experiments are carried out to examine the thermal comfort and energy performance of an office room with an integrated system under 12 cases, with different weather, heat load, TABS activation mode and with/without diffuse ceiling. From the view of thermal comfort, diffuse ceiling plays a beneficial role

improving thermal comfort in the occupied zone, especially in winter. When TABS works as a heated ceiling and air directly is supplied into the room, a high temperature gradient and high draught risk will be experienced by occupants, especially for those sit closed to the façade. These local discomforts can be effectively eliminated by combining with diffuse ceiling ventilation. In addition, the risk of discomfort by exposing to a warm ceiling is significantly reduced by diffuse ceiling, since the TABS is encapsulated and the radiation effect is restrained. Regarding whole body thermal comfort, occupants will feel 'slightly warm' by using integrated system in the transition and cooling season, since diffuse ceiling limits the cooling capacity of ventilation and TABS. However, the PMV/PPD values are still in the acceptable level, no discomfort is predicted.

From the view of energy performance, the integrated system presents opposite trends for heating and cooling conditions. Because the presence of plenum changes the radiation and convection heat transfer between TABS surface and the room by changing the view factors, the air–surface temperature difference and the air flow pattern. The results demonstrated that, diffuse ceiling promotes the heat transfer coefficient of TABS under heating conditions but reduces the value under cooling conditions. By considering both thermal comfort and energy performance, it could conclude that the integrated system increases the opportunity of using outdoor air directly for ventilation without thermal discomfort all year around. And the system shows a promising potential as a heating system than the stand along radiant heating ceiling from both thermal comfort and energy efficient considerations. However, a reduction of cooling capacity is predicted by using diffuse ceiling. TABS need to run with a lower temperature which limits the application of renewable cooling resources and raises the condensation risk. A further study of dynamic state needs to be performed in order to investigate the potential of night cooling and energy storage by the integrated system.

Finally, the air temperature in the plenum and surface temperature of diffuse ceiling reveals the fact that the air in the plenum is not perfectly mixing and that the air is not evenly distributed through the entire ceiling area, which is as a function of distance to the inlet. However, this does not lead to a thermal comfort issue in the occupied zone. No clear radiation cooling potential of diffuse ceiling is identified in this study, due to the low conductivity of suspended ceiling tiles. The performance of plenum and diffuse ceiling may be influenced by many design parameters, such as plenum inlet conditions, plenum height, obstructions within the plenum, diffuse ceiling panel types and suspension profiles. However, the research regarding the plenum and diffuse ceiling design is quite limited and no design guide is available at present. Thus, a further investigation should be conducted on the proper design of these parameters.

References

[1] J. Adnot, P. Riviere, D. Marchio, M. Holmstrom, J. Naeslund, J. Saba, I. Blanco, Energy Efficiency and Certification of Central Air Conditioners (EECCAC), ARMINES, France, 2003.

[2] N. Artmann, H. Manz, P. Heiselberg, Climatic potential for passive cooling of buildings by night-time ventilation in Europe, Appl. Energy 84 (February (2)) (2007) 187–201.

[3] C. Zhang, P. Heiselberg, P.V. Nielsen, Diffuse ceiling ventilation: a review, Int. J. Vent. 13 (1) (2014) 49–63.

[4] P.V. Nielsen, E. Jakubowska, The performance of diffuse ceiling inlet and other room air distribution systems, in: Clima 2010: 10th REHVA World Congress, 2010.

[5] C.A. Hviid, S. Svendsen, Experimental study of perforated suspended ceilings as diffuse ventilation air inlets, Energy Build. 56 (2013) 160–168.

[6] P. Jacobs, B. Knoll, Diffuse ceiling ventilation for fresh classrooms, in: 4th International Symposium on Building and Ductwork Air Tightness, 2009, pp. 1–7.

[7] E.M. Jakubowska, Air Distribution in Rooms with the Diffuse Ceiling Inlet (PhD thesis), Department of Civil Engineerging, Aalborg University, Denmark, 2007.

[8] L. Jacobsen, Air Motion and Thermal Environment in Pig Housing Facilities with Diffuse Inlet (PhD thesis), Department of Civil Engineering, Aalborg University, Denmark, 2008.

[9] L. Rong, B. Elhadidi, H.E. Khalifa, P.V. Nielsen, CFD modeling of airflow in a livestock building, in: 7th International Conference on Indoor Air Quality, Ventilation and Energy Conservation in Buildings, United States, 2010.

[10] P.V. Nielsen, R.L. Jensen, L. Rong, Diffuse ceiling inlet systems and the room air distribution, in: Clima 2010: 10th REHVA World Congress, 2010.

[11] P. Jacobs, E.C.M. Van Oeffelen, B. Knoll, Diffuse ceiling ventilation, a new concept for healthy and productive classrooms, Indoor Air (2008) 17–22.

[12] F.I.Z. Karlsruhe, Thermo-Active Building Systems, FIZ Kalsruhe, Germany, 2007.

[13] B.W. Olesen, Using building mass to heat and cool, ASHRAE J. (2012) 44–52.

[14] B. Lehmann, V. Dorer, M. Gwerder, F. Renggli, J. Tödtli, Thermally activated building systems (TABS): energy efficiency as a function of control strategy, hydronic circuit topology and (cold) generation system, Appl. Energy 88 (January (1)) (2011) 180–191.

[15] B. Lehmann, V. Dorer, M. Koschenz, Application range of thermally activated building systems tabs, Energy Build. 39 (May (5)) (2007) 593–598.

[16] S.B. Riffat, X. Zhao, P.S. Doherty, Review of research into and application of chilled ceilings and displacement ventilation systems in Europe, Int. J. Energy Res. 28 (March (3)) (2004) 257–286.

[17] S.J. Rees, P. Haves, An experimental study of air flow and temperature distribution in a room with displacement ventilation and a chilled ceiling, Build. Environ. 59 (2013) 358–368.

[18] F. Alamdari, D.J.G. Butler, P.F. Grigg, M.R. Shaw, U. Kingdom, Chilled ceiling and displacement ventilation, Renew. Energy 15 (1–4) (1998) 300–305.

[19] F. Causone, F. Baldin, B.W. Olesen, S.P. Corgnati, Floor heating and cooling combined with displacement ventilation: possibilities and limitations, Energy Build. 42 (December (12)) (2010) 2338–2352.

[20] M. Behne, Indoor air quality in rooms with cooled ceilings. Mixing ventilation or rather displacement ventilation? Energy Build. 30 (1999) 155–166.

[21] T. Yu, P. Heiselberg, B. Lei, M. Pomianowski, C. Zhang, A novel system solution for cooling and ventilation in office buildings: a review of applied technologies and a case study, Energy Build. 90 (2015) 142–155.

[22] C.A. Hviid, Integrated ventilation and night cooling in classrooms with diffuse ceiling ventilation, in: 11th Ökosan, 2011.

[23] ISO 8990-1996: Thermal Insulation. Determination of Steady-State Thermal Transmission Properties. Calibrated and Guarded Hot Box, International Standard, 1996.

[24] ISO 7730:2005: Ergonomics of the thermal environment – Analytical Determination and Interpretation of Thermal Comfort Using Calculation of the PMV and PPD Indices and Local Thermal Comfort Criteria, International Standard, 2005.

[25] H.B. Awbi, A. Hatton, Mixed convection from heated room surfaces, Energy Build. 32 (2000) 153–166.

[26] J. Fan, C.A. Hviid, H. Yang, Performance analysis of a new design of office diffuse ceiling ventilation system, Energy Build. 59 (2013) 73–81.

[27] P.O. Fanger, B.M. Ipsen, G. Langkilde, B.W. Olesen, N.K. Christensen, S. Tanabe, Comfort limits for asymmetric thermal radiation, Energy Build. 8 (1985) 225–236.

[28] EN 15377.2:2008, Heating Systems In Buildings – Design of Embedded Water Based Surface Heating and Cooling Systems – Part 2: Design, Dimensioning and Installation, European Standard, European Committee for Standardization, 2008.

[29] B.W. Olesen, New European standards for design, dimensioning and testing embedded radiant heating and cooling systems, in: Clima 2007: Wellbeing Indoor, Helsinki, Finland, 2007.

[30] F.S. Bauman, Underfloor Air Distribution (UFAD) Design Guide, American Society of Heating, Refrigerating and Air-Conditioning Engineers, Inc., USA, 2013.

Appendix C. Airflow Pattern and performance analysis of diffuse ceiling ventilation in an office room using CFD Study

Paper 3

AIRFLOW PATTERN AND PERFORMANCE ANALYSIS OF DIFFUSE CEILING VENTILATION IN AN OFFICE ROOM USING CFD STUDY

Chen Zhang[1], Qingyan Chen[2], Per K. Heiselberg[1], Michal Z. Pomianowski[1]
[1]Department of Civil Engineering, Aalborg University, Aalborg, 9200, Denmark
[2]School of Mechanical Engineering, Purdue University, West Lafayette, IN 47907, USA

ABSTRACT

Diffuse ceiling ventilation uses perforations in the suspended ceiling to deliver air into the occupied zone. Due to the complex geometry of the diffuser, it is not possible to build an exact geometrical model in CFD simulation. Two numerical models are proposed in this study, one is a simplified geometrical model and the other is a porous media model. The numerical models are validated by the full-scale experimental studies in a climate chamber. The results indicate that porous media model performed better on predicting air flow characteristic below diffuse ceiling and air velocity near the floor. However, the simplified geometrical model shows superior performance on calculating the diffuse ceiling surface temperature.

INTRODUCTION

The diffuse ceiling ventilation is an air distribution concept where the space above a suspended ceiling is used as a plenum and fresh air is supplied into the occupied zone through perforations in the suspended ceiling panels. As the large ceiling area serves as the supply opening, airflow is delivered into the occupied zone with very low velocity and with no fixed jet direction, hence the name 'diffuse'. The flow pattern in the room is normally controlled by the buoyance flow generated by heat sources. This ventilation concept was widely used in livestock buildings due to its low investment cost and high thermal comfort level(Jacobsen, 2008) (Rong, Elhadidi, Khalifa, & Nielsen, 2010.) as well as in clean rooms where high ventilation effectiveness is required (Brohus & Balling, 2004). In recent years, the applications and studies regarding utilization of diffuse ceiling ventilation in indoor spaces for humans are increasing gradually, especially for offices and classrooms with high heat loads and high ventilation demands.

The performance of diffuse ceiling ventilation in an office room was investigated by Nielsen et al. (2007) (Jakubowska, 2007) and compared with five other air distribution systems. Their investigations showed that diffuse ceiling ventilation presented superior performance on handling high heat loads with low draught risk in the occupied zone. Hviid et al. (2013) performed an experimental study in a climate chamber with two perforated tiles as diffuse ceiling supply. The results were in good agreement with

Nielsen's and no local discomfort in the occupant zone was found and the air change efficiency was comparable to mixing ventilation. On the other hand, they pointed out that a low pressure drop of 0.5 Pa to 1.5 Pa is enough to sustain the pressure of the plenum and ensure uni-directional flow through diffuse ceiling and that there is a radiation cooling potential of the ceiling. The other advantages such as modest investment costs, low energy consumption and low noise level was reported by Jacobs et al.(2009) from a pilot study in a classroom.

Studies of ventilation systems mainly use two approaches: experimental and numerical study. Compared with an experimental study, the numerical study is reputed for its low cost and time efficiency, as the boundary conditions can be easily changed to study different scenarios. The geometry of the diffuse ceiling diffuser is too complicated to be directly modelled in practical CFD-simulations. Therefore, simplified models that aim to describe the main characteristic of the diffuse ceiling ventilation needs to be developed.

Simplified models for some other supply diffusers have been extensively studied and been validated, such as momentum model and box model. In the momentum model, an initial jet momentum is imposed as a source term, and momentum and mass boundary conditions for the diffusers are decoupled for CFD simulations (Chen & Moser, 1991) (Srebric & Chen, 2003). The box method is conducted by defined the boundary conditions on an imaginary box surface around the diffuser(Skovgaard, M., Nielsen, 1991). One difficulty of this method is to specify the box size, which should have the boundaries in the fully developed region and avoid the impact of room air recirculation. On the other hand, in order to specify the boundary condition, either suitable jet relation or extensive measurement data is required. However, due to the unique properties of diffuse ceiling, these methods cannot effectively describe the air flow pattern and the flow characteristics of diffuse ceiling ventilation. First of all, the large ceiling area is used as supply diffuser, where the fully developed jet relation is not applicable and the measurement of the box boundary condition is unrealistic. Secondly, the use of a ceiling plenum to deliver air is one of the key features that distinguish diffuse ceiling ventilation from the conventional ducted air distribution system. The heat exchange between supply air and the thermal mass in the plenum will

influence the supply air temperature as it passing through the plenum. Therefore, the air will be supplied with non-uniform temperature and non-uniform amount through the diffuser. Although momentum method could introduce a correct momentum flow, it is impossible to predict the air temperature distribution and velocity distribution at the inlet boundary. Finally, the configurations of plenum and properties of diffuse ceiling panels have strong influence on the effectiveness of diffuse ceiling ventilation, and these parameters should be taken into account in the numerical model. Therefore, a simplified model needs to be established to effectively simulate diffuse ceiling ventilation.

Several numerical studies on diffuse ceiling ventilation haven been reported. Fan et al. (2013) simplified the diffuse ceiling as 4 long rectangular strips with the same effective area. They pointed out there is a slightly disagreement between numerical and experimental results due to the simplification of ceiling air passage, which cause overestimation/ underestimation of air movement in the room, especially in the region close to the ceiling. In Chodor's study (2013), they neglected the impact of the plenum and assumed the air was uniform distributed through the entire ceiling area with outdoor air temperature and with superficial velocity. Hviid (2013) had the similar assumption in his simulation. These studies focus on the characteristics of airflow in the conditioned space, however, the air distributed in the plenum and air flow through diffuse ceiling is not discussed in detail.

The purpose of this study is to propose a numerical model, which could effectively describe the air flow pattern of diffuse ceiling ventilation in both plenum and occupied zone. Two simplified models are built and compared, one is a simplified geometrical model and the other is a porous media model. The thermal comfort in the occupied zone is estimated by the temperature gradient and the velocity profile at different locations in the conditioned space. The air flow pattern in the plenum and through the diffuse ceiling is evaluated by the temperature distribution of plenum air and on the upper and lower surface of diffuse ceiling panel. Radiant ceiling system will work as a supplementary system to deal with additional heating or cooling demand during winter and summer. The impact of radiation on the accuracy of simplified models is also discussed. The numerical models are validated by experimental studies in different operating conditions.

EXPERIMENTAL DESCRIPTION

Diffuse ceiling and its physical properties

In this study, the diffuse ceiling is made by cement-wood panels, which are originally used for sound absorption, as shown in Figure 1. Each panel has the dimension of 35 mm in thickness, 600 mm in width and 1200 mm in length. The density of the ceiling

panel is measured to be 359.13 kg/m^3. The porosity is estimated through volumetric measurement, which is 65%. The thermal conductivity is measured by λ-Meter EP500 based on the guarded hot plate method, and the value is 0.085 W/m.K with a measurement error less than 1.0 %.

The pressure drop across the ceiling panel is measured as function of superficial velocity. The panel sample is placed in the centre of a pressure chamber, and the pressure difference across the sample is measured by FCO 510 micromanometer with an accuracy of 0.25%. The results are shown in Figure 2, indicated as pressure drop across a single panel.

Figure 1 Cement-wood panel
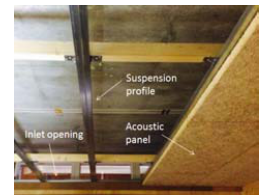
Figure 3 Diffuse ceiling setup
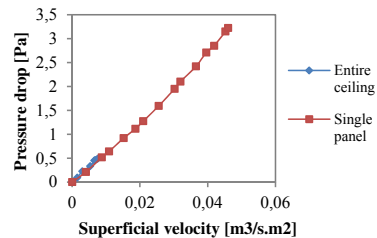
Figure 2. Function between pressure drop and superficial velocity for single panel and entire ceiling

Test chamber
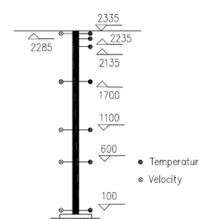
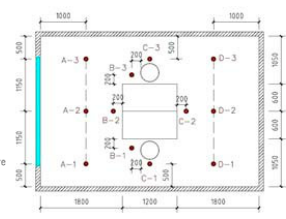Figure 4 Temperature and velocity sensors in the moveable columns

Figure 5 Measurement locations of air temperature and velocity in the conditioned space

In order to investigate the airflow pattern in the room with diffuse ceiling ventilation, a test system is installed in a climate chamber with a dimension of 4.8m * 3.3m * 2.72m (length * width * height). The diffuse ceiling is installed 0.35 m below the ceiling

concrete slab and is fixed by suspension profiles, as illustrated in Figure 3. The suspended ceiling panels cover the entire ceiling area and separate the space into two zones: the plenum and the conditioned space. The air is supplied into the plenum through three small windows located above the diffuse ceiling, with a geometric opening area of 0.0675 m^2. The exhaust is located in the conditioned space, at the bottom left corner of the front wall with a diameter of 160 mm. The air is drawn from the test chamber into a connected cooling chamber by means of an exhaust fan, and it will be re-supplied into the test chamber after cooling down by the air-handling unit located inside the cooling chamber.

The test room is set up to represent an office layout. Two workplaces are arranged, which consists of two desks with two computers (55W and 45 W), two monitors (16 W and 21.5 W) and two task lamps (54 W and 59 W). Two persons are simulated by thermal manikins (100 W for each). The overall heat load is 450.5 W (28.44 W/m2).

In the experiments, the air velocity and air temperature are measured in both plenum and conditioned space. Three moveable columns are located in the occupied zone, and in each column there are 7 thermocouples and 5 anemometers positioned at different heights to measure vertical temperature and velocity profiles, as indicated in Figure 4. Each column are moved to 4 positions, so that in total 12 positions have been measured in the occupied zone, as indicated in Figure 5. In the plenum, the thermocouples and anemometers are placed in the central line, at three different distances to the inlet (0.8 m, 2.4 mand 4.0 m). In addition, the surface temperature of diffuse ceiling panels and inner walls are measured. The temperatures are measured by K-type thermocouples with an accuracy of ± 0.15 K. The air velocities are measured by Dantec 54R 10 Hot sphere anemometer with a accuracy of ± 0.01 m/s +5% of reading. Finally, there are 5 pressure sensors located in the plenum and the conditioned space to determine the pressure drop across the diffuse ceiling and the pressure difference is recorded by FCO510 micromanometer.

Table 1

Test conditions in three scenarios

Case	ACH h^{-1}	Supply air temp ^{o}C	Slab surface temp ^{o}C	Heat load W
1	2	9.46	-	450.5
2	2	24.10	10.79	450.5
3	2	-6.87	27.34	450.5

Note: In scenario 1 where radiant slabs are not activated, slab surface temperature reacts to the air temperature and other wall temperatures. In scenarios 2 and 3, radiant slabs are activated and the slab surface temperature is controlled by water temperature.

Experiments are carried out in three scenarios with a supply air temperature range of 24.1 ^{o}C to -6.8 ^{o}C, which represents diffuse ceiling ventilation operating conditions at different seasons. A constant air change rate of 2 h^{-1} and a constant heat load of 450.5 W are used in all three scenarios. In order to keep an acceptable indoor environment, radiant slabs located above the diffuse ceiling serve as a supplementary system to deal with additional heating or cooling demand. The detail test conditions are listed in Table 1.

NUMERICAL MODEL

Simplified geometrical model

The simplified geometrical model approach is the most common method to simulate an air diffuser. The inlet boundary is set by reducing the inlet opening size, which is easy to implement in the CFD model. Heikkinen et al.(1993) pointed out that this method can produce good results for regions remote from the initial jet development.

Due to the special structure of the cement-wood panel (Figure 1), the effective opening area ratio of the diffuse ceiling does not equal to the panel's porosity and is difficult to be measured directly. Therefore, the effective opening area is calculated based on the pressure drop results obtained by measurement, as expressed by Eq (1).

$$C_d A = \frac{\dot{m}}{\sqrt{2\rho\Delta P}} \qquad (1)$$

Where: $\dot{m}$ is the mass flow rate, ΔP is the pressure drop across the diffuse ceiling, C_d is the discharge coefficient. A default C_d value of 0.6 is used in this study, which is suitable for the opening with low area ratio. Therefore, three slots opening with an effective area of 0.032 m^2 each are built to simulate the air passage of diffuse ceiling ventilation, as illustrated in Figure 6 (a).

The thermal process within the plenum is complex, which includes both the convective heat exchange between supply air and thermal mass and radiative heat exchange between diffuse ceiling panels and radiant slabs. Therefore, a surface-to-surface radiation model is activated in this model.

Porous media model

Due to the material properties of the wood-cement panel, a porous media model is adopted to simulate the flow through diffuse ceiling, as shown in Figure 6 (b). The basic idea of porous media model is to add a momentum sink in the governing momentum equation. The source term is composed of two parts: a viscous loss term and an inertial loss term(ANSYS, 2009). In laminar flows through porous media, the pressure drop is typically proportional to velocity, while at high flow velocity, the inertial loss will be dominant in the porous media, as expressed by Eq (2).

$$S_i = -\left(\frac{\mu}{\alpha}v_i + C_2 \frac{1}{2}\rho|v|v_i\right) \quad (2)$$

Where: v represent superficial velocity, α is the permeability, C_2 is inertial resistance factor. The viscous and inertial resistance coefficient $1/\alpha$ and C_2 are determined based on the function between pressure loss through porous media and superficial velocity obtained by experiments. In the experimental study, both the pressure drop across a single panel and the pressure drop across the entire ceiling are measured, as shown in Figure 2. Due to the large ceiling area and the limited capacity of the exhaust fan, only the small superficial velocities are performed when measured the entire ceiling pressure loss. The linear function between pressure drop and superficial velocity indicates the flow is laminar when it goes through the ceiling. These two pressure drop profiles correspond well with each other, revealing a fact that the cracks between ceiling panels and suspension system do not have apparent impact on the pressure drop. The viscous resistance and inertia resistance are calculated to be $1.14\ e^{+8}\ m^{-2}$ and $33055\ m^{-1}$, respectively.

| (a) | (b) |
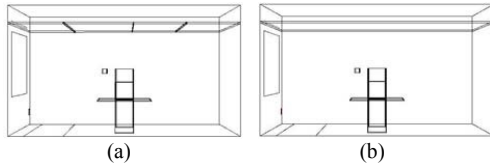
Figure 6 CFD model of the office room with diffuse ceiling (a) Simplified geometry model (b) Porous media model

The energy equation in porous media is modified on the conduction flux and the transient terms only, as expressed by Equation (3). An effective thermal conductivity of the medium is introduced as the volume average of the fluid conductivity and the solid conductivity.

$$\frac{\partial}{\partial t}\left(\gamma\rho_f E_f + (1-\gamma)\rho_s E_s\right) + \nabla\cdot\left(\bar{v}(\rho_f E_f + P)\right)$$
$$= \nabla\cdot\left[k_{eff}\nabla T - (\sum h_i J_i) + (\bar{\tau}\cdot\bar{v})\right] + S_f \quad (3)$$

Where: E_f is the total fluid energy, E_s is the total solid medium energy, γ is the porosity of the medium, and k_{eff} is the effective thermal conductivity of the medium.

Unfortunately, the porous media model is incompatible with radiation model because it is regarded as a fluid zone and the diffuse ceiling surfaces are treated as interiors between two fluid zones. In order to overcome this limitation, a radiation model is built separately, where the porous media is replaced by a solid material with the same thermal properties. The calculated surface temperatures (except diffuse ceiling surface temperature) is directly used as boundary inputs in the porous media model and heat exchanges between

porous media zone and the other zones (plenum and room) are calculated and treated as an energy source term S_f in the energy equation (3).

Turbulence model and Boundary conditions

As mentioned, the air flow through the diffuse ceiling with very low velocity and the flow is laminar. However, the convection air flow generated by the heat sources in the occupied zone increase the turbulence level. Thus, the Re-normalized group (RNG) k-ε model is appropriate for this situation, which provides an analytically derived differential formal for effective viscosity for low-Reynolds-number effects compared with the standard k-ε model (ANSYS, 2009). The boussinesq hypothesis is selected to model buoyancy-driven flow, with air thermal expansion coefficient of $0.343*10^{-3}\ K^{-1}$.

The geometrical model is created to represent the test chamber as it is physically, as shown in Figure 6. The entire model is divided into three zones: plenum, diffuse ceiling and room. As mentioned, three small windows above diffuse ceiling serves as inlet and a ventilation duct located in the same wall serves as outlet in the experiment. In order to simplify the geometrical model and generate a high quality mesh, the inlet and outlet are simplified as rectangular openings with the same area in the CFD model. The inlet is assumed to have a uniform profile, where the air temperature and velocity are kept the same as in the experiments. The outlet is simulated with zero pressure and zero gradient conditions for all the flow parameters.

The U-values of the walls are used as input for all the wall boundaries, and the measured air temperature in the cooling chamber zone and the surrounding zone are used as free stream temperatures. The heat released by heat sources consists of convection and radiation. For the model with radiation, the total heat loads are released from heat sources as surface heat fluxes. For porous media model where radiation is not compatible, the effect of radiation heat exchange has been presented on the surface temperature of enclosed walls. Therefore, only the convection heat flow boundary condition is specified for the heat sources.

Numerical methods

Mesh is an important factor for the high quality CFD model. The general idea is that fine grids must be used in areas with large gradients to minimize false diffusion and dispersive errors. In this study, structured meshes are generated in the entire computational domain and the finest meshes are generated in critical areas such as: diffuse ceiling, inlet, outlet, area closed to the walls and heat sources. A grid independency study is performed by models with different mesh densities. The total number of cells needed is determined to be 741,831for the simplified geometrical model and 669,262 for the porous media model.

The SIMPLE numerical algorithm is used. The criteria of convergence is set such that the residuals for u, v, w, k, ε less than 10^{-3}, and the residual for energy less than 10^{-6}.

RESULTS AND DISCUSSIONS

Air flow pattern in the conditioned space

Figure 7 and 8 illustrate the velocity and temperature distribution at the central plane of the office room in scenario 1. The air flow pattern predicted by the two models show a similar trend. The thermal plume generated by heat sources is the dominant driven force in the room with diffuse ceiling ventilation. The uprising buoyance flow above heat sources and the downward flow attached the wall generate air circulations in the room. Small jet flows below diffuse ceiling are observed in the simplified geometrical model, but its effect to the air flow pattern in the conditioned space is negligible compared to the buoyance driven flow. Relatively high air velocities are found at the ankle level in both models. However, the simplified geometrical model predicts high ankle velocities in both sides of the room, while, the porous media model indicates high ankle velocity mainly occurs in the side closed to the front wall (left side).
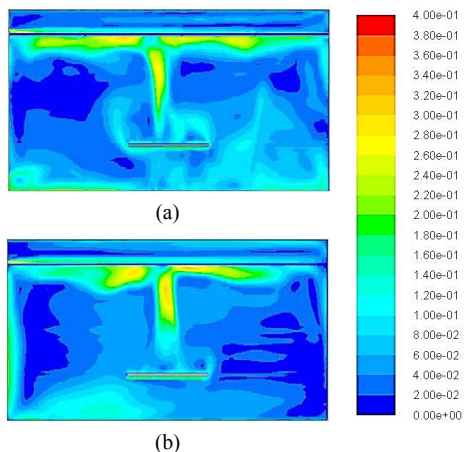
Figure 7 Velocity contour across the central plane of the room (a) Simplified geometrical model (b) Porous media model

The positive pressure in the plenum relative to the room enable air mixing in the plenum before it is supplied into the room and diffuse ceiling panels serve as a layer of insulation between the plenum and the conditioned space. Therefore, an air temperature difference between the plenum and the conditioned space will be expected, as shown in Figure 8. However, the air temperature is not uniform in the plenum due to its heat exchange with thermal mass (concrete slab and diffuse ceiling panel). The supply air temperature varies as a function of distance travelled through the plenum. Although air is supplied through the diffuse ceiling diffuser with non-uniform temperature, its impact on the room air temperature distribution is not obvious. The air temperature is predicted to be uniformly distributed in the occupied zone (except the region above heat sources), because of convection flows generated by the heat sources increases the mixing level.
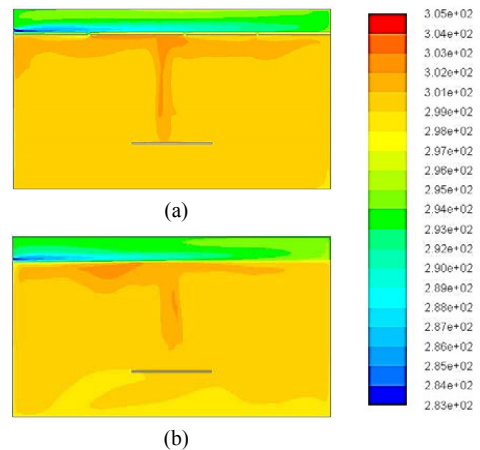
Figure 8 Temperature contour across the central plane of the room (a) Simplified geometrical model (b) Porous media model

Figure 9 and 10 show the vertical profiles of air temperature and velocity at four locations in the chamber, comparing the CFD modelling results with the measurement results. Although measurements are taken in many locations, the four locations along the central panel of the room are selected because they can represent the air flow characteristics in the room with diffuse ceiling ventilation. As indicated by Figure 9, a low vertical air temperature gradient is observed in the occupied zone. The temperature difference are less than 0.7 °C between the head and ankle level in all locations, which are much less than the limitation of 3 K required by ISO 7730 category B(ISO 7730, 2005). A good agreement has been reached between the computed air temperature and measured data in the occupied zone. The largest discrepancy is found in the region below the diffuse ceiling, where the CFD models overestimate the effect of the thermal plume. Compared with the simplified geometrical model, the porous media model gives a better prediction of the air temperature below diffuse ceiling, especially in location C-2 and D-2. This is because the porous media model allows air supply through the entire ceiling area, which is more close to the realistic air flow characteristics of diffuse ceiling ventilation.

Figure 10 indicates that the air velocity in the occupied zone is generally low, and no draught risk

is observed in all locations. A relatively high velocity is found at the ankle level closed to the front wall (A-2). The air velocity near the floor gradually reduces with increasing distance to the front wall. The porous media model show better performances on predicting the air velocity. The simplified geometrical model overestimate the air velocity near the floor and the velocity at location D-2. Both models indicate there is a peak velocity 5-10 cm below the diffuse ceiling, due to the thermal plume. More measured data is required in this region to validate this finding.
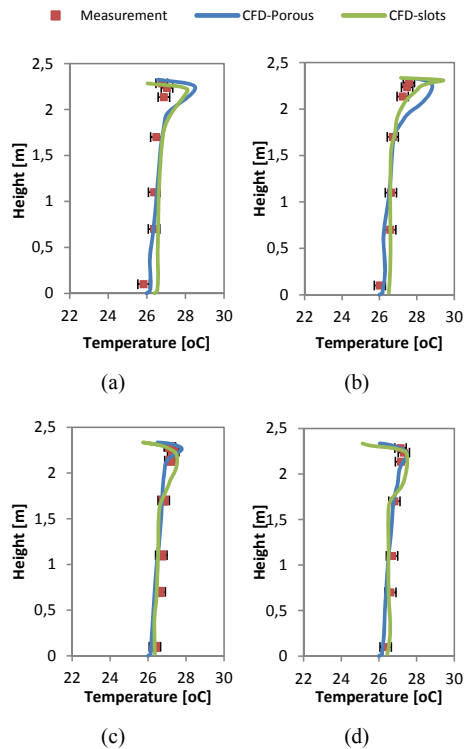
Figure 9 Comparison of the vertical temperature profile at different locations for scenario 1 (a) A-2 (b) B-2 (c) C-2 (d) D-2
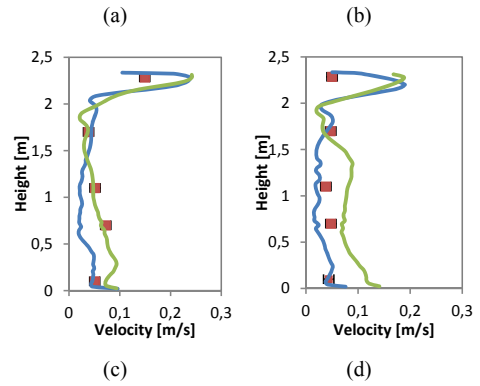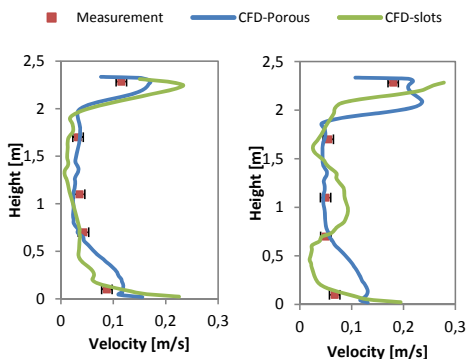
Figure 10 Comparison of the vertical velocity profile at different locations for scenario 1 (a) A-2 (b) B-2 (c) C-2 (d) D-2

Scenario 2 simulates a summer condition and scenario 3 simulates a winter condition, where the supply air temperature ranges from 24.1 to -6.87 ^{o}C and the radiant slabs run in cooling mode and heating mode, respectively. Due to the limited space in this paper, the comparison of vertical air temperature and velocity in these two scenarios will not be illustrated here. The effect of supply air temperature on the vertical temperature gradient of the conditioned space is not significant. The air temperature differences between head and ankle level are less than 0.4 ^{o}C in scenario 2 and less than 0.9 ^{o}C for scenario 3. However, the relative high velocity near the floor moves along the horizontal direction while the supply air temperature changes. In winter the cold downward flow generates a strong circulation close to the front wall. On the contrary, the warm supply air in summer allow a longer penetration length, thus, strong air circulation occurs at the end of the room. Generally, these two models give satisfactory prediction of the flow pattern in the conditioned space. Although the porous media model has smaller discrepancies to measured results, the difference between two models is quite limited.

Air distribution in the plenum and through diffuse ceiling

The thermal processes within the plenum have an important impact on the effectiveness of diffuse ceiling ventilation. An appropriate numerical model should be able to correctly predict the air flow pattern and thermal processes in the plenum and through the diffuse ceiling.

Figure 11 shows the relationship between plenum air temperature and the distance to plenum inlet in the three scenarios. As the air travels through the plenum, it is gradually warmed up or cooled down by heat transfer from the diffuse ceiling panels and from the radiant slabs, named as thermal decay. Both CFD models give acceptable predications on the thermal decay of plenum air. The largest disagreement occurs

in scenario 3, where the peak air temperature at the center is not predicted by the CFD models. This may be caused by a reverse flow occurring in this region due to the thermal plume from the heat sources. On the other hand, although the supply air temperature changes from -6.87 ^{o}C to 24.10 ^{o}C, the air temperature in the plenum stays relatively stable (14 ^{o}C to 22 ^{o}C). This indicates a significant pre-heating or pre-cooling effect of the plenum.

instead of predicting surface temperature, the porous media model calculates the air temperature through the diffuse ceiling panels. On the other hand, because the porous media model is incompatible with the radiation model, the impact of radiation heat transfer to/from the diffuse ceiling panel is calculated and treated as an energy source term in the energy equation. These assumptions cause the disagreement between the CFD simulations and the experiments.

(a)

(b)

(c)
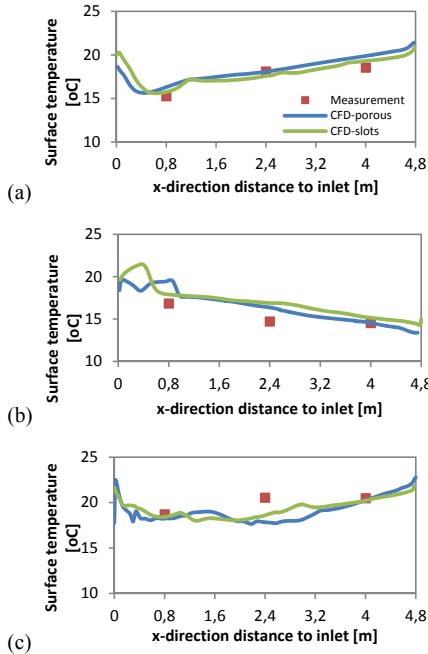
Figure 11 Plenum air temperature distribution (a) Scenario 1 (b) Scenario 2 (c) Scenario 3

As a medium between the plenum and the room, the diffuse ceiling panel has a complex heat exchange with these two zones. The diffuse ceiling surface temperatures are measured and simulated in the three scenarios, as presented by Figure 12. The measured data indicate that the surface temperatures are not uniformly distributed, but changes as a function of the distance to plenum inlet. In addition, a noticeable temperature difference between the diffuse ceiling lower and upper surface is observed, which reaches to 10 ^{o}C. The simplified geometrical model obtains a better agreement with the measured data, although the surface temperature drops in the positions, where the slot openings are built. The porous media model fails to predict the surface temperature of the diffuse ceiling panels, especially when the radiant slabs are activated (Scenario 2 and 3). This is because the porous media is treated as a fluid zone in the CFD software and the diffuse ceiling surfaces are regarded as interiors between two fluid zones. Therefore,

(a)

(b)

(c)

(d)

(e)
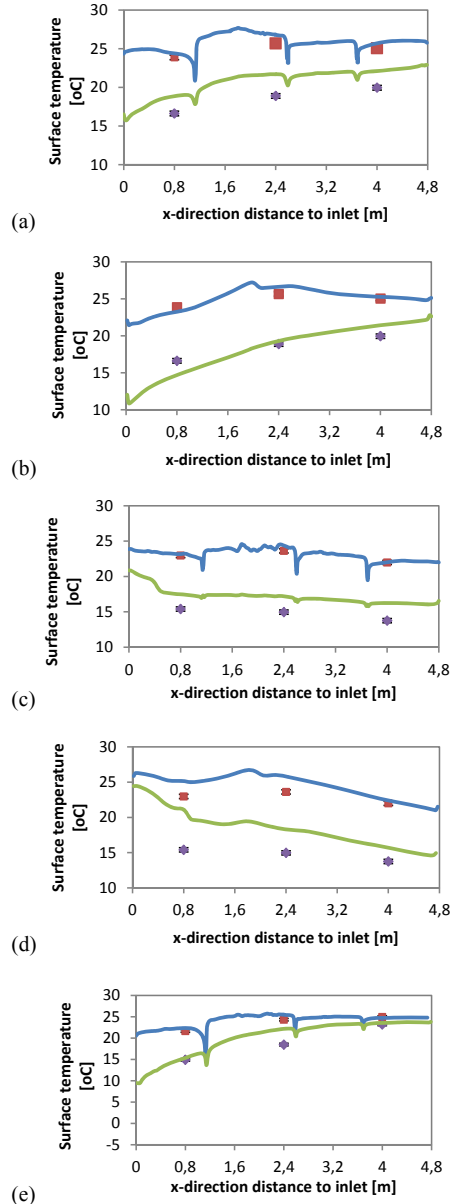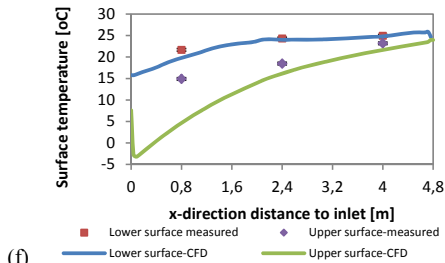
(f)

Figure 12 Diffuse ceiling surface temperature distribution. Scenario 1: (a) Simplified geometrical model (b) Porous media model; Scenario 2: (c) Simplified geometrical model (d) Porous media model; Scenario 3: (e) Simplified geometrical model (f) Porous media model

CONCLUSION

The objective of this research is to develop a simplified method on predicting the air flow pattern of diffuse ceiling ventilation in the CFD simulation. Two numerical models have been presented and compared, one is a simplified geometrical model and the other is a porous media model. The measured data obtained by the full-scale experiments are used to validate the numerical models.

Both the experimental results and the numerical results indicate that buoyancy flows generated by heat sources is the driving force for air distribution in a room with diffuse ceiling ventilation. The thermal plume increases the mixing level, creating a uniform temperature distribution in the occupied zone. A relative high velocity is observed at the ankle level near the front wall, however, no draught risk is predicted in any of the scenarios. A thermal decay of the supply air is observed in the plenum, due to the heat exchange between the air and the thermal mass (concrete slabs and diffuse ceiling panels). On the other hand, the plenum has a significant pre-heating or pre-cooling effect, enabling the air to be supplied into the room with an acceptable temperature.

Generally, the two numerical models reach good agreement with the measured data on the air temperature and velocity distribution in the occupied zone. The porous media model gives better predictions on the flow characteristic just through diffuse ceiling, and the air velocity near the floor. However, the simplified geometrical model shows superior performance on predicting the diffuse ceiling surface temperature. This is because of the limitations of the porous media model in the CFD software, where it is treated as a fluid zone and is incompatible with a radiation model.

REFERENCES

ANSYS, I. (2009). ANSYS FLUENT User's Guide.

Brohus, H., & Balling, K. D. (2004). Local Exhaust Efficiency in an Operating Room Ventilated by Horizontal Unidirectional Airflow. In Proceedings of Roomvent 2004. Coimbria Portugal.

Chen, Q. and A. Moser. (1991). Simulation of a Multiple-Nozzle Diffuser. Proceedings of 12th AIVC Con- ference 2:1-14.

Chodor, A. D., & Taradajko, P. P. (2013). Experimental and Numerical Analysis of Diffuse Ceiling Ventilation. Aalborg University.

Fan, J., Hviid, C. A., & Yang, H. (2013). Performance analysis of a new design of office diffuse ceiling ventilation system. Energy and Buildings, 59, 73–81.

Hviid, C. A. (2013). Numerical investigation of diffuse ceiling ventilation in an office under different operating conditions.

Hviid, C. A., & Svendsen, S. (2013). Experimental study of perforated suspended ceilings as diffuse ventilation air inlets. Energy and Buildings, 56, 160–168.

ISO 7730. (2005). Ergonomics of the thermal environment -- Analytical determination and interpretation of thermal comfort using calculation of the PMV and PPD indices and local thermal comfort criteria.

Jacobs, P., & Knoll, B. (2009). Diffuse ceiling ventilation for fresh classrooms. Proceedings of 4 th Intern. Symposium on Building and Ductwork Air tightness. Berlin, Germany.

Jacobsen, L. (2008). Air Motion and Thermal Environment in Pig Housing Facilities with Diffuse Inlet. Department of Civil Engineering, Aalborg University.

Lemaire, a. D., Chen, Q., Ewert, M., Heikkinen, J., Inard, C., Moser, a., … Whittle, G. (1993). IEA Annex 20: Air flow patterns within buildings. Room air and contaminant flow, evaluation of computational methods. Buildings, 82.

Nielsen, P. V, & Jakubowska, E. (2007). The Performance of Diffuse Ceiling Inlet and other Room Air Distribution Systems. Proceedings of Cold Climate HVAC 2009.Greenland.

Rong, L., Elhadidi, B., Khalifa, H. E., & Nielsen, P. V. (n.d.). CFD Modeling of Airflow in a Livestock Building. In IAQVEC 2010: The 7th International Conference on Indoor Air Quality, Ventilation and Energy Conservation in Buildings.

Skovgaard, M., Nielsen, P. V. (1991). Modelling Complex Inlet Geometries in CFD.

Srebric, J., & Chen, Q. (2003). Simplified numerical models for complex air supply diffusers. ASHRAE Transactions, 109 PART .
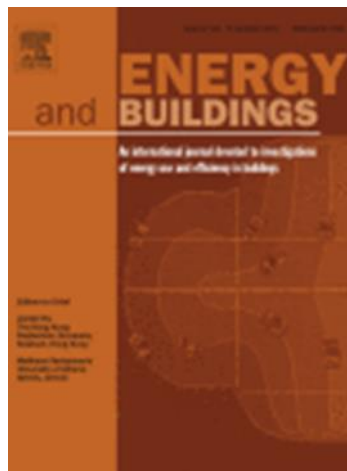
Appendix D. Parametrical analysis on the diffuse ceiling ventilation by experimental and numerical studies

Paper 4

Author's Right

Re: Add the article into Ph.D. thesis [ref 160704-007781] [160704-007781]

Dear Zhang,

Thank you for chatting with us.

Please be informed that as an author, you have the right to use your article for your thesis or dissertation as long as it is for non-commercial purposes.

I wish to advise that you do not need to obtain permission in some instances if you are the author of the article you wish to use. You also have certain rights in using your article.

For further details on this, please visit the link below:

https://www.elsevier.com/about/company-information/policies/copyright#permissions

Kind regards,

Marc Toneza

Researcher Support

Parametrical analysis on the diffuse ceiling ventilation by experimental and numerical studies

Chen Zhang*, Martin Heine Kristensen, Jakob Søland Jensen, Per Kvols Heiselberg, Rasmus Lund Jensen, Michal Pomianowski

Department of Civil Engineering, Aalborg University, Sofiendalsvej 11, Aalborg 9200, Denmark

ARTICLE INFO

ABSTRACT

This paper aims to investigate the performance of diffuse ceiling ventilation in a classroom. An experimental study is carried out in a test chamber to examine the impact of diffuse ceiling opening area on the system cooling capacity and thermal comfort. The results indicate that diffuse ceiling ventilation provides a satisfied thermal comfort level in the occupied zone even under a high ventilation rate and a high heat load condition. A design chart method is adopted to compare different diffuse ceiling configurations, and the results indicate that the system with a 18% diffuse ceiling opening area is able to handle the highest heat load without discomfort. On the other hand, a CFD model is built where the diffuse ceiling is simulated with a porous media zone. This model is validated by experimental results and further used to analyze the effect of heat load distribution and room height. The numerical results reveal that even distribution of heat sources gives a lower draught risk environment than centralized distribution. In addition, there is a significant increase on the draught risk with increase of room height.

© 2015 Elsevier B.V. All rights reserved.

1. Introduction

Nowadays, the most widely used ventilation systems in school buildings are mixing ventilation and displacement ventilation. In mixing ventilation, air is supplied to the room with high initial velocity and turbulence, which promotes good mixing with uniform temperature and pollution distribution in the occupied zone. On the contrary, the principle of displacement ventilation is to replace but not to mix the room air with fresh air, where the fresh and cold air is supplied close to the floor. Consequently, the highest velocity and the lowest temperature occur near the floor, and there is a vertical temperature gradient in the room [1]. Due to the concentrated flow through the inlets, draught problem always occurs in these two ventilation systems when high ventilation rate is required and air is supplied with low temperature [2]. As reported by Jacobs [3], high draught risk often leads to insufficient ventilation and poor air quality in the classroom. The indoor environment of classrooms has significant impact on pupils' health and learning efficiency. A recent study found that more than half of school children have some kind of allergy or asthma in the traditional

school buildings [4]. In addition, with a widespread study of Danish school, Toftum et al. [5] concluded that there is a strong association between classroom ventilation mode and learning outcome.

A novel ventilation concept was proposed recently, named as diffuse ceiling ventilation. In this air distribution system, the space above a suspended ceiling is used as a plenum and fresh air is supplied into the occupied zone through perforations in the suspended ceiling panels. Due to the large opening area, air is delivered into the occupied zone with very low velocity and with no fixed jet direction, hence the name 'diffuse'. Diffuse ceiling ventilation was widely used in livestock buildings due to its low investment cost and high thermal comfort level [6,7]. Recently, there has been a growing focus on the application of diffuse ceiling concept in indoor spaces for humans, especially for offices and classrooms with intense heat loads and high ventilation demands.

Nielsen et al. [8,9] investigated the performance of diffuse ceiling ventilation in an office room and compared it with five other air distribution systems. Their investigation showed that diffuse ceiling ventilation presented superior performance on handling high heat loads with low draught risk in the occupied zone. Hviid et al. [10] performed an experimental study in a climate chamber with two types of diffuse ceiling panels. The results were in good agreement with those of Nielsen that no local discomfort in the occupant zone was observed and the temperature and ventilation effectiveness were comparable to mixing ventilation. On the other hand,

* Corresponding author at: Aalborg University, Sofiendalsvej 11, Aalborg 9200 , Denmark. Tel.: +45 9940 7232.

E-mail address: cz@civil.aau.dk (C. Zhang).

they pointed out that a low pressure drop of 0.5 Pa to 1.5 Pa was enough to sustain the pressure of the plenum which ensured unidirectional flow through diffuse ceiling and there was a radiation cooling potential of the diffuse ceiling. The other advantages such as modest investment costs, low energy consumption and low noise level were reported by Jacobs et al. [2] with a pilot study in a Dutch classroom.

The previous studies have proved that buoyancy flow generated by heat sources is the dominant flow in a room with diffuse ceiling ventilation [10–12]. Because of the low impulse supply flow, the mixing in the room is dependent on the buoyance force. A tendency of displacement effect occurs at low heat loads and a development towards fully mixing with increasing heat load, as reported by Petersen [13]. Venkatasubbaiah et al. [14,15] conducted intensive studies on the buoyancy-induced flow in the ceiling vented room, and they revealed that flow behavior is significant influenced by the size and location of heat source. This finding was verified by Choder et al. [16] via an experimental study. They observed that equally distributed heat sources enable a higher cooling capacity of diffuse ceiling ventilation than the other heat sources locations, and that heat sources placed at floor level give a higher draught risk than if placed in the upper zone. Nielsen [17] further proved the benefit of an even distribution of heat sources and mentioned that the geometry of a room also impacts the performance of a diffuse ceiling ventilation.

Unlike the momentum driven ventilation systems, the inlet opening of diffuse ceiling ventilation is more flexible. As mentioned by Zhang et al. [18], the diffuse ceiling inlet can be divided into three types based on their air path. The air can be either supplied through the connection slots between ceiling panels (crack flow), or through perforations in the ceiling panels, or a combination of these two paths. In addition, the inlet can either occupy the whole ceiling area or part of the ceiling. However, the impacts of different air path and diffuse ceiling opening area on the system performance have not been discussed in detail in the previous studies.

This paper will conduct a parameter study on the supply opening area of diffuse ceiling with a full-scale experiment of a classroom layout. Besides thermal comfort evaluation, a design chart method is applied to compare different diffuse ceiling configurations and to find the optimal solution. Furthermore, a numerical model is built and validated by the experimental results. The validated CFD model is further used to analyze the effect of heat load locations and room height on the airflow pattern and draught risk in the room with diffuse ceiling ventilation.

2. Experimental study

2.1. Diffuse ceiling and its physical properties

In this study, the diffuse ceiling is made by cement-wood panels, which are originally for acoustic purpose, as shown in Fig. 1. Each panel has a dimension of 35 mm in thickness, 600 mm in width and 1200 mm in length. The density of the ceiling panel is measured to be 359 kg/m^3. The porosity is estimated through volumetric measurement, which is 65%. The thermal conductivity is measured by λ-Meter EP500 based on a guarded hot plate method, and the value is 0.085 W/m K with a measurement error less than 1.0%.

The ceiling panels are installed in the test room with a specific suspension system, as illustrated in Fig. 2. Because of the non-overlapping layout of the panels, it could be predicted that the air is supplied through both perforations in the panels and the slots between the panels. The amount of panel flow and crack flow can be evaluated by a pressure drop measurement.
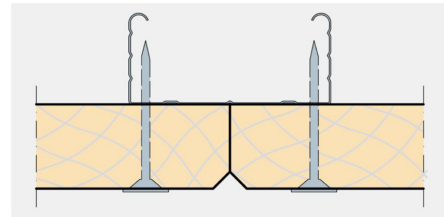

Fig. 1. Cement-wood ceiling panel.

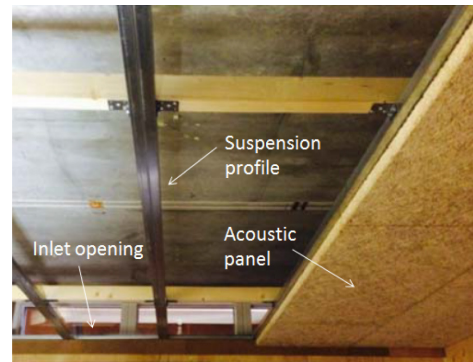**Fig. 2.** Suspension system of diffuse ceiling.

Fig. 3. Diffuse ceiling setup.

2.2. Test chamber

The experiments are carried out in a climate chamber with an inner dimension of 4.8 m × 3.3 m × 2.72 m (length × width × height), which is located at Aalborg University, Denmark. The test chamber is well-insulated and surrounded by a guarded zone with the purpose of reducing the heat gain or heat loss from the outside laboratory. The diffuse ceiling is installed 0.35 m below concrete slabs with the specific suspension system, as illustrated in Fig. 3. The diffuse ceiling panels cover the entire ceiling area and separate the space into two zones: a plenum and a conditioned space. The air is supplied into the plenum through three small windows located above the diffuse ceiling, with a total geometric opening area of 0.0675 m^2. The exhaust is mounted 80 mm below the diffuse ceiling in the wall opposite to the inlet, see Fig. 4. The air is drawn from the test chamber into a connected cold chamber by means of an exhaust fan, and the air will be re-supplied into the test chamber after it is conditioned by an air-handling unit located inside the cold chamber.
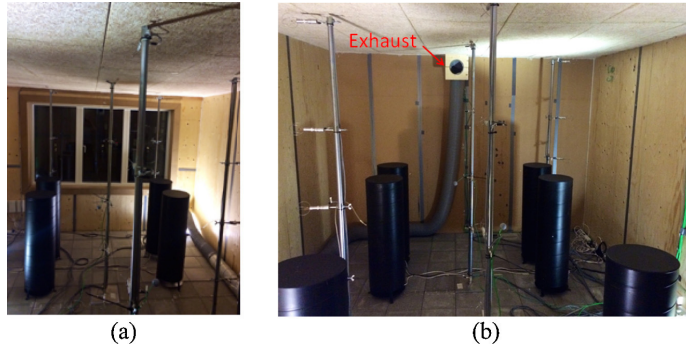
Fig. 4. The test chamber with a classroom layout (a) Front side (b) Back side.
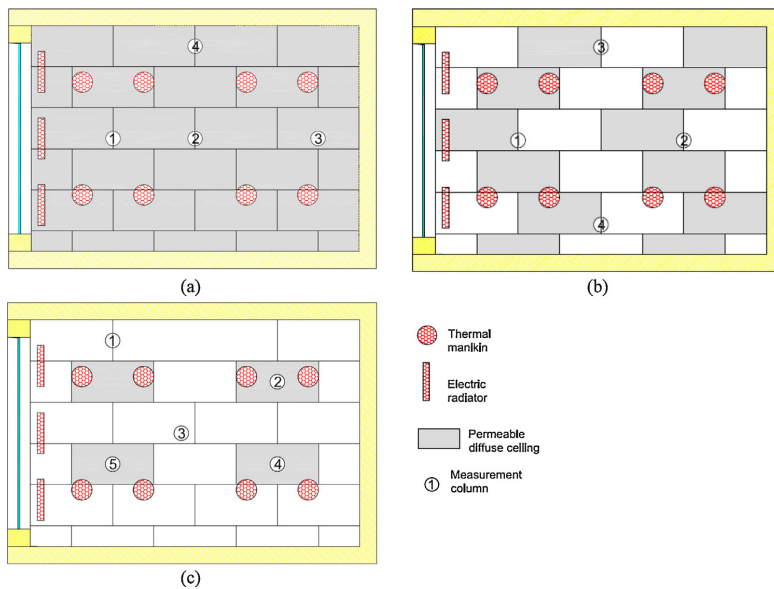

Fig. 5. Diffuse ceiling layouts and placement of measurement columns (gray panels are air permeable and white ones are covered by vapor barrier) (a) 100% DF (2) 50% DF (c) 18% DF.

The test room is set up to represent a classroom layout, as shown in Fig. 4. Eight thermal manikins with a heat load of 80 W each are used to simulate eight pupils with sedentary activity of 1.2 met. The thermal manikins are made by hollow black-painted metal barrels with a diameter of 0.3 m and a height of 1.0 m, and the heat is generated by an electric fan assisted heater hanging in the middle of the barrel. Besides eight thermal manikins, there are three electric radiators placed just below the big windows. They are used to maintain a desired indoor temperature under different operating conditions. The heat load of radiators varies in different cases and is recorded by a power meter.

The primary interest in the experiment is the diffuse ceiling opening area and its influence on the thermal comfort and system capacity. The tests are carried out with three diffuse ceiling opening ratios: 100%, 50% and 18%, as shown in Fig. 5. The changing of diffuse ceiling opening area is done by covering a vapor barrier on the suspended ceiling panels from the room side, as demonstrated in Fig. 6. Under each diffuse ceiling configuration, several tests are

conducted with different combinations of air flow rate and supply air temperature. Five supply air temperatures are determined to represent the system operation in different climates. In order to investigate comfort limit of the system, the air flow rate covers a wide range and reaches a very high value in the tests. Table 1 provides the details of test conditions.

2.3. Measurements

In the experiments, thermal comfort is evaluated by the vertical temperature gradient and the draught risk. Measurement columns are located in the critical regions within the occupied zone, which are determined based on the smoke visualization for each diffuse ceiling configuration. The placements of measurement columns for the three diffuse ceiling configurations are illustrated in Fig. 5. In each column, there are five Dantec hot-sphere anemometers with built-in thermistors located at five different heights (0.1 m, 0.6 m, 1.1 m, 1.7 m, 2.3 m). The measurement uncertainty of the air

Fig. 6. Reduced diffuse ceiling area by covering vapor barrier.

Table 1
Test conditions.

Case	DF (%)	$\Delta T = T_{ex} - T_{in}$ (°C)	ACR (h^{-1})
1–6	100	10	12–17
7–15		15	4–12
16–22		20	4–12
23–33		25	4–12
34–36		30	7–8
37–39	18	10	11–12
40–42		15	9–10
43–47		20	8–11
48–51		25	9–11
52–55		30	8–11
56–61	50	30	6–11
62–63		25	6–7
64–65		20	9–11
66–67		15	10–11
68–70		10	9–14

Note: ΔT is the temperature difference between exhaust and supply air.

velocity is ±5%, and the uncertainty of air temperature is ±0.1 K. The surface temperature of diffuse ceiling panels and inner walls are measured using K type thermocouples with an uncertainty of ±0.15 K. The pre-heating effect of the plenum is investigated by measuring the plenum air temperature with nine K-type thermocouples evenly distributed in the plenum. All the thermocouples are scanned every 10 s, and the temperatures are logged by a Helios Fluke data logger. Finally, there are five pressure sensors located in the plenum and the conditioned space in order to determine the pressure drop across the diffuse ceiling. The pressure difference is recorded by FCO510 micromanometer with an uncertainty of ±0.25%.

2.4. Design chart method

In this study, a design chart method is used to compare the system with different diffuse ceiling configurations. The design charts are drawn based on the measured results from the full-scale experiments.

In order to maintain an acceptable indoor thermal comfort, it is important to investigate the limit of a ventilation system regarding the possible air flow rate into the room and the temperature difference between supply and return in the design phase. A design chart method is proposed by Nielsen [8,19], which makes it is possible to compare different systems and find the most suitable one in a certain situation. The design chart can be expressed as a $q_0 - \Delta T_0$ chart, which encloses an area that supplies sufficient fresh air and ensures draught-free air movement in the occupied zone and a restricted vertical temperature gradient.

As mentioned by Nielsen [20], the limits shown in the design chart can be found using flow element theory. However, due to the large area of inlet in the diffuse ceiling ventilation, it may result in different types of important flow occurring between flow elements. Therefore, it is impossible to design this kind of systems based on flow element theory. Experiments and similarity principle are recommended in this situation [8]. In the room with fully developed flow, the non-dimensional velocity in the occupied zone is a function of Archimedes number. This phenomenon is called the similarity principle and expressed by the following equations:

$$\frac{u_{max}}{u_0} = func(Ar) \tag{1}$$

$$Ar = \frac{\beta \cdot g \cdot l \cdot \Delta T_0}{u_0^2} \tag{2}$$

where Ar is the Archimedes number, β is the expansion coefficient (1/K), g is the gravitational acceleration (m/s^2), ΔT_0 is the temperature difference between supply and return (K), u_0 is the supply air velocity and u_{max} is the maximum velocity in the occupied zone (m/s).

2.5. Experimental results

2.5.1. Thermal comfort

Due to the large amount of test cases, this paper will only include and present the cases representing the general tendencies. For each diffuse ceiling configuration, one case is selected. Case 22, Case 65 and Case 47 represent the diffuse ceiling opening ratio of 100%, 50% and 18%, respectively. All these cases operate with an air temperature difference ΔT of 20 °C and air change rate of 10.5 h^{-1}.

Fig. 7 illustrates the vertical temperature gradients with three different diffuse ceiling configurations. Low vertical temperature gradients in the occupied zone are observed in all cases. The maximum air temperature difference between head (1.7 m) and ankle level (0.1 m) is 0.88 °C, 1.09 °C and 0.62 °C in Case 22, Case 65 and Case 47, respectively, which is much lower than the limit of 3 °C in Category B ISO 7730 [21]. Regarding horizontal temperature distribution, an apparent temperature difference can be found just below the diffuse ceiling. In the 100% DF case, Column 1 is measured as 3–5 °C warmer than the other columns at 2.3 m height. This phenomenon can be explained by the airflow pattern predicted by CFD simulation, as shown in Fig. 11. The plume generated by the electric radiators forms a thermal layer below diffuse ceiling and blocks the supply into the occupied zone directly. The thermal plume becomes weak toward the back wall and enables more fresh air delivering into the room. In case 47, the temperature difference below diffuse ceiling even reaches to 17 °C. This is due to the fact that Column 2, 4 and 5 are located just below perforated ceiling panels, thus the temperature at these positions are close to the supply air temperature (plenum air temperature). However, Column 1 and 3 are placed below unperforated panels, where the air temperature is strongly influenced by the thermal plume. Although the large temperature difference is observed below the diffuse ceiling, the air temperature becomes very uniform in the occupied zone which indicates an effective mixing of thermal plume and fresh air is obtained in the occupied zone.

Fig. 8 shows the velocity profile in the test room. It needs to be noticed that these three cases aim to investigate the draught limit of the diffuse ceiling ventilation; therefore, very high heat loads (140–154 W/m^2) and very high air change rates (10.5 h^{-1}) are used compared with normal classroom conditions. Generally, high velocities are found at the ankle level in the occupied zone and the positions just below the diffuse ceiling. Although there is a high velocity at 1.7 m height in Case 47, the reason is not clear, which could be that the measurement point is too close to the thermal
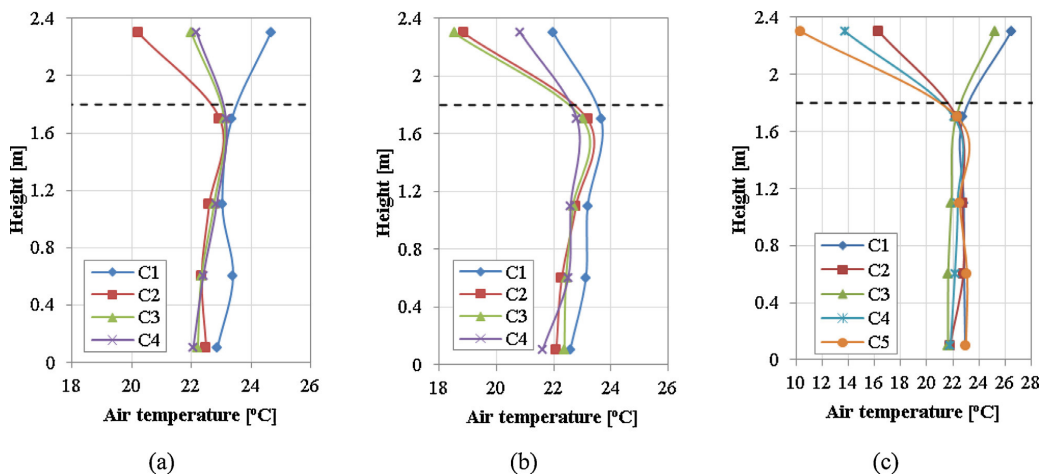
Fig. 7. Vertical air temperature (a) Case 22 with 100% DF (b) Case 65 with 50% DF (c) Case 47 with 18% DF.
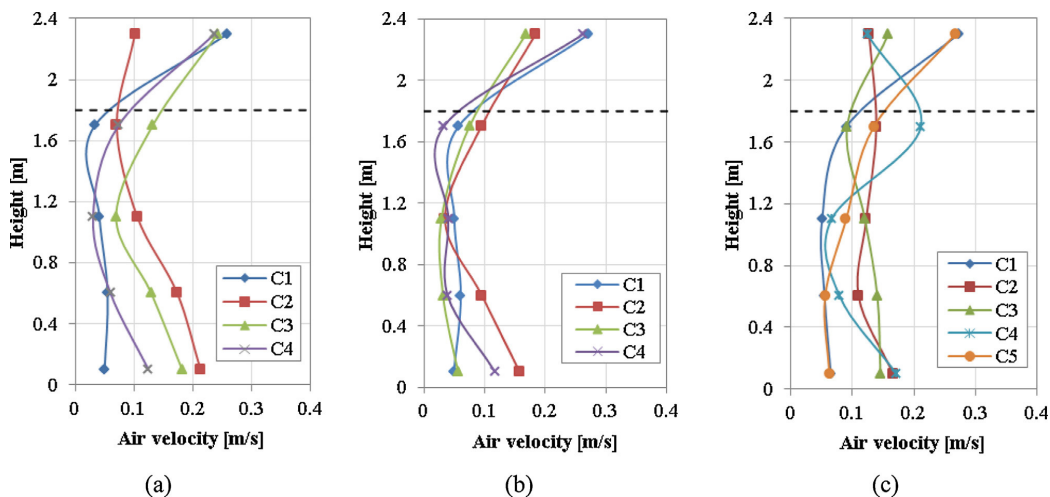

Fig. 8. Vertical air velocity (a) Case 22 with 100% DF (b) Case 65 with 50% DF (c) Case 47 with 18% DF.

manikin and is impacted by the thermal plume. The buoyancy flow generated by the electric radiators (1580–1770 W) is the driving force in the room. The uprising thermal plume attaches the ceiling and penetrates to the back side of the room from where it finally falls down attached to the back wall, which results in a strong vortex in the entire room. This phenomenon is supported by the velocity distribution from the CFD simulation, as indicated by Fig. 12. The air flow enters the occupied zone through the back side of the room at the floor level, exactly the positions high air velocities are observed in the experiments, as shown in Fig. 8. These results further prove that the diffuse ceiling ventilation system does not generate the draught by itself. Instead, it is the heat sources raising the draught risk.

2.5.2. Design chart

Fig. 9 shows the design chart for the diffuse ceiling ventilation with different opening areas. The design chart is based on the maximum velocity in the occupied zone of 0.2 m/s. However, it is impossible to control the air velocity in the occupied zone directly. Alternatively, it is calculated from the measured velocity with the same diffuse ceiling configuration and heat load condition, and it is assumed that the air flow in the room can be described as a fully developed turbulent flow [8,17]. Therefore, the similarity principle introduced in Section 2.4 can be applied.

The dashed line limits the minimum air flow rate of 7 l/s per occupant for the indoor air quality purpose required by Category B CR 1752 [22]. The $q_0 - \Delta T_0$ curve represents the maximum heat load that can be removed by the ventilation systems without creating draught. Because of the low vertical temperature gradient generated by diffuse ceiling ventilation, the limit of temperature gradient of 2.5 K/m is not considered in this case. The enclosed area of the design chart satisfies both the thermal comfort and indoor air quality requirements.

Fig. 9 shows that the cooling capacity of diffuse ceiling ventilation ranges from 40 W/m² to 100 W/m² depending on the diffuse ceiling configurations. The system with 18% opening area is able to
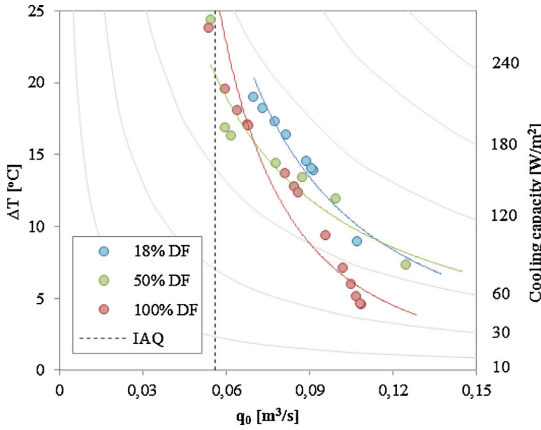
Fig. 9. Design chart for different diffuse ceiling opening areas.
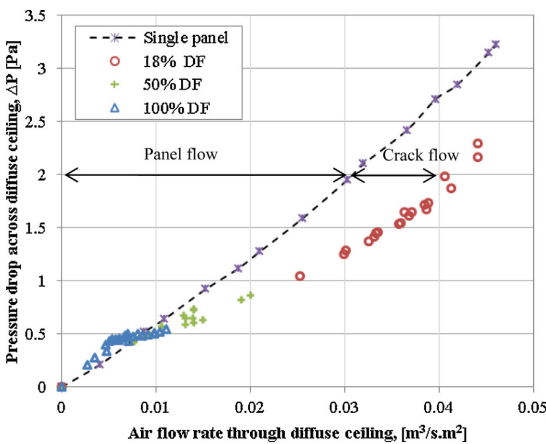
Fig. 10. Pressure drop for the different diffuse ceiling configurations.

handle the highest heat load without draught risk compared with the other two. This could be explained by the heat sources being located below the perforated diffuse ceiling panels in the 18% case. Consequently, the cold supply air can directly deal with the thermal plume from the heat sources. On the other hand, 18% of opening area can produce relatively higher momentum flow than the other two configurations, which to some extent influences the flow pattern of the room. On the contrary, the system with 100% opening area has the lowest cooling capacity. However, it can be observed that the cooling capacity of the system does not keep exactly constant while changing the air flow rate, especially in 100% DF case. This result indicates that the draught risk in the occupied zone is not totally independent of air flow rate.

2.5.3. Air path of diffuse ceiling ventilation

The air paths with different diffuse ceiling configurations are investigated by pressure drop measurements. Fig. 10 shows the relation between the pressure drop of a single panel and the pressure drop of the mounted diffuse ceiling. First of all, low pressure drop of the mounted diffuse ceiling is observed in all cases, even when the air change rate reaches $17\,h^{-1}$. The low pressure drop associated with diffuse ceiling ventilation allows a significant

reduction in the energy consumption of fan, and even makes it possible to work by natural ventilation. As reported by Jacobs et al. [2], the specific fan power decreased by 90–95% compared with conventional mixing ventilation.

The air path strongly depends on the diffuse ceiling configuration and air flow rate. It is clear that air is mainly supplied through the perforated panels in the case with 100% DF. The crack flow becomes more significant while reducing the diffuse ceiling opening area. On the other hand, panel flow is the dominant air path at low air flow rate. While increasing the air flow rate, the pressure drop as well as the crack flow increase. The crack flow is partly attributed to the suspension profile, where the non-overlapping layout leads to the air jet between panels. Meanwhile, the leakage through the vapor barrier is inevitable. The crack flow was studied by Nielsen et al. [11] through the smoke test. Their results indicated that high entrainment takes place in the micro-jets below the slots and penetrates to a depth of 0.25 m into the room. Therefore, it requires a distance of at least 0.25 m from the occupied zone to the ceiling surface.

3. Numerical studies

3.1. The computational fluid dynamic model

3.1.1. Porous media model

In order to further investigate the air flow pattern of diffuse ceiling ventilation, a computational fluid dynamics (CFD) model is built in the commercial software Fluent [23]. Due to the special structure of the wood-cement panel (see Fig. 1), it is too complicated to build the diffuse ceiling model directly. A porous media model is adopted in this study to simulate the flow through diffuse ceiling instead. The principle of porous media model is to add a momentum sink in the governing momentum equation. The source term is composed of two parts: a viscous loss term and an inertial loss term [24]. In laminar flows through porous media, the pressure drop is typically proportional to velocity, while at high flow velocity, the inertial loss will be dominant in the porous media, as expressed by the following equation:

$$S_i = -\left(\frac{\mu}{\alpha} v_i + C_2 \frac{1}{2} \rho |v| v_i \right) \tag{3}$$

where: v represent superficial velocity, α is permeability, C_2 is inertial resistance factor. The viscous resistance coefficient $1/\alpha$ and inertial resistance coefficient C_2 in the 100% DF cases are calculated to be $1.74e^{+8}\,m^{-2}$ and $263,366\,m^{-1}$, respectively. These coefficients are determined based on the function between pressure loss through diffuse ceiling and air flow rate obtained by experiments, as illustrated in Fig. 10.

In terms of the energy equation, modifications have been done on the conduction flux and the transient term in the porous media model, as expressed in Eq. (4). An effective thermal conductivity is introduced by considering the porosity of the medium.

$$\frac{\partial}{\partial t}\left(\gamma \rho_f E_f + (1 - \gamma) \rho_s E_s \right) + \nabla \cdot \left(\bar{v} \left(\rho_f E_f + P \right) \right)$$
$$= \nabla \cdot \left[k_{\text{eff}} \nabla T - \left(\sum h_i J_i \right) + (\bar{\tau} \cdot \bar{v}) \right] + S_f \tag{4}$$

Unfortunately, the porous media model is incompatible with radiation model because it is regarded as a fluid zone and the diffuse ceiling surfaces are treated as interiors between two fluid zones. In order to overcome this limitation, a radiation model is built separately, where the porous media is replaced by a solid material with the same thermal properties. The calculated surface temperatures (except diffuse ceiling surface temperature) is directly used as boundary inputs in the porous media model and heat exchanges

Table 2
Grid independence test.

	Mesh 1	Mesh 2	Mesh 3
Grid amount	283,264	613,716	1106,452
Mass balance (%)	0.00	0.00	0.00
Heat flux balance (%)	0.76	0.19	0.22
Average room air temperature (°C)	22.27	22.58	22.66

between porous media zone and the other zones (plenum and room) are calculated and treated as an energy source term S_f in the energy equation (4).

3.1.2. Boundary conditions

The CFD model is built to represent the test chamber as it is physically. In the experiments, three small windows above the diffuse ceiling serve as inlet and a ventilation duct located near the back wall serves as outlet. In order to simplify the geometrical model and generate high quality structure meshes, the inlet and outlet are simplified as a rectangular opening with the same opening area as in the experiments. Pupils and electric radiators are modeled as blocks with the same surface heat flux as in the experiments. The U-values of the walls are used as input for all the wall boundaries, and the measured air temperature in the cooling chamber and the surrounding zone are used as free stream temperatures.

3.1.3. Turbulence model and numerical methods

In this study, structured meshes are generated in the entire computational domain and the finest meshes are generated in critical areas such as: diffuse ceiling, inlet, outlet, area closed to the walls and heat sources. A grid independency study is performed by models with different mesh densities, as shown in Table 2. The results indicate that the difference between the results of mesh 2 and mesh 3 is very small; therefore, mesh 2 with 613,716 grids is used for comparison with the experimental results.

The air flow through the diffuse ceiling with very low velocity and the flow is almost laminar. However, the convection air flow generated by the heat sources in the occupied zone increases the turbulence level. Thus, the Re-normalized group (RNG) k–ε model is appropriate for this situation. The boussinsq hypothesis is selected to model buoyancy-driven flow, with air thermal expansion coefficient of 0.343×10^{-3} K^{-1}. The simulation uses the finite volume differencing scheme and SIMPLE numerical algorithm. The criteria of convergence is set such that the residuals for u, v, w, k, ε less than 10^{-3}, and the residual for energy less than 10^{-6}.

3.2. Validation of the CFD model

The CFD model can be used to study the air flow pattern in the room with diffuse ceiling ventilation and the model is validated by the measurement results. Figs. 11 and 12 illustrate the air temperature and velocity distribution across the central plane of the test room in Case 22. The air flow pattern indicates that the thermal plume generated by the heat sources is the dominant driven force in the room with diffuse ceiling ventilation. The uprising buoyancy flow above the electric radiators interacts with the downward supply flow through diffuse ceiling generates a strong air recirculation in the room level. The air vortex enters the occupied zone from the back side of the room alone the floor. The plume acts as a thermal blockage for the ventilation air flow, which restricts the fresh air into the area of occupants directly.

Fig. 13 illustrates the predicted velocity vector across the diffuse ceiling as a function of distance to the plenum inlet. It needs to notice that the velocity presented in Fig. 13 is the superficial velocity regardless the impact of porosity. A bi-directional air flow is observed across the diffuse ceiling. The reverse flow can be
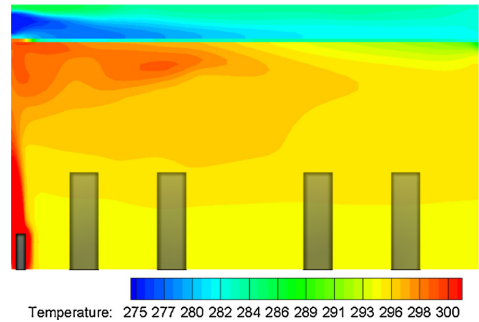
Fig. 11. Temperature contour across the central plane of the room.
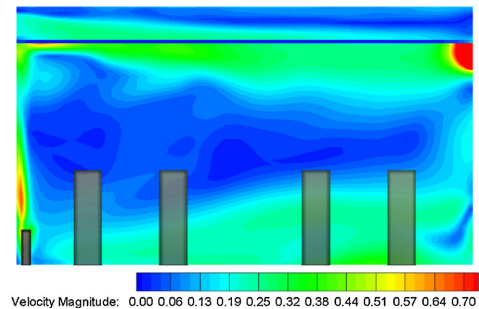
Fig. 12. Velocity contour across the central plane of the room.
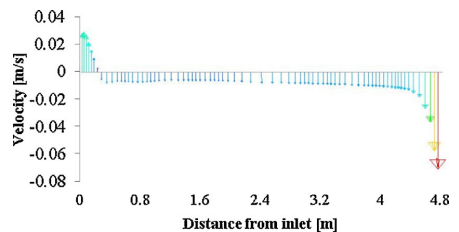
Fig. 13. Velocity distribution across the diffuse ceiling.

attributed to the strong thermal plume generated by the radiators (1650 W) and the low pressure drop between plenum and the room (0.5 Pa). Elmroth et al. [25] found out that the small pressure drop across the porous insulation makes it difficult to obtain a uni-directional airflow and uniform heat transfer over the entire surface area. However, by conducting a tracer-gas measurement under a pressure drop of 1.5–4.5 Pa, Jakubowska [26] did not observe any reverse flow into the plenum. A similar study was done by Hviid et al. [10], only insignificant reverse flow was observed under a pressure drop of 0.5–1.5 Pa. Compared with previous studies [10,26], the heat load of radiators is much more intense and centralized, the strong buoyancy flow may enhance the risk of reverse flow. On the other hand, as the air passing through the plenum, it is gradually warmed up by the thermal mass of the concrete slabs and diffuse ceiling panels, as shown in Fig. 11. Therefore, it can be predicted that air is supplied through the diffuse ceiling with non-uniform temperature. However, this non-uniform air supply does not lead to a non-uniform temperature distribution in the occupied zone, due to mixing by buoyance flow.
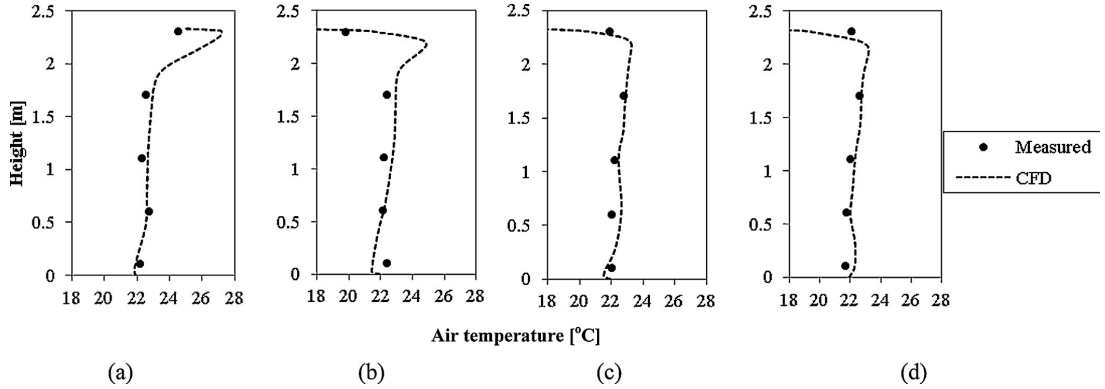
Fig. 14. Validation of the air temperature in Case 22 (a) Column 1, (b) Column 2, (c) Column 3 and (d) Column 4.
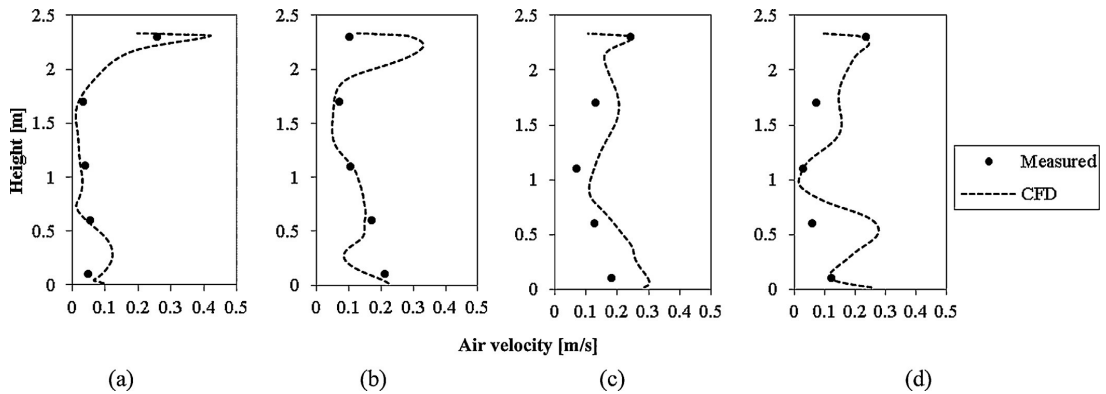

Fig. 15. Validation of the air velocity in Case 22 (a) Column 1, (b) Column 2, (c) Column 3 and (d) Column 4.

Figs. 14 and 15 shows the comparison between calculated and measured air temperature and air velocity profiles in the test room. Generally, there is a good agreement between the calculated and measured results. Both CFD simulation and experiment show the low temperature gradient in the occupied zone, which indicates a good mixing in the room. High air velocity is found at the ankle level, due to the air recirculation enter the occupied zone alone the floor. However, CFD model seems overestimate the air velocity in column 3 and 4. CFD model predicts that there is a temperature and velocity peak 5–10 cm below diffuse ceiling because of the thermal plume from radiators, especially in column 1 and column 2. However, this flow characteristic is not perfectly captured by the measured data, due to no sufficient measurement points located below diffuse ceiling. In further study, a detail measurement on the vertical temperature and velocity profiles below the diffuse ceiling should be performed.

3.3. Parameter study

Based on the above numerical method, we will further discuss the effect of heat sources location and the effect of room height. In the parameter study, diffuse ceiling is modelled with 100% opening area, and ventilation is operated with an air change rate of 4 h^{-1} and supply air temperature of 15.5 °C in all cases.

3.3.1. The location of heat sources

Based on the experimental study, it can be concluded that the buoyancy flow generated by the heat sources is the dominant flow in the room with diffuse ceiling ventilation. Therefore, the location of the heat sources is very important for the air flow pattern and also the thermal comfort. This study investigates four different heat load distributions (see Fig. 16), including: heat sources evenly distributed, located in the center, located in the front side of the room and located in the back side of the room. In each case, the heat load composes of eight pupils and each pupil releases 80 W heat as in the experiments, but electric radiators are not activated.

Fig. 17 shows the calculated velocity distribution in the vertical plane across the pupils. It is obvious that different heat load locations generate very different flow patterns. A strong air recirculation occurs when the heat sources are placed in one side of the room and the direction of recirculation is opposite to the heat source location, as shown in Fig. 17(c) and (d). When the heat sources located in the center of the room, two air recirculation zones occur around the heat sources. The air vortexes are asymmetrical where the stronger vortex occurs in the front side of the room. In the case with evenly distributed heat sources, no clear air recirculation is observed in the plane across the occupants. This results is supported by the findings by Nielsen [17]. By conducting a smoke test, they found that the flow pattern in the room with
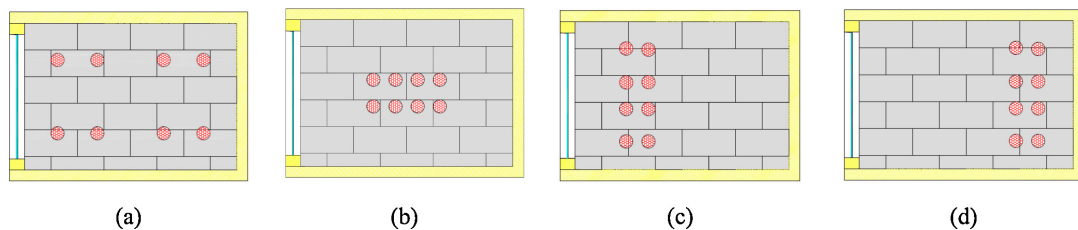
Fig. 16. Parameter study of different heat load distributions (a) evenly distributed, (b) centered, (c) front side and (d) back side.

Velocity Magnitude: 0.00 0.03 0.05 0.08 0.11 0.14 0.16 0.19 0.22 0.25 0.27 0.30
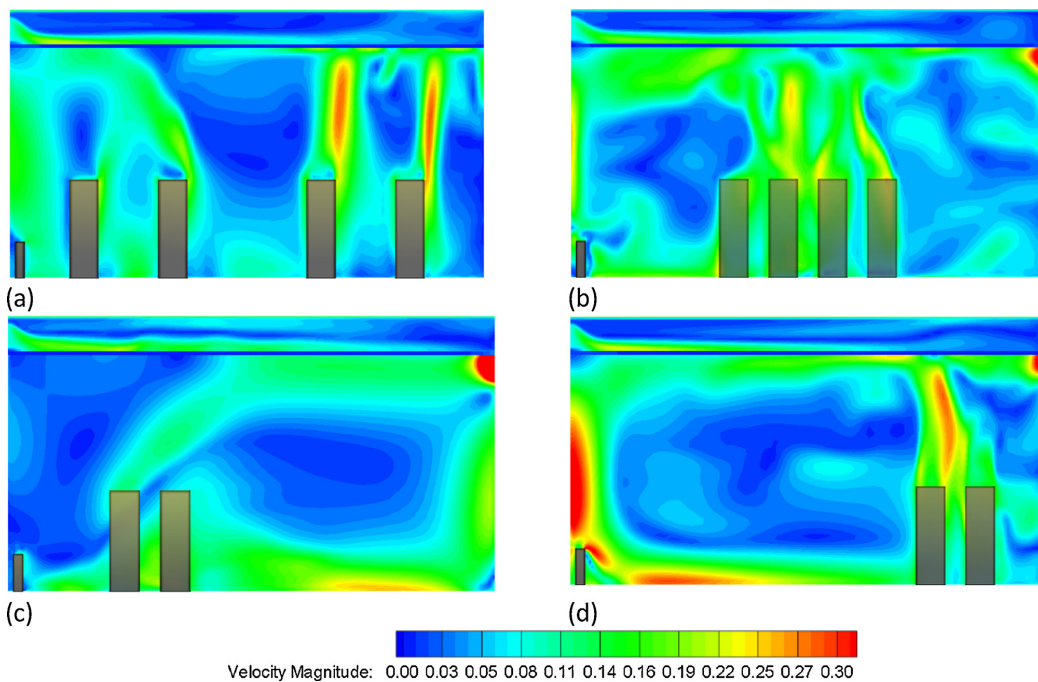
Fig. 17. Velocity distribution for different heat load layout (a) evenly distributed, (b) centered, (c) front side and (d) back side.

evenly distributed heat source is less stable than the other heat load layouts. The flow direction is either unclear or not consistent.

Both CFD calculated results and measured results indicate that maximum air velocity in the occupied zone occurs near the floor. Therefore, the draught risk is analyzed at the 0.1 m height across the central plane of the room, as illustrated in Fig. 18. An even distribution of heat sources gives the lowest draught risk compared to the others. As a matter of fact, an intense thermal plume occurs when the heat sources are centralized. The concentrated thermal plume will generate a strong air recirculation and lead to a large reverse flow entering the occupied zone at the floor level. On the other hand, the highest draught risk presents when the heat sources are located in the back side of the room, where the draught rate reaches approximate 20% at 0.7–1.2 m away from the inlet. On the contrary, the maximum draught rate in the case with front located heat sources is only 15%. This phenomenon indicates that air is not evenly distributed through the diffuse ceiling. A larger amount of air is supplied in a short distance to the inlet. Therefore, the downward air flow from diffuse ceiling meets the uprising thermal

plume and aggravates the recirculation. This could also explain the asymmetrical vortexes with the central location of heat sources.

3.3.2. Room height

Room geometry is also a crucial parameter when designing a ventilation system. For instance, displacement ventilation should be avoided in the room with low ceiling, due to the stratification principle. By performing an experimental study under two ceiling heights 2.5 m and 4.1 m, Nielsen [17] revealed that high ceiling will lead to an increase of velocity level in the room and a reduction of cooling capacity of the diffuse ceiling ventilation. The impact of room height on the draught risk with diffuse ceiling ventilation is investigated by CFD simulations in this study. Three room heights are discussed here: 2.335 m (as in the experiments), 3.0 m and 4.0 m. The heat sources are kept evenly distributed and with constant heat load of 80×8 W, as shown in Fig. 16(a).

The velocity distribution across the central plane of the room is demonstrated in Fig. 19. The air flow patterns show a similar
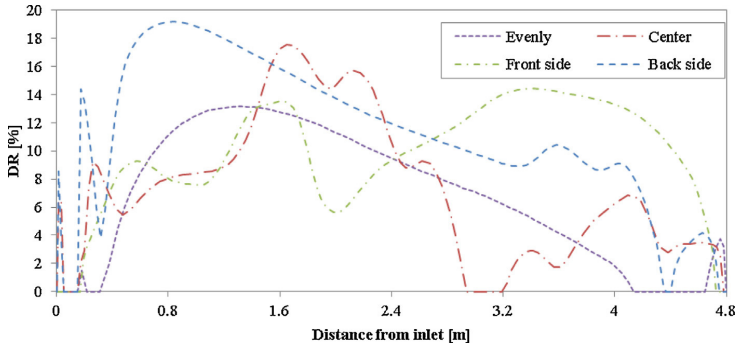
Fig. 18. Draught risk vs. heat load locations.

(a)   (b)   (c)

Velocity Magnitude: 0.00 0.03 0.05 0.08 0.11 0.14 0.16 0.19 0.22 0.25 0.27 0.30
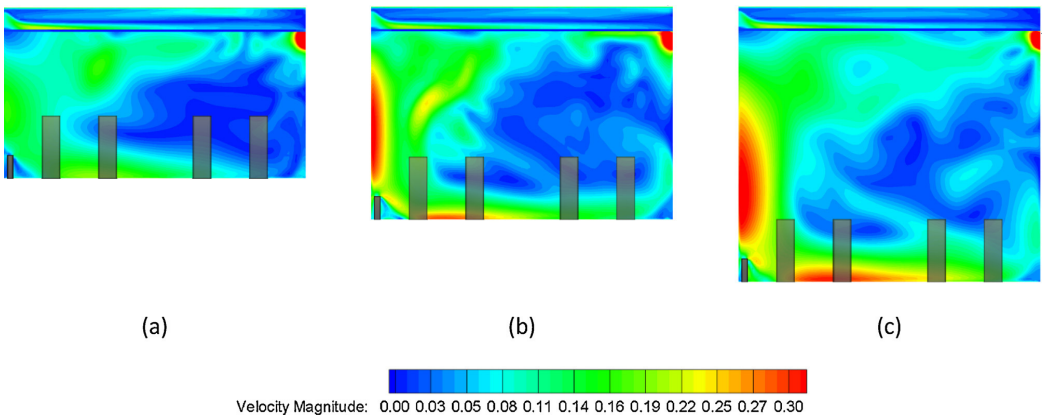
Fig. 19. Velocity distribution across the central plane of the room at different room height (a) 2.335 m, (b) 3.0 m and (c) 4.0 m.
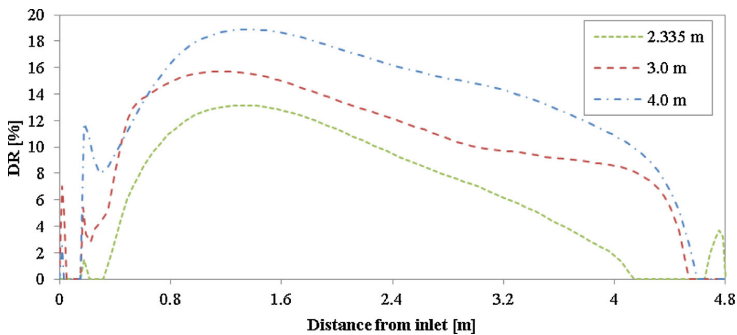
Fig. 20. Draught risk vs. room heights.

tendency under different room height, an air recirculation is formed in the room due to the interactions between the warmer buoyance flow and the cold fluid through the diffuse ceiling. However, the intensity and strength of the recirculation increases dramatically with increase of the room height. This is because the height of the room has impact on the amount of entrainment. The entrainment of ambient air is significant while the air is recirculated in the room and creates an additional acceleration of air flow.

Therefore, the draught risk is in direct proportion to the room height, as shown in Fig. 20. The maximum draught rate in 4.0 m height room approaching to 20% almost reaches the draught limit in ISO 7730 Category B [21]. While the draught rate in 2.335 m room is only 12%. However, the highest draught risk is observed at the same position approximately 1.2–1.4 m away from inlet, where is the position reverse flow entering into the occupied zone.

4. Conclusion

The objective of this study is to investigate the performance of diffuse ceiling ventilation in a classroom. Parametrical analysis is carried out by both experimental and numerical studies. In the experimental study, three diffuse ceiling configurations with opening area of 100%, 50% and 18%, respectively, are evaluated in terms of thermal comfort, cooling capacity and air paths. Generally, low temperature gradients in both vertical and horizontal directions indicate a fully mixing in the occupied zone. No draught risk is observed even with very high flow rate of $10.5 \, h^{-1}$ and high heat load of $140–154 \, W/m^2$. These findings further proves that diffuse ceiling ventilation has a superior performance in the room with intense heat load and high ventilation demand compared with conventional ventilation system.

Based on the design chart method, it is found that the system with 18% opening area is able to handle the highest heat load without thermal discomfort compared to the other configurations. However, it is too cursory to conclude that the smaller the opening area the higher the cooling capacity will be. Because the location of heat sources to location of the diffuse ceiling opening also play a crucial role. It will be interesting to investigate the interaction between heat sources location and diffuse ceiling opening location in the further study. On the other hand, the design chart demonstrates that the cooling capacity of diffuse ceiling is not constant with air flow rate, which indicates that the air flow rate to some extent still influences the draught risk in the occupied zone. Finally, the air path is analyzed by pressure drop measurement. Panel flow is the dominant path at low flow rate and with fully opening area. However, the crack flow becomes significant while increasing the air flow rate and reducing the diffuse ceiling opening area.

In the numerical study, a CFD model is built where the diffuse ceiling is defined as a porous media zone due to its special construction. The CFD model is validated by the experimental results and further used to study the effect of heat load distribution and room height. The air flow pattern indicates that the thermal plume generated by the heat sources is the dominant driven force in the room with diffuse ceiling ventilation. The interaction between the uprising thermal plume and downward supply flow forms an air recirculation in the room level. Consequently, the air flow pattern is strongly dependent on the location of heat sources. From the view of draught risk, it is recommended to even distribution of heat sources rather than concentrated placement. On the other hand, high ceiling room leads to a large amount of entrainment while the air is recirculated in the room, which results a high draught risk at the floor level. Therefore, it is not recommended to use diffuse ceiling ventilation in a high ceiling room.

Acknowledgements

References

[1] P.V. Nielsen, The 'Family Tree' of Air Distribution Systems, Roomvent, 2011.
[2] P. Jacobs, B. Knoll, Diffuse ceiling ventilation for fresh classrooms, in: Fourth Intern. Symposium on Building and Ductwork Air Tightness, 2009.
[3] P. Jacobs, E.C.M. Van Oeffelen, B. Knoll, Diffuse ceiling ventilation, a new concept for healthy and productive classrooms, Indoor Air (2008) 17–22, In: The Eleventh International Conference on Indoor Air Quality and Climate.
[4] T. Karimipanah, H.B. Awbi, M. Sandberg, C. Blomqvist, Investigation of air quality, comfort parameters and effectiveness for two floor-level air supply systems in classrooms, Build. Environ. 42 (2007) 647–655.
[5] J. Toftum, B.U. Kjeldsen, P. Wargocki, H.R. Menå, E.M.N. Hansen, G. Clausen, Association between classroom ventilation mode and learning outcome in Danish schools, Build. Environ. 92 (2015) 494–503.
[6] L. Jacobsen, Air Motion and Thermal Environment in Pig Housing Facilities with Diffuse Inlet, Department of Civil Engineering, Aalborg University, Denmark, 2008 (Phd thesis).
[7] L. Rong, B. Elhadidi, H.E. Khalifa, P.V. Nielsen, CFD modeling of airflow in a livestock building, in: The Seventh International Conference on Indoor Air Quality Ventilation and Energy Conservation in Buildings, 2010.
[8] P.V. Nielsen, Analysis and design of room air distribution systems, HVAC&R Res. 13 (6) (2007) 987–997.
[9] P.V. Nielsen, E. Jakubowska, The performance of diffuse ceiling inlet and other room air distribution systems, Cold Climate HVAC (2009).
[10] C.A. Hviid, S. Svendsen, Experimental study of perforated suspended ceilings as diffuse ventilation air inlets, Energy Build. 56 (Jan) (2013) 160–168.
[11] P.V. Nielsen, R.L. Jensen, L. Rong, Diffuse ceiling inlet systems and the room air distribution, in: Clima 2010: 10th REHVA World Congress, 2010.
[12] L. Jacobsen, P.V. Nielsen, S. Morsing, Prediction of indoor airflow patterns in livestock buildings ventilated through a diffuse ceiling, in: Ninth International Conference on Air Distribution in Rooms, 2004.
[13] S. Petersen, N.U. Christensen, C. Heinsen, A.S. Hansen, Investigation of the displacement effect of a diffuse ceiling ventilation system, Energy Build. 85 (2014) 265–274.
[14] K. Venkatasubbaiah, Y. Jaluria, Numerical simulation of enclosure fires with horizontal vents, Numer. Heat Transfer, A: Appl. 62 (2012) 179–196.
[15] R. Harish, K. Venkatasubbaiah, Numerical simulation of turbulent plume spread in ceiling vented enclosure, Eur. J. Mech. B: Fluids 42 (2013) 142–158.
[16] A.D. Chodor, P.P. Taradajko, Experimental and Numerical Analysis of Diffuse Ceiling Ventilation, Department of Civil Engineering, Aalborg University, Denmark, 2013 (Master thesis).
[17] P.V. Nielsen, R.W. Vilsbøll, L. Liu, R.L. Jensen, Diffuse ceiling ventilation and the influence of room height and heat load distribution, Healthy Build. Europe 2015 (2015) 2–9.
[18] C. Zhang, P. Heiselberg, P.V. Nielsen, Diffuse ceiling ventilation: a review, Int. J. Vent. 13 (1) (2014) 49–63.
[19] P.V. Nielsen, T.S. Larsen, C. Topp, Design methods for air distribution systems and comparison between mixing ventilation and displacement ventilation, in: Proceedings of the Seventh International Conference on Healthy Buildings, 2003.
[20] P.V. Nielsen, The influence of ceiling-mounted obstacles on the air flow pattern in air-conditioned rooms at different heat loads, Build. Serv. Eng. Res. Technol. 1 (4) (1980) 199–203.
[21] International Standard, ISO 7730:2005 Ergonomics of the Thermal Environment—Analytical Determination and Interpretation of Thermal Comfort Using Calculation of the PMV and PPD Indices and Local Thermal Comfort Criteria, 2005.
[22] CEN Report, CR 1752, Ventilation for Buildings—Design Criteria for the Indoor Environment, European Committee for Standardization, 1998.
[23] ANSYS Inc., Ansys Fluent Release 16.0, 2015, Available: http://www.ansys.com/ [Online].
[24] ANSYS Inc., ANSYS Fluent User's Guide, 2009.
[25] A. Elmroth, B. Fredlund, The Optima-house: Air Quality and Energy Use in a Single Family House with Counterflow Attic Insulation and Warm Crawl Space Foundation, Department of Building Science, Lund Institute of Technology, Sweden, 1996.
[26] E.M. Jakubowska, Air Distribution in Rooms with the Diffuse Ceiling Inlet, Department of Civil Engineering, Aalborg University, Denmark, 2007 (Master thesis).

Appendix E. Numerical analysis of diffuse ceiling ventilation and its integration with a radiant ceiling system

Paper 5

The paper presented in Appendix E is submitted to Building Simulation, minor revision 04.07.2016.

Author's Right

Copyright information: Building Simulation

Numerical analysis of diffuse ceiling ventilation and its integration with a radiant ceiling system

Chen Zhang[a,*], Per Kvols Heiselberg[a], Qingyan Chen[b], Michal Pomianowski[a]

[a] Department of Civil Engineering, Aalborg University, Sofiendalsvej 11, 9200 Aalborg, Denmark

[b] School of Mechanical Engineering, Purdue University, West Lafayette, IN 47907, USA

*Corresponding author's Tel: +45 9940 7232; E-mail: cz@civil.aau.dk

Numerical analysis of diffuse ceiling ventilation and its integration with a radiant ceiling system

Abstract

A novel system combining diffuse ceiling ventilation and radiant ceiling was proposed recently, with the aim of providing energy efficient and comfort environment to office buildings. Design of such a system is challenging because of the complex interactions between the two subsystems and a large number of design parameters encountered in practice. The study aimed to develop a numerical model that can reliably predict the airflow and thermal performance of the integrated system during the design stage. The model was validated by experiments under different operating conditions. The validated model was then applied to to evaluate the impacts of different design parameters on the system performance, including the diffuse ceiling panel, plenum height, plenum length, and inlet configuration. The simulation results demonstrated that diffuse ceiling panels with a high U-value can minimize its impact on the energy performance of radiant ceiling. Low plenum height was beneficial to the energy efficiency but aggravated the non-uniformity air distribution and further led to the draught problem in the occupied zone. This system was recommended to apply in the small offices instead of large, open spaces.

Keywords

Diffuse ceiling ventilation, Radiant ceiling, CFD, Parametric study, Thermal comfort, Energy efficiency

1. Introduction

Recently, a growing interest has been paid on a new ventilation system - diffuse ceiling ventilation. This ventilation concept uses an open space between ceiling slab and suspended ceiling as a plenum to distribute air. The conditioned air is delivered into occupied space through the perforation on the suspended ceiling panels and/ or slots between ceiling panels. Compared with traditional ventilation systems, diffuse ceiling ventilation has the potential to provide a more comfort environment with less energy cost. Because of the large ceiling area as air diffuser, the system has low- momentum supply flow and does not generate draught even by supplying cold outside air directly[1][2][3]. This ventilation concept is appropriate to the spaces with high thermal load and large ventilation demand, like offices and classrooms, where the draught is usually a major concern by using conventional mixing or displacement ventilation[4]. On the other hand, the suspended ceiling as air diffuser requires low- pressure drop due to its large surface area. In addition, the use of plenum eliminates the need for ductwork and the large size of the plenum creates a little restriction to the air flow[5]. Consequently, the amount of energy required to deliver air by this ventilation system is less than that required by fully-ducted system [4][6][7]. However, ventilation is a passive cooling approach, which is determined by the outdoor climate. An additional heating/cooling system is required when natural resources are inadequate. The radiant ceiling is a promising solution to work together with ventilation systems. Because it deals with heat load by both radiation and convection, it could provide a more comfort environment than the all-air system and able to make use of low-grade energy[8][9][10].

A schematic diagram of the system combined diffuse ceiling ventilation with the radiant ceiling is shown in Figure 1. In the integrated system, the suspended ceiling covers the radiant ceiling and consequently changes the heat transfer mechanism between the radiant surface and the rest of the room. Initial investigations have been done by full-scale experiments under steady-state conditions[11][12]. The results indicated that the diffuse ceiling ventilation increased the heating capacity of the radiant ceiling but decreased its cooling capacity. The thermal process in the plenum was more complicated than that with ducted systems. The direct contact between the supply air and the radiant ceiling enabled heat transfer to or from the air depending on the air-to-surface temperature difference and airflow rate, which resulted in a temperature variation on the plenum air. From the standpoint of thermal comfort, due to the preheating/precooling effect of the plenum, the air was supplied into the room with moderate temperature, which further reduced the risk of draught. The previous investigations showed that the diffuse ceiling ventilation and the radiant ceiling interact and complement with each other. Therefore, the system needs properly design and control, to fulfill both energy saving and thermal comfort purposes.

Figure 1

The most common integrated system is displacement ventilation with cooled ceiling. This combined system gives a rather superior performance on the air quality and thermal comfort to the VAV system [10][13]. However, the harmony of the combination is the key issue, since cooled ceiling creates a downward motion of air and suppresses the displacement flow. Therefore, the amount of heat load removed by cooled ceiling need be properly adjusted in order to maintain a low vertical temperature difference and a high air quality in the breathing zone [14][15]. At the same time, the entire cooling load needs to be lower than 100 W/m^2, and the room height is required to be higher than 2.5 m [16]. The possibility of radiant floor and displacement ventilation was also discussed by several studies [17][18]. They mentioned that floor cooling did not lead to an increase in draught risk, but vertical temperature gradient must be controlled carefully in the cooling case. Although the integrations of ventilation and radiant systems have been widely studied, the knowledge regarding the combination of diffuse ceiling ventilation and the radiant ceiling is very limited.

As mentioned above, the design of the integrated system is challenging due to the interactions between its two subsystems. In this study, the primary objective was to optimize the energy performance of the radiant ceiling and provided a more uniform air distribution through the diffuse ceiling. The design process would need to define a large number of parameters, such as diffuse ceiling configuration, plenum geometry, shape and location of the plenum inlet, obstruction within the plenum, etc., which would have impacts on these interactions. To explore the effect of different design parameters on the airflow pattern and thermal performance, one can use experimental and/or numerical approaches. Experimental study is regarded to be more reliable but also more expensive and time-consuming than numerical investigation. Therefore, it is desirable to develop a validated numerical model that could provide a reliable prediction of the integrated system during the design stage.

Numerical evaluation on the two subsystems has been reported in many articles. For diffuse ceiling ventilation, Fan [2] simplified the diffuse ceiling supply into four slot openings. They observed slight disparities in the air velocity distribution, especially near the ceiling and the floor. This was because the simplification of the air pathway resulted in an overestimation or underestimation of the air movement in the conditioned space. Chodor et al. [19] assumed the outdoor air directly supplied into the room without going through the plenum, and they also assumed a uniform air distribution through the suspended ceiling. They oversimplified the inlet boundary conditions and neglected the thermal process within the plenum, which led to a discrepancy in the airflow prediction inside of the room. Zhang et al. [20] proposed a porous media

model, which could efficiently predict the airflow characteristics through the diffuse ceiling panels. However, this study focused on the airflow pattern in the conditioned space, and no detail discussion regarding the plenum was available. For the radiant ceiling system, Tye-Gingras et al. [21] coupled a semi-analytic radiant model with a 2D CFD model to analyze the comfort and energy consumption of the radiant ceiling. However, this study neglected the impact of ventilation on the airflow pattern, and only considered the buoyancy force from heat sources. Myhren et al. [22] used a validated CFD model to compare different radiant heating systems, where a surface-to-surface method was implemented to deal with the radiation heat exchange. The previous studies mainly focus on the individual system, but the study regarding the integrated system was limited. In addition, the air distribution and thermal process within the plenum should also be addressed in this study, where the heat exchange between radiant ceiling and supply air mainly takes place.

This study aimed to develop a validated numerical model for the system with diffuse ceiling ventilation and the radiant ceiling. This model should be able to predict the airflow pattern and thermal performance both in the plenum and in the occupied zone. This investigation then used the validated model to conduct a series of parametric studies, including the diffuse ceiling panels, plenum height, room length, and plenum inlet configuration, for optimal design of the integrated system. It needs to notice that both the experiments and numerical simulations presented in this study were conducted under steady-state condition, where the effect of thermal masses (ceiling slab and suspended ceiling) was not the focus of this study.

2. Experimental setup

To develop a validated numerical model, we needed reliable and high-quality experimental data. This section describes the experimental facility and the measurement technique.

2.1 Test facility

Figure 2

The full-scale experimental facility was an environmental chamber located inside a laboratory. As illustrated in Figure 2, the environmental chamber consisted of two parts: a climate chamber simulating the outdoor environment and a test chamber simulating an office with a ceiling plenum. The lower zone in the test chamber represented an office with an inner dimension of 4.8 m* 3.3 m *2.72 m, see Figure 3. In the office, there were two workstations with two PC, two lamps as well as two thermal manikins, which corresponded to a heat load of 450.5 W or 28.4 W/m^2 floor area.

Figure 3

There were two glazing areas in the façade between the climate chamber and the test chamber. The lower glazing area, with three panels and overall dimensions of 2.4 m × 1.4 m, was closed during the experiments. The upper glazing area, with three panels and overall dimensions of 2.4 m × 0.35 m, was opened to function as plenum inlets. The inlet opening could be controlled by adjusting their opening angle, and it kept a geometrical opening area of 0.0207 m^2 (0.01 m × 0.69 m × 3 panels). The exhaust duct was in the lower corner of the façade and had 160 mm diameter. The exhaust air was drawn into the climate chamber using a fan, and then treated by an AHU unit when it passed through the climate chamber, finally re-supplied to the plenum. The façade had an effective U-value of 0.61 W/m2.K and the other enclosures were well insulated to minimize the heat transfer from the lab.

2.2 Diffuse ceiling and radiant ceiling

The diffuse ceiling panels were the type of wood-cement panels typically used for acoustic purposes, but they were permeable to air. The ceiling panels were positioned 0.35 m below the concrete slabs by a suspension system, which separated test chamber into a ceiling plenum and a conditioned space as shown in Figure 4. The diffuse ceiling panels had a thickness of 35mm and a density of 359kg/m^3. The thermal conductivity of the ceiling panels, measured with a λ-Meter EP500 by a guarded hot plate method, was 0.085 W/m K. The porosity was estimated to be 65% by means of a volumetric measurement. The high porosity ensured a low-pressure drop across the ceiling panel. According to previous measurements [23], the pressure drop through the diffuse ceiling was less than 2 Pa when the airflow rate was less than or equal to 0.03 m^3/s·m^2. Since there were small cracks between the ceiling panels, the pressure drop across the whole diffuse ceiling was even lower.

Figure 4

The radiant ceiling was composed of four concrete slabs with embedded water-carrying pipes, each with dimensions of 3.560 m × 1.197 m × 0.200 m. The water pipes with a diameter of 20 mm were embedded 4 mm above the lower surface of the concrete slab. The water circuit connected to both heating and cooling units, where a three-way valve used to control the water temperature. The water flow was controlled and recorded by a Brunata HGQ flow meter.

2.3 Case setup

Measurements were conducted for three cases with different boundary conditions, as shown Table 1. In winter, the radiant ceiling was operated as a heated ceiling with a surface temperature of 27.34 ºC. In moderate seasons, the radiant ceiling was not activated, and ventilation was used to remove the load for the entire space. While in summer, radiant ceiling took charge of the whole heat load and ran with a surface temperature of 10.79 ºC. The radiant surface temperature was below the dew point temperature in summer, and there was a risk of condensation in practice. However, the experimental study aimed to identify the possibility and limitation of the integrated system, even the case with condensation risk was still tested.

Table 1

The experiments focused on the airflow and thermal performance in both the plenum and the occupied space. The vertical temperature gradient and velocity gradient in the office were measured with the use of three moveable poles, in each pole located seven thermocouples and five anemometers, as shown in Figure 5 (a). During the experiment, each pole was moved to four different positions within the office, so that the measurements were conducted at a total of 12 locations in the occupied zone. Figure 5 (b) shows the measuring points in the plenum. A total of nine thermocouples were evenly distributed at the mid-height of the plenum to measure the temperature variation of plenum air. The surface temperatures of the walls, floor, radiant ceiling, and diffuse ceiling panels were also measured. The experiment used 115 K-type thermocouples for monitoring the air and surface temperatures, with an uncertainty of ± 0.15 K. The thermocouples measured the temperatures every 10 s, and the data was recorded by a Helios Fluke data logger. The velocities were measured by the hot-sphere anemometers with an uncertainty of ± 0.01 m/s +5% of the readings. The air velocities were recorded by a 54N10 Dantec multichannel flow analyzer.

Finally, the pressure drop through the diffuse ceiling was measured with FCO510 micro-manometers (uncertainty ± 0.25 %) by placing the pressure sensors at various locations in the plenum and in the center of the office, as shown in Figures 5. Detailed information about the measurements was described in Zhang [11] and Yu [12].

Figure 5

3. Numerical models

The numerical study used a CFD model to solve the airflow and temperature distributions in the plenum and the occupied space. The commercial CFD programme Fluent [24] was used in this study. The CFD simulations require a suitable model to specify the airflow through the diffuse ceiling panels. As the radiant ceiling has a large temperature difference from the rest of the surfaces in the room, a suitable radiation model is essential to analyse the radiative heat transfer in space. This effort would provide the necessary boundary conditions for the porous media model. The CFD model also requires a suitable turbulence model for solving the airflow and temperature distribution in the occupied space. This section discusses the numerical models used for the investigation.

3.1 A porous media model for the diffuse ceiling panels

The diffuse ceiling panels used in this study had a porous property because of the structure of the wood-cement material. It was impossible to model the air diffusion through the panels directly. A porous media model was implemented to simulate the air diffusion in this study. As flow through the porous media zone, it experiences both the viscous resistance and inertial resistance. The porous media model was developed by adding a momentum source term in the governing equation, based on Darcy-Forchheimer Law [25]. When the flow goes through the porous panels with very low velocity, the viscous term is dominant. However, for high-velocity flow, the inertial effect becomes significant. The momentum source term can be expressed by:

$$S_M = -\left(\frac{\mu}{\alpha}v + C_2\frac{1}{2}\rho|v|v\right) \qquad (1)$$

The viscous resistance coefficient $1/\alpha$ and inertial resistance coefficient C_2 were determined by the properties of the wood-cement board, such as porosity and equivalent perforation diameter. These two coefficients were derived from experimental data in the form of pressure drop as a function of velocity through the porous media, where $1/\alpha = 1.14 \times 10^8$ m^{-2} and $C_2 = 33055$ m^{-1}. Detailed information about pressure drop measurement and results can be found in Zhang et al.[23].

The energy equation for the porous panels was modified on the conduction flux only, where an effective thermal conductivity k_{eff} was introduced to consider the effect of both the fluid and solid conductivities.

$$\nabla \cdot \left(\bar{v}(\rho_f E_f + P)\right) = \nabla \cdot \left[k_{eff}\nabla T + (\bar{\tau} \cdot \bar{v})\right] + S_E \qquad (2)$$

$$k_{eff} = \gamma k_f + (1-\gamma)k_s \qquad (3)$$

3.2 Radiation model

Radiative heat transfers occur between the radiant ceiling, diffuse ceiling panel and the rest of the room surfaces. Unfortunately, our CFD program with the porous media model treated the diffuse ceiling panel as flow cells and thus could not calculate the radiative heat exchange directly. In order to determine the radiative heat exchanges, a separate model was built by specifying the diffuse ceiling panels with the corresponding solid materials. A surface to surface method was implemented to calculate the radiative heat transfer between surfaces by use of the Stefan-Boltzmann law and view factors. The radiative heat flux leaving a given surface is expressed [25]:

$$q_{rad,k} = \varepsilon_k \sigma T_k^4 + \rho_k \sum_{j=1}^{N} F_{kj}q_{rad,j} \qquad (4)$$

In the radiation model, the wall boundaries were specified by the U-value together with the outdoor temperature or called free stream temperature. The radiant ceiling was specified by a uniform surface temperature, and the temperature decay along the pipe was assumed to be negligible (less than 3 ºC in the

measurements). The internal heat sources were treaded as surface heat fluxes on the manikins, computers, and task lamps.

The calculated results obtained from the radiation model included the surface temperatures of the walls and radiative heat flux of the diffuse ceiling panels.

3.3 Boundary conditions

The wall temperatures obtained from the radiation model were then used as boundary conditions in the porous media model for the detail calculation on the air velocity and air temperature distribution. Instead of directly specifying the diffuse ceiling's surface temperature, the radiative heat flux to the diffuse ceiling panels was applied as an energy source S_E.

The heat sources released heat through both convection and radiation. The effect of radiative heat flow has been already considered in the radiation model. A feasible approach was to estimate the radiative heat flow and to specify the convective heat flow boundary condition for the heat sources [26]. ASHRAE Handbook provides default convective fraction for different heat sources [27]. The convective fraction of occupants with moderately active office work was approximate 50%, while the values of computers and desk lamps were 90% and 50%, respectively.

3.4 Turbulence model

The airflow through diffuse ceiling panels could be laminar because of the very low velocity. However, the room airflow was turbulent because of strong thermal plumes from various heat sources and convective heat transfer through the room enclosure. The Re-normalized group (RNG) k-ε model was recommended by Chen [28] to model the turbulent flow in the indoor environment. Yang et al also proved the accuracy of the k-ε model for the porous media zone [29].

3.5 Geometrical model

The geometrical model used in CFD, as shown in Figure 6, was a simplified version of the environmental chamber facility. This model included the plenum, the diffuse ceiling, and the occupied office. The three lower glazing panels were consolidated as a window and the three upper glazing panels into an inlet. A ventilation duct located in the lower left corner of the façade was treated as an exhaust. In order to generate high-quality meshes for the indoor space, the inlet and exhaust were built as rectangular openings with the effective areas as in the experiment. The air supply through the inlet was assumed to have a uniform profile. The exhaust was treated as outflow boundary with zero diffusion flux for all flow variables.

Figure 6

3.6 Numerical algorithm for CFD

As shown in Figure 6, structured meshes were built in the entire space. The finest meshes were generated in the areas with large gradient, for example, the diffuse ceiling, inlet, outlet, walls, and heat sources. Chen et al. [30] recommended systematically refining the grid size to verify the numerical model. A common approach is to double the mesh number and then to compare the two mesh solutions. Three mesh solutions were constructed in the grid independent study, and the results for exhaust air temperature and average air velocity at position A2 are presented in Table 2. The comparison indicates that the calculation with Mesh 2 produced accurate results for air velocity at A2, and the deviation in exhaust air temperature was less than 0.11% with Mesh 3. The increase in cell number from 760,235 to 1,027,309 did not result in a significant improvement in the simulated results, but cost more computing time and needed larger computational resources. Consequently, Mesh 2, with 760,235 cells, was used for further investigation in this study.

The solution method was the SIMPLE algorithm. The convergence criterions were set that the absolute residuals should be less than 10^{-3} except that for energy less than 10^{-6}. Table 2 shows the unbalance rate for

mass and heat flux, where the mass reached a complete balance state and the heat flux unbalance in the range of 0.09%–0.2%.

Table 2

4. Model Validation

In this section, we will present the computed airflow pattern for the test chamber with the integrated system and compare the calculated temperature and velocity distributions with the corresponding experimental data. The objective is to validate the numerical model for predicting the performance of the integrated system.

4.1 Temperature distribution

The vertical temperature profile at position A2 was selected to analyze the temperature distribution in the office. Figure 7 showed the comparison between the calculated results and the measured ones for the three cases. The numerical model provided a satisfactory prediction on the temperature distribution in the occupied zone, with deviations of less than 0.36 ℃ in all three cases. The largest deviation occurred below the diffuse ceiling. The CFD model seems to have overestimated the effect of the thermal plume generated by the heat sources, which led to a 2 ℃ higher air temperature in this region. It is well known that the wall function used in the RNG k-ε model cannot correctly predict the convective heat transfer at solid surfaces. Therefore, to keep the calculated results sufficiently close to the measured ones for exhaust and average air temperatures, a high convective fraction was applied to specify the thermal boundary of the heat sources. In addition, the measurements were not free from errors, which could also have contributed to the discrepancy.

Figure 7

In the integrated system, complex thermal processes take place within the plenum. Therefore, the numerical model should be able to provide a reliable prediction in the plenum. Figure 8 presented the horizontal temperature distribution at the mid- height of the plenum for the three cases. It was clear that the CFD model can predict the relation between air temperature variation and the distance from the plenum inlet. Although the deviations between the simulated temperatures and measured ones can reach 2 ℃ in some points, considering the large temperature range of the supply air from -7 oC to 24 oC, the deviations can be regarded as acceptable. In winter, the cool supply air entered the plenum from the left. As it passed through the plenum, it was gradually warmed up by the heat transferred from the radiant surface on the top and from the diffuse ceiling panel on the bottom (heat conducted from the room side). In the summer, by contrast, the air in the plenum was gradually cooled down by cooled ceiling. In the moderate season, although the radiant ceiling was not activated, the air was still warmed up by heat transfer from the upper zone and the room side.

Figure 8

4.2 Air flow pattern and velocity distribution

Figure 9 illustrates the predicted airflow pattern across the central plane in the three cases. The rising buoyancy flow from the heat source and the downward flow along the wall generated a air recirculation in the room and caused reverse flow entering the occupied zone along the floor. In different cases, the vortex moved from one side of the room to the other depending on the operating conditions. In winter, the outdoor air was supplied to the plenum at a low temperature, and because of gravity, a large amount of air dropped to the surface of the diffuse ceiling and penetrated into the room at a location close to the plenum inlet. In contrast, warm supplied air could travel further in the plenum and was gradually cooled down by the thermal

mass. Therefore, a relatively large amount of air was delivered to the room at the far end. This phenomenon explains the fact that the air distribution through the diffuse ceiling was not perfectly uniform, which depended on the supplied air condition and the thermal process within the plenum.

Figure 9

Figure 10 showed the CFD calculated and measured velocities at position A2. Overall, good agreement has been reached. However, a relative larger discrepancy existed below the diffuse ceiling. As mentioned above, this was due to the overestimation of the convective flow from the heat sources.   Both calculated and measured results showed low air velocities exist in the occupied zone by using this system. A relative high velocity occurred at the floor in winter case. However, it was still lower than the limit of 0.18 m/s[31], no draught risk would be expected.

Figure 10

5. Parameter analysis

Most previous studies have pointed out the need to expose the radiant ceiling to the rest of the room to optimize energy efficiency. However, in the integrated system, the radiant ceiling is encapsulated by the diffuse ceiling panels. Therefore, the properties of diffuse ceiling panels have a remarkable impact on the thermal performance of radiant ceiling. Two different diffuse ceiling panels were analyzed: one was wood-cement panel as used in the experiment, and the other was aluminum (Al) panel. The Al panel was chosen as an example because it is the most commonly used type of suspended ceiling in practice, and it has significantly higher conductivity than does wood-cement panel. The Al panel was expected to perform differently from the wood-cement panel.

On the other hand, from an architectural standpoint, it is preferable to reduce plenum height in order to maintain sufficient headroom. It is important to identify the minimum plenum height at which an acceptable air distribution within the plenum could be achieved. Plenum length is also an important parameter because airflow may not reach the end of the plenum if the length exceeds a certain value. Finally, the plenum inlet configuration and location determine the momentum of supply air and the airflow pattern in the plenum.

This study aimed to identify the impact of different design parameters on the thermal performance and airflow pattern in the room with the integrated system. The study used the validated CFD model for investigating the sensitivity of the design parameters, including the diffuse ceiling panel, plenum height, plenum length, and inlet configuration. This section details our effort.

5.1 The effect of diffuse ceiling panels

Two types of diffuse ceiling panels were compared regarding their impact on system performance under different operating conditions. One was wood-cement panel, and the other was Al panel. The Al panel had a thickness of 5 mm and thermal conductivity of 202.4W/m.K, corresponding to a U-value of 40480 W/m^2. K. The U-value of wood-cement panel was only 2.43 W/m^2.K. To limit the number of variables, it was assumed they had the same porosity and the same pressure resistance. In addition, to avoid the influence of the materials' emissivity on the radiative heat exchange, it was assumed that the Al panel was painted into black and had the same emissivity as the wood-cement panel.

Table 3

Table 3 presents the CFD results with the two different diffuse ceiling panels. From the standpoint of energy performance, the diffuse ceiling panel with a high U-value was benefit to the radiant ceiling cooling capacity. An enhancement of 22% was achieved by using Al panels. This was because the Al panels enabled a larger temperature difference between the plenum air and radiant surface in the cooling mode. In addition, the surface-to-surface temperature difference between the radiant ceiling and diffuse ceiling panels also increased when the Al panels were used, and therefore an increase in radiative heat exchange could be expected as well.

However, the opposite effect was found in the heating mode, where the heating capacity of the radiant ceiling was reduced by 13%, from 516 W with the wood-cement ceiling panels to 450 W with the Al panels. Both convective and radiative heat exchange were reduced by the use of Al panels. This was due to the decrease in both air-to-surface temperature difference and surface-to-surface temperature difference with the Al panels in the winter case. In the moderate season, the radiant ceiling was not activated. The diffuse ceiling had an indirect influence on the heat conducted from the floor above. The Al panels restricted the amount of heat transfer from the upper zone and maintained a slightly lower indoor temperature than did the wood-cement panels.

According to previous studies [12][11], the diffuse ceiling ventilation promotes the radiant ceiling' heating capacity but decreases its cooling capacity in comparison with the stand-alone radiant system. In summer, radiant ceiling needed to run with a very low surface temperature to keep an acceptable indoor temperature, thus limiting the use of renewable energy resources and simultaneously raising the condensation risk. Based on this parametrical study, diffuse ceiling with a high U-value can minimize this impact and enable the radiant ceiling to cool down the room with a relatively higher surface temperature. Thus, it is recommended to utilize diffuse ceiling panels with high U-value, if the system was designed to provide cooling most of the time.

The U-value of diffuse ceiling panels did not show a notable impact on the airflow pattern. Therefore, detailed comparison of the velocity and temperature distributions were not discussed here.

5.2 The effect of plenum height

The study was performed on plenums varying from 5 cm to 35 cm in height under the boundary conditions of the winter case. The winter case was chosen as an example because the cold outdoor air would cause deterioration of the uniform air distribution through the diffuse ceiling and would enhance the draught risk in the occupied zone, see Figure 9 (a). Thus, this case is more representative than the others.

As depicted in Table 3, a reduction in the plenum height had a positive effect on the energy efficiency of the radiant ceiling. The convective heat transfer from the radiant ceiling to the plenum increased from 205 W to 461 W when the plenum height decreased from 35 cm to 5 cm. The low-height plenum forced cold supply air to contact the warm radiant surface directly with a high velocity, which enhanced both the convective coefficient and the air-to-surface temperature difference. As a result, the convective heat exchange increased dramatically. Although the radiant heat transfer from the radiant ceiling decreased because of the change in the diffuse ceiling surface temperature and view factors, the total heating capacity still increased from 516 W to 636W as the plenum height was reduced from 35 cm to 5 cm. Consequently, the air temperature in the room increased by approximately 3 ºC.

Regarding air distribution, low plenum height reduced the uniformity of the air distribution through the diffuse ceiling. Figure 11 (a) illustrates the delivered airflow ratio through the diffuse ceiling. A uniform distribution would result in a delivered airflow ratio of 100% at all distances from the inlet. In all cases, high

proportions of air were delivered at a short distance from the plenum inlet, and the air delivery gradually decreased as the distance from the plenum inlet increased. Furthermore, the reduction in plenum height exacerbated the situation. The distribution variation exceeded 120% with the 5 cm plenum, while the variation for the 35 cm plenum was less than 100%. The large distribution variation can be attributed to the low-pressure drop through the diffuse ceiling panels and also to the extremely low supply-air temperature.

Another important design consideration is the need to minimize the variation in supply air temperature. Figure 11 (b) shows air distribution just above the diffuse ceiling, which could present the supply air temperature. Because of the heat exchange with the radiant ceiling, the thermal decay on the supply air was significant in all cases. However, the low height plenum limited the mixing of air in the plenum and aggravated the temperature variation. When the plenum as low as 5 cm, the cold outdoor air was directly delivered to the room at a short distance from the plenum inlet, no mixing could be expected in this case.

<div align="center">

Figure 11

</div>

Plenum height influences the air distribution through the diffuse ceiling, and thus it affects the airflow performance in the occupied zone. The velocity distributions at a height of 0.1 m were analyzed and compared under different plenum heights, as illustrated in Figure 12. When the plenum height decreased, reverse flow with high velocity penetrated from the front of the room to the entire room, and the air velocity increased significantly. The air velocity reached 0.25 m/s in the case with a plenum height of 5 cm, which would result in a draught problem. The asymmetric distribution of velocity along the y-axis can be attributed to two factors. First, the exhaust was at the left corner of the façade ($x = 0$, $y = 3.1$, $z = 0.25$), which to some extent impacted the local air velocity. Second, because of the random and asymmetric nature of the turbulent flow, the airflow would not have produced a perfectly symmetric pattern [32].

Although the temperature variation in the plenum reached 30 $^{\circ}$C, the air temperature in the occupied zone was very uniform. An effective mixing between supply air flow and convective flow from heat sources was observed. In order to keep this article brief, the plot of temperature distribution in the occupied zone was not shown here.

<div align="center">

Figure 12

</div>

5.3 The effect of plenum length

The effect of plenum length on the air distribution was investigated by doubling the plenum length, and its effect on the radiant ceiling energy performance was also discussed here. Because the room geometry was doubled, the heat loads were doubled accordingly and were located symmetrically along the x-axis. In addition, the air flow rate was doubled to maintain the ACH of 2 h^{-1}. Plenum height was kept at 35 cm, as in the experimental measurements. Only the winter case was studied, as for the reason discussed in Section 5.2.

The doubled plenum length did not result in an exact doubling of the heat released from the radiant ceiling, as shown in Table 3. The total heat flow of the radiant ceiling was 965 W when the length of the room was 9.6 m, which was only 87% greater than that at the original length of 4.8 m. As expected, both air velocity and temperature differences decreased as the air traveling further in the plenum. Consequently, both convective and radiative heat fluxes were weakened by the increase in plenum length.

Figures 13 showed that doubling the plenum length causes deterioration in the uniformity of the air distribution through the diffuse ceiling. The variation reached 140% when the room length was 9.6 m, while

the variation in the 4.8 m case was less than 100%. Furthermore, it can be observed that there were two "jumps" in the curve at distances of approximately 2.2 m and 6.7 m from the plenum inlet. These jumps were because that the rising thermal plume reached the diffuse ceiling and acted as thermal blockages for the ventilation air flow. Therefore, low air delivery was found at these two locations. The temperature variation increased 3 oC by doubling the plenum length. The degree of temperature variation was determined by the amount of heat transfer from the thermal mass and also by the residence time of the supply air within the plenum. The greater the travel distance of the supply air, the larger the temperature variation will be.

Figure 13

Figure 14 presents the velocity distribution at a height of 0.1 m in the room with doubled length. In this room, the high draught region penetrated approximately half of the room deep. The air velocity in the occupied zone even reached 0.32 m/s, significantly higher than the limit of 0.18 m/s. The occupants situated near the façade experienced significantly greater draught than the ones located near the back wall. The temperature variation along the length of the room was negligible (less than 1 ºC). From the standpoint of both energy efficiency and thermal comfort, it can be concluded that the integrated system is suitable to use in a small space, for instance, a single office room.

Figure 14

5.4 Effect of plenum inlet configuration

Two different inlet configurations were studied, as illustrated in Figure 15. The original plenum inlet setup served as a reference, where the glazing opening was simplified as a slot opening located just above the diffuse ceiling. The other configuration was a square opening located at one corner of the plenum, which simulated a duct opening. The reason for constructing a square opening instead of a round one was to simplify the mesh. Both inlets had the same effective opening area, and the plenum height was 35 cm in both cases.

Figure 15

From the standpoint of energy performance, the squared opening slightly enhanced the energy efficiency of the radiant ceiling by increasing the convective heat exchange, as shown in Table 3. This can attribute to the location of the plenum inlet. The slot opening was located just above the diffuse ceiling, resulting in the distribution of cool supply air along the ceiling panels. The square opening was located closer to the radiant surface, where the cool supply air had more contact with the warm radiant surface, which led to greater heat exchange. The increase in the heating capacity resulted in a slight increase in the air temperature in both the plenum and the occupied space.

A plot of predicted velocity distribution across the diffuse ceiling is shown in Figure 16. Different flow patterns were generated by using different inlet configurations, as illustrated by the streamline. For the square opening, a high velocity was observed in the corner of the plenum because of its centralized configuration. Because of a large recirculation of plenum air, the minimum velocity was found at the other corner near the façade. In contrast with the square opening, the slot opening enabled the injected air to be more evenly distributed along the y- direction. The air velocity gradually decreased as the air traveled along the plenum, and the minimum velocity was at the far end of the plenum. The temperature variation of the delivered air was more significant with the square inlet, where the maximum delivered air temperature was 27.7 ºC and the minimum temperature was 8.1 ºC. The values for the reference inlet were 27.1 ºC and 11.8 ºC, respectively. To keep this article brief, a plot of the temperature distribution is not shown here.

Figure 16

Figures 17 present the velocity distributions at 0.1 m height in the room with the square opening. A large amount of air delivered in the corner through diffuse ceiling caused the penetration of airflow into the occupied zone at the corner of the room. However, high air velocity occurred only near the wall and did not increase the local draught risk. The maximum air velocity in the occupied zone was similar to that in the reference case, which was approximately 0.18 m/s. The lowest air temperature occurred in the corner, although the air temperature difference in the occupied zone was still less than 1 °C.

Figure 17

6. Conclusions

The objective of this study was to develop a numerical model for the system combined diffuse ceiling supply with radiant ceiling. The air diffusion through the diffuse ceiling was simulated by a porous media model. The radiative heat exchange was calculated by a separate radiation model, and then applied as boundary conditions for the porous media model. The numerical model was validated by measured results from the full-scale test facility under different operating conditions. The CFD calculated results agreed well with the measured one on both temperature and velocity. This numerical model was proved that it able to use for predicting the airflow pattern and thermal performance in the room with the integrated system.

The validated numerical model was further applied in a series of parametric studies, to analyze the effects of different design parameters. Several conclusions can be drawn:

1. The previous study indicated that the presence of diffuse ceiling increased the heating capacity of the radiant ceiling but decrease its cooling capacity. Therefore, radiant ceiling needs to run with a low surface temperature to maintain an acceptable indoor environment. The simulated results in this study showed that diffuse ceiling panels with a high U-value can reduce its impact on the radiant ceiling, making it possible to use a high surface temperature for cooling.
2. A low plenum height enabled the supply air to contact the radiant surface directly and enhanced the energy efficiency of the radiant ceiling. However, the reduction in plenum height caused deterioration in the uniformity of the air distribution through the diffuse ceiling and thus led to an increase in draught risk in the occupied zone. Simulated results indicated that a plenum height below 10 cm would result in a significant draught at floor level.
3. Doubling the plenum length had negative impacts on both the energy performance of radiant ceiling and the comfort level in the occupied zone. The results indicated that the integrated system is suitable to use in a small office rather than a large, open space.
4. The plenum inlet configuration had an impact on the air distribution in both the plenum and the occupied zone. To enhance the energy efficiency of the radiant ceiling, the plenum inlet should be located close to the radiant surface. Additional plenum inlet configurations should be investigated in the future.

Compared with conventional radiant ceiling and separated ventilation system, the two subsystems interact and complement with each other in the integrated system. The system showed a promising opportunity as a heating system and the potential to use the natural cooling resource without compromise thermal comfort. However, a reduction in the radiant ceiling's cooling capacity could not be neglected. A dynamic state

investigation would be interesting in the further study, which focuses on the night cooling potential and the thermal storage capacity of the ceiling slab and diffuse ceiling panel.

Nomenclature

C_2 inertial resistance factor [1/m]

E_f total fluid energy [m^2/s^2]

F_{kj} view factor between surfaces k and j

k_{eff} effective thermal conductivity of the medium [W/m.K]

k_f fluid thermal conductivity [W/m.K]

k_s solid medium thermal conductivity [W/m.K]

P pressure [Pa]

q_{rad} radiative heat flux [W/m^2]

S_M momentum source term [N/m^3]

S_E energy source term [W/m^3]

V superficial velocity [m/s]

α permeability [m^2]

ε_k emissivity

μ dynamic viscosity [kg/m.s]

γ porosity of the medium

ρ air density [kg/m^3]

ρ_k reflection coefficient

τ shear stress [Pa]

σ Stefan-Boltzmann constant, $5.67*10^{-8}$ [$W/m^2.K^4$]

References

[1]   P. Jacobs and B. Knoll, "Diffuse ceiling ventilation for fresh classrooms," in *4 th Intern. Symposium on Building and Ductwork Air tightness*, 2009, pp. 1–7.

[2]   J. Fan, C. A. Hviid, and H. Yang, "Performance analysis of a new design of office diffuse ceiling ventilation system," *Energy Build.*, vol. 59, pp. 73–81, Apr. 2013.

[3]   P. V Nielsen and E. Jakubowska, "The Performance of Diffuse Ceiling Inlet and other Room Air Distribution Systems," in *COLD CLIMATE HVAC*, 2009.

[4]   C. A. Hviid and S. Svendsen, "Experimental study of perforated suspended ceilings as diffuse ventilation air inlets," *Energy Build.*, vol. 56, pp. 160–168, Jan. 2013.

[5]   F. S. Bauman, *Underfloor Air Distribution (UFAD) Design Guide*. USA: American Society of Heating, Refrigerating and Air-Conditioning Engineers, Inc., 2013.

[6]   P. Jacobs, E. C. M. Van Oeffelen, and B. Knoll, "Diffuse ceiling ventilation, a new concept for healthy and productive classrooms," in *Indoor Air*, 2008, pp. 17–22.

[7]   E. M. Jakubowska, "Air distribution in rooms with the diffuse ceiling inlet," Department of Civil Engineerging, Aalborg University, 2007.

[8]   L. Su, N. Li, X. Zhang, Y. Sun, and J. Qian, "Heat transfer and cooling characteristics of concrete ceiling radiant cooling panel," *Appl. Therm. Eng.*, vol. 84, pp. 170–179, 2015.

[9]   N. Arcuri, R. Bruno, and P. Bevilacqua, "Influence of the optical and geometrical properties of indoor environments for the thermal performances of chilled ceilings," *Energy Build.*, vol. 88, pp. 229–237, 2015.

[10]   J. Niu and J. v d Kooi, "Indoor climate in rooms with cooled ceiling systems," *Build. Environ.*, vol. 29, no. 3, pp. 283–290, 1994.

[11]   C. Zhang, P. K. Heiselberg, M. Pomianowski, T. Yu, and R. L. Jensen, "Experimental study of diffuse ceiling ventilation coupled with a thermally activated building construction in an office room," *Energy Build.*, vol. 105, pp. 60–70, 2015.

[12]   T. Yu, P. Heiselberg, B. Lei, M. Pomianowski, C. Zhang, and R. Jensen, "Experimental investigation of cooling performance of a novel HVAC system combining natural ventilation with diffuse ceiling inlet and TABS," *Energy Build.*, vol. 105, pp. 165–177, 2015.

[13]   A. Novoselac and J. Srebric, "A critical review on the performance and design of combined cooled ceiling and displacement ventilation systems," *Energy Build.*, vol. 34, no. 5, pp. 497–509, Jun. 2002.

[14]   S. J. Rees and P. Haves, "An experimental study of air flow and temperature distribution in a room with displacement ventilation and a chilled ceiling," *Build. Environ.*, vol. 59, pp. 358–368, Jan. 2013.

[15]   H. Brohus, "Influence of a Cooled Ceiling on Indoor Air Quality in a Displacement Ventilated Room Examined by Means of Computational Fluid Dynamics," in *ROOMVENT, 6th International conference on air distribution in rooms*, 1998, pp. 53–60.

[16]   S. B. Riffat, X. Zhao, and P. S. Doherty, "Review of research into and application of chilled ceilings and displacement ventilation systems in Europe," *Int. J. Energy Res.*, vol. 28, no. 3, pp. 257–286, Mar. 2004.

[17]   F. Causone, F. Baldin, B. W. Olesen, and S. P. Corgnati, "Floor heating and cooling combined with displacement ventilation: Possibilities and limitations," *Energy Build.*, vol. 42, no. 12, pp. 2338–2352, Dec. 2010.

[18]   M. Krajčík, R. Tomasi, A. Simone, and B. W. Olesen, "Experimental study including subjective evaluations of mixing and displacement ventilation combined with radiant floor heating/cooling system," *HVAC&R Res.*, vol. 19, no. 8, pp. 1063–1072, 2013.

[19]   A. D. Chodor and P. P. Taradajko, "Experimental and Numerical Analysis of Diffuse Ceiling Ventilation," Aalborg University, 2013.

[20]   C. Zhang, M. H. Kristensen, J. S. Jensen, P. K. Heiselberg, R. L. Jensen, and M. Pomianowski, "Parametrical analysis on the diffuse ceiling ventilation by experimental and numerical studies," *Energy Build.*, vol. 111, pp. 87–97, 2016.

[21]   M. Tye-Gingras and L. Gosselin, "Comfort and energy consumption of hydronic heating radiant ceilings and walls based on CFD analysis," *Build. Environ.*, vol. 54, pp. 1–13, Aug. 2012.

[22]   J. A. Myhren and S. Holmberg, "Flow patterns and thermal comfort in a room with panel, floor and

wall heating," *Energy Build.*, vol. 40, no. 4, pp. 524–536, Jan. 2008.

[23] C. Zhang, P. K. Heiselberg, M. Pomianowski, T. Yu, and R. L. Jensen, "Integrated solution in an office room with diffuse ceiling ventilation and thermally activated building constructions," *Energy Procedia*, vol. 78, pp. 2808–2813, 2015.

[24] ANSANSYS Inc., "Ansys Fluent release 16.0.," 2015. [Online]. Available: http://www.ansys.com/.

[25] I. ANSYS, *ANSYS FLUENT User's Guide*. 2009.

[26] J. Srebric and Q. Chen, "An example of verification , validation , and reporting of indoor environment CFD analyses (RP-1133)," *ASHRAE Trans.*, vol. 108, no. 2, pp. 185–194, 2002.

[27] R. and A.-C. E. American Society of Heating, *2009 ASHRAE Fundamentals Handbook (SI)*, vol. 30329, no. 404. 2009.

[28] Q. Chen, "Comparison of Different K-E Models for Indoor Air Flow Computations," *Numer. Heat Transf. Part B Fundam. An Int. J. Comput. Methodol.*, vol. 28, no. 3, pp. 353–369, 1995.

[29] Y.-T. Yang and C.-H. Chen, "Numerical simulation of turbulent fluid flow and heat transfer characteristics of heated blocks in the channel with an oscillating cylinder," *Int. J. Heat Mass Transf.*, vol. 51, no. 7–8, pp. 1603–1612, 2008.

[30] Q. Y. Chen, D. Ph, and A. Member, "A procedure for verification , validation , and reporting of indoor environment CFD analyses," vol. 8, no. 2, pp. 201–216, 2002.

[31] CEN Report, "CR 1752, Ventilation for buildings - Design criteria for the indoor environment," 1998.

[32] H. Jin, F. Bauman, and T. Webster, "Testing and modeling of underfloor air supply plenums," *ASHRAE Trans.*, vol. 112, no. 2, pp. 581–591, 2006.

Figure
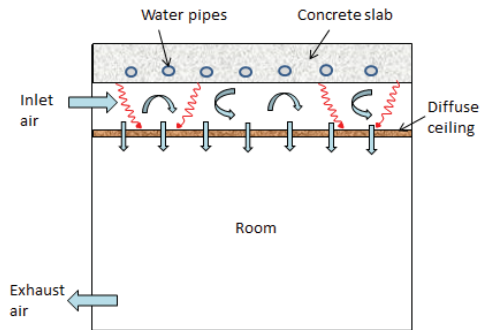
Fig.1 Schematic diagram of the integrated system
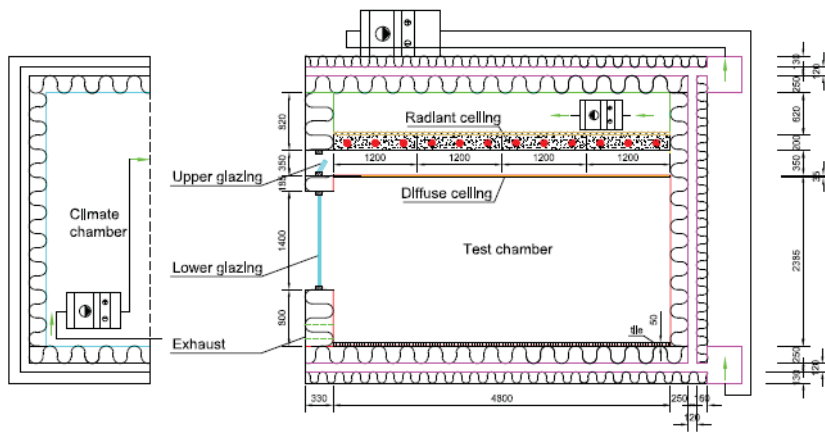
Fig.2. Vertical section view of environmental chamber

Fig.3. The test chamber with an office layout

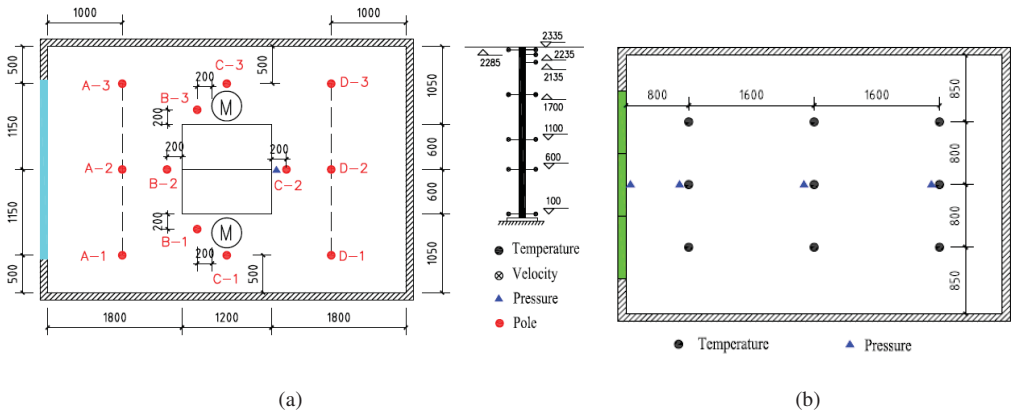Fig.4. Diffuse ceiling panels and radiant ceiling

(a)

(b)

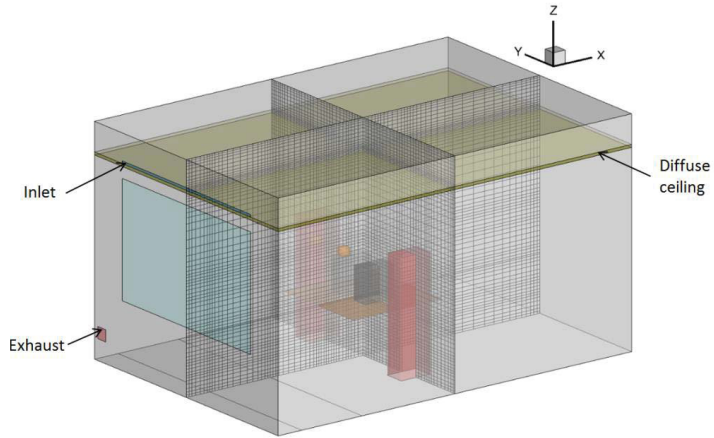Fig. 5 Measuring locations in plan view (a) Office (b) Plenum

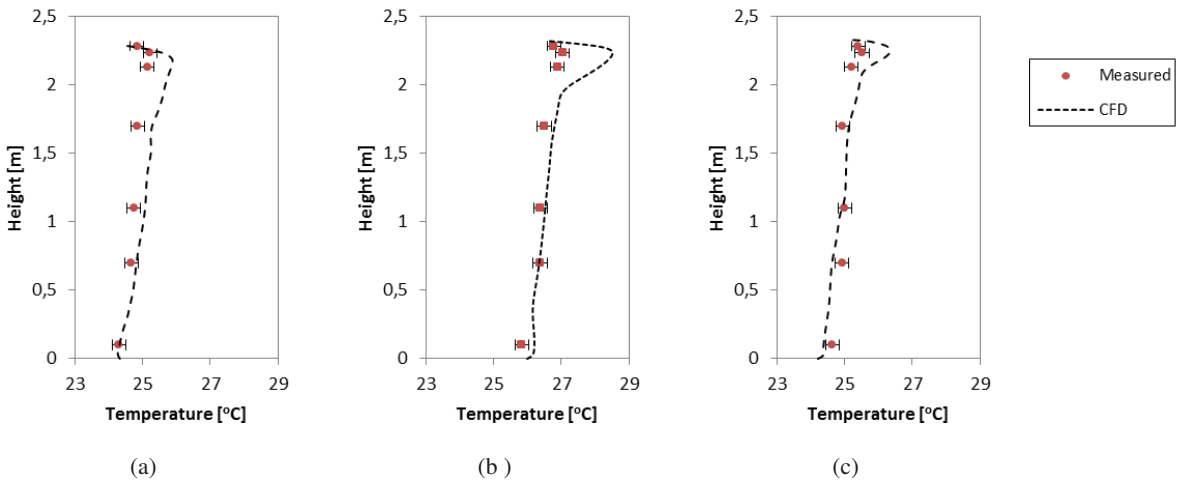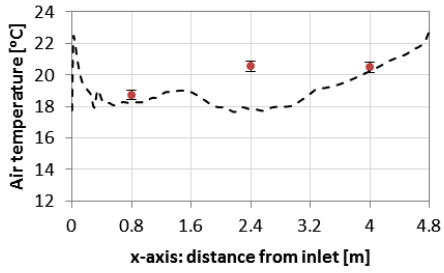Fig.6. Geometrical model and mesh distribution of the integrated system in an office room
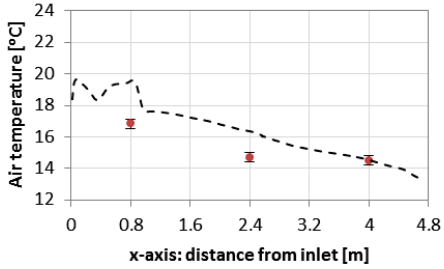

(a)

(b)

(c)

Fig.7. Vertical temperature profile at A2: (a) Winter, (b) Moderate season, and (c) Summer
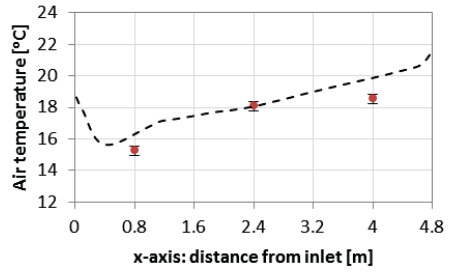
Fig.8. Air temperature distribution at the mid-height of the plenum: (a) Winter, (b) Moderate season, and (c) Summer

Velocity Magnitude: 0.00 0.03 0.07 0.10 0.13 0.17 0.20 0.23 0.26 0.30
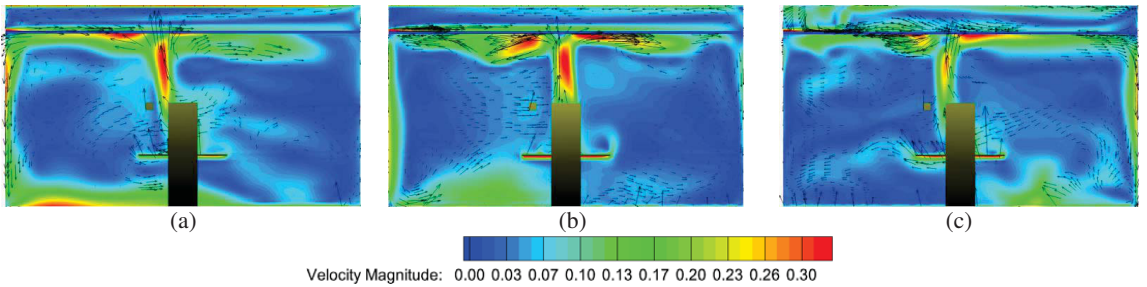
Fig.9. Velocity vector across the central plane, unit m/s: (a) Winter, (b) Moderate season, and (c) Summer
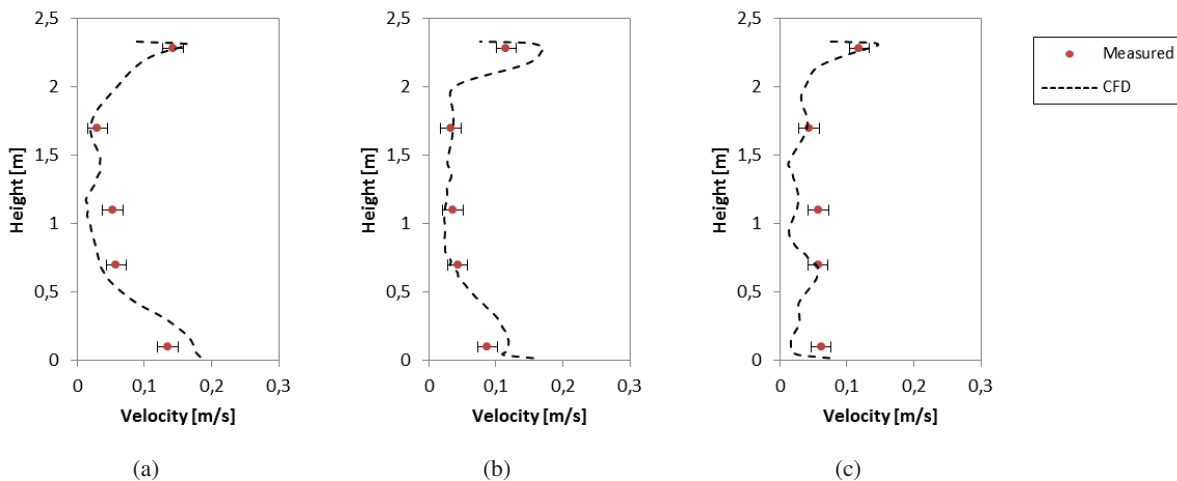
Fig.10. Vertical velocity profile at A2: (a) Winter, (b) Moderate season, and (c) Summer
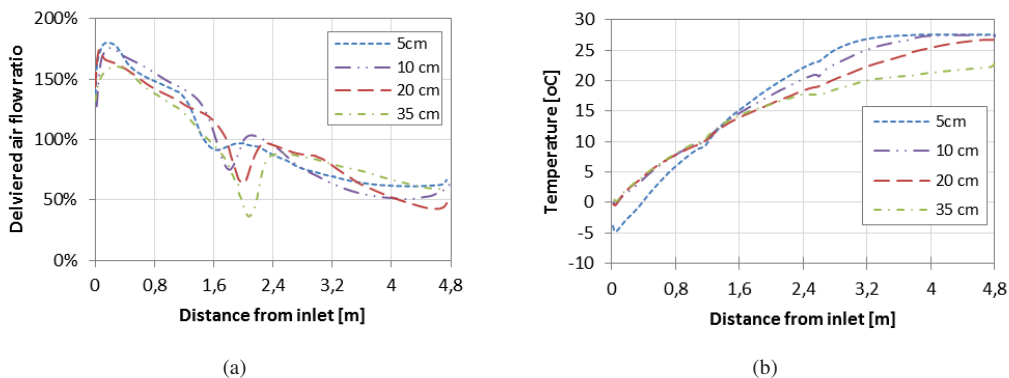
Fig. 11. Air distribution through the diffuse ceiling with different plenum heights (a) Delivered air flow ratio (b) Supply air temperature distribution
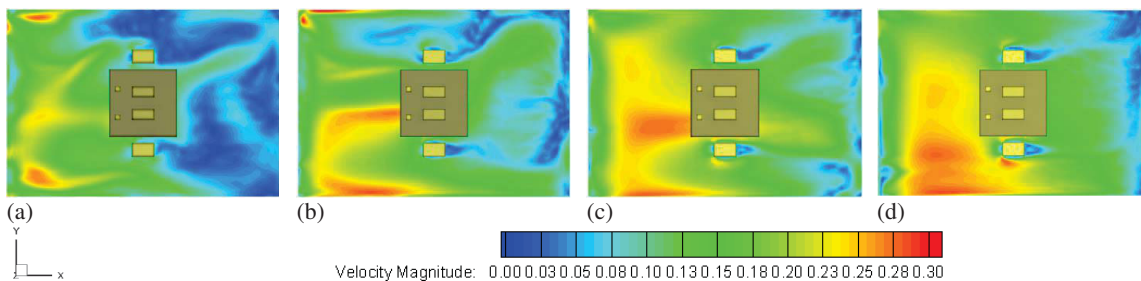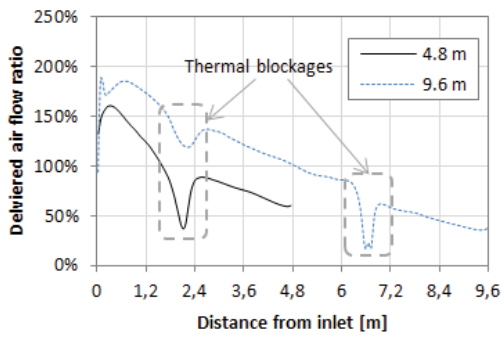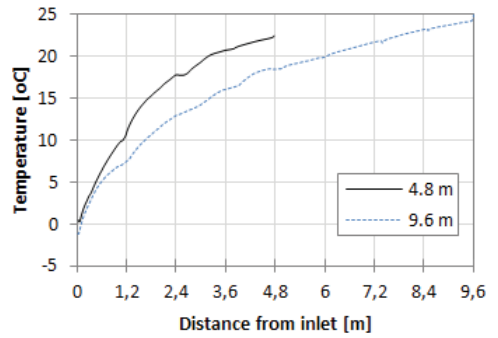

Velocity Magnitude: 0.00 0.03 0.05 0.08 0.10 0.13 0.15 0.18 0.20 0.23 0.25 0.28 0.30

Fig. 12. Velocity distribution at a height of 0.1 m with different plenum heights, unit m/s: (a) 35 cm, (b) 20 cm, (c) 10 cm, and (d) 5 cm

Fig. 13. Air distribution through the diffuse ceiling with different plenum lengths (a) Delivered air flow ratio (b) Supply air emperature distribution
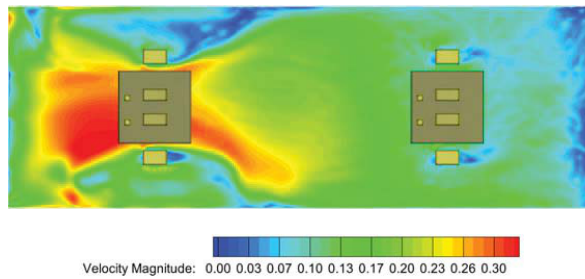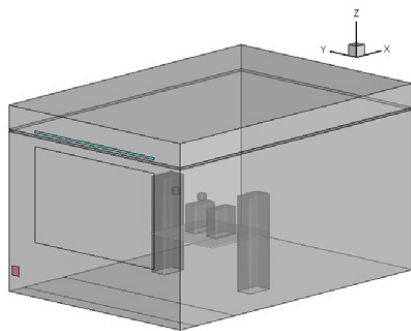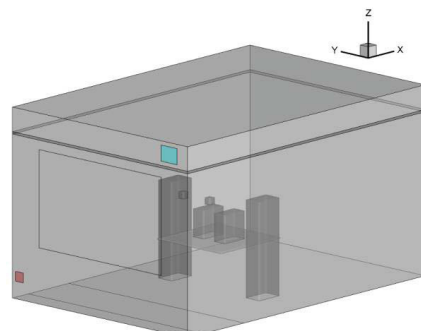

Fig.14. Velocity distribution at a height of 0.1 m in the room with doubled length, unit m/s

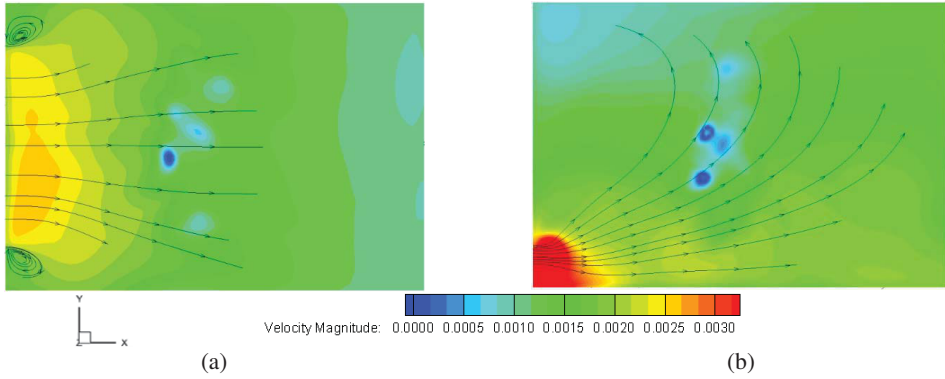Fig. 15. Plenum inlet configurations: (a) slot opening and (b) square opening

Fig. 16. Superficial velocity distribution across the diffuse ceiling with different plenum inlet configurations, unit m/s: (a) slot opening and (b) square opening
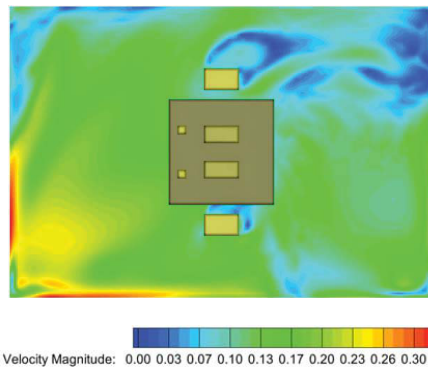

Fig. 17. Velocity distribution at a height of 0.1 m with the square opening, unit m/s

Table

Table 1. Test conditions for the three cases

Case	ACH	Supply air temp.	Radiant ceiling surface temp.	Interior heat load
	h⁻¹	ºC	ºC	W
Winter	2	-6.87	27.34	450.5
Moderate season	2	9.46	-	450.5
Summer	2	24.10	10.79	450.5

Table 2. Grid independence study

Variable	Mesh 1	Mesh 2	Mesh 3
Number of cells	353,312	760,235	1,027,309
Exhaust air temperature [ºC]	25.95	26.25	26.28
Air velocity at A2 [m/s]	0.065	0.068	0.068
Mass unbalance [kg/s]	0.00	0.00	0.00
Heat flux unbalance [W]	0.56	0.89	0.40
Heat flux unbalance [%]	-0.12%	-0.20%	-0.09%

Table 3. CFD results with different design parameters

Design Parameter	Operating condition				CFD calculated results			
	Description	Supply air temp.	Radiant ceiling surface temp.	Plenum air temp.	Room air temp.	Radiant ceiling heating/cooling capacity	Radiant ceiling radiative heat flow	Radiant ceiling convective heat flow
		ºC	ºC	ºC	ºC	W	W	W
Diffuse ceiling panel	Wood-cement	-6.87	27.34	18.70	25.11	516.61	311.52	205.09
	Al			20.24	23.62	449.68	258.69	190.99
	Wood-cement	9.46	-	19.55	26.72	-	-	-
	Al			22.20	25.94	-	-	-
	Wood-cement	24.10	10.79	16.56	24.46	-461.11	-172.29	-288.82
	Al			17.48	22.17	-556.74	-235.98	-320.76
Plenum height	35 cm	-6.87	27.34	18.70	25.11	516.61	311.52	205.09
	20 cm			18.82	26.04	540.10	272.66	267.44
	10 cm			19.00	27.94	603.86	203.88	399.98
	5 cm			20.36	28.76	636.44	175.08	461.37
Plenum length	4.8 m	-6.87	27.34	18.70	25.11	516.61	311.52	205.09
	9.6 m			18.58	25.05	965.03	576.07	388.96

| Plenum inlet | Original | -6.87 | 27.34 | 18.70 | 25.11 | 516.61 | 311.52 | 205.09 |
| | Corner | | | 19.33 | 25.32 | 540.67 | 294.28 | 246.39 |

SUMMARY

Diffuse ceiling ventilation is an innovative ventilation concept where the suspended ceiling serves as air diffuser to supply fresh air into the room. Compared with conventional ventilation systems, diffuse ceiling ventilation can significantly reduce or even eliminate draught risk due to the low momentum supply. In addition, this ventilation system uses a ceiling plenum to deliver air and requires less energy consumption for air transport than full-ducted systems. There is a growing interest in applying diffuse ceiling ventilation in offices and other commercial buildings due to the benefits from both thermal comfort and energy efficient aspects.

The present study aims to characterize the air distribution and thermal comfort in the rooms with diffuse ceiling ventilation. Both the stand-alone ventilation system and its integration with a radiant ceiling system are investigated. This study also presents the development and validation of a numerical model for predicting the airflow pattern and thermal behavior in the room with diffuse ceiling ventilation. The validated model is further used to investigate the effect of different design parameters on the system performance.